Experimental, Modelling and Optimization Insights for the Enhancement of Butanol Production using Phosphonium based Ionic Liquids

Submitted in Partial Fulfillment of the Requirements

for the Degree of

DOCTOR OF PHILOSOPHY

By

Dharamashibhai V. Rabari

Department of Chemical Engineering
Indian Institute of Technology Guwahati
February, 2015

Certificate

It is certified that the work contained in this thesis entitled **"Experimental, Modelling and Optimization Insights for the Enhancement of Butanol Production using Phosphonium based Ionic Liquids"**, by Dharamashibhai V. Rabari, has been carried out under my supervision and that this work has not been submitted elsewhere for a degree.

February 2015
IIT Guwahati

Dr. Tamal Banerjee
Associate Professor
Department of Chemical Engineering
Indian Institute of Technology Guwahati

Acknowledgements

It is my great privilege to sincerely thank several people who have supported me to complete my Doctoral Dissertation.

At the foremost, I would like to express my sincere gratitude to my research advisor **Dr. Tamal Banerjee** for his invaluable guidance throughout my research work. He will always be the source of positive energy that generated my keen interest in research. His positive attitude, smiling face and kind nature encouraged me to make research as my passion. His motivational and inspiring quotes improved my thinking ability, problem solving ability and technical writing skills. I got the opportunity to improve my research skills and personality under his leadership.

I would like to thank my Doctoral Committee members, **Dr. Kaustubha Mohanty** and **Dr. Amit Kumar**, Department of Chemical Engineering and **Dr. Manas Das**, Department of Mechanical Engineering. Their valuable inputs and evaluation during my research progress kept the flow of research work in the right direction.

I am indebted to **Prof. Ramgopal Uppaluri**, **Dr. Dipankar Bandyopadhyay**, **Dr. Mahuya De**, **Dr. A K Dasmahapatra** and **Dr. Prakash Kotecha** for their research oriented teaching during my course work. The knowledge gained during course work helped me in formulating my research objective. I also thank **Dr. Vijay Moholkar**, Head, Department of Chemical Engineering, for his administrative support. Furthermore, I would like to thank other Faculty and Staff members of Department of Chemical Engineering for their valuable support during my research. .

I am grateful to **Central Instrument Facility**, for providing me the necessary support for sample analysis using Nuclear Magnetic Resonance (NMR) Spectrometer. Without the help of **Mr. Kh. Kesho Singh** (Technical Superintendent, NMR) and **Mr. Kiran Indukari** (Teaching Assistant, NMR), it would not have been possible to analyze so many samples in such a short time.

My sincere gratitude to **Dr. Milind Joshipura** and **Mr. Nikunj Patel**, Nirma University for their assistance in modelling Equation of State in my research work.

I deeply acknowledge **Dr. A. Praveen Kumar**, **Mr. C V Manohar** and **Mr. V. Pasumurthi**, members of my research group, for their valuable assistance in learning the basics of NMR characterization and molecular dynamics simulation. I thank **Mr. Santhi Pilli**, **Ms. Sanjukta Bhoi**, **Mr. Anand Bharti**, **Ms. Basudhrity Banerjee**, **Mr. Mood Mohan**, **Ms. Reema Biswas**, **Mr. Suman Mahato**, **Mr. Ankit Bishnoi**, **Mr. Debanjan Dey**, **Mr. Pyarimohan Dehuri**, **Mr. Pratik Swain**, **Ms. Upasana Mahanta** and **Mr. Gaurab Sarkar** for providing a co-operative research environment.

I am extremely thankful to my senior research scholars, **Dr. Prashant Mishra**, **Mr. Ruhit Konwar**, **Mr. Manish Kamal**, **Ms. Chitrita Kundu**, **Mr. Sujoy Bose**, **Mr. Sankar Chakma**, **Mr. Jay Bhasarkar** and **Mr. Rajeev Parmar** for their help and encouragement.

I would like to thank my friends **Mr. Brijesh Kumbhani**, **Mr. Shrenik Patel** and **Mr. Nagendra Kumar**, Department of Electronics and Electrical Engineering and **Mr. Hardik Pandya**, Department of Computer Science and Engineering, for their assistance in learning LATEX.

My sincere thanks to friends **Mr. Himadri Sahu**, **Mr. Spatak Rarotra**, **Mr. Sunny Kumar**, **Mr. Suman Saha**, **Mr. Rahul Patwa**, **Mr. Rahul Ramteke**, **Mr. Supriyo Mondal**, **Mr. Abhik Bhattacharjee**, **Mr. Bhaskar Medhi**, **Mr. Proloy Das**, **Mr. Kulbhusan Samal**, **Mr. Abhay Tawalare**, **Mr. Piyush Patel**, **Mr. Prashant Thakar**, **Mr. Harsh Amin**, **Mr. Mayur Kevat**, **Mr. Jay Prajapati** and many more for making my stay at IIT Guwahati memorable.

Words of motivation and encouragement from some of my friends and relatives were only a call away. They always appreciated my efforts and outcomes of my research work. My sincere gratitude to **Late Dr. N. Subramanyam**, **Dr. Nitin Padhiyar**, **Dr. Sanjay Patel**, **Mr. S. B. Thakor**, **Dr. Parin Shah**, **Mr. Nimish Shah**, **Mr. H. R. Patel**, **Ms. Payal Mehta**, **Mr. Rahul Shah**, **Mr. Anand Patel**, **Ms. Nilofer Lakhani**, **Mr. Hitesh Patel**, **Mr. Anand Metre**, **Mr. Lalsingh Pawar**, **Mr. Ashok Kalor**, **Mr. L. V. Rabari**, **Mr. B. V. Rabari**, **Mr. Amrut Desai**, **Ms. Amthi Desai**, **Ms. Amba Desai**, **Mr. Jayram Desai**, **Mr. Vishnu Desai**, **Mr. Sagar Rabari**, **Mr. Rajesh Aal**, **Mr. Mukesh Desai**, **Mr. Ketan Desai**, **Mr. Ravi Kodiatar** and many more.

My whole hearted gratitude goes to my **father**, **Late mother**, **wife Rekha** and **daughter** as well as **Dr. Tamal Banerjee's** family whose blessings and boundless patience kept my morale high during the course of my study.

Above all I am thankful to GOD for giving me a wonderful and healthy life.

Sincerely
Dharamashibhai V. Rabari

Abstract

Butanol, a potential fuel produced by Acetone-Butanol-Ethanol (ABE) fermentation has a low conversion. The bacteria *Clostridium acetobutylicum* and *Clostridium beijerinckii* convert the substrate into acetone-butanol-ethanol with proportion of 3:6:1 under anaerobic conditions. The butanol concentration in product stream higher than 10 g/L retards the growth of microbes resulting in a low yield. This necessitated the use of Liquid Liquid Extraction for the removal of butanol from ABE streams. Thus the extraction of butanol by hydrophobic Ionic Liquids (ILs) have been proposed in the present work. In order to evaluate the potential of ILs, three Hydrophobic ILs, trihexyl(tetradecyl) phosphonium bis(2,4,4-trimethylpentyl)phosphinate ([TDTHP][Phosph]), trihexyl(tetradecyl) phosphonium dicyanamide ([TDTHP][DCA]) and trihexyl(tetradecyl) phosphonium decanoate ([TDTHP][DEC]) were chosen for experimental studies. The choice of ILs were made due to the fact that they are lighter than water and thus have been considered as solvents for butanol extraction from aqueous solution. As density plays a major role in piping and vessel design, the density of the phosphonium ILs along with imidazolium ILs have been measured at 298.15-328.15 K. These experimental densities were then correlated with nine different models. Among these models, two equation of state based cohesion factor models gave Absolute Average Deviation (%AAD) within the range 0.20%-0.45%. Molecular Dynamics (MD) strategy was also used to predict the density of ILs and the deviation was around 5% from experimental values.

The butanol distribution coefficient for all three ternary systems containing

[TDTHP][Phosph],[TDTHP][DCA] and [TDTHP][DEC] have been found within 19-59, 25-95 and 17-173 respectively. [TDTHP][Phosph] and [TDTHP][DCA] have been also used as solvent for simultaneous removal of ethanol and butanol from aqueous solution. Both ILs have shown more affinity towards butanol than ethanol, as butanol is more non polar than ethanol. The highest butanol selectivity (3709) and ethanol selectivity (2584) were found for 0.268 molar ratio of ethanol to butanol (identical with ABE outlet concentration) and 72.65 molar ratio of water to [TDTHP][Phosph]. The butanol distribution coefficient (4-123) was higher than ethanol distribution coefficient (3-20) for quaternary system containing [TDTHP][Phosph]. Similarly the butanol and ethanol distribution coefficient for the quaternary system containing [TDTHP][DCA] were obtained within 5-44 and 3-13 respectively. The ternary and quaternary experimental tie line data were then corrleated with the Gibb's Free Energy models namely Non Random Two Liquids (NRTL), UNIversal QUAsiChemical (UNIQUAC) and the quantum chemical based COnductor like Screening MOdel- Segment Activity Coefficient (COSMO-SAC) model. NRTL and UNIQUAC models gave deviation less than unity for all systems indicating an excellent fit. COSMO-SAC gave deviation within 10-20% which is reasonably accurate considering the method to be priori.

The binary interaction parameters for both quaternary systems generated by NRTL model were then used for optimization of multistage extractor. Particle Swarm Optimization (PSO) with the Isothermal Sum Rate (ISR) method was used for the cost function minimization for two systems namely [TDTHP][DCA]-ethanol-1-butanol-water and [TDTHP] [Phosph]-ethanol-1-butanol-water at T=298.15 K and p=1 atm. PSO parameters such as Global Local best Inertia Weight (GLbestIW) gave a less Average

number of iterations (42) and satisfactory Success rate (64%) as compared to conventional Linear Decreasing Inertia Weight (LDIW). For the system containing [TDTHP][DCA], the optimum solution was $1.1253{\cdot}10^{11}$ INR/year with 3 stages and 3.9891 kmol/hr solvent flow rate. The cheaper IL [TDTHP][Phosph] gave lesser cost ($4.526 \cdot 10^{10}$ INR/year) as compared to [TDTHP][DCA]. Further [TDTHP][Phosph] loss in raffinate phase was found to be half as compared to [TDTHP][DCA]. Ethanol efficiency was found to increase by an order of magnitude with a $(1/100)^{th}$ reduction in [TDTHP][Phosph] cost. Similarly a cost reduction of [TDTHP][DCA] by 100 times resulted in a 100% extraction efficiency for both alcohols.

Contents

List of Figures

List of Tables

Nomenclature

Abbreviations

AAD	Absolute Average Deviation
ABE	Acetone-Butanol-Ethanol
ACO	Ant Colony Optimization
AIT	Average number of ITerations
BIP	Binary Interaction Paramaeters
B3LYP	Becke, three-parameter, Lee-Yang-Parr
$CDCl_3$	Chloroform-D
CEOS	Cubic Equation Of State
CHELPG	CHarges from Electrostatic Potentials using a Grid based method
COSMO-RS	COnductor like Screening MOdel for Real Solvents
COSMO-SAC	COnductor like Screening MOdel - Segment Activity Coefficient
DE	Differential Evolution
DMSO	DiMethyl Sulfone Oxide
GA	Genetic Algorithm
GEPOL	GEometry of POLyhedron
GLbestIW	Global-average Local best Inertia Weight
GLbestAC	Global-average Local best Acceleration Coefficient
HETS	Height Equivalent to Theoretical Stages
IL	Ionic Liquid
ISR	Isothermal Sum Rate Method
LDIW	Linear Decreasing Inertia Weight
LLE	Liquid Liquid Equilibria
MD	Molecular Dynamics
MESH	Material Equilibrium Summation and Enthalpy equations
MW	Molecular Weight

NMR	Nuclear Magnetic Resonance
nop	Number Of Population
NRTL	Non-Random Two-Liquid model
OPLS-AA	Optimized Potentials for Liquid Simulations- all atoms
PCM	Polarizable Continuum Model
PSO	Particle Swarm Optimization
PSRK	Predictive-Soave-Redlich-Kwong
RDF	Radial Distribution Function
RMSD	Root Mean Square Deviation
RTIL	Room Temperature Ionic Liquid
SA	Simulated Anneling
SD	Standard Deviation
SOMA	Self Organizing Migrating Algorithm
SR	Success Rate
TZVP	Triple Zeta Valence Potential
UNIQUAC	UNIversal QUAsiChemical

ILs cations and anions	
[Ac]	Acetate
[BMIM]	1-Butyl-3-methylimidazolium
[Cl]	Chloride
[DCA]	Dicyanamide
[DEC]	Decanoate
[DMIM]/[Im10.1]	1-Decyl-3-methylimidazolium
[eFAP]	Tris(pentafluoroethyl)trifluorophosphate
[EMIM]	1-Ethyl-3-methylimidazolium
[$EtSO_4$]	Ethyl Sulfate
[HMIM]	1-Hexyl-3-methylimidazolium
[HOhMIM]	1-(6-hydroxyhexyl)-3-methylimidazolium
[MCH]	1-methyl-1-cyclohexanoate

[$MDEGSO_4$]	Diethylene glycol monomethyl ether sulfate
[$MeSO_3$]	Methane Sulfonate
[$MeSO_4$]	Methyl Sulfate
[Mnaph]	2-methyl-1-naphthoate
[MOcIM]	1-methyl-3-octylimidazolium
[Mo10.1]	4-decyl-4-methylmorphonium
[MTOA]	Methyl trioctyl ammonium
[$OcSO_4$]	Octyl Sulfate
[OCT]	Octanoate
[OMIM]	1-Octyl-3-methylimidazolium
[PF_6]	Hexafluorophosphate
[Phosph]	bis(2,4,4-trimethylpentyl)phosphinate
[P_{4441}]	Tributyl methyl phosphonium
[SCN]	Thiocyanate
[TCB]	Tetracyanoborate
[TDA]	Tetrakis(decyl)-ammonium
[TDTHP]	Tetradecyltrihexylphosphonium
[TEMA]	Tris(2-hydroxyethyl)-methylammonium
[Tf_2N]	Bis-(trifluoromethyl sulfonyl)imide

Latin Symbols

A_{ij}	UNIQUAC interaction parameter between component i and j
A^{PCM}	Overall surface in Polarizable Continuum Model, in^2
A_{ws}	Standard segment area, cm^2/mol
$A_i(\sigma)$	The surface area with a charge density of value σ
a_{eff}	Area of the standard surface segment, $\mathring{A}^2$
a_n	Area of the segment n, $\mathring{A}^2$
c/C	Number of components in the LLE system
$C_{Capital}$	Capital cost, $INR/year$
C_{col}	Column cost, $INR/year$

C_{pack}	Packing cost, *INR/year*
C_{Solute}	Cost for solute loss in raffinate phase, *INR/year*
$C_{Solvent}$	Cost for solvent loss in raffinate phase, *INR/year*
C_{Total}	Total cost, *INR/year*
c_{hb}	Hydrogen bonding interaction constant
D	Column diameter, m
d_{mn}	The distance between segment m and n, $\AA$
E^I	Extract phase flow rate, *kmol/hr*
E_j	Extract phase flow rate through stage j, *kmol/hr*
E_{mf}	Misfit energy
E_{hb}	Hydrogen bonding energy
F	Feed flow rate, *kmol/hr*
$F(N,Sol)$	Augmented objective function in optimization, *INR/year*
F_j	Feed flow rate over stage j, *kmol/hr*
f_{decay}	The empirical parameter
G_{ji}/g_{ji}	Average interaction energy for the interaction of molecules of component j with molecules of component i
$\Delta \underline{G}_{i/s}^{*res}$	The restoring solvation free energy
g_{best}	Global best position for particles in PSO
H_i	Peak area under NMR spectra of component i
$iter_{max}$	Maximum number of iterations in PSO
$K_{i,j}$	Distribution coefficient of component i over stage j
$k_{r,ij}$	Bond potential for bond between atoms i and j in OPLS-AA Force field, *kcal/mole*
$k_{\theta,ijk}$	Angle potential for angle among atoms i, j and k in OPLS-AA Force field, *kcal/mole*
l	Staverman-Guggenheim combinatorial term parameter
m	Number of tie lines
N_{av}	Avagrado's number

N	Number of stages
Obj	Objective function
Obj_C	Cost objective function in PSO
$P^{HB}(\sigma)$	The Gaussian type probability over charge density distribution
P_b	Atmospheric Pressure, *bar*
P_c	Critical Pressure, *bar*
$p_{best,i}$	Individual best position for particle i in PSO
$p_s(\sigma)$	Screening charge density distribution
q_i	Normalized surface area parameter for the Staverman-Guggenheim combinatorial term
R	Universal gas constant, $JK^{-1}mol^{-1}$
R^{II}	Raffinate phase flow rate, *kmol/hr*
R_j	Raffinate phase flow rate through stage j, *kmol/hr*
r_{eff}	The radius of the standard surface segment, $\AA$
r_i	Normalized volume parameter for the Staverman-Guggenheim combinatorial term
r_{ij}	Bond length between atoms i and j in OPLS-AA Force field, $\AA$
$r_{0,ij}$	Equilibrium bond length between atoms i and j in OPLS-AA Force field, $\AA$
r_n	The radius of the segment n, $\AA$
S	Selectivity
Sol	Solvent flow rate in PSO, *kmol/hr*
s	Penalty parameter in PSO
T	Temperature, K
T_b	Boiling Temperature, K
T_c	Critical Temperature, K
T_r	Reduced Temperature
U	Potential function in MD Force field
V_c	Critical volume, cm^3/mol

V_i	Velocity of particle i in PSO
V_{max}	Maximum limit for particle velocity in PSO
$V_{m,ijkl}$	Dihedral potential for angle among atoms, i, j, k and l, $kcal/mol$
V_{ws}	Standard segment volume, cm^3/mol
V^{PCM}	Overall volume in Polarizable Continuum Model, in^3
w	Weight factor
X_i	Position of particle i in PSO
X_{LB}	Lower bound limit for particle position in PSO
X_{UB}	Upper bound limit for particle position in PSO
${x_i}^I$	Mole fraction of component i of phase I in the LLE system
$x_{i,j}$	Mole fraction of component i in raffinate phase over stage j in ISR
${\hat{x}_i}^I$	Mole fraction of component i of phase I in the LLE system predicted by model
$y_{i,j}$	Mole fraction of component i in extract phase over stage j in ISR
Z/CN	Coordination number
z_i	Feed concentration of component i

Greek Symbols

α	NRTL non-randomness parameter
$\alpha(T_r)$	Cohesion factor expression
α'	Misfit energy constant
β or K_i	Distribution Coefficient
δ	Compound specific adjustable parameter in density models
γ_i or $\gamma_{i/s}$	Activity coefficient of component i in a solution (Extract or Raffinate)
$\gamma_{i,j}$	Activity coefficient of component i over stage j in ISR
$\Gamma_s(\sigma)$	Segment Activity Coefficient
ε_{ij}	Geometric mean of Van der Waals interaction parameters for atoms, i and j, $kcal/mol$
σ_{hb}	Hydrogen bonding interaction cutoff

σ_{acc}	Larger value of σ_m and σ_n
σ_{don}	Smaller value of σ_m and σ_n
σ_{ij}	Geometric mean of atomic diameter of atoms, i and j, $\mathring{A}$
σ_m	Apparent charge density distribution of the segment m, $e/\mathring{A}^2$
σ_n^*	Original charge density distribution of the segment n, $e/\mathring{A}^2$
θ	Area fraction in UNIQUAC equation
θ_{ijk}	Bond angle between atoms i, j and k in OPLS-AA Force field, *degrees*
$\theta_{0,ijk}$	Equilibrium bond angle between atoms i, j and k in OPLS-AA Force field, *degrees*
τ_{ij} or τ_{ia}	NRTL interaction parameter between component i and j/a
φ_{ijkl}	Dihedral angle among atoms, i, j, k and l, *degrees*
ω	Acentric factor
Φ	Segment fraction in UNIQUAC equation
$\phi(x)$	Penalty function in PSO
Ψ	Flow rate ratio of extract to feed
ρ_c	Critical density, g/cm^3
ρ_s	Saturated density, g/cm^3
ρ_0 or ρ_{model}	Predicted or reference density, g/cm^3

1

Introduction

Since the last few decades, there is an imbalance between energy supply and demand due to the rapid population growth and limited fossil fuel availability. Scientists and engineers are trying to diminish this gap by exploring alternative energy sources like biomass, wind and solar energy. During 1910-1920, fermentation processes were developed to produce bio-fuels which were later scaled commercially. These biotechnologies became obsolete due to costly raw material, low product yield and strong competition with petrochemical industries which started supplying cheaper products in 1960s. Instability in crude supply and prices from middle-east countries motivated

other countries to reintroduce bio-fuels as alternative energy fuels in 1970-1980. With economic consideration, many upstream and downstream processes have been developed to overcome past challenges like low product concentration and high product recovery cost. Thus in this regard, fermentation processes have been developed to provide energy fuels like ethanol and butanol. Though the alcohols are conventionally used as blending components with gasoline, butanol has more calorific value, more hydrophobicity and lesser flammability than ethanol. Therefore in the current work, the research interest is towards the enhancement of butanol than that of ethanol.

1.1 ABE Fermentation

Weizmann [1] developed the famous ABE fermentation process to produce acetone that could be used for the production of cordite (smokeless propellant) during World War I [1]. ABE fermentation had been implemented at industrial scale till it became obsolete due to the growth of petroleum industry. Considering alcohols as biofuels, this process became viable recently which produces acetone-butanol-ethanol with proportion of 3:6:1. The bacteria *Clostridium acetobutylicum* and *Clostridium beijerinckii* convert the substrate into products under anaerobic conditions. The major challenge in this process is the cell growth inhibition if butanol concentration is higher than 1.5 wt%, resulting in low product yield. In ABE process, the research findings can be categorized as; (a) to find the best biomass waste (substrate) for fermentation, (b) to increase the tolerance limit (alcohols concentration) for bacteria by genetic modification and (c) to remove butanol from the fermentation broth simultaneously during fermentation (*in-situ* separation).

Biomass containing higher sugar and starch content provides a better raw material for butanol production [2]. *Clostridium acetobutylicum* and *Clostridium beijerinckii* had recently been modified to increase the product yield [3, 4]. The tolerance level for bacteria has been improved up to 3 wt% butanol and 16 wt% ethanol in ABE product stream [5, 6]. Different separation techniques like distillation, extraction, gas stripping, adsorption and pervaporation had been earlier used for butanol extraction and enhancement from ABE product stream [2, 7, 8]. Distillation is a more energy-intensive step as the product

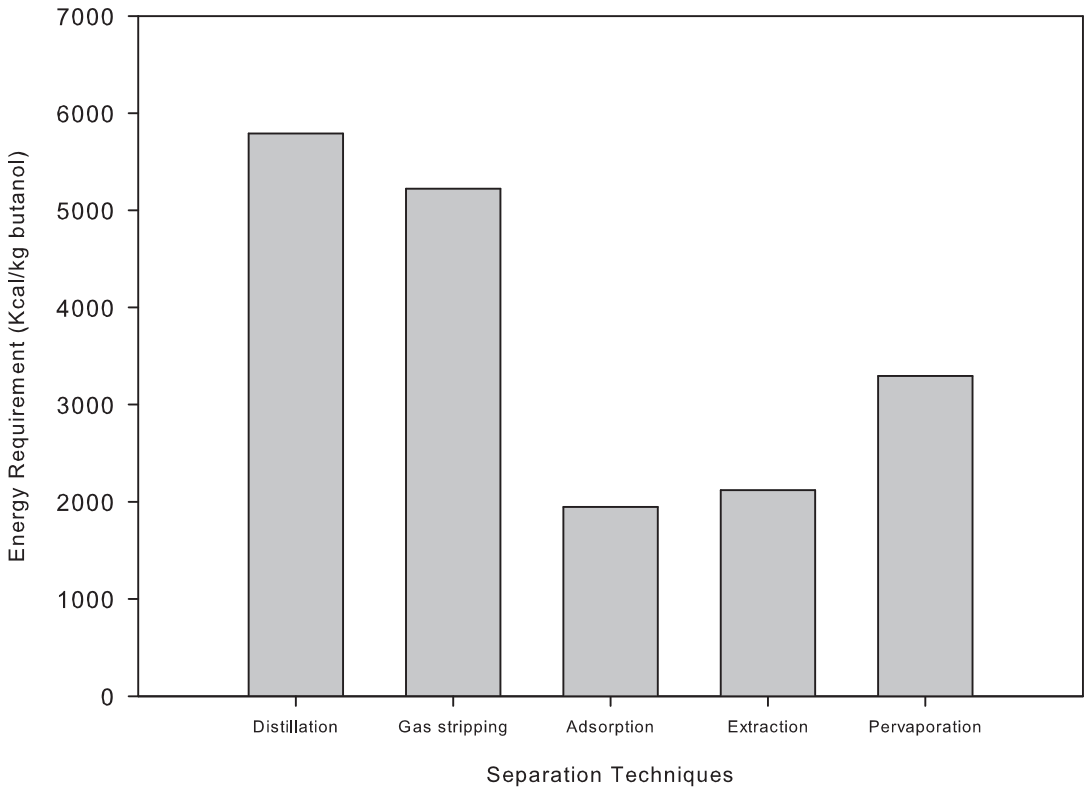

FIGURE 1.1: Energy Requirements for Butanol Removal by Various Separation Techniques [9]

stream contains large amount of water (higher volatile than butanol). Qureshi et al. [9] have compared the energy requirement per unit mass of butanol removal by different separation techniques (Figure 1.1). It is observed that the energy efficient techniques are

liquid liquid extraction and adsorption. The adsorption process requires energy of the order of 2000 kcal per 1 kg butanol production. Further the capacity of the adsorbent was found to be very low, hence adsorption for butanol removal was not used at an industrial scale [2]. Clogging or fouling are the main drawbacks in case of membrane separation [3]. Keeping the limitations in mind, extraction has been considered as an appropriate technique for butanol removal in the present work. Different organic solvents like oleyl alcohol [10], glyceryl tributyrate [11] and mesitylene [12] have been earlier used for bio-butanol extraction. However the major issue in using organic solvent is its toxicity to microorganism and evaporation to environment. Considering the environmental impact, we therefore propose Ionic Liquid (IL) as a solvent for the extraction of butanol from aqueous streams.

1.2 Ionic Liquids

Ionic liquids are salts those consist of organic cations and inorganic/organic anions. Room Temperature Ionic Liquids (RTIL) are liquid at room temperature. They are known as designer solvents due to the possibility of large number of ILs (cation and anion combinations) which impart specific properties. These solvents are more attractive due to desirable special properties, such as wider liquid range, negligible vapor pressure at room temperature, tunable viscosity, low flammability, high heat capacity and favorable solvation properties for polar and nonpolar compounds [13–19]. These solvents are more stable at high temperature and/or in presence of chemicals and are suitable for the extraction of inorganic and organic compounds [5, 18, 20–25].

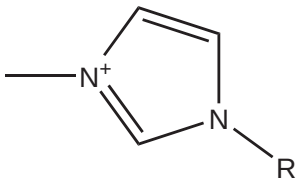

1-alkyl-3-methylimidazolium

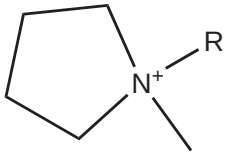

1-alkyl-1-methylpyrrolidinium

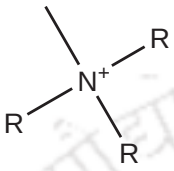

trialkylmethylammonium

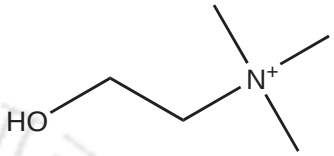

2-hydroxyethyltrimethylammonium

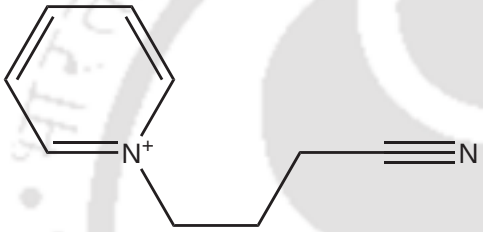

1-(3-cyanopropyl)pyridinium

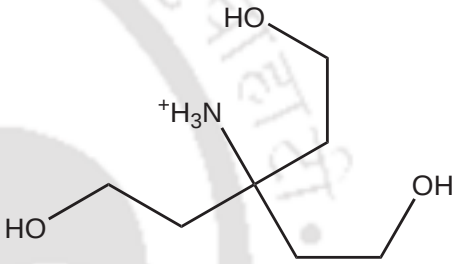

tris(2-hydroxyethyl)methyl ammonium

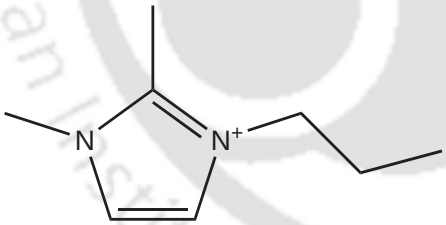

1,2-dimethyl-3-propylimidazolium

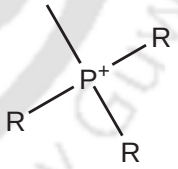

trialkylmethylphosphonium

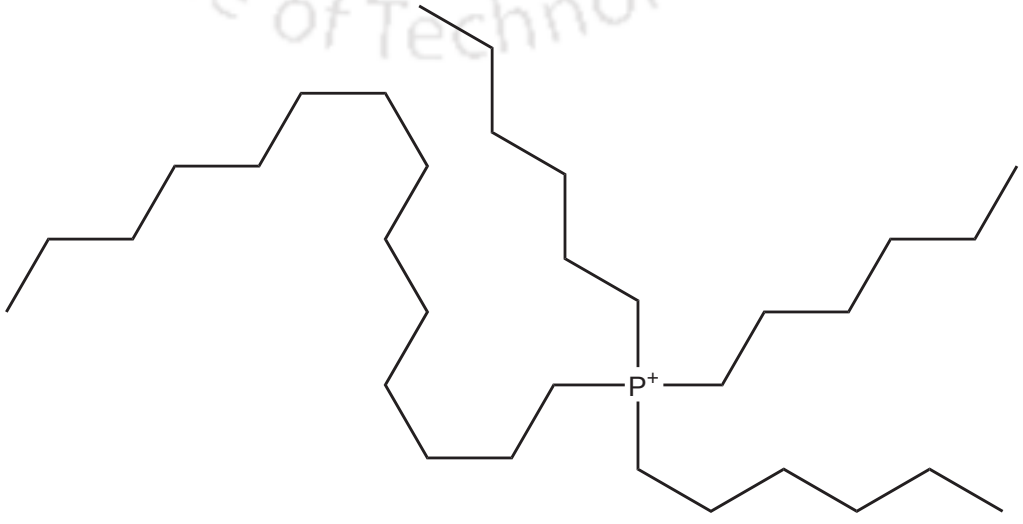

trihexyltetradecylphosphonium

FIGURE 1.2: Some commercial IL cations

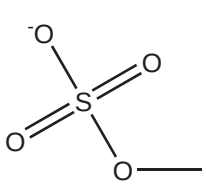

methyl sulfate

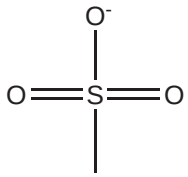

methanesulfonate

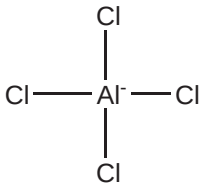

tetrachloroaluminate

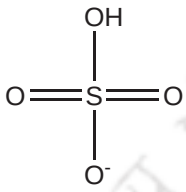

hydrogensulfate

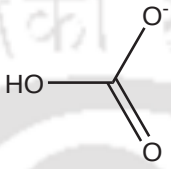

hydrogencarbonate

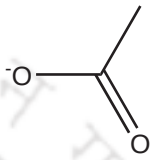

acetate

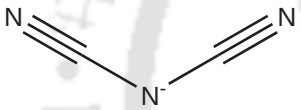

dicyanamide

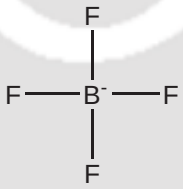

tetrafluoroborate

Cl-

chloride

thiocyanate

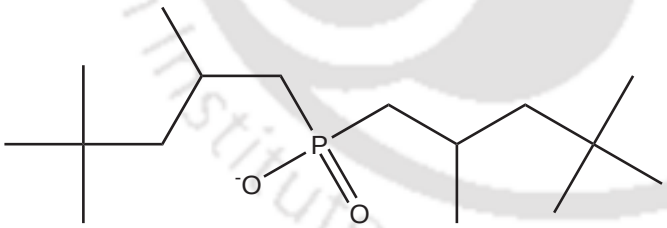

bis(2,4,4trimethylpentyl)phosphinate

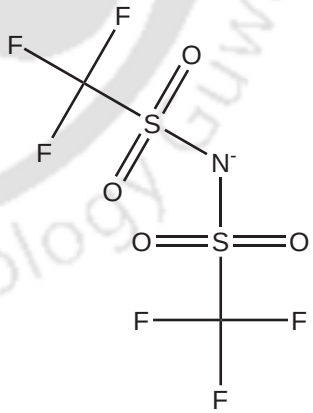

bis(trifluoromethylsulfonyl)imide

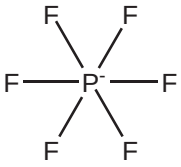

hexafluorophosphate

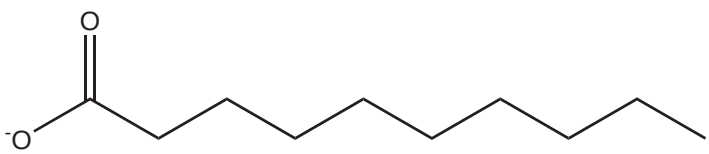

decanoate

FIGURE 1.3: Some commercial IL anions

The physical properties of these solvents can be tuned by suitable combination of cation and anion. Different types of room temperature ILs are based on cations such as alkylammonium, tetraalkylammonium, tetraalkylphosphonium, 1,3-dialkylimidazolium, and N-alkylpyridinium. Cations such as 1-alkylpiperidinium and 1,3-dialkylimidazolium salts are formed with anions possessing low nucleophilicity such as bis(trifluoromethylsulfonyl)imide, hexafluorophosphate, tetrafluoroborate, perfluoroalkylsulfonate, thiocynate, nitrate, acetate, ethyl sulphate and methane sulfonate. Some commercially available cations and anions are shown in Figs. 1.2-1.3. The applications of ILs covers many research domains like catalysis [26–34], nanotechnology [35], azeotropic separation [36], liquid-liquid extraction [37–39], metal extraction [40], aromatic-aliphatic separation [41, 42], membrane science [43, 44] and gas absorption [45–47].

1.3 Butanol Enhancement using Ionic Liquids

The Liquid Liquid Extraction process can be adopted via two approches namely (a) hydrophilic ILs [25] and (b) hydrophobic ILs [5, 21–24]. Hu et al. [25] have selected the former approach to separate water from 1-butanol using 1-(2-hydroxyethyl)-3-methylimidozoliumtetrafluoroborate. When compared to second approach, the first approach is not appropriate as IL rich phase contains large amount of water thereby becoming an energy intensive step [5, 23]. Hydrophilic ILs work in instances where there is concentrated feed mixture of 1-butanol and water. However in many situations, separation from dilute feed stream becomes challenging.

Ha et al. [21] have tested selectivity and distribution coefficient of butanol in water using different imidazolium based hydrophobic ILs. Garcia-Chavez et al. [5] have reported the potential of different nonflourinated ILs for the extraction of 1-butanol from water and validated their results with oleyl alcohol as solvent. In their work, they have compared selectivity values for 1-butanol in water using different ammonium based, phosphonium based and immidazolium based ILs. Pereiro and Rodriguez [48] have studied the extraction of ethanol from hexane/heptane by 1-ethyl-3-methylimidazolium ethyl sulfate ([EMIM][$EtSO_4$]). Simoni et al. [22] have shown that less number of stages are required in the extraction of 1-butanol from aqueous solution using 1-hexyl-3-methylimidazolium tris(pentafluoroethyl) trifluorophosphate ([HMIM][eFAP]) as compared to 1-(6-hydroxyhexyl)-3-methylimidazolium bis-(trifluoromethylsulfonyl)imide ([HOhMIM][Tf_2N]). In another work, Chapeaux et al. [23] used 1-hexyl-3-methylimidazoliumbis(trifluoromethylsulfonyl) imide to separate 1-butanol and ethanol from water. Domanska and Krolikowski [24] have shown the effect of alkyl chain length on selectivity and distribution coefficient of 1-butanol in water with tetracyanoborate based ILs. Nann et al. [49] have used four ILs containing ions such as 1-decyl-3-methylimidazolium, 4-decyl-4-methylmorpholinium, bis(trifluoromethylsulfonyl)imide and tetracyanoborate for the extraction of 1-butanol from aqueous solution at 308.15 K and 323.15 K. They found the selectivity of 1-butanol over water ranging from 53 to 144. Davis and Morton III [50] investigated the ternary LLE data for water-1-butanol-1-butyl-3-methylimidazolium bis(trifluoromethylsulfonyl) imide or 1-hexyl-3-methylimidazolium bis(trifluoromethylsulfonyl)imide at 298.15 K.

Kubiczek and Kamiński [51] have extracted all three components, namely acetone, butanol and ethanol from water using 1-hexyl-3-methylimidazolium hexafluorophosphate ([HMIM][PF_6]) and 1-butyl-3- methylimidazolium bis(trifluoromethylsulfonyl)imide ([BMIM] [Tf_2N]). They found the distribution coefficients for butanol (≈1.4) and acetone (≈1.1) are higher than ethanol (≈0.2) for a [HMIM][PF_6]/water mass ratio of 0.625 [51]. [BMIM][Tf_2N] also showed a similar trend for separation [51]. Kubiczek and Kamiński [51] have also replicated the same experiment at higher temperature (323.15 K). However, the temperature for ABE fermentation process is maintained at 308.15-310.15 K as it represents favorable environment for microorganism growth [52]. The ILs studied for butanol extraction till date are heavier than water. It should be noted that density plays an important role during design as it relates to the fluid handling cost. Some phosphonium based ILs are lighter than water and they have been used for extraction of organic components from aqueous solution [53–55]. Chowdhury et al. [53] have reported the highest selectivity (≈9) for ethanol extraction by the IL, trihexyl(tetradecyl) phosphonium bis(2,4,4-trimethylpentyl)phosphinate ([TDTHP][Phosph]) for 0.3 ethanol mole fraction in feed. Keeping this in mind we will focus our attention on the phosphonium based cation, as they are less dense than water.

1.4 Objectives

From the detailed literature study, the following objectives for the thesis have been defined:

Objective 1: *Measurement of pure property (density) of Ionic Liquids at different temperatures and Modelling by Cubic Equation Of State (CEOS) approach and Molecular Dynamics (MD) approach.*

There is an absence of experimental data on the thermodynamic properties of Phosphonium ILs. Considering the fact, prediction or even correlation of their thermophysical properties is essential and useful for engineering applications. The density of any IL is an important property as it is useful in piping, vessel designing and phase equilibrium calculations. Thus an attempt has been made to predict the density using the CEOS approach and then validate the same using experimentally measured liquid densities. The second strategy namely MD calculations were also used to validate the experiments.

Objective 2: *Measurement of Liquid Liquid Equilibrium (LLE) data for IL-Butanol-Water*

As discussed earlier, hydrophilic ILs are usually used for concentrated feed mixture of 1-butanol and water. Separation from dilute feed stream becomes challenging hence hydrophobic ILs are preferred. In this work, phosphonium based ILs are chosen as they are lighter than water and more thermally stable even at high temperature as compared to ammonium, imidazolium and pyridinium based ILs.

Objective 3: *Measurement of Liquid Liquid Equilibrium (LLE) data for IL-Ethanol-Butanol-Water*

Acetone in ABE product stream is more volatile as compared to ethanol and butanol, hence it can be vaporized in distillation. Thus the hydrophobic phosphonium based ILs

can be used for the preferential extraction of ethanol and butanol. The selectivity and distribution coefficient for each alcohol have been measured in the LLE process with phosphonium based ILs as solvents.

Objective 4: *Modelling of Experimental LLE data with NRTL, UNIQUAC and COSMO-SAC model.*

The experimental equilibrium data obtained in Objective 3 can be correlated with Gibb's Free energy models such as Non-Random Two-Liquid (NRTL) and UNIversal QUAsiChemical (UNIQUAC). Further the quantum chemical based COSMO-SAC model was also attempted to predict the extract (IL rich phase) and raffinate (Water rich phase) composition. The binary interaction parameters generated in the modelling was then used in the process optimization flowsheet. Thus an attempt was made to transform laboratory data into process design at industrial scale.

Objective 5: *Optimization of Multistage Extractor from NRTL binary interaction parameters.*

A multistage extractor containing more than two components requires detailed design like temperature, pressure, flow rate and composition on each stage. In this thesis, the traditional Isothermal Sum Rate (ISR) method has been considered for the stagewise calculation. We have optimized the number of stages and solvent flow rate by minimizing the multistage extractor cost for extraction of butanol and ethanol from aqueous solution using phosphonium based ILs. In such a process, Particle Swarm Optimization (PSO) was used as an optimization algorithm.

1.5 Organization

The thesis is organized into the following chapters.

Chapter 2 describes the experimental density measurement and the prediction of Ionic Liquid densities using a cohesion based CEOS. The temperature dependency of the cohesion factor in the cubic equation of state is used to predict the densities of seven commercial ILs namely, 1-Ethyl-3-methylimidazolium methane sulfonate [EMIM][$MeSO_3$], 1-Ethyl-3-methylimidazolium acetate [EMIM][Ac],1-Ethyl-3-methylimidazolium Thiocynate [EMIM][SCN], 1-Ethyl-3-methylimidazolium ethyl sulphate [EMIM][$EtSO_4$], Tris(2-hydroxyethyl)-methylammonium methyl sulphate [TEMA][$MeSO_4$], Trihexyl(tetradecyl) phosphonium bis(2,4,4-trimethylpentyl) phosphinate ([TDTHP][Phosph]) and Trihexyl(tetradecyl) phosphonium dicyanamide ([TDTHP][DCA]). The density of two ILs, [TDTHP] [DCA] and Trihexyl(tetradecyl) phosphonium decanoate ([TDTHP][DEC]) have further been predicted by MD approach.

Chapter 3 presents the experimental Liquid Liquid Equilibrium data for the ternary systems containing different phosphonium based ILs with water and butanol. The hydrophobic ILs namely [TDTHP] [Phosph], [TDTHP] [DCA] and [TDTHP] [DEC] having density lower than water has been specially chosen to recover butanol from water. The selectivity and distribution coefficient were also discussed for the extraction 1-butanol from water. The equilibrium data were then correlated with NRTL, UNIQUAC and COSMO-SAC model.

Chapter 4 presents the experimental Liquid Liquid Equilibrium data for the quaternary systems namely, [TDTHP] [Phosph]-ethanol-butanol-water and [TDTHP] [DCA]-ethanol-butanol-water. The effect of ethanol/butanol and water/IL molar ratio on selectivity and distribution coefficient were also studied in detail. The feed points are chosen such that the concentration of feed points are identical with ABE product concentration. The equilibrium data were then correlated with NRTL, UNIQUAC and COSMO-SAC model.

Chapter 5 describes the optimization of multistage extractor from the binary interaction parameters which were generated by NRTL model using experimental LLE data as obtained in Chapter 4. Particle Swarm Optimization along with Isothermal Sum Rate algorithms have been used to obtain the optimized solvent to feed flow rate and the number of theoretical stages for a multistage extractor.

2

Pure Ionic Liquid Properties

2.1 Introduction

There is an absence of experimental data on various thermodynamic properties of ILs. Considering the fact, prediction or even correlation of their thermophysical properties is essential and useful for engineering applications. The density of any IL is an important property because it is useful in phase equilibrium calculations, piping and vessel designing. In case of unavailability of experiment data, there are models available in literature [56–58] for density predictions. However most of the correlations, available in the literature, were derived for organic substances [58]. The experimental densities of seven commercial ILs, namely, 1-Ethyl-3-methylimidazolium methane sulfonate [EMIM][$MeSO_3$], 1-Ethyl-3-methylimidazolium acetate [EMIM][Ac], 1-Ethyl-3-methylimidazolium Thiocynate [EMIM][SCN], 1-Ethyl-3-methylimidazolium ethyl sulphate [EMIM][$EtSO_4$], Tris(2-hydroxyethyl)-methylammonium methyl sulphate [TEMA][$MeSO_4$], Trihexyl(tetradecyl) phosphonium bis(2,4,4-trimethylpentyl) phosphinate [TDTHP][Phosph] and Trihexyl (tetradecyl) phosphonium bis(2,4,4-trimethylpentyl) dicyanamide [TDTHP][DCA] (Fig. 2.1) were measured and predicted by different models in this chapter. Out of these models, two models based on cohesion factor of cubic equation of state were chosen from literature [59, 60] along with one newly derived cohesion factor expression [61]. The deviation between measured and predicted density was checked and the best model with minimum deviation was selected. In the subsequent section, IL density was predicted using cohesion factor based equation of state. The concluding section predicts and compares the density of ILs, namely, Trihexyl(tetradecyl) phosphonium bis(2,4,4-trimethylpentyl) dicyanamide [TDTHP][DCA] and Trihexyl(tetradecyl) phosphonium bis(2,4,4-trimethylpentyl)

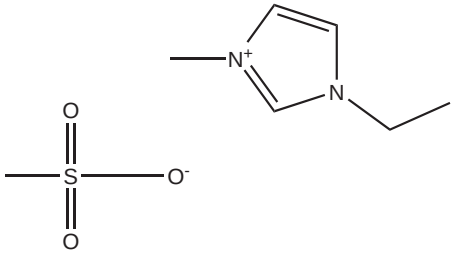

1-Ethyl-3-methylimidazolium methane sulfonate

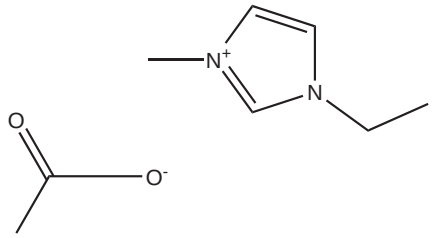

1-Ethyl-3-methylimidazolium acetate

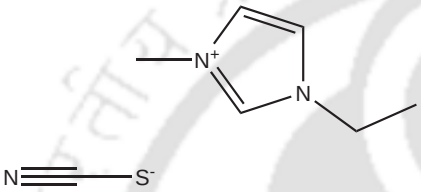

1-Ethyl-3-methylimidazolium thiocyanate

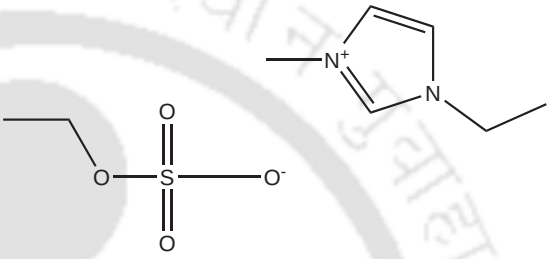

1-Ethyl-3-methylimidazolium ethyl sulphate

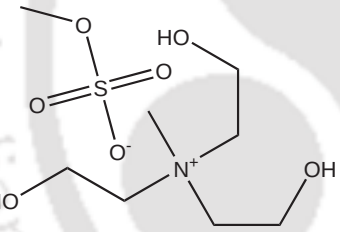

Tris(2-hydroxyethyl)-methylammonium methyl sulphate

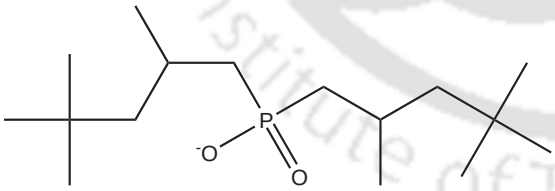

Bis(2,4,4-trimethylpentyl)phosphinate

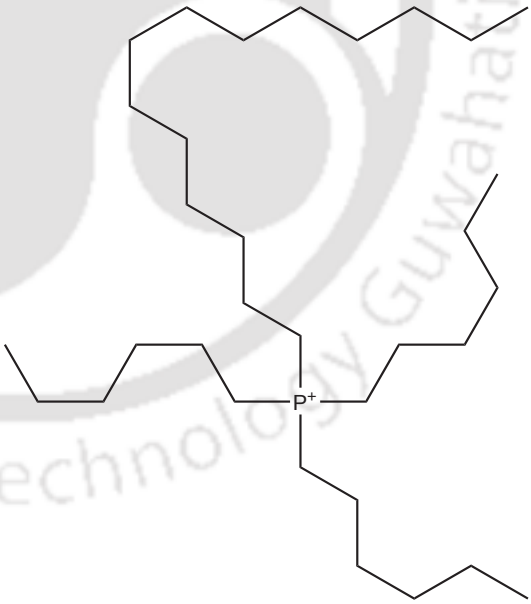

Tetradecyl(trihexyl) phosphonium

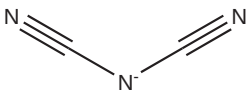

Dicyanamide

FIGURE 2.1: Seven ILs used for density measurement and prediction

decanoate [TDTHP][DEC] at T=298.15 K by classical Molecular Dynamics simulation (Section 2.3.2).

2.2 Experimental Methodology

All seven ILs were provided by Sigma Aldrich, Germany. The purities of ILs were more than 95% and were used as received from the supplier. To remove volatile compounds from all the ILs, 0.1 Pa vacuum was applied for at least 48 hours as a pretreatment operation. Digital densitometer (Anton Paar DMA-4500M model) with vibrating tube was used for the measurement of density. U-shaped tube (made of borosilicate glass) with sample was excited to vibrate at its characteristic frequency relating to the density of sample. Densitometer converts this frequency into density. The densitometer considers the viscosity correction factor, compensates ambient air pressure, and detects bubble in sample injection automatically. The instrument was calibrated using air and ultra-pure water in the temperature range of 293.15-328.15 K and further compared with the values reported in Anton Paar densitometer reference manual [62]. The uncertainty in density measurement was $\pm 1 \times 10^{-5} g \cdot cm^{-3}$ and the accuracy was $5 \times 10^{-5} g \cdot cm^{-3}$. The temperature was automatically controlled by densitometer with a resolution of 0.01 K and an accuracy of 0.03 K. The densities of all seven ionic liquids were measured within 293.15-328.15 K with 5 K interval.

2.3 Computational Details

The computational details are divided into two sections namely, density prediction and modelling (Section 2.3.1) and molecular dynamics simulation (Section 2.3.2).

2.3.1 Density Prediction and Modelling

Several authors [56–60] have suggested different models for density predictions [56–60]. Correlations with adjustable parameters are available which are specific to compounds. Some models are based on principle of corresponding states and others are based on group contribution methods. Most of the models require critical properties of ILs. Critical properties can be estimated using several group contribution methods [63–66]. In this work, modified Lydersen-Joback-Reid method [63–66] was used to predict critical properties of ILs (Eqs. 2.1-2.4). Acentric factor was calculated using the calculated critical pressure, critical temperature and normal boiling point by Rudkin's model [63–67] (Eq. 2.5). The groups along with the critical properties calculated via modified Lydersen-Joback-Reid method are given in Table 2.1.

$$T_b = 198.2 + \sum n\Delta T_b \tag{2.1}$$

$$T_c = \frac{T_b}{\left[A + B\sum n\Delta T_c - \left(\sum n\Delta T_c\right)^2\right]} \tag{2.2}$$

$$P_c = \frac{MW}{\left[C + \sum n\Delta P_c\right]^2} \tag{2.3}$$

$$V_c = D + \sum n\Delta V_c \tag{2.4}$$

TABLE 2.1: Group considered in Modified Lydersen-Joback-Reid method [66]

	Groups	$MW_i =$	$\Delta T_c =$	$\Delta P_c =$	$\Delta V_c =$	$\Delta T_b =$
Without Rings	$-CH_3$	15.035	0.027	0.303	66.810	23.580
	$-CH_2-$	14.027	0.016	0.216	57.110	22.880
	>CH-	13.019	0.2E-03	0.114	45.700	21.740
	>C<	12.011	-0.021	0.054	21.780	18.25
	-OH	17.008	0.072	0.134	30.400	92.880
	-O-	16.000	0.005	0.130	15.610	22.420
	>C=O	28.011	0.025	0.234	69.760	94.970
	=O (other)	16.000	0.027	0.204	44.030	-10.500
	>N-	14.007	-0.003	0.030	26.700	11.740
	-CN	26.018	0.051	0.369	89.320	125.660
	-P	30.974	-0.008	0.178	67.010	34.860
	-S-	32.066	0.001	0.690	184.670	117.520
With Rings	$-SO_2$	64.065	-0.056	-0.061	112.190	147.240
	=CH-	13.019	0.011	0.169	42.550	26.730
	>N-	14.007	0.006	0.054	25.170	68.160

$$\omega = \frac{(T_b - 43)(T_c - 43)}{(T_c - T_b)(0.7T_c - 43)} \log\left[\frac{P_c}{P_b}\right] - \frac{(T_c - 43)}{(T_c - T_b)} \log\left[\frac{P_c}{P_b}\right] + \log\left[\frac{P_c}{P_b}\right] - 1 \qquad (2.5)$$

where A-D are constants [63–66] (A=0.5703, B=1.0121, C=0.2573, D=6.75). T_b, T_c, P_b, P_c and V_c represent, boiling point (K), critical temperature (K), atmospheric pressure (bar), critical pressure (bar) and critical volume (cm^3/mol) respectively. Here n is the number of functional group present in the structure, MW, molecular weight, and ω,

acentric factor. Δ sign indicates the contribution of the respective group to the critical properties and normal boiling point of compound. Due to the lack of experimental

TABLE 2.2: Estimated critical properties of ILs*

Property	[EMIM] [$MeSO_3$]	[EMIM] [Ac]	[EMIM] [SCN]	[TEMA] [$MeSO_4$]	[EMIM] [$EtSO_4$]	[TDTHP] [Phosph]	[TDTHP] [DCA]
MW	206.27	170.21	169.25	275.33	236.29	773.29	549.91
T_b (K)	667.38	615.11	717.32	865.10	712.68	1374.80	1231.08
T_c (K)	1026.03	864.11	1013.63	1092.14	1067.49	1879.92	1527.01
V_c (cm^3/mol)	587.06	544.63	666.44	744.34	659.78	2964.61	2145.42
P_c (bar)	48.13	30.44	22.26	35.24	40.46	5.51	7.65
ω	0.33	0.57	0.39	1.53	0.37	-0.14	0.57

* calculated by Eqs. 2.1- 2.5

critical properties, authors [63–66] have tested the accuracy and consistency of these values by determining the density of ILs, for which experimental data are available. They could show that the method proposed by Reid (modified Lydersen-Joback-Reid method [63–66]) was appropriate for the prediction of critical properties. Predicted values of critical properties, normal boiling point and acentric factor for seven ILs used in this work are shown in Table 2.2. Nine different models were chosen for the prediction of density as shown in Table 2.3. The first seven models (Table 2.3) are based on correlations namely; Reid et al. [58] (RR)(Model 1), Mchaweh et al. [58] (MH)(Model 2), Yen & Woods [58] (YW) (Model 3), Racket [58] (RA) (Model 4), Yamada & Gunn [58] (YG) (Model 5), Hankinson & Thomson [58] (HT) (Model 6), and Linear Generalized Model [58] (LGM)(Model 7).

According to literature [58], these seven models show minimum deviation from the experimental values of density and proved to be better alternative for the estimation of density. Further Nasrifar and Moshfeghian [59] proposed a model for the estimation of density of refrigerant fluids in conjunction with Predictive-Soave-Redlich-Kwong (PSRK) [59–61]. Recently Valderrama and Forero [66] have shown that PRNSM1 cohesion factor model can predict the vapour pressure of IL's accurately. In the present study, Nasrifar's density model (NM) was used in conjunction with PRNSM1 and original SRK cohesion factor expressions. NM model [59] is represented by Eqs. 2.6-2.7.

$$\rho_s = \rho_0 \rho_c \left[1 + \delta(\alpha(T_r) - 1)^{\frac{1}{3}}\right] \tag{2.6}$$

$$\rho_0 = 1 + d1\left(1 - \frac{T_r}{\alpha(T_r)}\right)^{\frac{1}{3}} + d2\left(1 - \frac{T_r}{\alpha(T_r)}\right)^{\frac{2}{3}} + d3\left(1 - \frac{T_r}{\alpha(T_r)}\right) + d4\left(1 - \frac{T_r}{\alpha(T_r)}\right)^{\frac{4}{3}} \tag{2.7}$$

where ρ_s, ρ_0, ρ_c are respectively, saturated density, predicted or reference density and critical density; T_r (T/T_c) the reduced temperature and d_1, d_2, d_3, d_4: global constants [59] independent of compounds (d_1=1.1688, d_2=1.8177, d_3= -2.6581, d_4=2.1613). The term $\alpha(T_r)$ is the cohesion factor expression.

The expressions for PRNSM1 and SRK cohesion factor are given by Eqs 2.8- 2.9 respectively.

PRNSM1 cohesion factor [61]:

$$\alpha(T_r) = \left[1 + (1.3676\omega + 0.4132)(1 - T_r^{0.5})\right]^2 \tag{2.8}$$

TABLE 2.3: Density prediction models [58–61, 66]

Sr. No.	Model Name	Model Equation
1	Reid et al. (RR)	$\rho = \rho_c \left[1 + 0.85(1 - T_r) + (1.6916 + 0.984\omega)(1 - T_r)^{\frac{1}{3}}\right]$
2	Mchaweh et al. (MH)	$\rho(T) = \rho_c \left(1 + 1.169\tau^{\frac{1}{3}} + 1.818\tau^{\frac{2}{3}} - 2.658\tau + 2.16\tau^{\frac{4}{3}}\right)$, $\tau = 1 - \frac{\frac{T}{T_c}}{\left[1+m\left(1-\sqrt{\frac{T}{T_c}}\right)\right]^2}$, $m = 0.480 + 1.574\omega - 0.176\omega^2$
3	Yen and Woods (YW)	$\rho = \rho_C \left[1 + \sum_{i=1}^{4} k_i (1 - T_r)^{i/3}\right]$ where $k_1 = 17.4425 - 214.578Z_C + 989.625Z_C^2 - 1522.06Z_C^3$, $k_2 = -3.28257 + 13.6377Z_C + 107.4844Z_C^2 - 384.211Z_C^3$ (if $Z_C < 0.26$), $k_2 = 60.2091 - 402.063Z_C + 501Z_C^2 + 641Z_C^3$ (if $Z_C > 0.26$), $k_3 = 0$, $k_4 = 0.93 - k_2$
4	Racket (RA)	$\rho = \rho_C Z_C^{-(1-T_r)^{2/7}}$
5	Yamada and Gunn (YG)	$\rho = \rho_C (0.29056 - 0.08775\omega)^{-(1-T_r)^{2/7}}$
6	Hankinson and Thomson (HT)	$\rho = \frac{\rho_C}{\left[V^{(0)}\left(1-\omega V^{(1)}\right)\right]}$ where $V^{(0)} = 1 - 1.5281(1 - T_r)^{1/3} + 1.4390(1 - T_r)^{2/3} - 0.8144\,(1 - T_r) + 0.19045(1 - T_r)^{4/3}$, $V^{(1)} = \left(-0.296123 + 0.386914T_r - 0.0427258T_r^2 - 0.0480645T_r^3\right) / (T_r - 1.00001)$

7	Linear Generalized Model (LGM)	$\rho = \left(\frac{A}{B}\right) + \left(\frac{2}{7}\right) \cdot \left\{\frac{A \cdot \ln B}{B}\right\} \frac{(T - T_b)}{(T_c - T_b)}$, $A = a + b \cdot \frac{M}{V_c}$ $B = \left(\frac{c}{V_c} + \frac{d}{M}\right) \cdot V_c^2$ where a=0.3411, b=2.0443, c=0.5386, d=0.0393 and δ=1.0476
8	Predictive-Soave-Redlich-Kwong (PSRK) Equation of State with NSM1 alpha function (NMPRNSM1)	$\rho_s = \rho_0 \rho_c \left[1 + \delta(\alpha(T_r) - 1)^{\frac{1}{3}}\right]$, $\rho_0 = 1 + d1 \left(1 - \frac{T_r}{\alpha(T_r)}\right)^{\frac{1}{3}} + d2 \left(1 - \frac{T_r}{\alpha(T_r)}\right)^{\frac{2}{3}} + d3 \left(1 - \frac{T_r}{\alpha(T_r)}\right) + d4 \left(1 - \frac{T_r}{\alpha(T_r)}\right)^{\frac{4}{3}}$, $\alpha(T_r) = \left[1 + (1.3676\omega + 0.4132)(1 - T_r^{0.5})\right]^2$
9	Predictive-Soave-Redlich-Kwong (PSRK) Equation of State with Original derived alpha function (NMSRK)	$\rho_s = \rho_0 \rho_c \left[1 + \delta(\alpha(T_r) - 1)^{\frac{1}{3}}\right]$, $\rho_0 = 1 + d1 \left(1 - \frac{T_r}{\alpha(T_r)}\right)^{\frac{1}{3}} + d2 \left(1 - \frac{T_r}{\alpha(T_r)}\right)^{\frac{2}{3}} + d3 \left(1 - \frac{T_r}{\alpha(T_r)}\right) + d4 \left(1 - \frac{T_r}{\alpha(T_r)}\right)^{\frac{4}{3}}$, $\alpha(T_r) = \left[1 + m(1 - T_r^{0.5})\right]^2$, $m = 0.480 + 1.574\omega - 0.176\omega^2$

SRK cohesion factor:

$$\alpha(T_r) = \left[1 + m(1 - T_r^{0.5})\right]^2 \tag{2.9}$$

where

$$m = 0.480 + 1.574\omega - 0.176\omega^2 \tag{2.10}$$

δ is the adjustable parameter specific to the compound under consideration. We now focus our attention to the computational details involving MD simulation in the subsequent section.

2.3.2 Molecular Dynamics Simulation

The structures of the phosphonium-based ILs namely, [TDTHP][DCA] and [TDTHP][DEC] were drawn using the molecule editing software Avogadro [68] (Fig. 2.2). Thereafter their molecular geometries were optimized using Gaussian 03 package at B3LYP/SDD level. The partial atomic charges were derived from this geometry according to the CHELPG procedure [69]. Cubic boxes each containing 150 molecules of IL were built for both [TDTHP][DCA] and [TDTHP][DEC] using Packmol freeware [70]. All MD simulations were performed using parallel NAMD package [71] in the OPLS-All Atom force field, where the potential function used has the general form:

$$\begin{aligned} U = & \sum_{ij}^{bonds} \frac{k_{r,ij}}{2}(r_{ij} - r_{0,ij})^2 + \sum_{ijk}^{angles} \frac{k_{\theta,ijk}}{2}(\theta_{ijk} - \theta_{0,ijk})^2 \\ & + \sum_{ijkl}^{dihedrals} \sum_{m=1}^{4} \frac{V_{m,ijkl}}{2}\left[1 + (-1)^m \cos\left(m\varphi_{ijkl}\right)\right] \\ & + \sum_i \sum_{j \neq i} \left\{ 4\varepsilon_{ij} \left[\left(\frac{\sigma_{ij}}{r_{ij}}\right)^{12} - \left(\frac{\sigma_{ij}}{r_{ij}}\right)^{6} \right] + \frac{1}{4\pi\varepsilon_0}\frac{q_i q_j}{r_{ij}} \right\} \end{aligned} \tag{2.11}$$

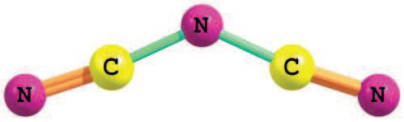

(a) Dicyanamide anion

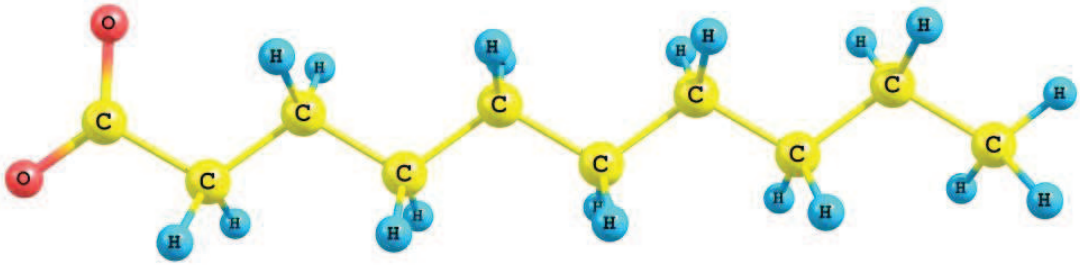

(b) Decanoate anion

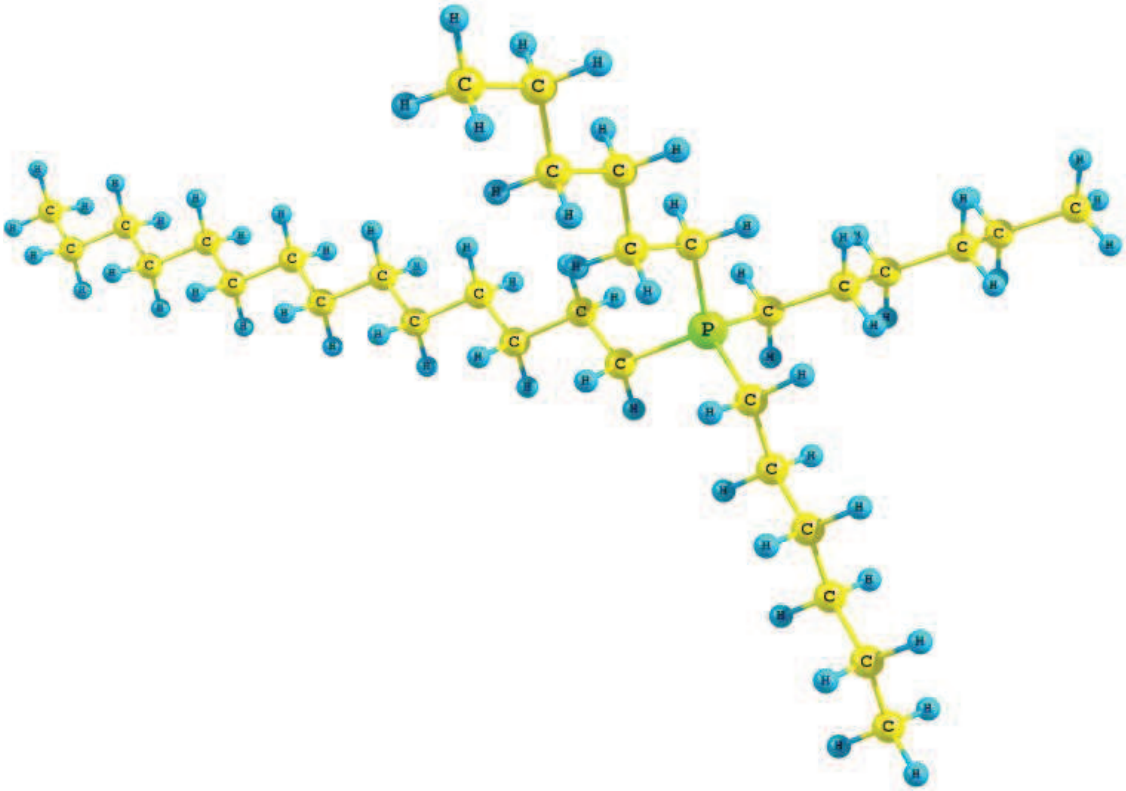

(c) Trihexyl tetradecyl phosphonium cation

FIGURE 2.2: Three-dimensional structures of phosphonium-based ionic liquids under MD study

where the individual terms correspond to the bonding interactions such as bonds, angles, dihedrals (the first three terms) and the non-bonded interactions like van der Waal and electrostatics (the fourth and fifth term). The effective values of σ and ε are calculated using geometric mean. All simulations were performed with a time step of 1 *fs*. Periodic Boundary Conditions (PBC) were employed in three dimensions. The temperature and pressure were controlled by a Langevin thermostat and Berendsen barostat respectively. An atom-based cutoff of 15 Å was employed to calculate nonbonded interactions. A switching function was used till 13.5 Å to bring both the coulombic and van der Waal interactions smoothly to zero at the cutoff distance. The subsequent pair list is updated once every 10 steps where a distance of 16.5 Å was necessary to be included in the *pair list*. The 1-4 electrostatic interactions were scaled by a factor of 0.5 [72]. The calculations of nonbonded and electrostatic interactions were performed once every 1 and 2 steps respectively. The NAMD configuration file, PDB file, PSF file and Force field parameter file for both ILs are shown in APPENDIX A.

2.4 Results and Discussion

2.4.1 Experimental Liquid Densities

Initially the experimental values of density for [EMIM][SCN] were compared with the experimental values from literature [73]. As shown in Figure 2.3, data points agree remarkably well with %Absolute Average Deviation (%AAD) equal to 0.055. The density values were found to depend on the nature of anion; i.e, the ethyl sulphate anion has less density (1.2367 *gm/cc*) compared to the less bulky methane sulphonate anion (1.2443

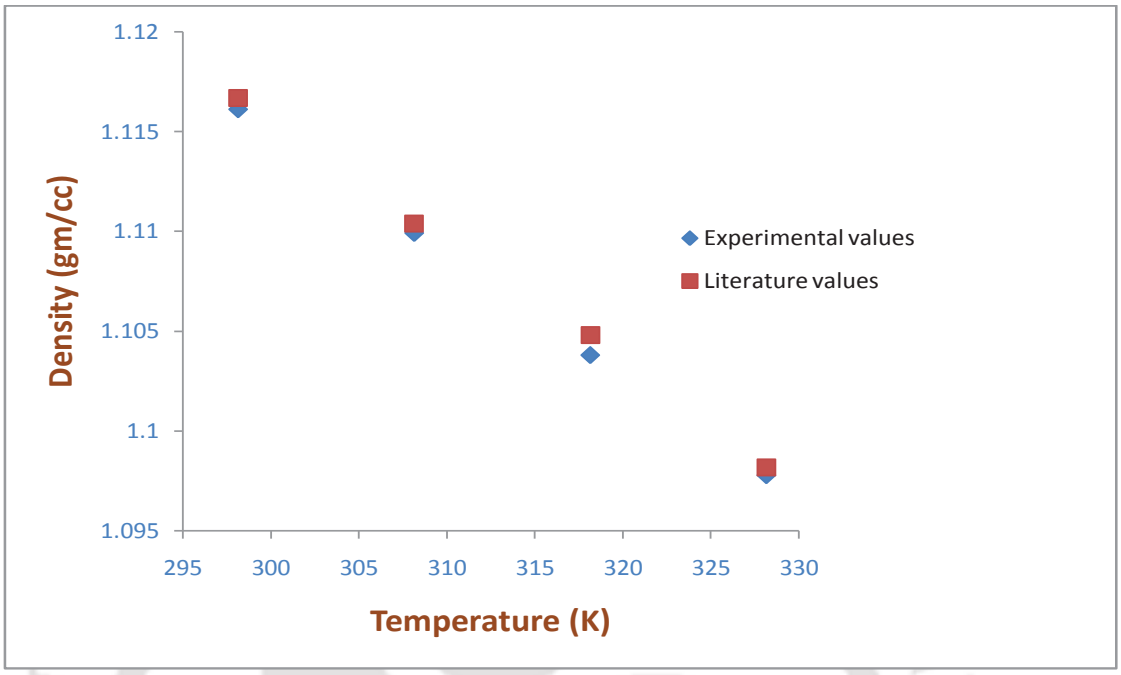

FIGURE 2.3: Comparison of experimental density of [EMIM][SCN] with literature values [73]

gm/cc) with 1-ethyl-3-methylimidazolium cation. The densities of seven ionic liquids were measured within 293.15-328.15 K with 5 K interval. To further benchmark our experimental studies, the experimental densities for seven ILs at $T = 298.15$ K and p=1 atm. are compared with reported data [42, 73–91] in Table 2.7. The results shows excellent agreement with literature values.

2.4.2 Correlative Liquid Density Prediction

Using the nine models listed in Table 2.3, the densities were predicted. NM model was described in section 2.3.1. This model requires a δ value for the density prediction. δ values for all the IL's were regressed from experimental data by minimizing the objective

TABLE 2.4: Comparison of Experimental densities with literature values at T=298.15 K and p= 1 atm. for seven ILs

Ionic liquid	Experimental Density ($g \cdot cm^{-3}$)	Literature densities($g \cdot cm^{-3}$)
[EMIM][$MeSO_3$]	1.2409	1.2424[74], 1.241[75], 1.2399[76], 1.2438[77], 1.2345[42]
[EMIM][Ac]	1.0983	1.0993[74], 1.0996[78], 1.102[79], 1.0978[80], 1.0977[81]
[EMIM][SCN]	1.1161	1.1166[73], 1.117[74], 1.1159[77], 1.118[87]
[TEMA][$MeSO_4$]	1.3443	1.3441[88]
[EMIM][$EtSO_4$]	1.2332	1.2375[82], 1.237[83], 1.2378[84], 1.2373[85], 1.2398[86]
[TDTHP][Phosph]	0.8908	0.8853[16], 0.8864[89, 90]
[TDTHP][DCA]	0.9003	0.899[16], 0.898[91]

function (Eq. 2.12) for both the cohesion factor expressions (Eqs. 2.8- 2.9)

$$f(\delta) = \sum_{i}^{n} \left[\frac{\rho_{i,exp} - \rho_{i,cal}}{\rho_{i,exp}} \right] \tag{2.12}$$

where n is no. of data points, $\rho_{i,exp}$ and $\rho_{i,cal}$ are experimental density and calculated saturated density respectively. Optimized values of δ for all seven ILs are shown in Table 2.5 for the derived NMPRNSM1 model and NMSRK Model. Further the accuracy of all models was checked by %Average Absolute Deviation (%AAD). The deviations were measured as:

$$\%AAD = \frac{100}{n} \sum_{i=1}^{n} \left| \frac{\rho_{exp} - \rho_{model}}{\rho_{exp}} \right|_i \tag{2.13}$$

TABLE 2.5: Optimized value of δ for ILs with NMPRNSM1 and NMSRK models

Ionic liquid	Optimized adjustable parameter* (δ)	
	NMPRNSM1	NMSRK
[EMIM][$MeSO_3$]	0.0962	0.0751
[EMIM][Ac]	0.0882	0.0561
[EMIM][SCN]	0.3531	0.3166
[TEMA][$MeSO_4$]	0.0451	0.0444
[EMIM][$EtSO_4$]	0.1919	0.1702
[TDTHP][Phosph]	0.0591	0.1261
[TDTHP][DCA]	0.0328	0.0399

* calculated by Eq. 2.12

where ρ_{exp} and ρ_{model} are the experimental and predicted density values respectively. Densities predicted by all the nine models for all ILs were compared with the experimental values of density (Table 2.6 and Figs. 2.4- 2.10). It can be observed that the density deviations predicted by correlative models are higher in magnitude as compared to the CEOS based cohesion models with $\%AAD$ of 0.1975% and 0.4499% for model 8 and 9 respectively. On closer inspection, Model 7 (5.008%) proved better as compared to other correlative models since authors [58] have considered wide variety of ILs during the development of this model.

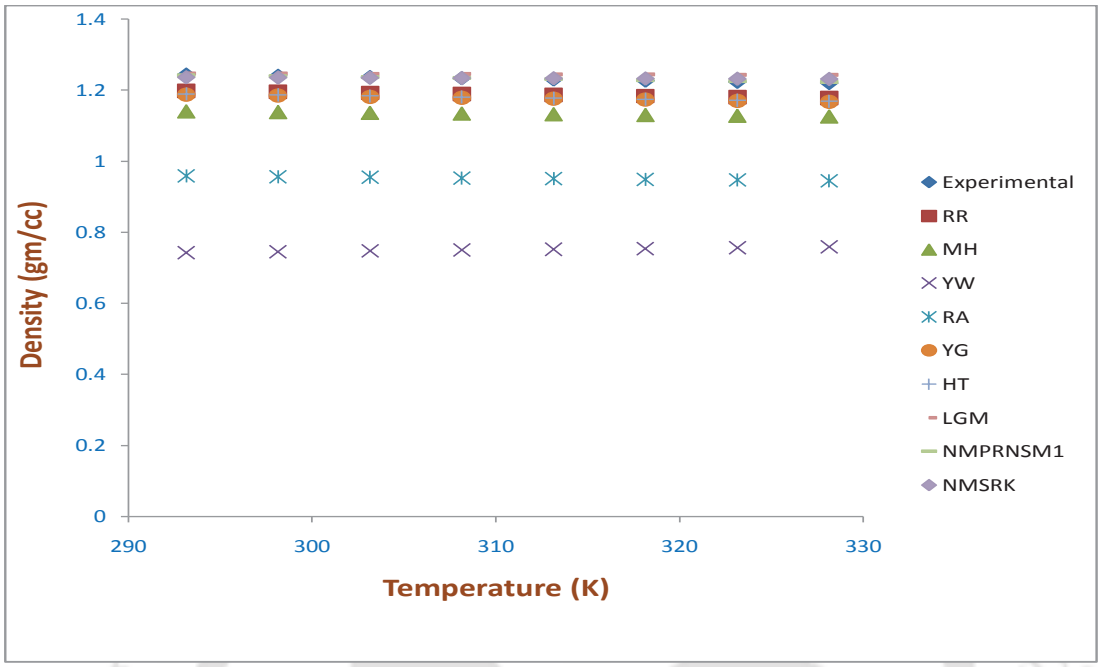

FIGURE 2.4: Densities at different temperatures for [EMIM][$MeSO_3$] at p=1 atm.

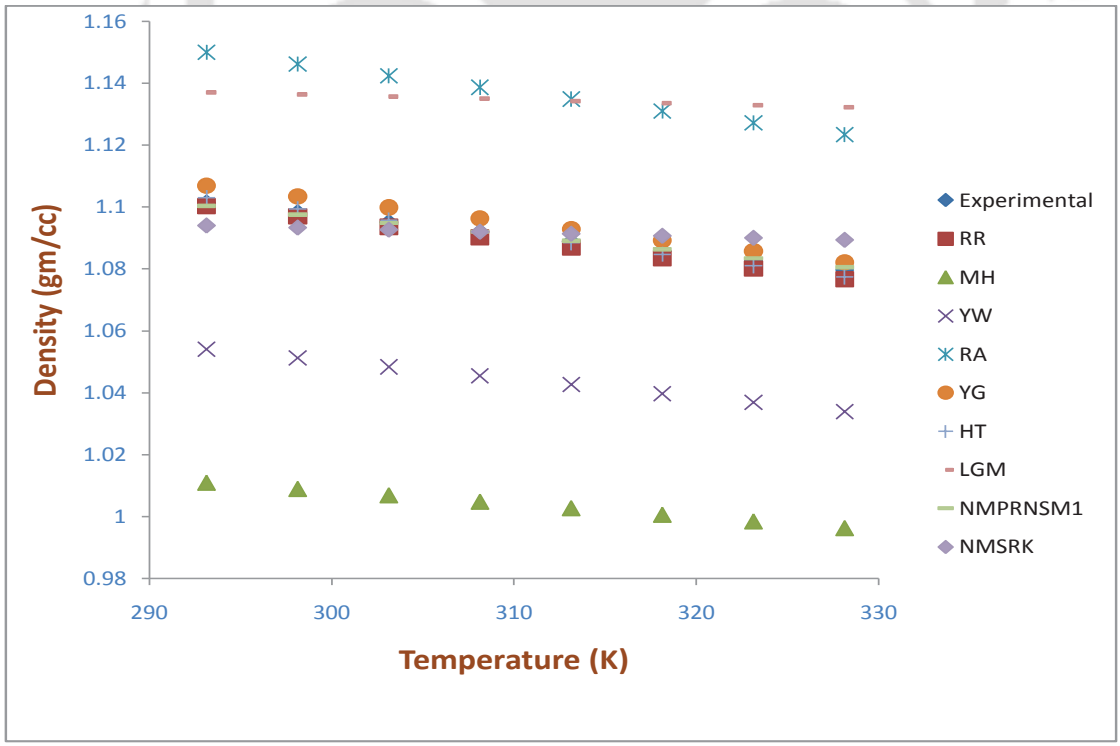

FIGURE 2.5: Densities at different temperatures for [EMIM][Ac] at p=1 atm.

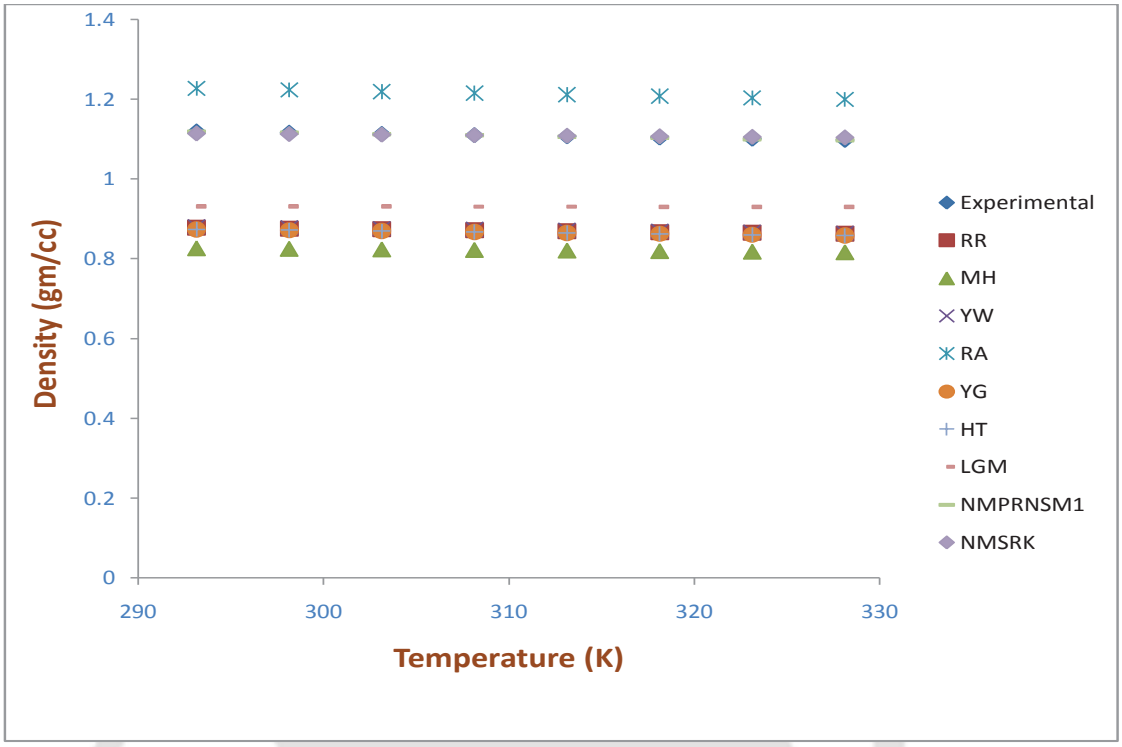

FIGURE 2.6: Densities at different temperatures for [EMIM][SCN] at p=1 atm.

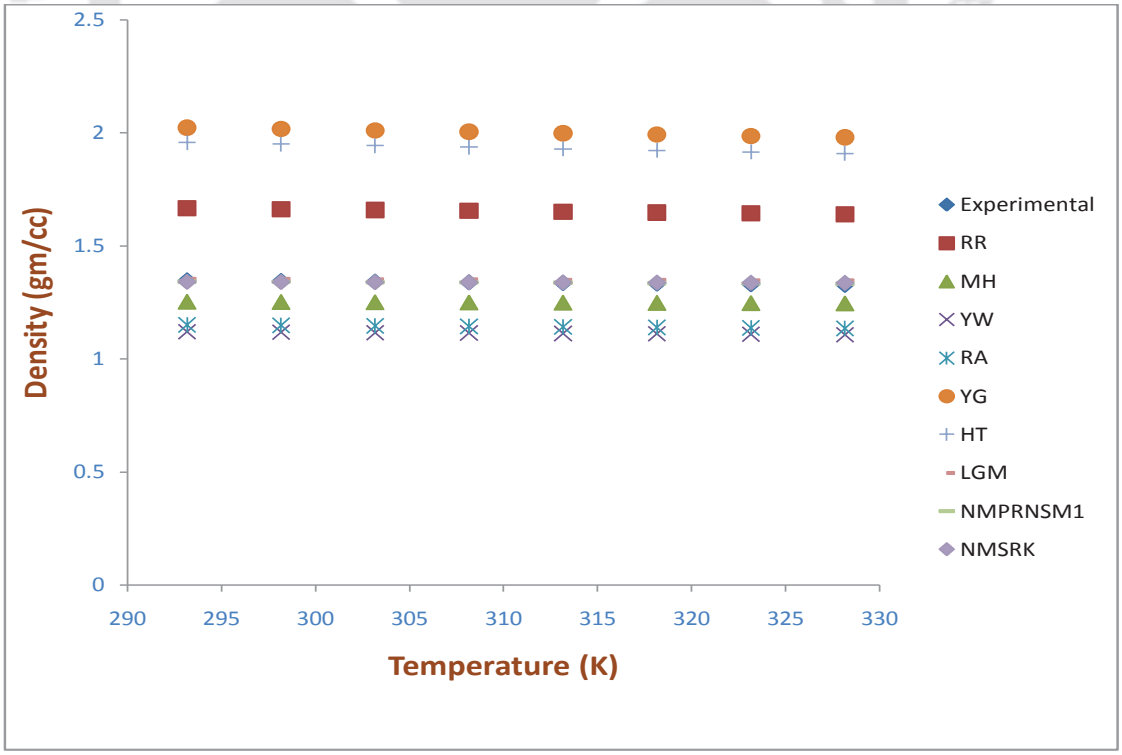

FIGURE 2.7: Densities at different temperatures for [TEMA][$MeSO_4$] at p=1 atm.

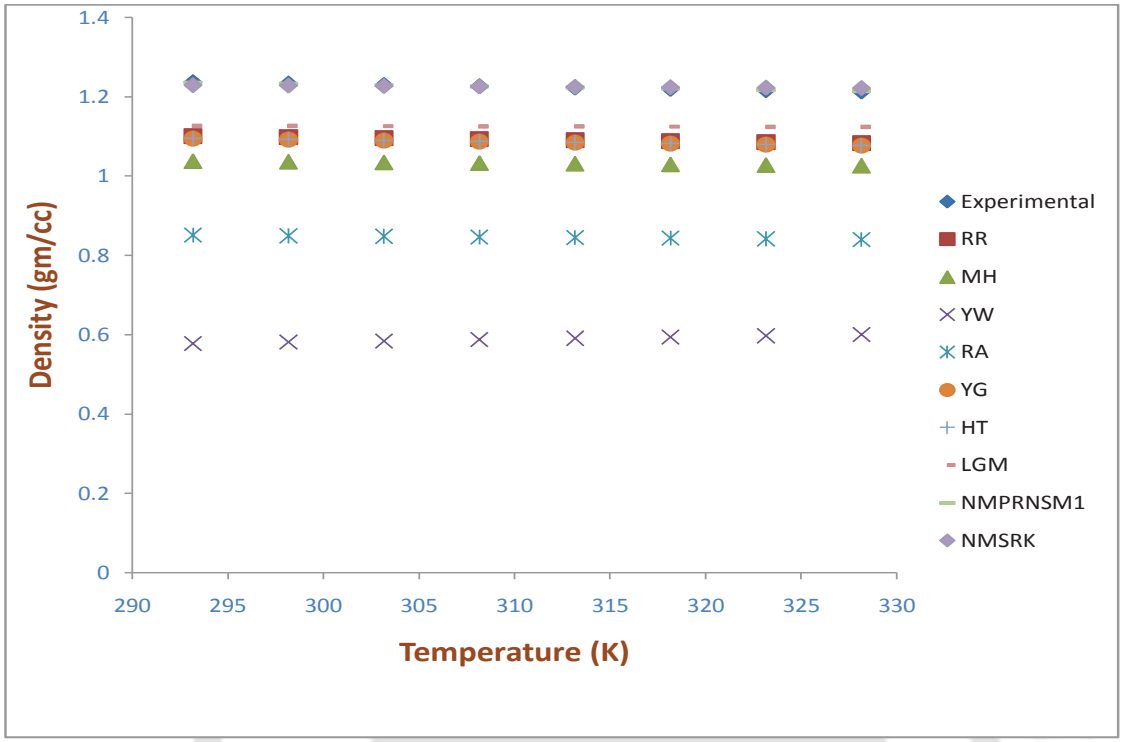

FIGURE 2.8: Densities at different temperatures for [EMIM][$EtSO_4$] at p=1 atm.

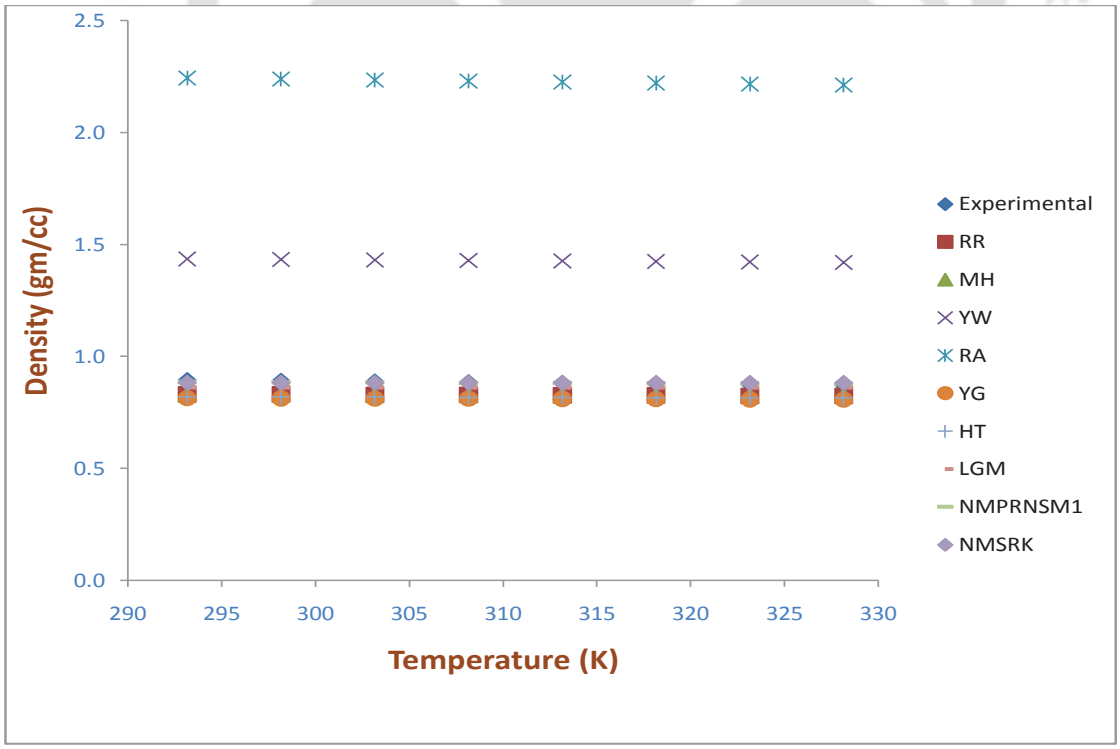

FIGURE 2.9: Densities at different temperatures for [TDTHP][Phosph] at p=1 atm.

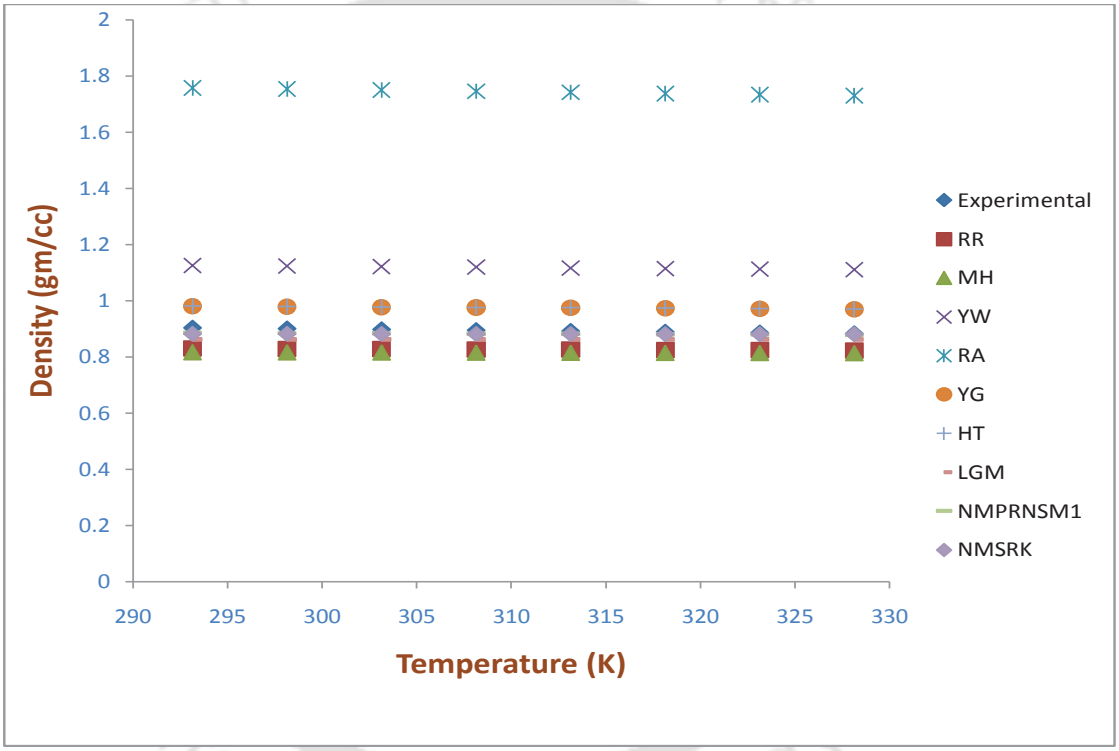

FIGURE 2.10: Densities at different temperatures for [TDTHP][DCA] at p=1 atm.

TABLE 2.6: Experimental and predicted densities for seven ILs*

[EMIM][$MeSO_3$]										
Temp (K)	Experimental	Model 1	Model 2	Model 3	Model 4	Model 5	Model 6	Model 7	Model 8	Model 9
293.15	1.2444	1.1982	1.1408	0.7426	0.9586	1.1880	1.1900	1.2478	1.2420	1.2359
298.15	1.2409	1.1953	1.1388	0.7450	0.9567	1.1852	1.1870	1.2472	1.2393	1.2352
303.15	1.2374	1.1924	1.1368	0.7474	0.9548	1.1824	1.1841	1.2466	1.2366	1.2346
308.15	1.2339	1.1895	1.1348	0.7497	0.9529	1.1795	1.1811	1.2460	1.2339	1.2339
313.15	1.2305	1.1865	1.1328	0.7520	0.9510	1.1767	1.1781	1.2454	1.2312	1.2332
318.15	1.2270	1.1836	1.1308	0.7542	0.9491	1.1738	1.1751	1.2448	1.2284	1.2325
323.15	1.2237	1.1807	1.1287	0.7565	0.9472	1.1710	1.1721	1.2442	1.2256	1.2319
328.15	1.2203	1.1777	1.1266	0.7586	0.9453	1.1681	1.1691	1.2435	1.2229	1.2312
%AAD**		3.5907	7.9892	39.0691	22.7438	4.3950	4.2736	1.0931	0.1147	0.4491
[EMIM][Ac]										
293.15	1.1015	1.1002	1.0110	1.0541	1.1500	1.1069	1.1031	1.1370	1.1004	1.0940

298.15	1.0983	1.0969	1.0089	1.0512	1.1462	1.1034	1.0995	1.1363	1.0976	1.0934
303.15	1.0951	1.0936	1.0069	1.0484	1.1424	1.0999	1.0958	1.1356	1.0948	1.0927
308.15	1.0920	1.0902	1.0048	1.0455	1.1387	1.0963	1.0921	1.1349	1.0920	1.0920
313.15	1.0889	1.0869	1.0027	1.0426	1.1349	1.0928	1.0885	1.1342	1.0892	1.0913
318.15	1.0858	1.0835	1.0006	1.0397	1.1311	1.0892	1.0848	1.1336	1.0863	1.0907
323.15	1.0828	1.0801	0.9984	1.0368	1.1273	1.0857	1.0811	1.1329	1.0834	1.0900
328.15	1.0797	1.0767	0.9963	1.0339	1.1234	1.0821	1.0774	1.1322	1.0805	1.0893
%AAD**		0.1835	7.9592	4.2643	4.2371	0.3675	0.1066	4.0441	0.0479	0.4472
[EMIM][SCN]										
293.15	1.1192	0.8785	0.8270	0.8804	1.2277	0.8739	0.8745	0.9316	1.1194	1.1142
298.15	1.1161	0.8763	0.8256	0.8781	1.2238	0.8717	0.8723	0.9314	1.1163	1.1128
303.15	1.1130	0.8742	0.8242	0.8759	1.2200	0.8696	0.8700	0.9311	1.1131	1.1113
308.15	1.1099	0.8720	0.8228	0.8736	1.2161	0.8674	0.8677	0.9309	1.1099	1.1099
313.15	1.1069	0.8698	0.8213	0.8714	1.2123	0.8652	0.8655	0.9306	1.1067	1.1085

318.15	1.1038	0.8676	0.8199	0.8691	1.2084	0.8631	0.8632	0.9304	1.1035	1.1071
323.15	1.1008	0.8655	0.8184	0.8669	1.2045	0.8609	0.8609	0.9301	1.1003	1.1057
328.15	1.0978	0.8633	0.8169	0.8646	1.2007	0.8587	0.8587	0.9299	1.0971	1.1043
%AAD**		21.4303	25.8398	21.2843	9.5412	21.8429	21.8175	16.0267	0.0226	0.2976
[TEMA][$MeSO_4$]										
293.15	1.3472	1.6669	1.2535	1.1208	1.1517	2.0240	1.9575	1.3530	1.3429	1.3406
298.15	1.3443	1.6632	1.2525	1.1190	1.1493	2.0179	1.9506	1.3520	1.3414	1.3399
303.15	1.3414	1.6596	1.2515	1.1172	1.1470	2.0117	1.9437	1.3510	1.3400	1.3392
308.15	1.3385	1.6559	1.2504	1.1154	1.1446	2.0055	1.9369	1.3501	1.3385	1.3385
313.15	1.3357	1.6522	1.2494	1.1136	1.1423	1.9993	1.9300	1.3491	1.3370	1.3378
318.15	1.3329	1.6485	1.2483	1.1117	1.1399	1.9932	1.9232	1.3481	1.3355	1.3372
323.15	1.3302	1.6448	1.2472	1.1099	1.1375	1.9870	1.9163	1.3472	1.3340	1.3365
328.15	1.3274	1.6410	1.2461	1.1080	1.1351	1.9807	1.9095	1.3462	1.3325	1.3358
%AAD**		23.6929	6.5301	16.6569	14.4903	49.7468	44.5884	0.9281	0.2011	0.3223

[EMIM][$EtSO_4$]										
293.15	1.2367	1.1008	1.0376	0.5775	0.8510	1.0938	1.0953	1.1269	1.2348	1.2295
298.15	1.2332	1.0983	1.0360	0.5808	0.8494	1.0913	1.0927	1.1264	1.2320	1.2284
303.15	1.2298	1.0957	1.0343	0.5840	0.8479	1.0888	1.0901	1.1260	1.2292	1.2274
308.15	1.2263	1.0932	1.0327	0.5872	0.8463	1.0863	1.0874	1.1256	1.2263	1.2263
313.15	1.2229	1.0906	1.0310	0.5904	0.8448	1.0838	1.0848	1.1252	1.2235	1.2253
318.15	1.2195	1.0881	1.0293	0.5936	0.8432	1.0813	1.0821	1.1247	1.2206	1.2243
323.15	1.2162	1.0855	1.0276	0.5967	0.8416	1.0787	1.0795	1.1243	1.2178	1.2233
328.15	1.2128	1.0829	1.0259	0.5998	0.8400	1.0762	1.0768	1.1239	1.2149	1.2222
%AAD**		10.8427	15.7477	51.9215	30.9584	11.4026	11.3173	8.1051	0.0939	0.3899
[TDTHP][Phosph]										
293.15	0.8940	0.8308	0.8551	1.4353	2.2435	0.8138	0.8211	0.8626	0.8861	0.8823
298.15	0.8908	0.8298	0.8541	1.4330	2.2392	0.8129	0.8202	0.8626	0.8850	0.8821
303.15	0.8877	0.8288	0.8531	1.4307	2.2348	0.8121	0.8193	0.8626	0.8838	0.8819

308.15	0.8846	0.8278	0.8520	1.4284	2.2305	0.8113	0.8184	0.8626	0.8827	0.8817
313.15	0.8815	0.8268	0.8510	1.4262	2.2261	0.8104	0.8175	0.8626	0.8815	0.8815
318.15	0.8784	0.8258	0.8500	1.4239	2.2218	0.8096	0.8166	0.8627	0.8804	0.8813
323.15	0.8753	0.8248	0.8490	1.4216	2.2174	0.8088	0.8157	0.8627	0.8792	0.8812
328.15	0.8723	0.8238	0.8479	1.4193	2.2130	0.8079	0.8148	0.8627	0.8781	0.8810
%AAD**		6.3130	3.5687	61.6327	152.3368	8.1751	7.3755	2.3102	0.4397	0.6586
[TDTHP][DCA]										
293.15	0.9033	0.8308	0.8164	1.1256	1.7573	0.9808	0.9819	0.8626	0.8861	0.8823
298.15	0.9003	0.8298	0.8159	1.1234	1.7534	0.9793	0.9803	0.8626	0.8850	0.8821
303.15	0.8974	0.8288	0.8155	1.1212	1.7495	0.9778	0.9786	0.8626	0.8838	0.8819
308.15	0.8945	0.8278	0.8150	1.1191	1.7456	0.9762	0.9770	0.8626	0.8827	0.8817
313.15	0.8916	0.8268	0.8146	1.1169	1.7416	0.9747	0.9753	0.8626	0.8815	0.8815
318.15	0.8887	0.8258	0.8141	1.1148	1.7377	0.9732	0.9737	0.8627	0.8804	0.8813
323.15	0.8858	0.8248	0.8137	1.1126	1.7338	0.9716	0.9720	0.8627	0.8792	0.8812

328.15	0.8829	0.8238	0.8132	1.1105	1.7298	0.9701	0.9704	0.8627	0.8781	0.8810
%AAD**		8.1674	3.3794	25.1948	95.2447	9.2339	9.3091	2.5489	0.4629	0.5848
Global %AAD		10.6029	10.1449	31.4319	47.0789	15.0234	14.1126	5.0080	0.1975	0.4499

* Model number indicates Sr. No. of Table 2.3

** $\%AAD = \frac{100}{n}\sum_{i=1}^{n}\left|\frac{\rho_{exp}-\rho_{model}}{\rho_{exp}}\right|_i$

Among all these models, Model 8 (NMPRNSM1) and Model 9 (NMSRK) fare reasonably well as compared to other models with minimum %AAD values of 0.1147 and 0.4491 for [EMIM][$MeSO_3$] respectively. It should be noted that Models 8 and 9 are based on alpha function of PSRK equation. Both models are specific to compounds, so experimental values of density are required for regression of adjustable compound specific parameter δ (Table 2.5). Model 8 gave smooth variation of density with temperature as compared to model 9 (Figs. 2.4- 2.10). Thus selection of alpha function (Eqs. 2.8- 2.9) plays an important role in the equation of state calculation. However it is evident that irrespective of nature of IL, the improvement in prediction for modified cohesive factor (Eq. 2.8 and NMPRNSM1) is around 2.5 times better than the original cohesive factor expression (Eq. 2.9 and NMSRK). The %AAD for all models with different ILs is tabulated in Table 2.6. It shows good agreement of experimental densities with predicted densities for all seven ILs.

2.4.3 MD simulation results

A brief minimization of 10000 steps was performed to make the system ready for dynamic simulations. Upon successful minimization, the system was equilibrated for 1 *ns* in a NPT ensemble at 300 K and 1 atm. The volume of the system was monitored during this stage and at the end of 1 *ns* dynamics, the volume was found to be fully equilibrated (Fig. 2.11). The Radial Distribution Function (RDF), *g(r)* plots of phosphonium cation (central atom P) in dicyanamide (central atom N) and decanoate (central atom C, O=C<) anion systems are shown in Fig. 2.12. From the value of *g(r)*, the first solvation shell was observed at 5 Å, and second solvation shell at 10 Å for dicyanamide anion

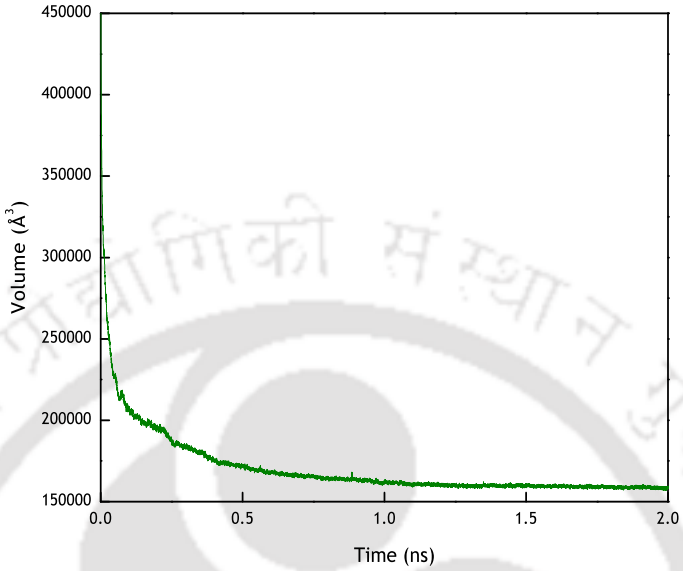

(A)

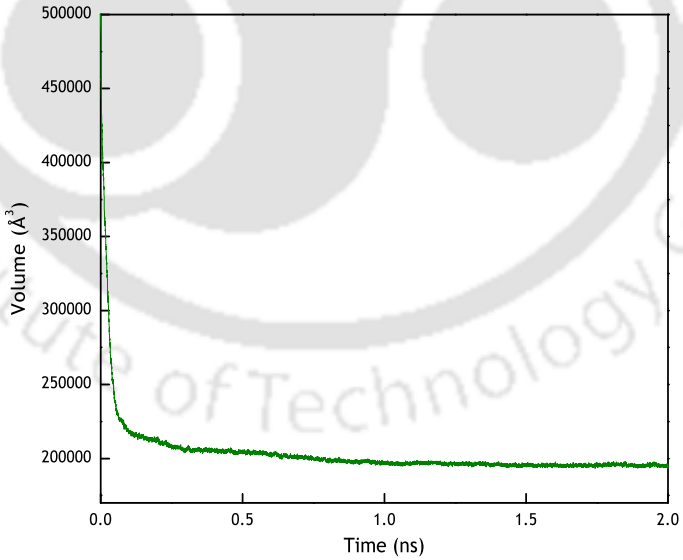

(B)

FIGURE 2.11: Volume as a function of simulation time during Equilibriation for (A) [TDTHP][DCA] and (B) [TDTHP][DEC]

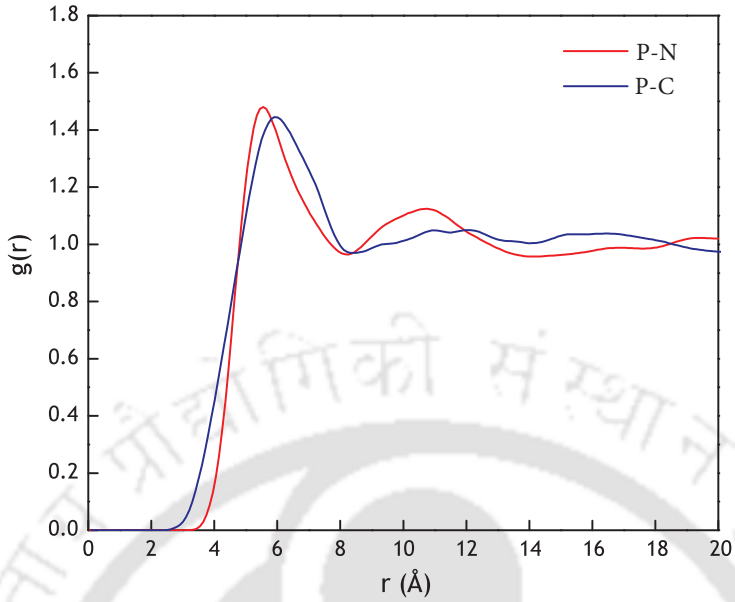

FIGURE 2.12: Radial distribution function for both ILs (P: central phosphorous atom in [TDTHP] cation; N: central nitrogen atom in [DCA] anion; C: carbon atom, O=C< in [DEC] anion)

system, while the first solvation shell for decanoate system was observed at 6 Å. The two systems being pure phosphonium ILs had comparable density values of 857.47 and 830.96 kg/m^3 [92] respectively, the RDF peak positions and heights are relatively close in their magnitude. The physical similarity of the two pure IL systems ([TDTHP][DCA] and [TDTHP][DEC]) continues in terms of Coordination Number (CN) of anions for the first solvation shell around the phosphonium cation, as the CN of anions are 2.20 and 2.00 respectively. The system temperature was found oscillating (±1%) around the

TABLE 2.7: Measured and predicted densities of Phosphonium Ionic Liquids under study

Ionic liquid	Measured Density [92](kg/m^3)	Predicted Density (kg/m^3)	Deviation(%)
[TDTHP][DCA]	898.00	857.47	4.51
[TDTHP][DEC]	883.00	830.96	5.89

target value of 298.15 K. At time=2 *ns*, both the systems became stable and the box volume were then measured to estimate the density. The measured density at T=298.15 K are compared with the reported values in literature [92] in Table 2.7. For both ILs, the density deviation were around 5% from the literature value [92].

3

Ionic Liquids as an Extraction Media in Ternary Systems

3.1 Introduction

Environment regulations motivate scientists and researchers to develop clean technologies for sustainable development. Researchers amplify their efforts to convert separation processes like extraction and distillation into clean technologies. The knowledge of thermodynamic properties like equilibrium data and activity coefficient at infinite dilution are required for adequate separation. Liquid Liquid Equilibrium (LLE) data helps in the selection of solvent for the selective separation of solute component. In addition to this economic aspect, clean technology also considers ecological aspect. Since last few decades, eco-friendly solvents like ILs had been considered as better replacement for conventional volatile solvents [20, 93]. Various hydrophobic ILs [5, 22] have shown better selectivity for butanol separation from aqueous solution and are more economical when compared to hydrophilic ILs [25] for extraction of water. As discussed earlier, the ILs considered in literature [5, 21–24, 49, 50] for butanol extraction are heavier than water. Considering fluid handling cost and economic aspect, we have chosen such ILs namely [TDTHP][Phosph], [TDTHP][DCA] and [TDTHP][DEC] as solvents since they are lighter than water. The physiochemical properties of these ILs are already discussed in Chapter 2 extensively.

For a mixture containing more than two components, the composition analysis by calibration methods like density and refractive index are difficult. The composition analysis can be carried out by Nuclear Magnetic Resonance (NMR) spectroscopy [42, 94–96]. ^{1}H NMR spectroscopy is a characterization technique that is based on magnetic properties of the proton (^{1}H). ^{1}H nuclei in magnetic field absorb and re-emit electromagnetic radiation. The magnetic properties of hydrogen atom effect the amount

of radiated energy. Hydrogen in aromatic functional group gives a chemical shift peak at more than 7 ppm while aliphatic hydrogen gives a peak less than 7 ppm. In the case of butanol separation by phosphonium ILs, there is an absence of aromatic hydrogen in all systems. If the system contains aromatic and aliphatic components, ^{1}H NMR characterization is thus easier. So we have performed a benchmarking system namely, aliphatic-aromatic separation by ammonium and phosphonium ILs. The ILs namely Tris (2-hydroxyethyl) methylammonium methylsulfate [TEMA][$MeSO_4$] and Tributyl methyl phosphonium methyl sulphate [P_{4441}][$MeSO_4$] (Fig. 3.1) were chosen for the purpose. We have measured three different ternary systems, namely, (*a*) [TEMA][$MeSO_4$] (1)-Benzene (2)-Hexane (3); (*b*) [TEMA][$MeSO_4$] (1)-Toluene (2)-Heptane (3) and (*c*) [P_{4441}][$MeSO_4$] (1)-Thiophene (2)-Cyclohexene (3) at T=298.15 K and p=1 atm. In addition to aromatic-aliphatic separation, we have considered the separation of lower alcohol such as 1-propanol from aqueous solution using [TDTHP][Phosph] as solvent. After gaining sufficient confidence in NMR spectroscopy characterization, we have concentrated on the extraction of butanol by three different ILs, namely [TDTHP][Phosph], [TDTHP][DCA] and [TDHP][DEC] (Figs. 2.1- 2.2). The LLE process was again carried out at T=298.15 K and p=1 atm.

3.2 Chemicals and Materials

Benzene (S R L chemicals, India), hexane (Sigma Aldrich, Germany), toluene (Sigma Aldrich, Germany), heptane (Rankem, India), thiophene (Sigma Aldrich, Germany), cyclohexene (Sigma Aldrich, Germany), 1-propanol (Sigma Aldrich, Germany) and 1-butanol (Sigma Aldrich, Germany) were supplied at 99% purity. In order to test

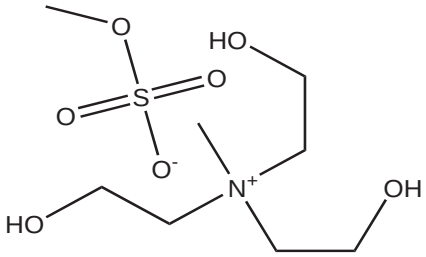

Tris (2-hydroxyethyl) methylammonium methyl sulfate

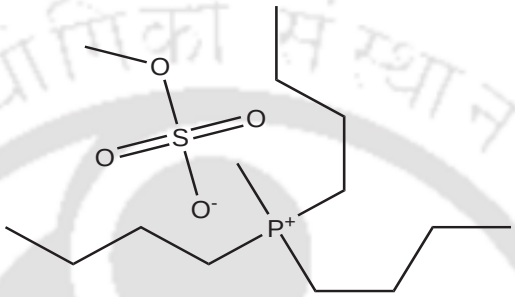

Tributyl methyl phosphonium methyl sulfate

FIGURE 3.1: Structure of ILs used in benchmarking aromatic-aliphatic separation

the purity of benzene, hexane, toluene, heptane, thiophene, cyclohexene, 1-propanol and 1-butanol, the densities of the pure components were measured at atmospheric pressure with Anton Par DMA-4500 digital vibrating U-tube densitometer. The obtained densities were within ±1% of the reported values. The ILs namely $[P_{4441}][MeSO_4]$, $[TEMA][MeSO_4]$, [TDTHP][Phosph], [TDTHP][DCA] and [TDTHP][DEC] (> 95% purity) were supplied by Sigma Aldrich, Germany. For the removal of impurities, the ILs were introduced in an oil bath for 24 h at 353 K. This is further attached to a high vacuum line, so that the impurities in small amounts were removed. Thereafter ^1H NMR was performed so as to validate the purity of the ILs. Dimethyl sulfone oxide-D_6 (DMSO-D_6) and chloroform-D ($CDCl_3$) were used as NMR solvent and were supplied by Merck, Germany. All chemicals with their purity, purification method and analysis method are reported in Table 3.1.

TABLE 3.1: Chemicals Purity and Purification Methods

Chemical Name	Source	Purification Method	Purity (Mole fraction)	Analysis Method
Benzene	S R L Chemicals, India	-	0.99	Density method
Hexane	Sigma Aldrich, Germany	-	0.99	Density method
Toluene	Sigma Aldrich, Germany	-	0.99	Density method
Heptane	Rankem, India	-	0.99	Density method
Thiophene	Sigma Aldrich, Germany	-	0.99	Density method
Cyclohexene	Sigma Aldrich, Germany	-	0.99	Density method
1-propanol	Sigma Aldrich, Germany	-	0.99	Density method
1-butanol	Sigma Aldrich, Germany	-	0.99	Density method
[TEMA][$MeSO_4$]	Sigma Aldrich, Germany	Vacuum drying	0.99	^{1}H NMR
[P_{4441}][$MeSO_4$]	Sigma Aldrich, Germany	Vacuum Drying	0.99	^{1}H NMR
[TDTHP][Phosph]	Sigma Aldrich, Germany	Vacuum drying	0.99	^{1}H NMR
[TDTHP][DCA]	Sigma Aldrich, Germany	Vacuum drying	0.99	^{1}H NMR
[TDTHP][DEC]	Sigma Aldrich, Germany	Vacuum Drying	0.99	^{1}H NMR
$CDCl_3$	Merck, Germany	-	0.998	^{1}H NMR
DMSO-D_6	Merck, Germany	-	0.998	^{1}H NMR

3.3 Aromatic-Aliphatic Separation by ILs

3.3.1 Experimental Procedure and Analysis

The samples were prepared using the tie line information provided by Matuszek et al. [31], where a similar system was studied. In this process, the average mole fraction of the component(s) in both the phases was considered as the feed composition. This implies that knowing the average mole fraction of the reported data, the feed concentration of the current experiment can be taken as an initial input. This helped us in preparing different mixture points with solute composition ranging from 0.05 mole fraction to 0.9 mole fraction. It also covers the entire area in the ternary diagram. There after individual volumes were found from mole fraction, molecular weight and density values. The total volume was kept at 5 ml and was then inserted into 15 ml cuvette after covering with parafilm so as to prevent loss of compounds to atmosphere. The cuvettes were kept on shaking for 6 h at 100 rpm with temperature set to 298.15 K. Equilibrium time of 12 h was provided after which two layers were separated with the help of 2 ml syringes. Mixture points exhibiting two phases after equilibrium have been analyzed to obtain the extract and raffinate compositions. Feed compositions which are homogenous after equilibrium have been rejected as its location is outside the binodal curve. The layers were then transferred to 5 ml cuvettes.

^{1}H NMR spectra is a convenient tool for measuring the tie lines compositions at equilibrium [95–100]. Initially the phases were separated by 2 ml syringes for all the data points. A fixed amount of sample (0.1 ml) was then removed from both the phases using a micropipette. Here a fixed volume of the $CDCl_3$ (0.3 ml) was then taken and mixed

with the sample (0.1 ml) in NMR tubes (thrift Grade). The NMR tube corresponding to each tie line and phase were then inserted in a NMR spectrometer of 11.74 Tesla (400 *MHz* response of ^{1}H). In case of ammonium based IL, from the ^{1}H NMR shifts, the peak areas of the hydrogen atom of each component (i.e IL, aromatic and aliphatic) can be divided into three zones (Figs. 3.2- 3.3).

In the first zone, the aliphatic compound had peaks in the range of 0.5 ppm to 1.5 ppm. For second zone, the IL; [TEMA][$MeSO_4$] having -CH_3 peak of the anion along with the N-CH_2 group and the O-CH_2 hydrogen atoms of the cation lies between 3-5 ppm. Thus the second zone consisted of 17 hydrogen atoms. The third zone was between 7 ppm to 8.5 ppm and is mainly due to the aromatic hydrogen atoms of benzene or toluene. The raffinate phase is free from any ionic liquid because of the absence of peaks between 3-6 ppm (Fig. 3.2). This agrees well with our previous work [41] on aromatic extraction. Separate equations are formed by adding the respective areas of hydrogen in each zone which are then solved simultaneously. In case of [P_{4441}][$MeSO_4$] containing system, cyclohexene was easily identified because of its double bond, which was detected at the 5.6 ppm. Aromatics are usually detected between 6.5 ppm to 8.5 ppm. Thiophene is an aromatic sulphur component which was detected at 7 *ppm* (Figs. 3.4- 3.5). For [P_{4441}][$MeSO_4$], the anion methyl sulfate peak was detected at 3.85 ppm, so all three types of protons have been taken for quantitative analysis.

Thereafter composition calculation for all compounds via NMR spectrum was done using this formula:

$$x_i = \frac{H_i}{\sum_{i=1}^{3} H_i} \tag{3.1}$$

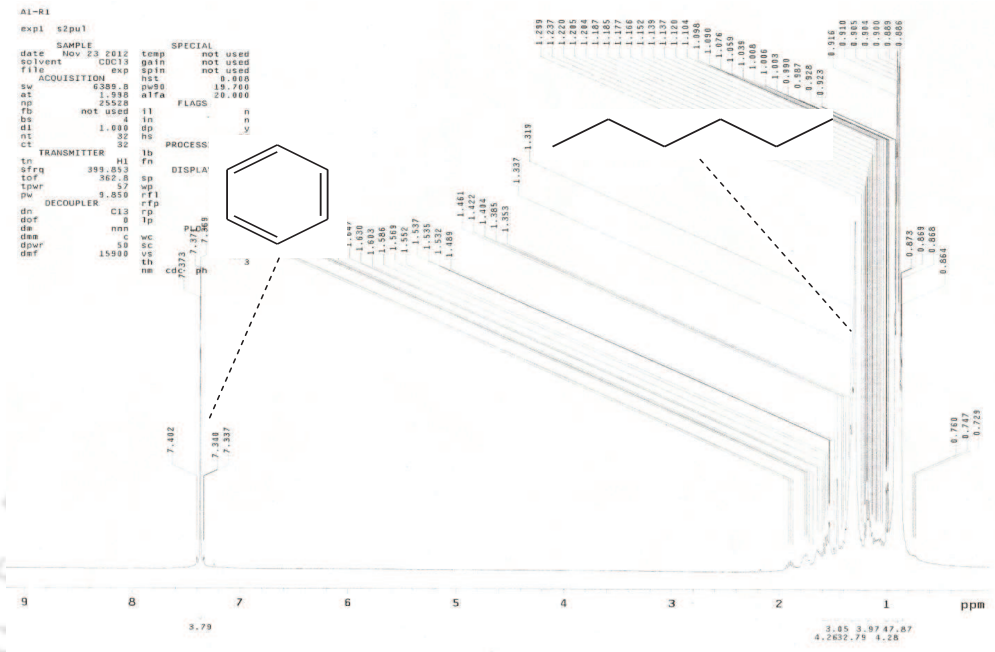

FIGURE 3.2: Raffinate phase ^{1}H NMR spectra for the system: [TEMA][$MeSO_4$] (1) - Benzene (2) - Hexane (3) at T=298.15 K and p=1 atm.

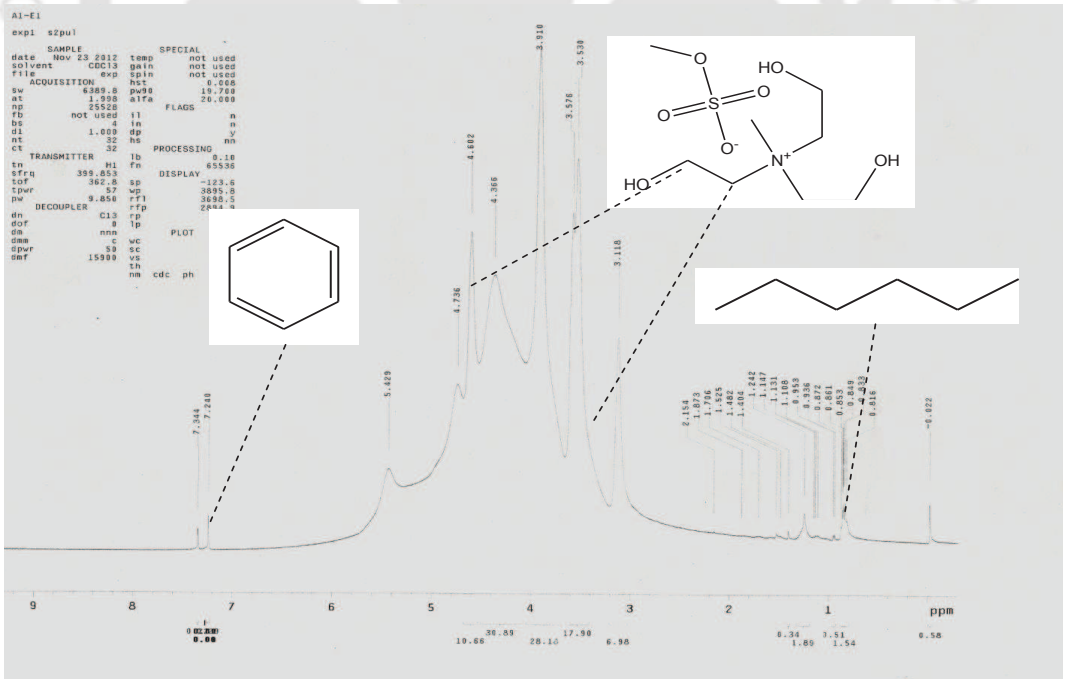

FIGURE 3.3: Extract phase ^{1}H NMR spectra for the system: [TEMA][$MeSO_4$] (1) - Benzene (2) - Hexane (3) at T=298.15 K and p=1 atm.

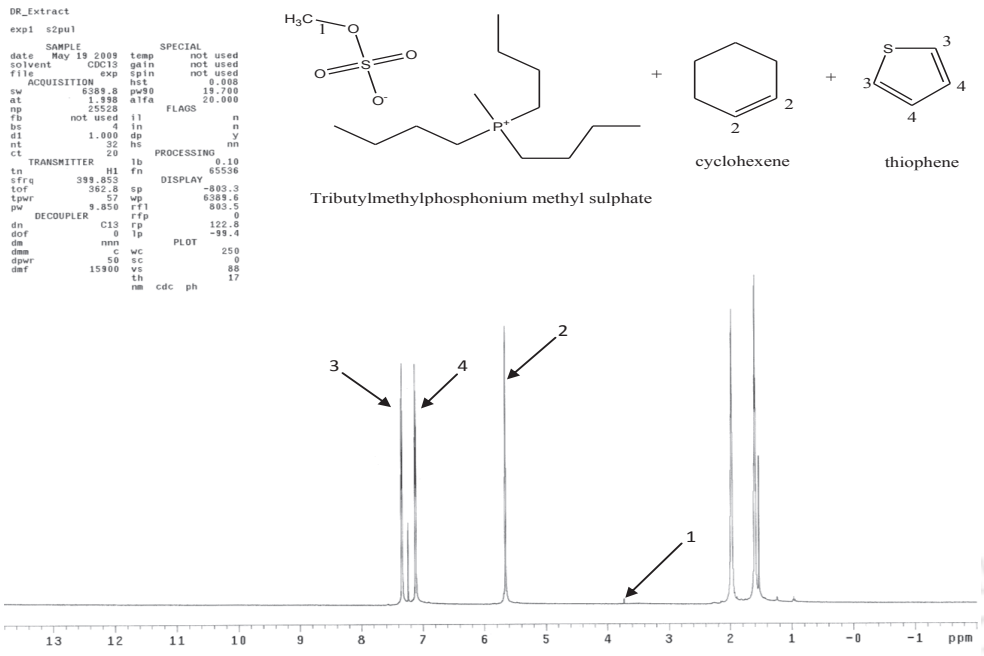

FIGURE 3.4: Raffinate phase ^{1}H NMR spectra for the system: $[P_{4441}][MeSO_4]$ (1) - Thiophene (2) - Cyclohexene (3) at T=298.15 K and p=1 atm.

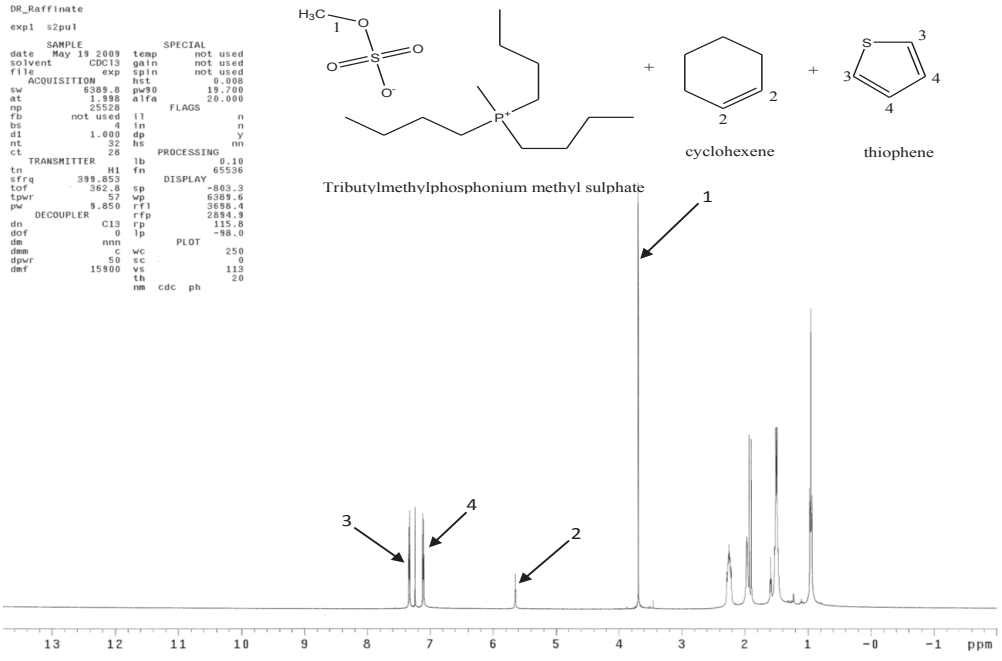

FIGURE 3.5: Extract phase ^{1}H NMR spectra for the system: $[P_{4441}][MeSO_4]$ (1) - Thiophene (2) - Cyclohexene (3) at T=298.15 K and p=1 atm.

Here x_i the mole fraction of samples and H_i is the single hydrogen peak area for component. For checking the accuracy we prepared known mixtures of both IL-solute and water-solute in the homogenous region and then obtained the ^{1}H NMR by $CDCl_3$. The results obtained by the peak integration were found to be in fairly good agreement with the known composition. The results gave a standard deviations of $<$0.007 for each compound. The maximum absolute deviation was found to be 0.010 in mole fraction in $CDCl_3$. In this work uncertainty in mole fraction composition obtained was $\pm$0.001 for both the phases.

3.3.2 Results and Discussions

LLE experimental data for the systems: [TEMA][$MeSO_4$] (1)- benzene (2)- hexane (3), [TEMA][$MeSO_4$] (1)-toluene (2)- heptane(3); and [P_{4441}][$MeSO_4$] (1) - thiophene(2) - cyclohexene(3) were performed at T= 298.15 K and p=1 atm.. The experimental tie lines for all systems are reported in Tables 3.2- 3.4.

The experimental tie lines are plotted in Figs. 3.6-3.8. It can be seen that the hexane composition in extract phase (Table 3.2) is negligible as compared to the corresponding heptane composition (Table 3.3). The hexane composition being almost equal to zero combined with absence of IL in raffinate phase points out to very low cross contamination in the single stage extraction process. This agrees well with the reported work of Matuszek et al. [31] on the separation of thiophene and heptane using [TEMA][$MeSO_4$] IL. The tie line slope of IL (1)-Benzene (2)-Hexane (3) (Fig. 3.6) resembles the reported ternary systems of hexane-benzene- 1-butyl-3-methylimidazolium methylsulfate ([BMIM][$MeSO_4$]) [101]

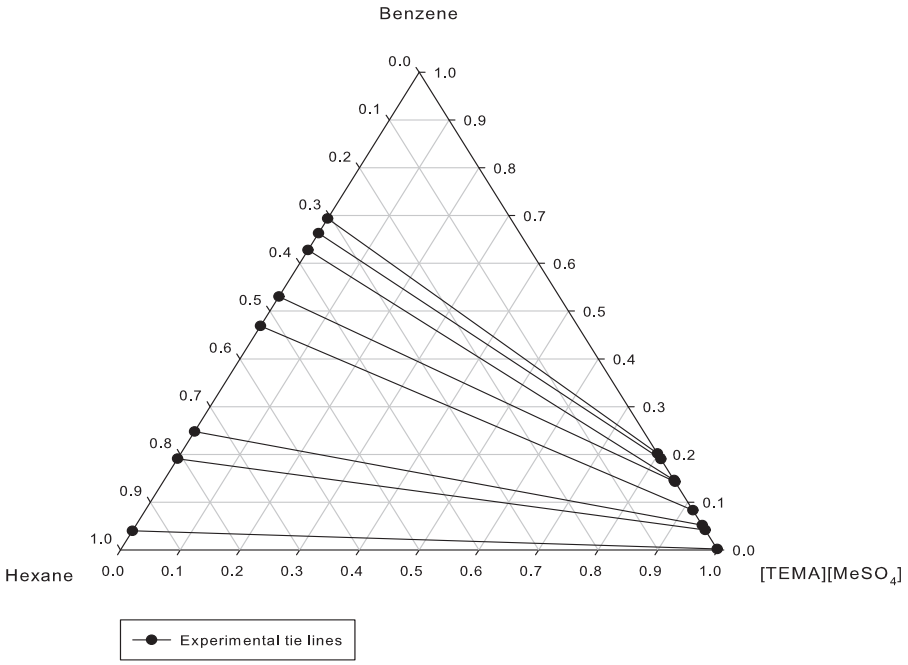

FIGURE 3.6: Experimental tie lines for the system:[TEMA][$MeSO_4$] (1) - Benzene (2) - Hexane (3) at T=298.15 K and p=1 atm.

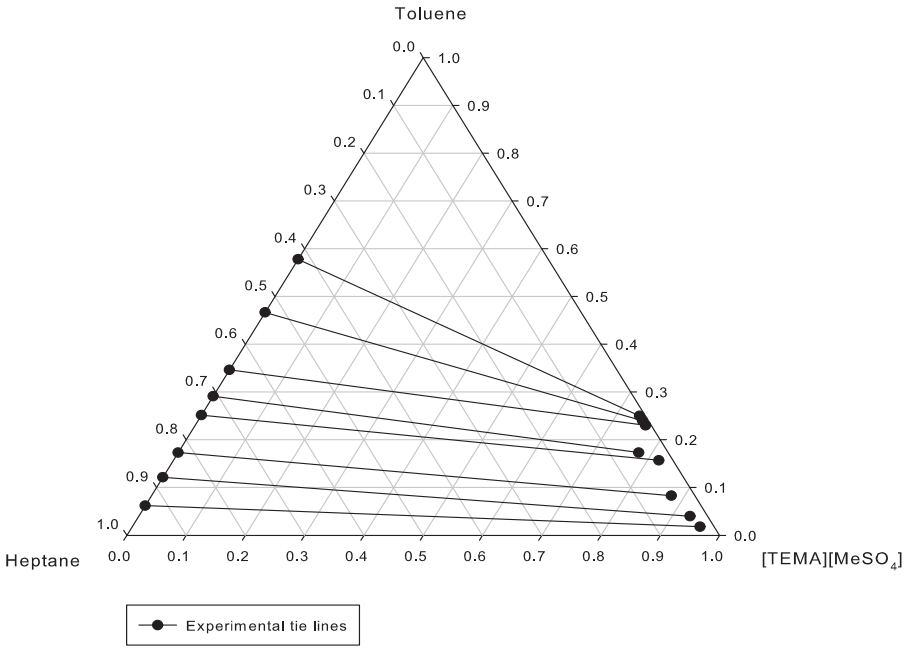

FIGURE 3.7: Experimental tie lines for the system:[TEMA][$MeSO_4$] (1) - Toluene (2) - Heptane (3) at T=298.15 K and p=1 atm.

TABLE 3.2: Experimental tie-line data for [TEMA][$MeSO_4$] (1) -Benzene (2) - Hexane (3) at 298.15 K and 1 atm.

Sr. No.	Extract Phase			Raffinate Phase			Distribution coefficient (β)	Selectivity (S)
	x_{IL}	x_{be}	x_{he}	x_{IL}	x_{be}	x_{he}		
1	0.997	0.002	0.001	0.000	0.040	0.960	0.050	48.000
2	0.957	0.042	0.001	0.000	0.191	0.809	0.220	177.895
3	0.947	0.052	0.001	0.000	0.248	0.752	0.210	157.677
4	0.916	0.083	0.001	0.000	0.469	0.531	0.177	93.972
5	0.856	0.143	0.001	0.000	0.531	0.469	0.269	126.303
6	0.853	0.146	0.001	0.000	0.628	0.372	0.232	86.484
7	0.808	0.191	0.001	0.000	0.663	0.337	0.288	97.084
8	0.797	0.202	0.001	0.000	0.694	0.306	0.291	89.066

and (C_6-C_9)-benzene- 1-ethyl-3-methylimidazolium methylsulfate ([EMIM][$MeSO_4$]) [102]. The [P_{4441}][$MeSO_4$] based ternary system studied in this work (Table 3.4) contains negligible IL concentration of 0.006 mole fraction in the raffinate phase. As obvious from Figs. 3.6- 3.7, the ternary plots for [TEMA][$MeSO_4$]-benzene-hexane and [TEMA][$MeSO_4$]-toluene-heptane system indicates negative sloping of all the tie lines. This implies that the distribution coefficients are low which is evident in Tables 3.2- 3.3. However, the selectivities obtained for both the systems are higher as compared to the thiophene-heptane separation [31]. On closer inspection, the values of distribution ratios are lower than one and are less than the values reported in the separation of thiophene and heptane using the same IL [31]. This implies that the solvent requirement or the

TABLE 3.3: Experimental tie-line data for [TEMA][$MeSO_4$] (1) -Toluene (2) - Heptane (3) at 298.15 K and 1 atm.

Sr. No.	Extract Phase			Raffinate Phase			Distribution coefficient (β)	Selectivity (S)
	x_{IL}	x_{to}	x_{ht}	x_{IL}	x_{to}	x_{ht}		
1	0.958	0.018	0.024	0.000	0.062	0.938	0.290	11.347
2	0.930	0.040	0.030	0.000	0.121	0.879	0.331	9.686
3	0.877	0.083	0.040	0.000	0.173	0.827	0.480	9.919
4	0.819	0.157	0.024	0.000	0.252	0.748	0.623	19.417
5	0.777	0.173	0.050	0.000	0.291	0.709	0.595	8.430
6	0.760	0.230	0.010	0.000	0.346	0.654	0.665	43.474
7	0.750	0.240	0.010	0.000	0.467	0.533	0.514	27.392
8	0.740	0.250	0.010	0.000	0.578	0.422	0.433	18.253

solvent to feed (S/F) ratio will be higher [103]. The selectivity is defined as:

$$S = \left(x^E_{be}/x^R_{be}\right)\Big/\left(x^E_{he}/x^R_{he}\right), = \left(x^E_{to}/x^R_{to}\right)\Big/\left(x^E_{ht}/x^R_{ht}\right), = \left(x^E_{th}/x^R_{th}\right)\Big/\left(x^E_{cy}/x^R_{cy}\right) \tag{3.2}$$

where S, is the selectivity. x_{be}, x_{to} and x_{th} are the mole fraction of benzene, toluene and thiophene respectively. x_{he}, x_{ht} and x_{cy} are the mole fraction of hexane, heptane and cyclohexene respectively. The superscripts E and R represent extract and raffinate phase respectively. The distribution coefficient is defined as the ratio of mole fraction of the solute in the extract phase (IL rich phase) to the mole fraction of the solute in the raffinate phase (hydrocarbon rich phase) and is given by

$$\beta = x^E_{be}/x^R_{be}, = x^E_{to}/x^R_{to}, = x^E_{th}/x^R_{th} \tag{3.3}$$

TABLE 3.4: Experimental tie-line data for $[P_{4441}][MeSO_4]$ (1) - Thiophene (2) - Cyclohexene (3) at 298.15 K and 1 atm.

Sr. No.	Extract Phase			Raffinate Phase			Distribution coefficient (β)	Selectivity (S)
	x_{IL}	x_{th}	x_{cy}	x_{IL}	x_{th}	x_{cy}		
1	0.709	0.043	0.248	0.000	0.031	0.969	1.377	5.378
2	0.652	0.122	0.226	0.000	0.103	0.897	1.182	4.685
3	0.538	0.213	0.249	0.000	0.199	0.801	1.068	3.436
4	0.468	0.312	0.220	0.000	0.364	0.636	0.857	2.478
5	0.291	0.471	0.239	0.006	0.493	0.501	0.954	2.003
6	0.251	0.519	0.230	0.006	0.566	0.428	0.917	1.708
7	0.223	0.548	0.229	0.000	0.615	0.385	0.890	1.496

The distribution coefficient (Table 3.2) were found to increase from 0.05 to 0.29 with increasing benzene mole fraction in raffinate phase for $[TEMA][MeSO_4]$ (1)-benzene (2)-hexane (3) system. This is consistent with the earlier reported work of benzene-hexane separation with the IL: 1-butyl-3-methylimidazolium methylsulfate ($[BMIM][MeSO_4]$) [101] and 1-ethyl-3-methylimidazolium methylsulfate ($[EMIM][MeSO_4]$) [102] respectively. However for $[TEMA][MeSO_4]$(1)-toluene (2)-heptane (3) system (Table 3.3) the distribution coefficient values did not have any specific trend. The selectivities obtained in this work for benzene-hexane (Table 3.2) separation decreases with the increase in aromatic concentration in raffinate phase. However the values (48-178) are better than the reported work using the IL: 1-ethyl-3-methylimidazolium octyl sulfate ($[EMIM][OcSO_4]$) [104], 1-methyl-3-octylimidazolium diethylene-glycol monomethyl ether sulfate ($[MOcIM][MDEGSO_4]$) [105] and 1-octyl-3-methylimidazolium chloride ([OMIM][Cl])

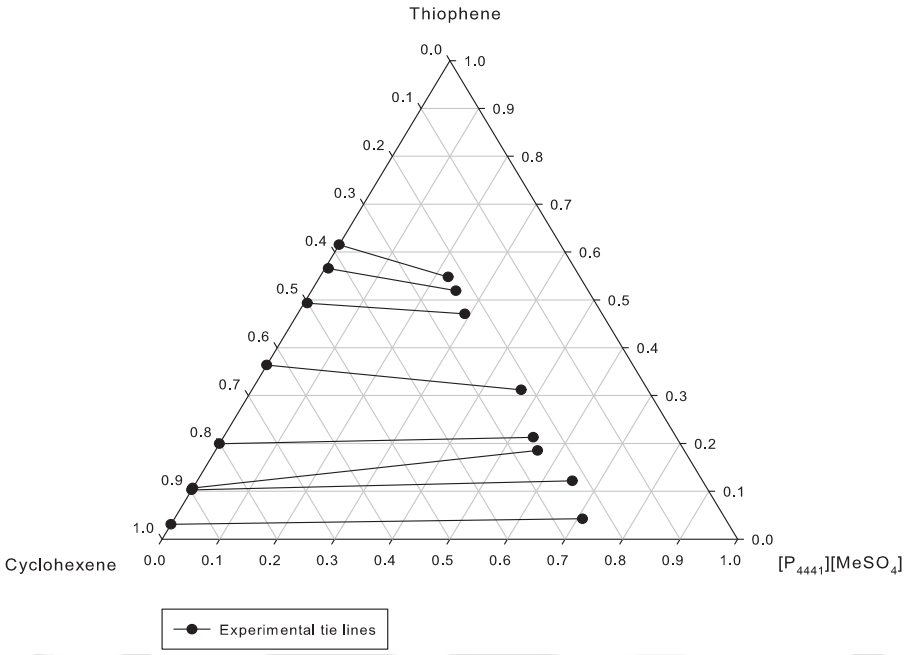

FIGURE 3.8: Experimental tie lines for the system:[P_{4441}][$MeSO_4$] (1) - Thiophene (2)-Cyclohexene (3) at T=298.15 K and p=1 atm.

[106]. The IL's gave selectivity values in the range of 1.3-2.7, 0.6-1.8 and 0.9-6.0 respectively for benzene-heptane separation [104–106]. It should also be noted that the selectivity values are higher than the ones reported by the pyridinium based ionic liquid 1-ethyl-3-methylpyridinium ethylsulfate for benzene [107] and ethylbenzene [102] separation. Thus after confirming our experimental methodology with IL-Aromatic-Aliphatic system, we now proceed with the LLE measurements of IL-butanol-water system.

3.4 Butanol Extraction by Phosphonium based ILs

3.4.1 Experimental Procedure and Analysis

Initially, different ternary mixtures (IL, 1-propanol/1-butanol and water) of 5 ml were prepared in 15 ml cuvettes. Similar experimental procedure and sample preparation for ^{1}H NMR were carried out as done earlier for aromatic-aliphatic separation. Here we have provided more time for mixing (8 hrs) and settling (20 hrs) for checking the turbidity of the mixture. Water in $CDCl_3$ solvent shows a peak at 1.6-1.9 ppm instead of 1.58 ppm due to the shift in peak of a mixture containing non-polar solvent [108]. The extract phase of [TDTHP][Phosph] based system shows a presence of water (Fig. 3.9). Extract phase ^{1}H NMR spectra (Figs. 3.10- 3.11) confirmed the absence of water peak in case of systems containing [TDTHP][DCA] and [TDTHP][DEC]. Karl Fischer titration (Metrohm Make, 787 KF Titrino Model) was also performed to verify the absence of water in extract phase. In raffinate phase, water showing peak at $\sim$ 3.8 ppm [109] was utilized for the characterization and quantification of water molecule (Figs. 3.12-3.14). 1-butanol and 1-propanol were characterized by methylene group (-CH_2) attached to hydroxyl group (-OH) for a peak at $\sim$ 3.4-3.6 ppm.

From the raffinate phase ^{1}H NMR spectra (Figs. 3.12-3.14), it is clear that the concentration of each IL is zero. It should be noted that as per earlier work [15], 102 hydrogen atoms of [TDTHP][Phosph] shows peaks between 0.79 and 2.33 ppm. Here the quantification of [TDTHP][Phosph] was carried out by subtracting peak area corresponding to all H atoms of propanol/butanol and water from total area for extract phase. ^{1}H NMR (400MHz, δ/ppm; $CDCl_3$) for [TDTHP][DCA] and [TDTHP][DEC]

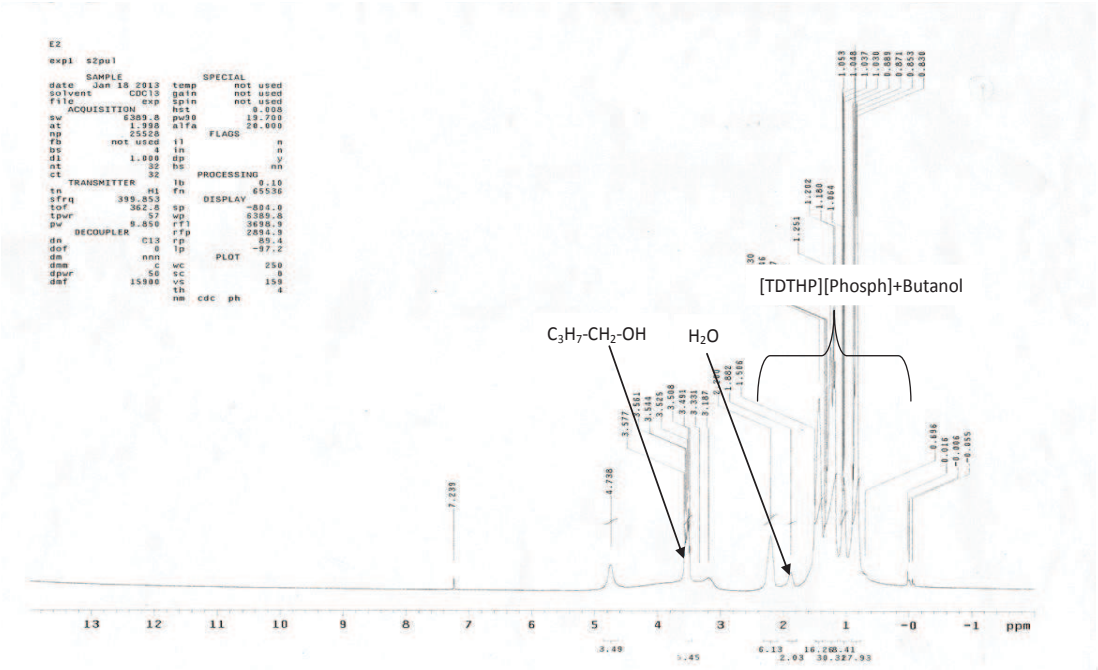

FIGURE 3.9: Extract phase ^{1}H NMR spectra for the system: [TDTHP][Phosph] (1) - 1-Butanol (2) - Water (3) at T=298.15 K and p=1 atm.

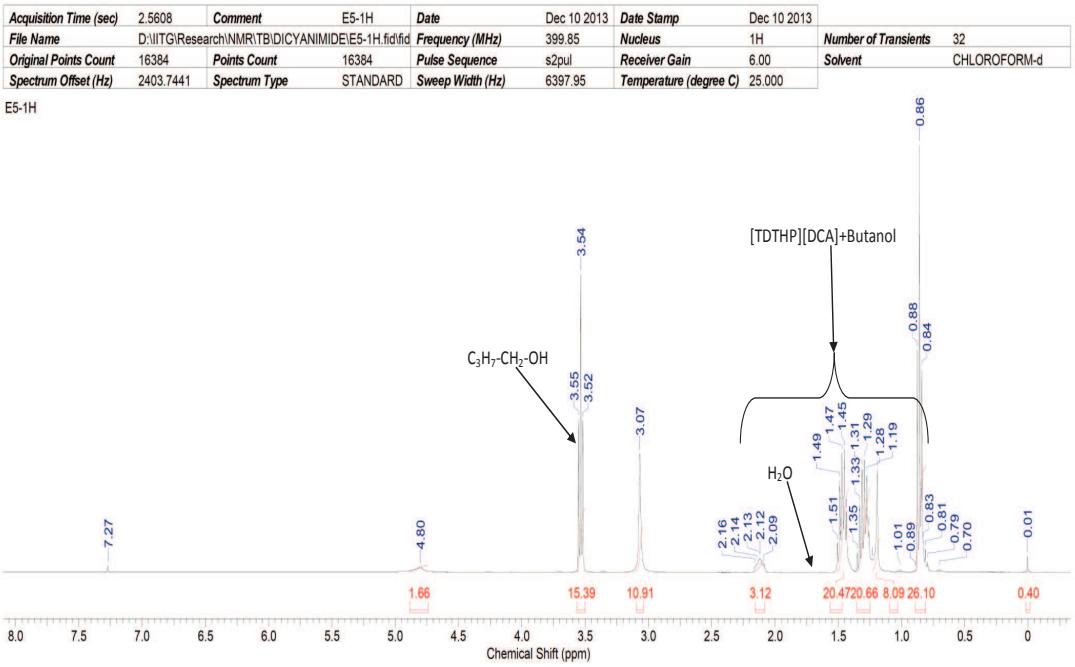

FIGURE 3.10: Extract phase ^{1}H NMR spectra for the system: [TDTHP][DCA] (1) - 1-Butanol (2) - Water (3) at T=298.15 K and p=1 atm.

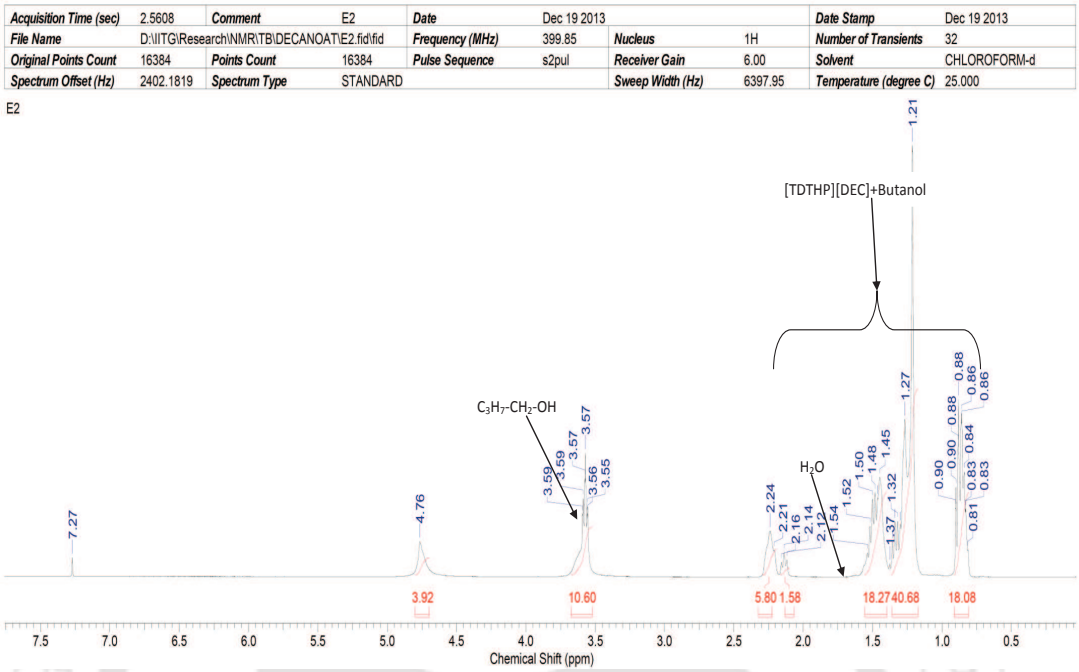

FIGURE 3.11: Extract phase ^{1}H NMR spectra for the system: [TDTHP][DEC] (1) - 1-Butanol (2) - Water (3) at T=298.15 K and p=1 atm.

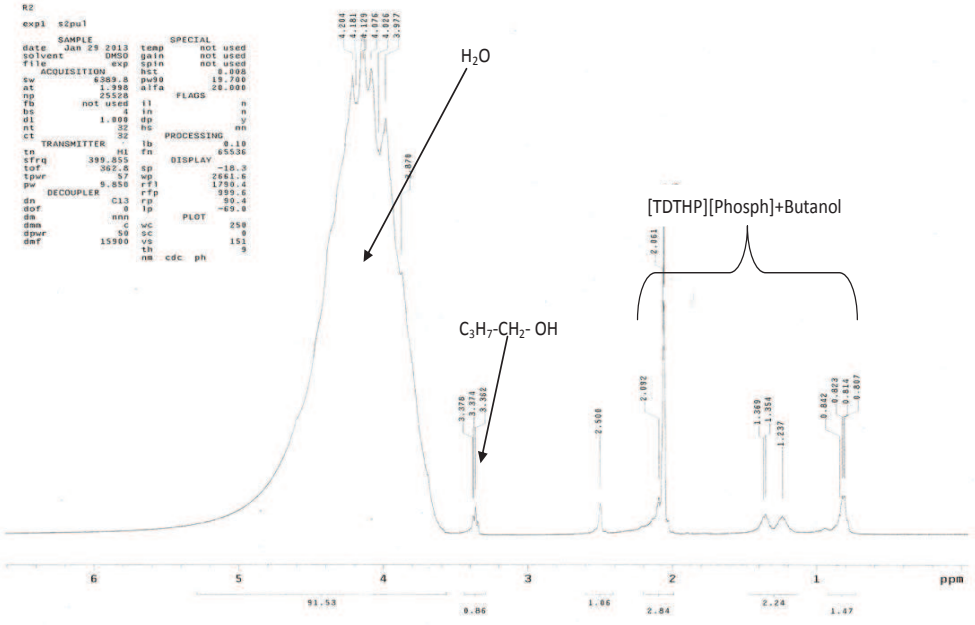

FIGURE 3.12: Raffinate phase ^{1}H NMR spectra for the system: [TDTHP][Phosph] (1) - 1-Butanol (2) - Water (3) at T=298.15 K and p=1 atm.

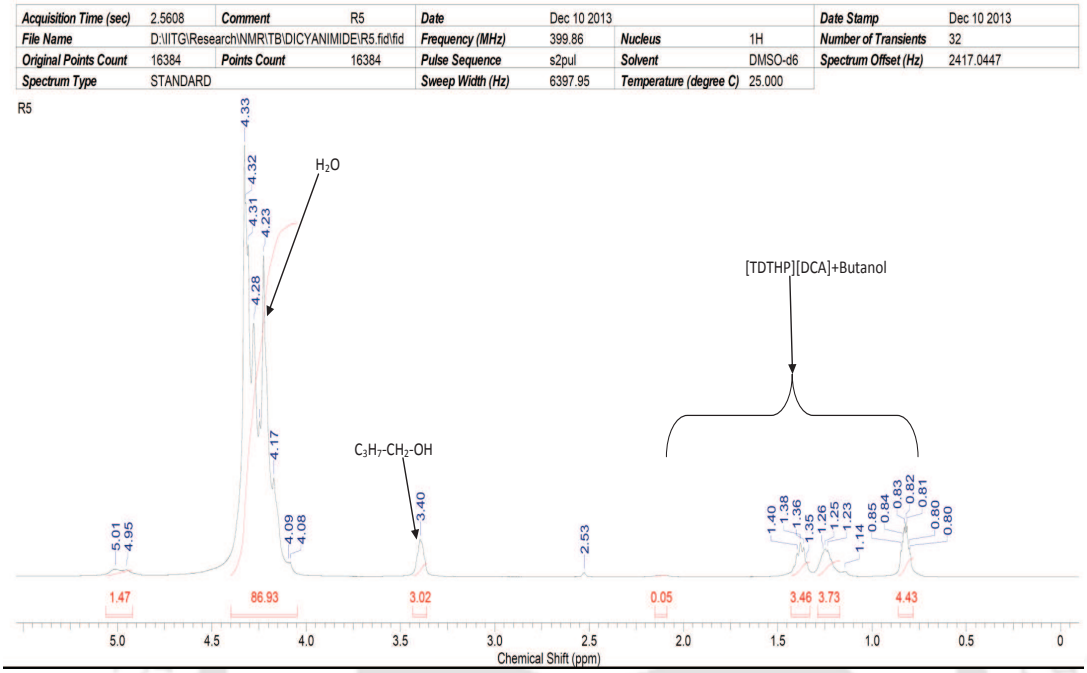

FIGURE 3.13: Raffinate phase ^{1}H NMR spectra for the system: [TDTHP][DCA] (1) - 1-Butanol (2) - Water (3) at T=298.15 K and p=1 atm.

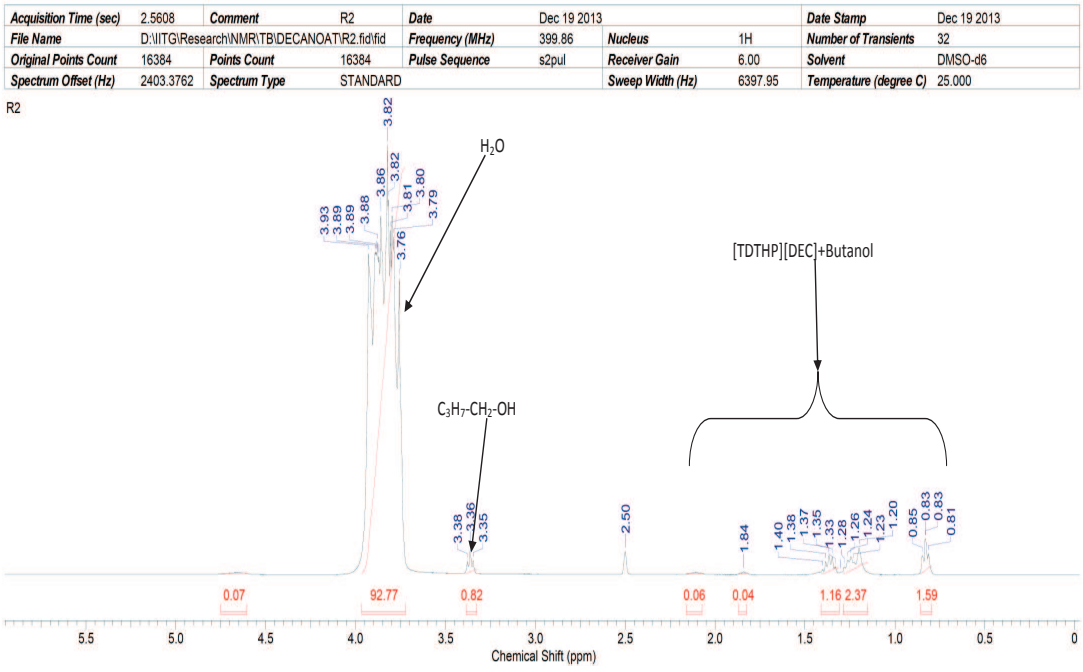

FIGURE 3.14: Raffinate phase ^{1}H NMR spectra for the system: [TDTHP][DEC] (1) - 1-Butanol (2) - Water (3) at T=298.15 K and p=1 atm.

were labelled [110] as 0.79-0.85 (m, 12 H), 1.2-1.3 (m, 32 H), 1.4-1.5 (m, 16 H); and 2-2.3 (m, 8 H), 0.79-0.96 (m, 15 H), 1.2-1.3 (m, 46 H), 1.4-1.5 (m, 16 H) and 2-2.3 (m, 10 H) ppm respectively (Figs. 3.10-3.11, 3.13-3.14). Thus for the estimation of mole fraction, 48 hydrogen atoms of [TDTHP][DCA] and 62 hydrogen atoms of [TDTHP][DEC] all lying in the range of 1.2-1.5 ppm were taken as reference peaks. The uncertainty of the mole fraction measurements has been conducted in a similar manner as performed for aliphatic-aromatic separation. For both phases, the uncertainty obtained in mole fraction composition was ±0.001.

3.4.2 Results and Discussions

Experimental ternary data for four systems namely [TDTHP][Phosph] (1)- 1-propanol (2) - water (3), [TDTHP][Phosph] (1)- 1-butanol (2) - water (3), [TDTHP][DCA] (1)- 1-butanol (2) - water (3) and [TDTHP][DEC] (1)- 1-butanol (2) - water (3) were measured at 298.15 K and 1 atm (Tables 3.5-3.8 and Figs. 3.15-3.18). The extraction effectiveness are represented by distribution coefficient (β) and Selectivity (S) for equilibrium biphasic systems. Eqs. 3.2-3.3 can be rewritten as,

$$S = \frac{\left(x_b^E / x_b^R\right)}{\left(x_w^E / x_w^R\right)} \tag{3.2}$$

$$\beta = \left(\frac{x_b^E}{x_b^R}\right)_{eq} \tag{3.3}$$

Here, x_b and x_w are the molefraction of butanol and water, respectively.

Large value of distribution coefficient is desirable since it indicates lesser solvent requirement for particular degree of separation. [TDTHP][Phosph] shows higher

TABLE 3.5: Experimental tie line data for the system [TDTHP][Phosph] (1) - 1-Propanol (2) - Water (3) at T=298.15 K and p=1 atm.

Sr. No.	Extract Phase			Raffinate Phase			Distribution coefficient (β)	Selectivity (S)
	x_{IL}	x_p	x_w	x_{IL}	x_p	x_w		
1	0.353	0.448	0.199	0.000	0.028	0.972	16.000	78.151
2	0.418	0.388	0.194	0.000	0.014	0.986	27.714	140.857
3	0.189	0.63	0.181	0.000	0.038	0.962	16.579	88.116
4	0.063	0.744	0.193	0.000	0.067	0.933	11.104	53.681
5	0.275	0.531	0.194	0.000	0.03	0.97	17.700	88.500
6	0.517	0.297	0.186	0.000	0.009	0.991	33.000	175.823
7	0.65	0.179	0.171	0.000	0.008	0.992	22.375	129.801
8	0.685	0.144	0.172	0.000	0.003	0.997	48.000	278.233

TABLE 3.6: Experimental tie line data for the system [TDTHP][Phosph] (1) - 1-Butanol (2) - Water (3) at T=298.15 K and p=1 atm.

Sr. No.	Extract Phase			Raffinate Phase			Distribution coefficient (β)	Selectivity (S)
	x_{IL}	x_b	x_w	x_{IL}	x_b	x_w		
1	0.672	0.151	0.177	0.000	0.000	1.000	-	-
2	0.568	0.276	0.156	0.000	0.007	0.993	39.429	250.978
3	0.403	0.415	0.182	0.000	0.007	0.993	59.286	323.465
4	0.341	0.456	0.203	0.000	0.008	0.992	57.000	278.542
5	0.289	0.503	0.208	0.000	0.011	0.989	45.727	217.424
6	0.251	0.541	0.208	0.000	0.026	0.974	20.808	97.436
7	0.16	0.612	0.228	0.000	0.032	0.968	19.125	81.197
8	0.092	0.724	0.184	0.000	0.038	0.962	19.053	99.612

TABLE 3.7: Experimental tie line data for [TDTHP][DCA] (1) - 1-Butanol (2) - Water (3) at T=298.15 K and p=1 atm.

Sr. No.	Extract Phase			Raffinate Phase			Distribution coefficient (β)
	x_{IL}	x_b	x_w	x_{IL}	x_b	x_w	
1	0.631	0.369	0.000	0.000	0.000	1.000	-
2	0.250	0.750	0.000	0.000	0.011	0.989	68.182
3	0.167	0.833	0.000	0.000	0.013	0.987	64.077
4	0.055	0.945	0.000	0.000	0.017	0.983	55.588
5	0.093	0.907	0.000	0.001	0.037	0.962	24.514
6	0.731	0.269	0.000	0.000	0.000	1.000	-
7	0.523	0.477	0.000	0.000	0.005	0.995	95.400
8	0.355	0.645	0.000	0.000	0.009	0.991	71.667

TABLE 3.8: Experimental tie line data for [TDTHP][DEC] (1) - 1-Butanol (2) - Water (3) at T=298.15 K and p=1 atm.

Sr. No.	Extract Phase			Raffinate Phase			Distribution coefficient (β)
	x_{IL}	x_b	x_w	x_{IL}	x_b	x_w	
1	0.524	0.476	0	0.000	0.003	0.997	158.667
2	0.249	0.751	0	0.001	0.007	0.992	107.286
3	0.104	0.896	0	0.001	0.045	0.954	19.911
4	0.065	0.935	0	0.001	0.054	0.945	17.315
5	0.69	0.31	0	0.001	0.002	0.997	155.000
6	0.376	0.624	0	0.001	0.006	0.993	104.000
7	0.296	0.704	0	0.000	0.007	0.993	100.571
8	0.827	0.173	0	0.000	0.001	0.999	173.000

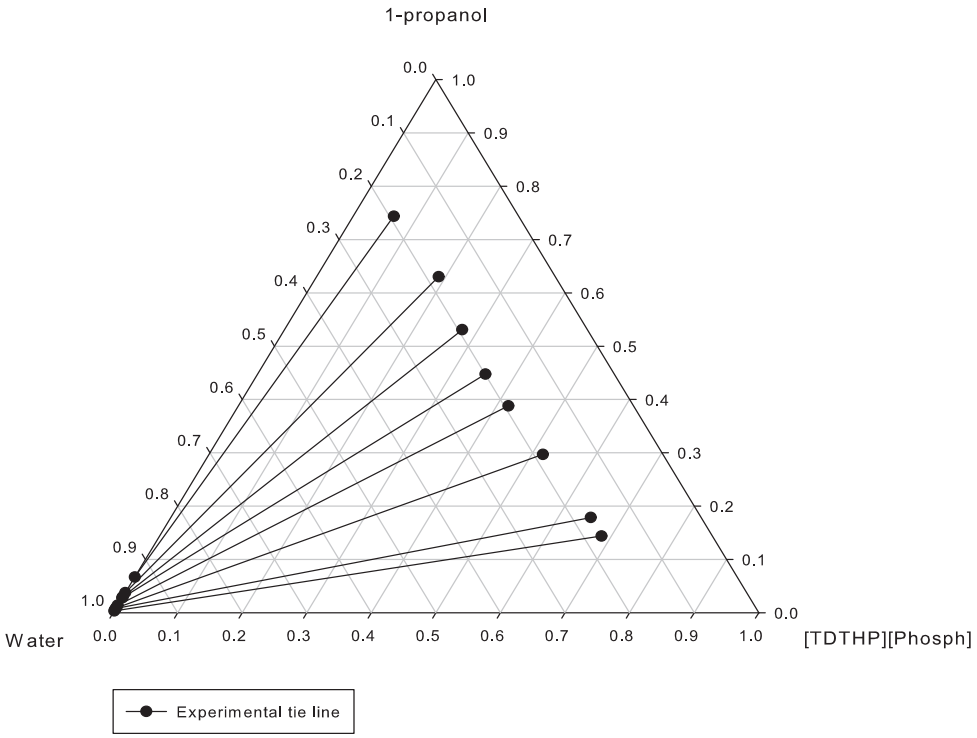

FIGURE 3.15: Experimental tie lines for the system: [TDTHP][Phosph] (1) - 1-Propanol (2) - Water (3) at T=298.15 K and p=1 atm.

distribution coefficient for butanol extraction (19-59) than propanol recovery (11-48) (Tables 3.5-3.6). This is due to the higher polarity of propanol as compared to butanol resulting in more solubility in water. The distribution coefficient varied in the range of 25-95 and 17-173 for ternary systems namely [TDTHP][DCA] and [TDTHP][DEC] respectively (Tables 3.7-3.8). These values are much higher than 0.7-2.2 as obtained by Ha et al. [21] for different imidazolium based ILs containing tetrafluoroborate, trifluoromethanesulfonate, hexafluorophosphate, and bis(trifluoromethylsulfonyl)imide anions. Further the positive sloping of the tie lines indicate butanol favorably partitions into the IL phase (Figs. 3.16-3.18). The distribution coefficient for [TDTHP][DCA] is twice as compared to the ILs reported by Nann et al. [49] that is, 1-decyl-3-methylimidazolium, tetracyanoborate

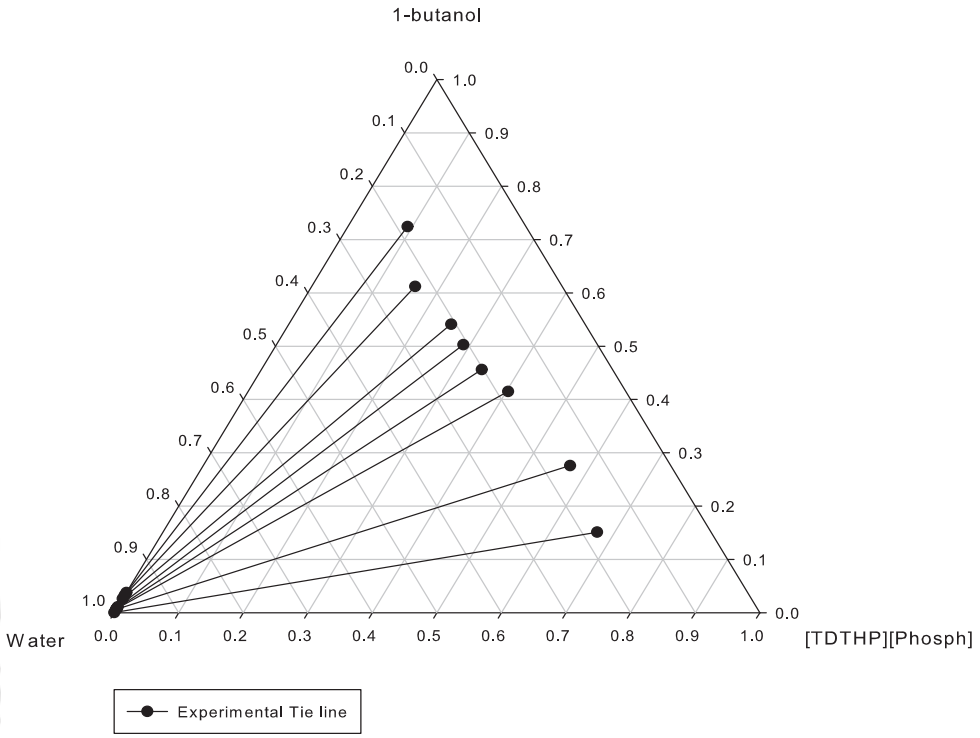

FIGURE 3.16: Experimental tie lines for the system: [TDTHP][Phosph] (1) - 1-Butanol (2) - Water (3) at T=298.15 K and p=1 atm.

([Im10.1][TCB]), 4-decyl-4-methylmorpholinium tetracyanoborate ([Mo10.1][TCB]), 1-decyl-3-methylimidazolium bis(trifluoromethylsulfonyl) ([Im10.1][Tf_2N]), and 4-decyl-4-methylmorpholinium bis-(trifluoromethylsulfonyl)imide ([Mo10.1][Tf_2N]). Further it was also observed that the distribution coefficients for [TDTHP][Phosph] and [TDTHP][DEC] are twelve and seven times respectively higher as compared to the same IL's [49]. Thus we can conclude that [TDTHP][Phosph] and [TDTHP][DEC] more favorably extract butanol from aqueous streams. The distribution coefficient for the present three systems are compared with literature data [49] in Fig. 3.19.

It should be noted that the ternary diagram is wider than that obtained in case of 1-hexyl-3-methylimidazolium bis(trifluoromethylsulfonyl)imide by Chapeaux et al. [23]. It is an indication of better separation with wide range of feed concentration. In addition,

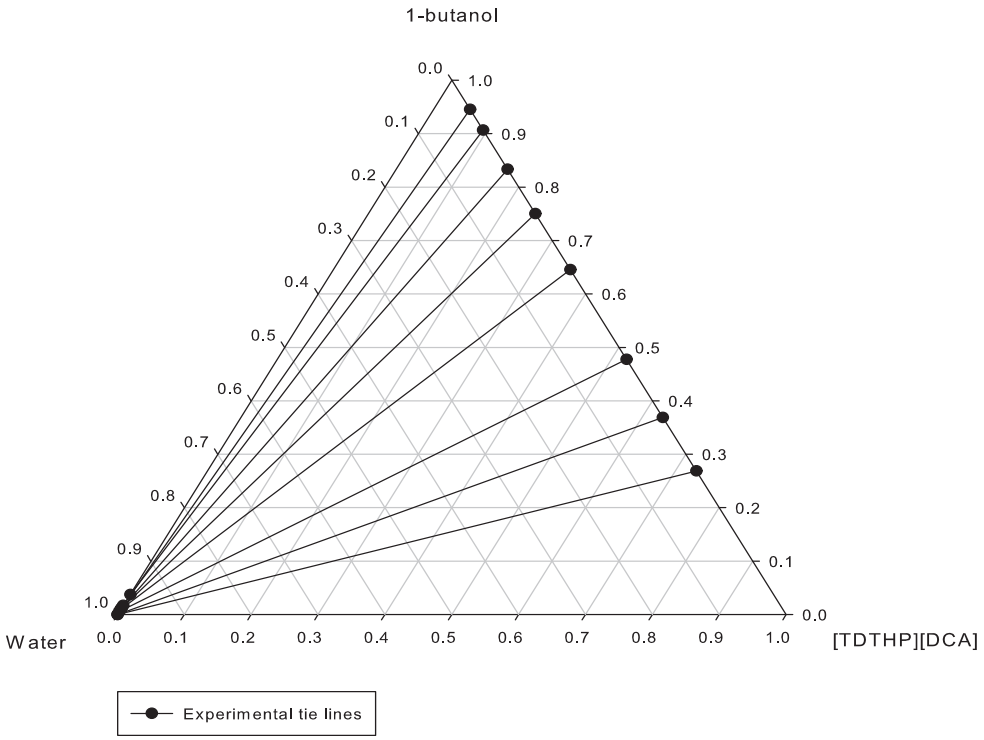

FIGURE 3.17: Experimental tie lines for the system: [TDTHP][DCA] (1) - 1-Butanol (2) - Water (3) at T=298.15 K and p=1 atm.

the solvent requirement or the solvent-feed ratio will be less as compared to imidazolium based ILs for a particular degree of separation.

Selectivity is the ability to separate 1-butanol from water. Higher values of selectivity indicate better selective separation of 1-butanol. For ternary system containing [TDTHP][Phosph], the mole fraction of butanol in raffinate phase is very low resulting in higher selectivity (Table 3.6). For the other two systems, the molefraction of water in extract phase is nearly zero, hence selectivity approaches infinity as per Eq. 3.2. Also Tables 3.7-3.8 and Figs. 3.17-3.18 represent negligible concentration of IL and water in either phase. It implies [TDTHP][DCA] and [TDTHP][DEC] are completely immiscible with water in ternary system. This confirms the findings of Cascon and Choudhary [111] for the IL: [TDTHP][DCA] where SILM-based pervaporation of 1-butanol indicated

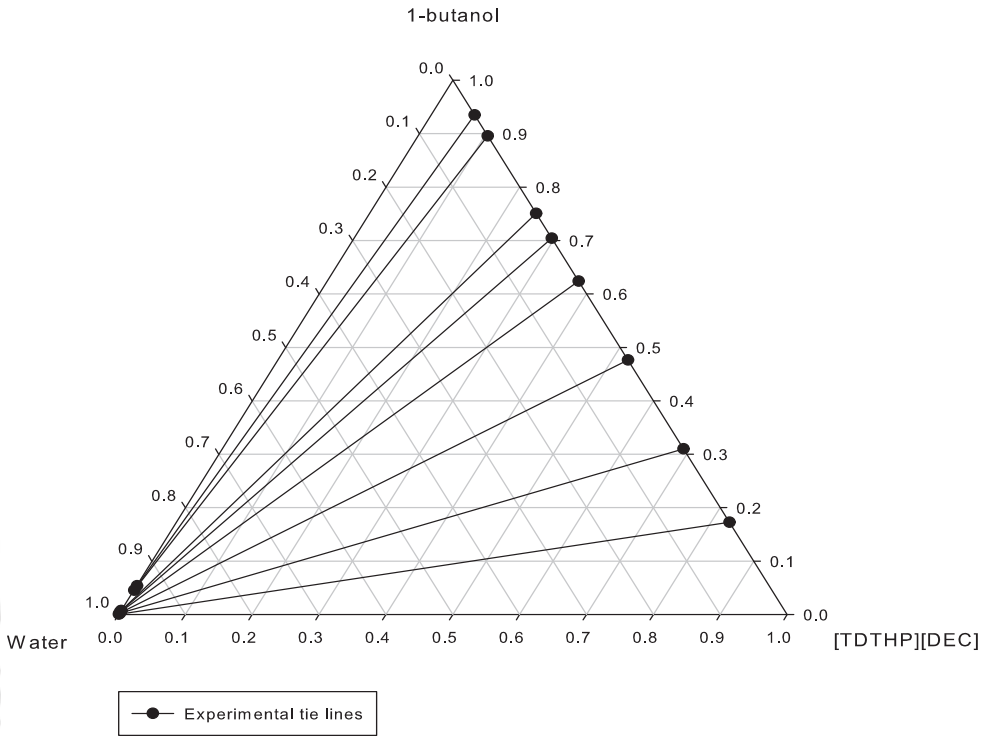

FIGURE 3.18: Experimental tie lines for the system: [TDTHP][DEC] (1) - 1-Butanol (2) - Water (3) at T=298.15 K and p=1 atm.

high affinity for the alcohol. This is due to the strong hydrogen bonding between the dicyanamide anion and 1-butanol. Hydrogen bond energy [112] between dicyanamide ion with butanol (60.8 kJ/mole) is more as compared to that with water (53.9 kJ/mole). This is contrary to the measurements by Freire et al. [17] where [TDTHP][DCA] and [TDTHP][DEC] were found to be more miscible with water. However hydrogen bond between the anions and butanol alters the miscibility of the ILs with butanol and water. It can be seen from Figs. 3.16-3.18 that the amount of water content in [TDTHP][Phosph] is more as compared to [TDTHP][DCA] and [TDTHP][DEC]. This is attributed to the more electronegative atoms (1 Phosphorous and 2 Oxygen atoms) in [Phosph] anion thereby forming a strong bond with water [112]. In the subsequent section, the experimental LLE data were modelled with NRTL, UNIQUAC and the quantum chemical

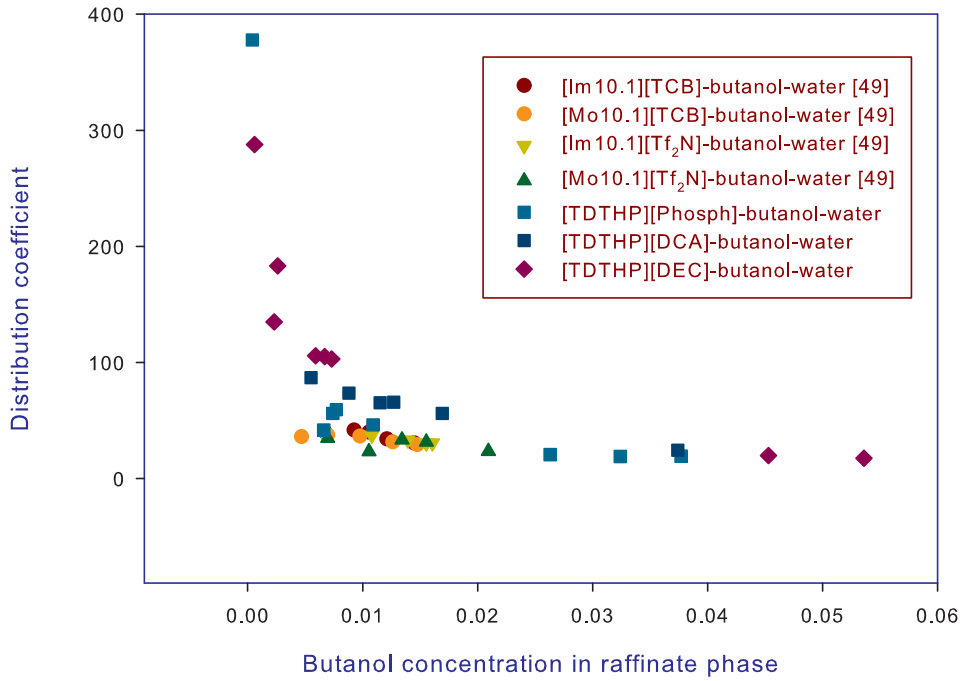

FIGURE 3.19: Comparison of Distribution Coefficient with imidazolium based cations at ambient conditions

based COSMO-SAC model.

3.5 LLE Modeling

3.5.1 Gibb's Free energy Models

Gibb's free energy models namely Non-Random Two-Liquid (NRTL) [113] and UNIversal QUAsiChemical (UNIQUAC) [114] were used to correlate experimental tie line data. Both models equations are described in Table 3.9. Polarizable Continuum Model (PCM) [115] with GEPOL algorithm was used to predict volume parameter (r) and surface area parameter (q) of ILs in UNIQUAC model. For the estimation of r and q of the

phosphonium based ILs, Eqs. 3.4 and 3.5 [115] has been used as:

$$r_{pred} = \frac{(V^{PCM} in^3)(1 \times 10^{-8} cm) N_{av}}{V_{ws}} \tag{3.4}$$

$$q_{pred} = \frac{(A^{PCM} in^2)(1 \times 10^{-8} cm)^2 N_{av}}{A_{ws}} \tag{3.5}$$

Here N_{av} is the Avagrado's number. The standard segment volume $V_{ws}(15.17\ cm^3/mol)$ and area $A_{ws}(2.5 \times 10^9 cm^2/mol)$ are discussed in our previous work [115]. The output file of PCM contains the overall surface (A^{PCM}) and the overall volume (V^{PCM}) of the phosphonium ILs under consideration. The parameters values are reported in Table 3.10. For both NRTL and UNIQUAC models (Table 3.9), modelling procedure is described in the following algorithm as per our earlier work [116].

Algorithm for NRTL/UNIQUAC model

Step 1: Start

Step 2: Compute feed concentration of component i (z_i) from experimental concentration of component i in both phases.

$$z_i = \frac{x_i^I + x_i^{II}}{2} \tag{3.6}$$

Here x_i^I and x_i^{II} are the mole fraction of component i in phases I (Extract) and II (Raffinate), respectively.

Step 3: Predict activity coefficient of component i (γ_i) in both phases by NRTL/UNIQUAC model (Equations in Table 3.9) with the help of the objective function

in GA(Eq. 3.14).

$$\gamma_i^I \hat{x}_i^I = \gamma_i^{II} \hat{x}_i^{II} \tag{3.7}$$

where $\hat{x}_i^I$ and $\hat{x}_i^{II}$ are the mole fraction of component i in phases I and II predicted by NRTL/UNIQUAC, respectively.

Step 4: Compute distribution coefficient of component i (K_i) from activity coefficient of component i.

$$K_i = \frac{x_i^I}{x_i^{II}} = \frac{\gamma_i^{II}}{\gamma_i^I} \tag{3.8}$$

Step 5: Solve the Isothermal flash algorithm for extract to feed (Ψ) ratio.

$$f(\Psi) = \sum \frac{z_i(1 - K_i)}{1 + \Psi(K_i - 1)} = 0 \tag{3.9}$$

subject to,

$$F z_i = E^I x_i^I + R^{II} x_i^{II} \tag{3.10}$$

and

$$\Psi = E^I / F \tag{3.11}$$

where F, E^I, R^{II} are flow rate of feed, extract and raffinate phase respectively. If step 5 is converged then go to step 6, otherwise go to step 3 and invoke GA toolbox for new set of binary interaction parameters (τ_{ij}/τ_{ji} or A_{ij}/A_{ji} as reported in Table 3.11). Thereafter repeat steps 4 and 5.

Step 6: Calculate the mole fractions in both phases

$$\hat{x}_i^{II} = \frac{z_i}{1 + \Psi(K_i - 1)} \tag{3.12}$$

$$\hat{x}_i^{I} = K_i \hat{x}_i^{II} \tag{3.13}$$

Step 7: End

TABLE 3.9: NRTL and UNIQUAC models

Model	Equations
NRTL[113]	$\ln\gamma_i = \frac{\sum_{j=1}^{c}\tau_{ji}G_{ji}x_j}{\sum_{k=1}^{c}G_{ki}x_k} + \sum_{j=1}^{c}\left[\frac{G_{ij}x_j}{\sum_{k=1}^{c}G_{kj}x_k}\left(\tau_{ij} - \frac{\sum_{i=1}^{c}\tau_{ij}G_{ij}x_i}{\sum_{k=1}^{c}G_{kj}x_k}\right)\right]$, $G_{ji} = \exp(-\alpha_{ji}\tau_{ji})$
UNIQUAC[114]	$\ln\gamma_i = \ln\left(\frac{\Phi_i}{x_i}\right) + \frac{z}{2}q_i\ln\left(\frac{\theta_i}{\Phi_i}\right) + l_i - \frac{\Phi_i}{x_i}\sum_{j=1}^{c}x_j l_j + q_i\left(1 - \ln\sum_{j=1}^{c}\theta_j\tau_{ji} - \sum_{j=1}^{c}\frac{\theta_j\tau_{ij}}{\sum_{k=1}^{c}\theta_k\tau_{kj}}\right)$, $\tau_{ji} = \frac{g_{ji}-g_{ii}}{RT} = \frac{A_{ji}}{T}$, $\theta_i = \frac{q_i x_i}{q_T}$, $q_T = \sum_k q_k x_k$, $\Phi_i = \frac{r_i x_i}{r_T}$, $r_T = \sum_k r_k x_k$, $l_i = \frac{z}{2}(r_k - q_k) + 1 - r_k$

TABLE 3.10: UNIQUAC Volume and Surface area structural parameters for components

Sr. No.	Compound	Volume parameter (r)	Surface area parameter (q)
1	[TDTHP][Phosph]*	9.83	6.26
2	[TDTHP][DCA]*	8.37	5.81
3	[TDTHP][DEC]*	8.77	5.96
4	1-propanol	2.25	3.13
5	1-butanol	3.92	3.67
6	Water	0.92	1.4

* calculated from Banerjee et al. [115]

These predicted concentration are incorporated with GA [116] to minimize objective function (Eq. 3.14). The difference between experimental mole fractions and those predicted by either NRTL or UNIQUAC is the objective function (Obj) which is non-linear in nature. Here the objective function Obj is minimized. However GA always deals with the maximization, therefore Obj on right side of Eq. 3.14 is preceded by a minus sign.

$$Maximize : Obj \begin{pmatrix} with respect to A_{ij} \\ where i,j=1,2,3 \\ and j \neq i \end{pmatrix} = -\sum_{k=1}^{m}\sum_{l=I}^{II}\sum_{i=1}^{c} w_{ik}^{l}\left(x_{ik}^{l} - \hat{x}_{ik}^{l}\right)^2 \tag{3.14}$$

Here m and c, refer to the number of tie lines and the number of components (viz. 3 for the present systems) respectively. x_{ik}^{l} and $\hat{x}_{ik}^{l}$ are the experimental and predicted mole fraction for component i in the k^{th} tie line of phase l, respectively. w represents weight factor.

The maximization would occur with respect to six binary interaction parameters (τ_{ij} and A_{ij} for NRTL and UNIQUAC model respectively). The number of generation and the number of population (possible random solutions) in GA were specified at 200 and 100 as per our earlier work by a Singh et al. [116]. Each solution represents a set of six parameters i.e A_{12}/τ_{12}, A_{13}/τ_{13}, A_{21}/τ_{21}, A_{23}/τ_{23}, A_{31}/τ_{31} and A_{32}/τ_{32}. GA operators (crossover and mutation) usually alter the random solution after each iteration till the termination criteria is satisfied. The optimization results corresponding to the lowest Obj are reported in Table 3.11. The Root Mean Square Deviation (RMSD) represents

deviation from experimental tie line data as shown in Eq. 3.15:

$$RMSD(in\%) = \left[\sum_{k=1}^{m}\sum_{i=1}^{c}\sum_{l=I}^{II}\frac{\left(x_{ik}^{l}-\hat{x}_{ik}^{l}\right)^{2}}{2mc}\right]^{1/2} \times 100 \qquad (3.15)$$

For all ternary systems, RMSD values are less than unity (Table 3.11). This implies that tie lines predicted by both models overlap experimental tie lines (Figs. 3.20-3.27).

TABLE 3.11: NRTL and UNIQUAC interaction parameters for ternary systems at T=298.15 K and p=1 atm.

i-j	NRTL Model Parameters				UNIQUAC Model Parameters			
	τ_{ij}	τ_{ji}	Obj^{*}	%RMSD**	A_{ij}/K	A_{ji}/K	Obj^{*}	%RMSD**
[TDTHP][Phosph] (1)- 1-Propanol (2)- Water (3)								
1-2	-0.11	-0.61			-314.85	-384.76		
1-3	16.72	8.73	-1.10 x10^{-4}	0.15	578.04	-171.19	-4.50 x10^{-4}	0.31
2-3	16.19	2.95			675.00	-40.32		
[TDTHP][Phosph] (1)- 1-Butanol (2)- Water (3)								
1-2	15.89	-9.04			-75.89	-55.06		
1-3	14.49	8.47	-3.8 x10^{-4}	0.28	569.69	-166.37	-1.48 x10^{-3}	0.56
2-3	16.91	3.22			395.36	-27.33		
[TDTHP][DCA] (1)- 1-Butanol (2)- Water (3)								
1-2	-1.93	10.45			-0.21	-155.56		
1-3	15.71	10.47	-7.24 x10^{-5}	0.12	1000	-51.98	-1.12 x10^{-3}	0.48
2-3	20	4.56			1000	-15.75		
[TDTHP][DEC] (1)- 1-Butanol (2)- Water (3)								
1-2	-4.77	17.99			-232.11	38.2		
1-3	17.24	5.45	-8.75 x10^{-5}	0.14	1000	-87.58	-1.46x10^{-3}	0.55
2-3	20	3.28			1000	-58.53		

* Calculated by Eq. 3.14

** Calculated by Eq. 3.15

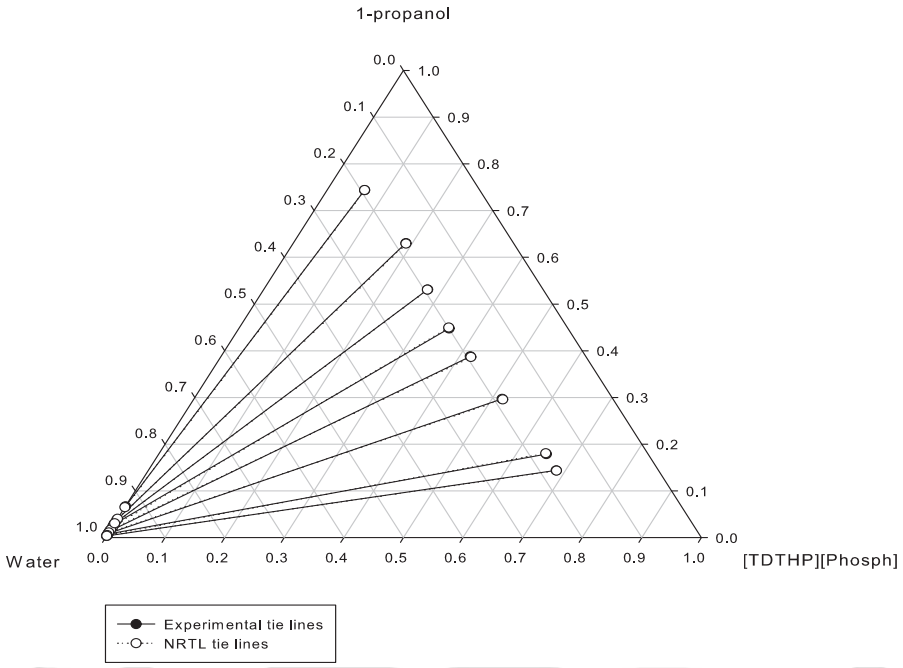

FIGURE 3.20: Experimental and NRTL correlated tie lines for the system: [TDTHP][Phosph] (1) - 1-Propanol (2) - Water (3) at T=298.15 K and p=1 atm.

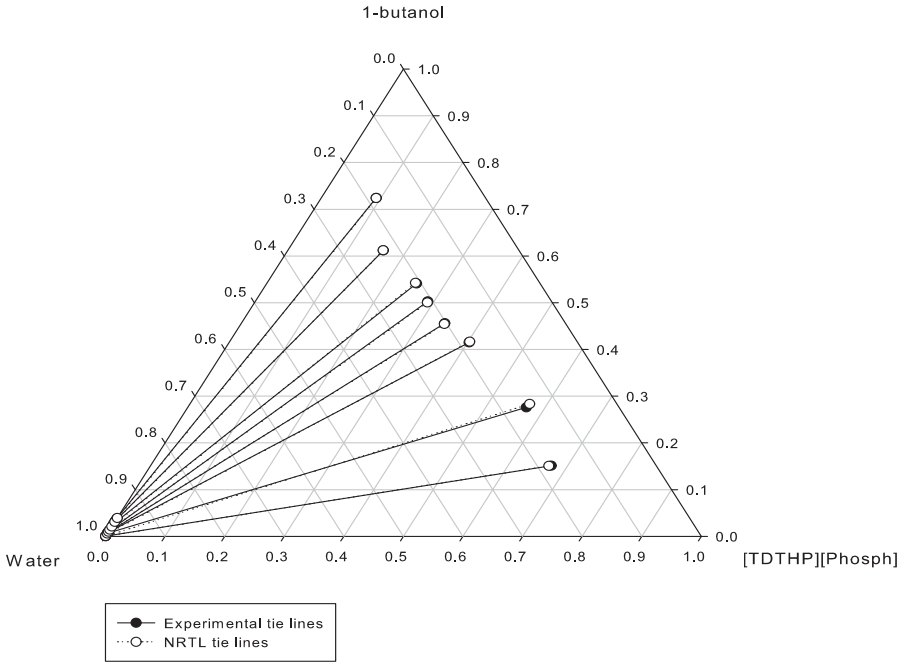

FIGURE 3.21: Experimental and NRTL correlated tie lines for the system: [TDTHP][Phosph] (1) - 1-Butanol (2) - Water (3) at T=298.15 K and p=1 atm.

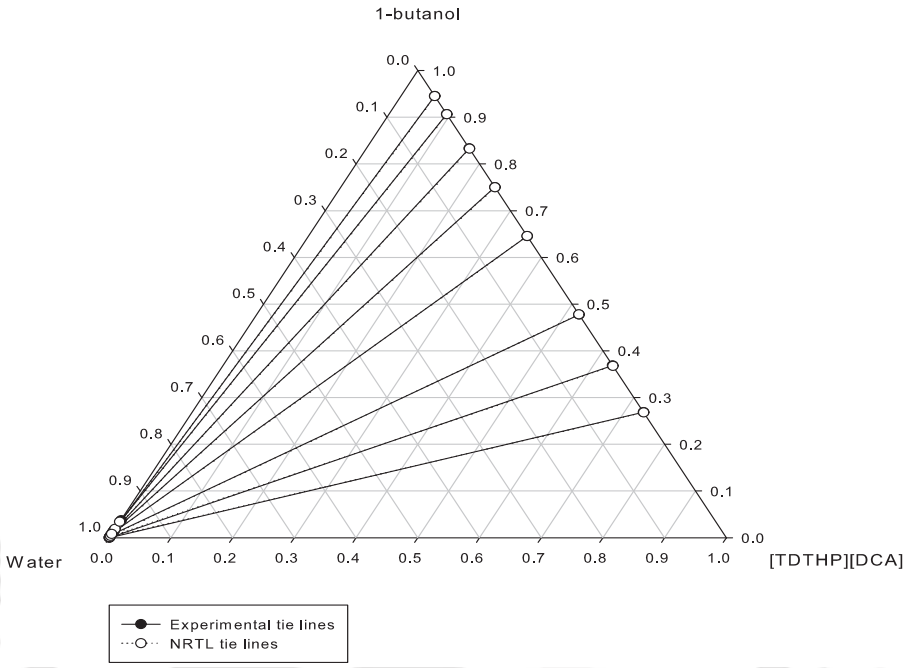

FIGURE 3.22: Experimental and NRTL correlated tie lines for the system: [TDTHP][DCA] (1) - 1-Butanol (2) - Water (3) at T=298.15 K and p=1 atm.

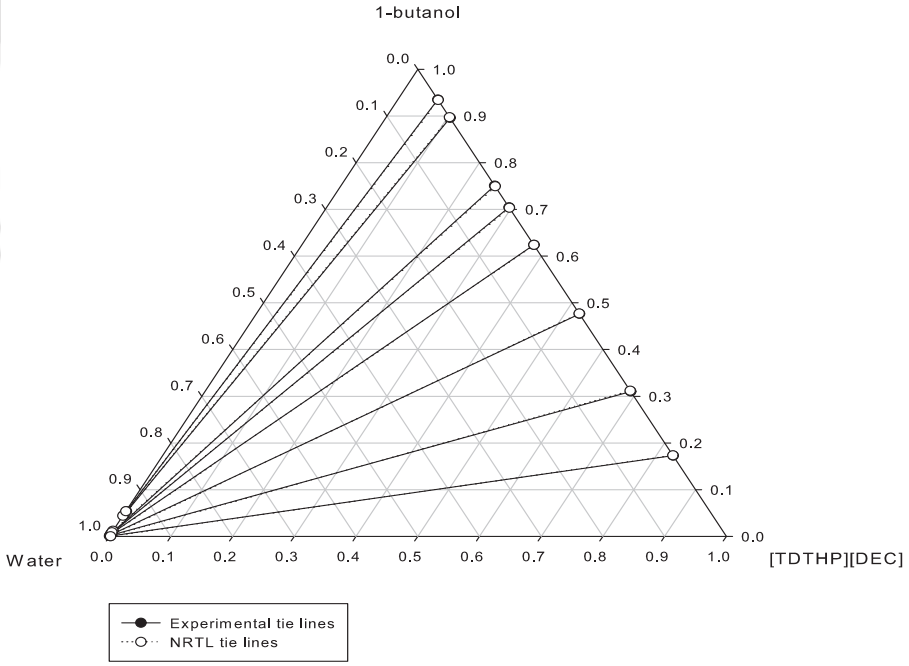

FIGURE 3.23: Experimental and NRTL correlated tie lines for the system: [TDTHP][DEC] (1) - 1-Butanol (2) - Water (3) at T=298.15 K and p=1 atm.

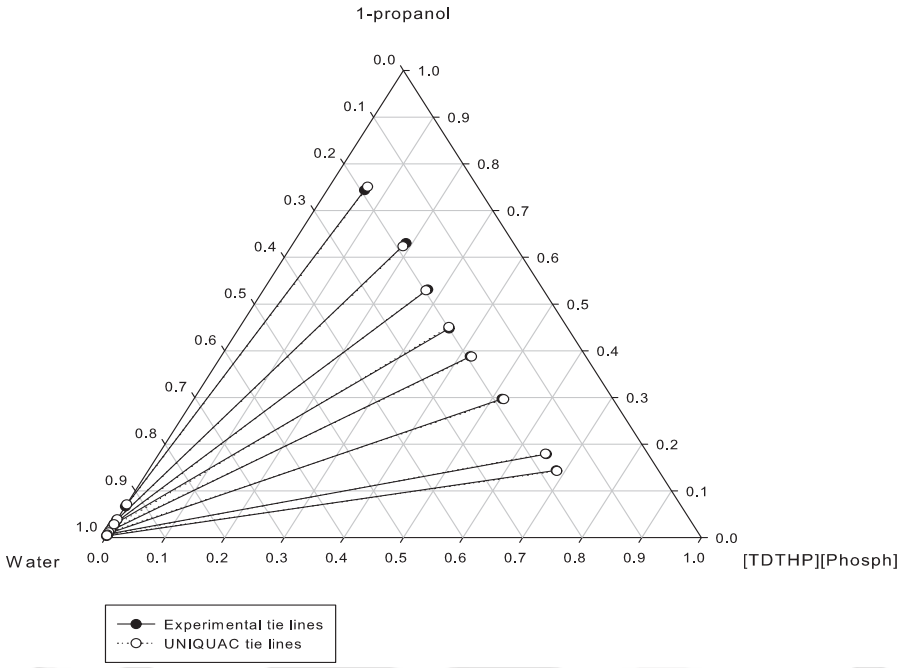

FIGURE 3.24: Experimental and UNIQUAC correlated tie lines for the system: [TDTHP][Phosph] (1) - 1-Propanol (2) - Water (3) at T=298.15 K and p=1 atm.

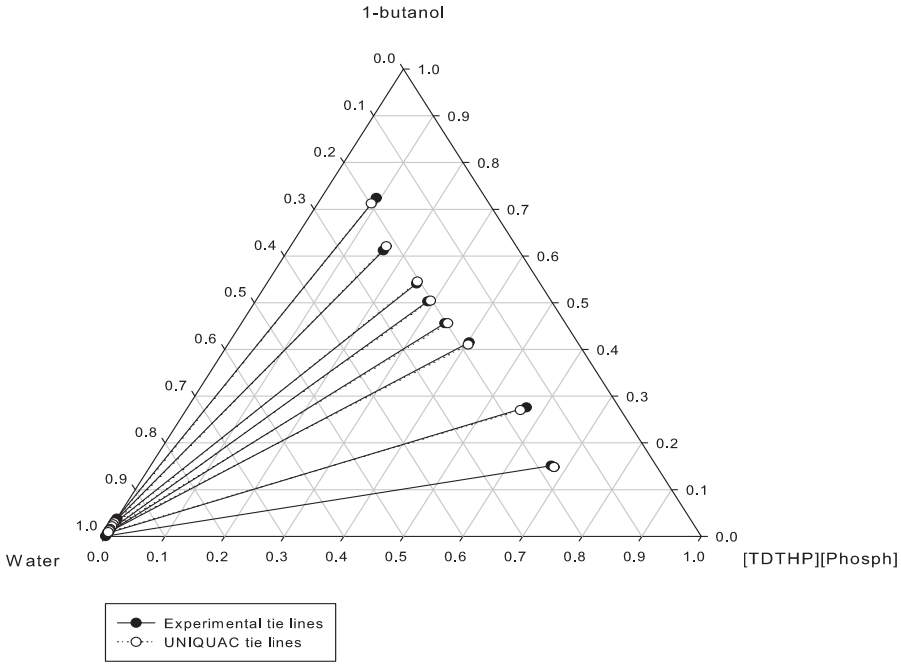

FIGURE 3.25: Experimental and UNIQUAC correlated tie lines for the system: [TDTHP][Phosph] (1) - 1-Butanol (2) - Water (3) at T=298.15 K and p=1 atm.

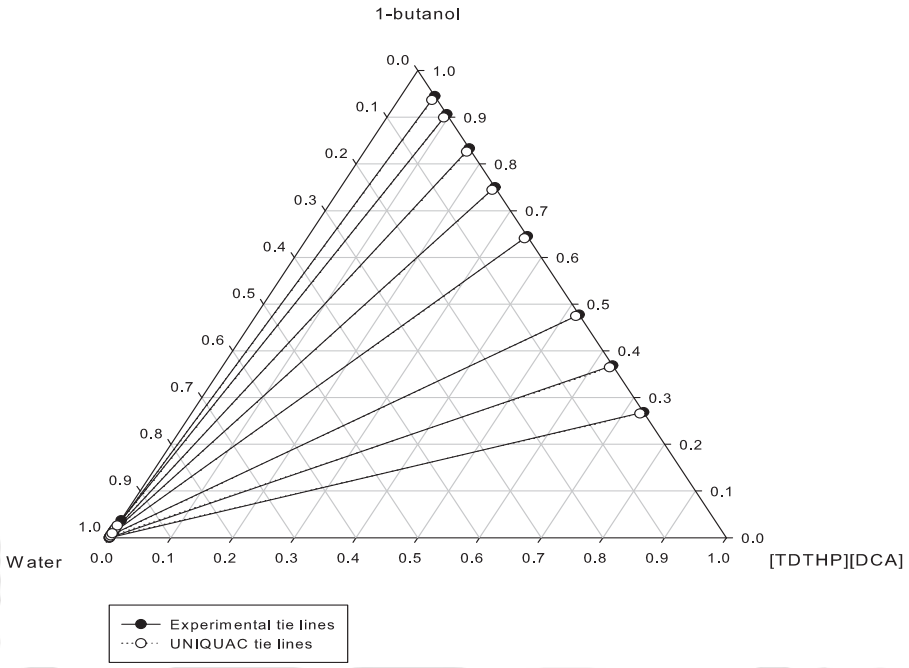

FIGURE 3.26: Experimental and UNIQUAC correlated tie lines for the system: [TDTHP][DCA] (1) - 1-Butanol (2) - Water (3) at T=298.15 K and p=1 atm.

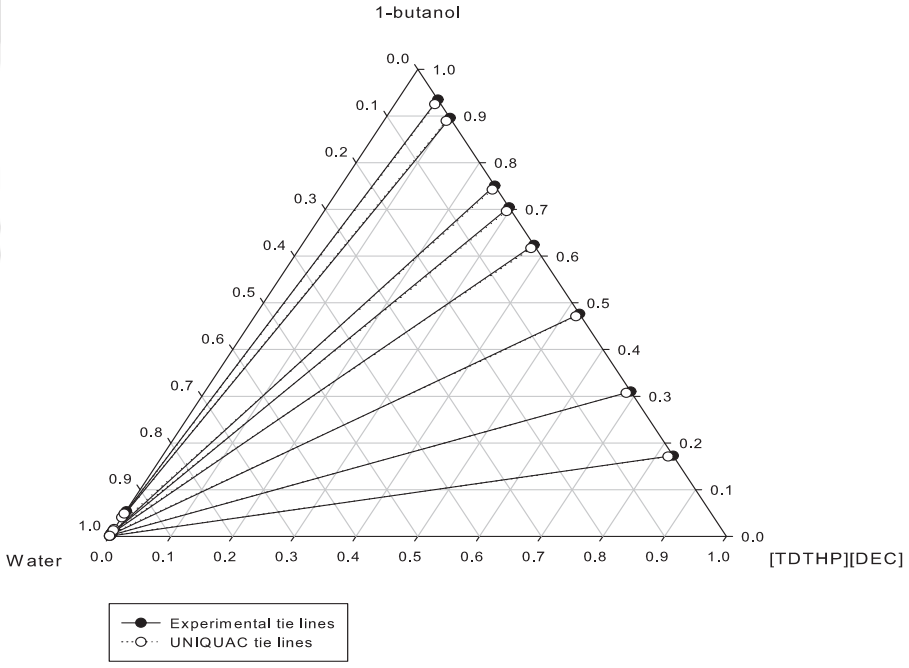

FIGURE 3.27: Experimental and UNIQUAC correlated tie lines for the system: [TDTHP][DEC] (1) - 1-Butanol (2) - Water (3) at T=298.15 K and p=1 atm.

3.5.2 COSMO-SAC Model (COnductor like Screening MOdel-Segment Activity Coefficient)

In the original COSMO-SAC [117] model, the activity coefficient $\gamma_{i/s}$ of solute i in the solution s is derived from

$$\ln \gamma_{i/s} = \frac{\Delta \underline{G}^{*res}_{i/s} - \Delta \underline{G}^{*res}_{i/i}}{RT} + \ln \gamma^{SG}_{i/s} \tag{3.16}$$

Where $\Delta \underline{G}^{*res}$ is the restoring solvation free energy, superscript SG denotes Staverman-Guggenheim [94, 117] combinatorial term which is,

$$\ln \gamma^{SG}_{i/s} = \ln \frac{\phi_i}{x_i} + \frac{z}{2} q_i \ln \frac{\theta_i}{\phi_i} + l_i - \frac{\phi_i}{x_i} \sum_j x_j l_j \tag{3.17}$$

where $\theta_i = \frac{x_i q_i}{\sum_j x_j q_j}$, $\phi_i = \frac{x_i r_i}{\sum_j x_j r_j}$ and $l_i = \frac{z}{2}(r_i - q_i) - (r_i - 1)$. Here, x_i is the mole fraction of component i, r_i and q_i are the normalized volume and surface parameters for i; z is the coordination number, usually taken to be 10. The summation is over the species of the mixture. The restoring solvation free energy accounts for nonideality due to the difference in molecular interactions, which are calculated from the interaction between the surface screening charges when the molecules are in close contact. The screening charges are obtained from the first principle solvation calculation of the molecule in a perfect conductor known as COSMO calculation. In the COSMO calculation, the surface of the molecule is dissected in small segments and screening charges are determined for each segment such that the net potential everywhere at the surface is zero (perfect screening). These charges are averaged so as to obtain apparent screening charges to be used in COSMO-SAC model. Initially the quantum chemistry package Gaussian [118] was used

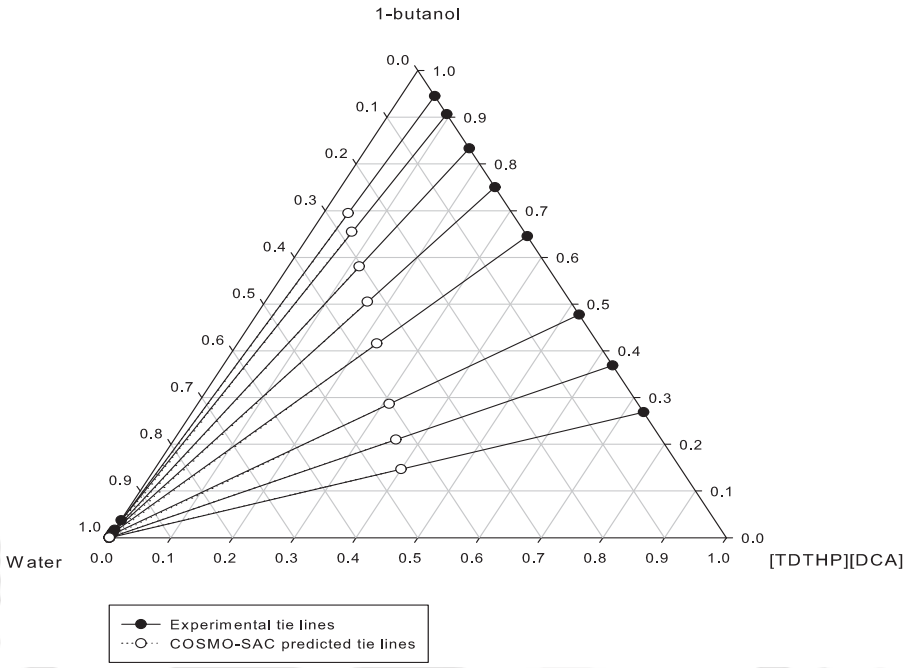

FIGURE 3.28: Experimental and COSMO-SAC predicted tie lines for the system: [TDTHP][DCA] (1) - 1-Butanol (2) - Water (3) at T=298.15 K and p=1 atm.

for geometry optimization of all species. The geometries were optimized at B3LYP level of theory [119] and 6-31G* basis set. Using the optimized geometry, COSMO calculation was done at P BVP86 level of density functional theory [120]. The triple zeta valence potential (TZVP) [121] basis set in combination with the density fitting basis set DGA1 [122] was used for the COSMO calculation. The resulting geometries, energies and surface screening charges densities of the individual molecules are then stored in a COSMO file. In the case of IL, the COSMO file was generated separately for the cation and anion. Based on the COSMO file, the sigma profiles for the molecules have been calculated as explained in the original reference [123]. The averaging algorithm is given by

$$\sigma_m = \frac{\sum_n \sigma_n^* \frac{r_n^2 r_{eff}^2}{r_n^2 + r_{eff}^2} \exp\left(-\frac{d_{mn}^2}{r_n^2 + r_{eff}^2}\right)}{\sum_n \frac{r_n^2 r_{eff}^2}{r_n^2 + r_{eff}^2} \exp\left(-\frac{d_{mn}^2}{r_n^2 + r_{eff}^2}\right)} \tag{3.18}$$

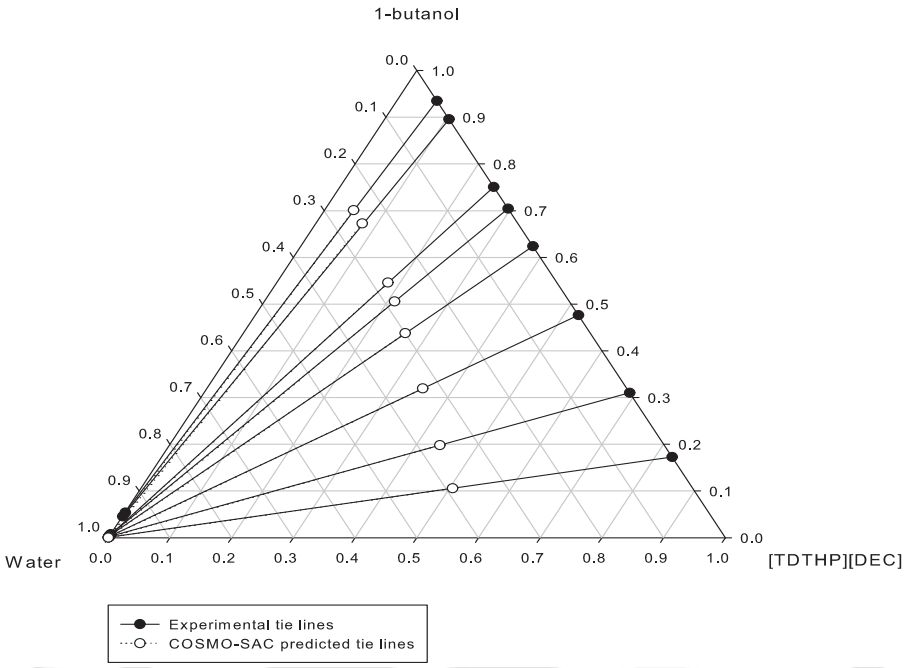

FIGURE 3.29: Experimental and COSMO-SAC predicted tie lines for the system: [TDTHP][DEC] (1) - 1-Butanol (2) - Water (3) at T=298.15 K and p=1 atm.

where $r_{eff} = \sqrt{a_{eff}/\pi}$, is the radius of the standard surface segment, $r_n = \sqrt{a_n/\pi}$, is the radius of the segment n and d_{mn} is the distance between segment m and n. σ^* and σ^* are charge density after and before charge averaging process; $\sigma_n = q_n/a_n$ is charge density of segments. The three dimensional screening charge density distribution is quantified using histogram known as σ-profile $p(\sigma)$, which is the probability of finding a surface segment with screening charge density σ i.e. $p(\sigma) = A_i(\sigma)/A_i$ where $A_i(\sigma)$ is the surface area with a charge density of value σ and a_i is the total surface area of species i. For a mixture, the σ-profile is determined from the area weighted average of contributions from all its components, i.e.

$$p_s(\sigma) = \frac{\sum_i x_i A_i p_i(\sigma)}{\sum_i x_i A_i} \tag{3.19}$$

The exchange energy contains contributions from electrostatic interactions, which is referred as misfit energy E_{mf}, and is calculated by electrostatic interactions between a pair of segments and hydrogen bonding energy E_{hb}, which occurs when an electropositive atom (hydrogen) forms additional bonds with an electronegative atom like oxygen, nitrogen or fluorine. The expressions of these two terms are given by Eqs. 3.20- 3.21.

$$E_{mf} = \left(\alpha'/2\right)\left(\sigma_m + \sigma_n\right)^2 \tag{3.20}$$

$$E_{hb} = c_{hb} \min\left[0, \max\left(0, \sigma_{acc} - \sigma_{hb}\right) \min\left(0, \sigma_{don} + \sigma_{hb}\right)\right] \tag{3.21}$$

$$\Delta W\left(\sigma_m, \sigma_n\right) = E_{mf} + E_{hb} \tag{3.22}$$

where α' is a constant for the misfit energy that is calculated from the surface area of a standard segment (a_{eff}=6.32 Å^2) [124].

$$\alpha' = \frac{0.64 \times 0.3 \times a_{eff}^{3/2}}{\varepsilon_0} \tag{3.23}$$

Here $\varepsilon_0 = 2.395 \times 10^{-4}$ $(e^2 mol)/(kcal\text{Å})$ and c_{hb}=75006 $(kcal\text{Å}^4)/(mole^2)$ [124] is a constant for the hydrogen bonding interaction. σ_{hb}=0.0084 $e/\text{Å}^2$ [124] is cutoff value for hydrogen bonding interactions; σ_{acc} and σ_{don} are the larger and smaller values of σ_m and σ_n; max and min indicate that the larger and smaller values of their arguments are used, respectively. The segment activity coefficient $\Gamma(\sigma)$ is defined as;

$$\ln \Gamma_s\left(\sigma_m\right) = -\ln\left\{\sum_{\sigma_n} p_s\left(\sigma_n\right) \Gamma_s\left(\sigma_n\right) \exp\left[-\frac{\Delta W\left(\sigma_m, \sigma_n\right)}{kT}\right]\right\} \tag{3.24}$$

This equation is solved iteratively. Finally, we obtain the restoring free energy of molecule in solvent or mixture as

$$\frac{\Delta G_{i/s}^{*res}}{RT} = n_i \sum_{\sigma_m} p_i(\sigma_m) \ln \Gamma_s(\sigma_m) \tag{3.25}$$

The activity coefficient is then calculated by :

$$\ln \gamma_{i/S} = n_i \sum_{\sigma_m} p_i(\sigma_m) \left[\ln \Gamma_S(\sigma_m) - \ln \Gamma_i(\sigma_m)\right] + \ln \gamma_{i/S}^{SG} \tag{3.26}$$

This equation is referred as the COSMO-SAC model. Once the activity coefficient is known, then the prediction of tie lines or mole fractions in either phase involving LLE can be predicted using the Eqs. 3.6-3.13 . The COSMO-SAC predicted tie line compositions gave RMSD deviation of 18.67% for the system containing [TDTHP][DCA] (Fig. 3.28). Similarly RMSD for the system containing [TDTHP][DEC] was 16.21% (Fig. 3.29).

4

Simultaneous Extraction of Ethanol and Butanol from Aqueous Solution

4.1 Introduction

As discussed earlier, acetone is highly volatile, it can be removed by simple distillation followed by alcohol extraction. Therefore in the present chapter, we have attempted to extract ethanol and butanol from water using [TDTHP][Phosph] and [TDTHP][DCA]. ILs have been found to be a better solvent for extraction of both alcohols [53, 125–127]. We have generated Quaternary LLE equilibrium data for two quaternary systems namely, [TDTHP][Phosph](1)- Ethanol(2)- 1-butanol(3)- Water(4) and [TDTHP][DCA](1)- Ethanol(2)- 1-butanol(3)- Water(4). The experimental data were then correlated with NRTL, UNIQUAC and COSMO-SAC models.

4.2 Experimental Procedure

4.2.1 Chemicals and Materials

Ethanol (Sigma Aldrich, Germany) was supplied at 99% purity. Ethanol purity was verified by measuring its density at atmospheric pressure with Anton Par DMA-4500 digital vibrating U-tube densitometer. The obtained densities was within ±1% of the reported values. The purity and purification methods for other chemicals are described in Table 3.1.

4.2.2 Process Analysis

The sample preparation and experimental procedure are described in Chapter 3. Considering the ABE product concentration, three feed points were also prepared with

same ethanol to butanol molar ratio (0.268) but different water to IL molar ratio (9^{th}, 10^{th} and 11^{th} tie line of Table 4.1). For both quaternary systems, the methylene group (-CH_2) attached to hydroxyl group (-OH) in both alcohols show separate peaks at ∼3.65 ppm (Figs. 4.1-4.4) in both phases hence these peaks were used to characterize both alcohols. The peaks were distinguished as a triplet peak for butanol and quartet peak for ethanol as per n+1 rule conjunction with Pascal's triangle [128] (Fig. 4.5).

The characterization of water and ILs have already been described in Chapter 3. For the measurement of single hydrogen representing IL, the total area represented by IL (by subtracting total area of all components - total area represented by all hydrogens of other three components except IL) was divided by total number of hydrogen in respective IL as shown in Figs. 4.1-4.4. The concentration of each compound in individual phase was calculated by using the single hydrogen peak area of each component i (H_i) as given in Eq. 4.1.

$$x_i = \frac{H_i}{\sum_{i=1}^{4} H_i} \tag{4.1}$$

where x_i is the mole fraction of individual component.

4.2.3 Results and Discussions

Liquid Liquid Equilibrium (LLE) data were measured at 298.15 K and 1 atm for both quaternary systems namely [TDTHP][Phosph] (1)- ethanol (2)- 1-butanol (3) - water (4) (Fig. 4.6) and [TDTHP][DCA] (1)- ethanol (2)- 1-butanol (3) - water (4) (Fig. 4.7). From both figures, It can be seen that few tie lines are pointing towards ethanol apex representing more extraction of ethanol as compared to butanol. The extraction efficiency

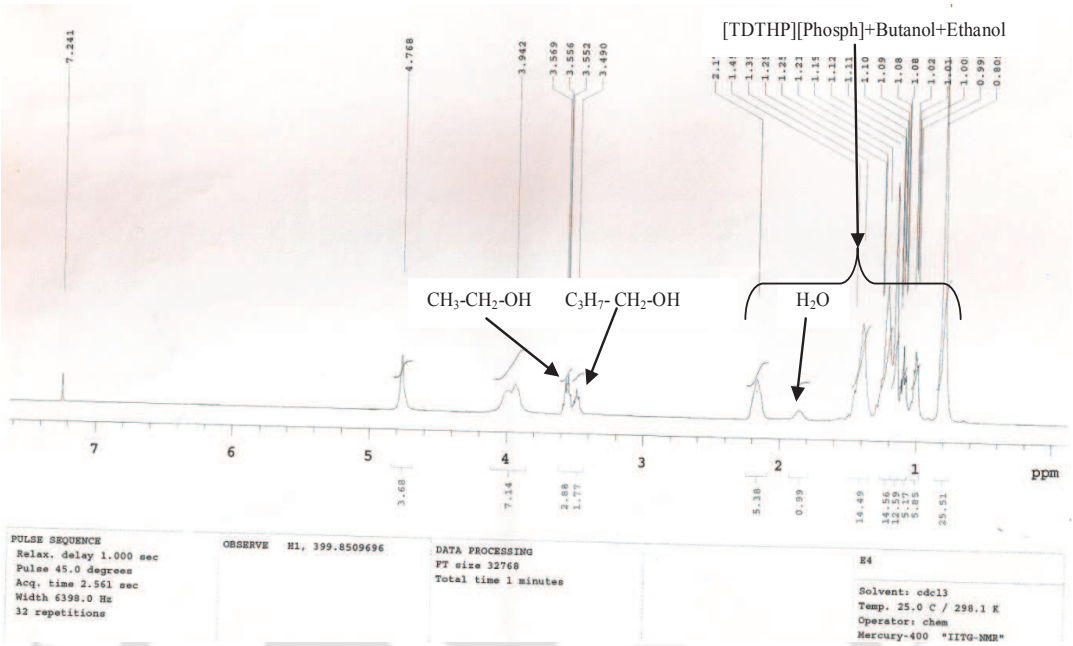

FIGURE 4.1: Extract phase ^{1}H NMR spectra for the system: [TDTHP][Phosph] (1) - Ethanol (2) - 1-Butanol (3) - Water (4) at T=298.15 K and p=1 atm.

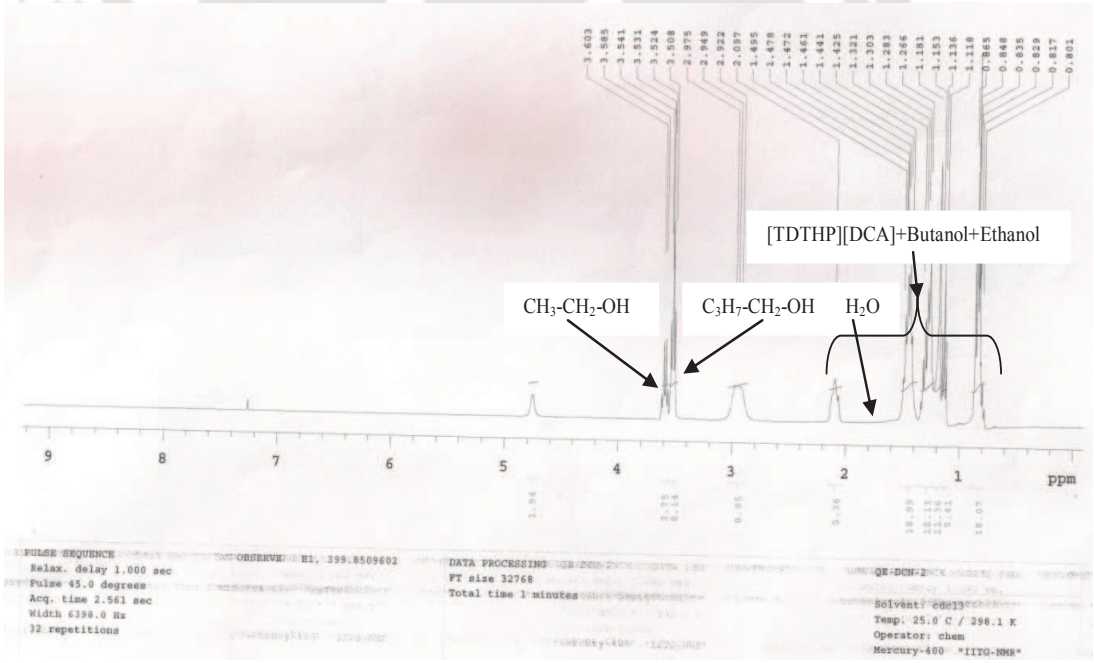

FIGURE 4.2: Extract phase ^{1}H NMR spectra for the system: [TDTHP][DCA] (1) - Ethanol (2) - 1-Butanol (3) - Water (4) at T=298.15 K and p=1 atm.

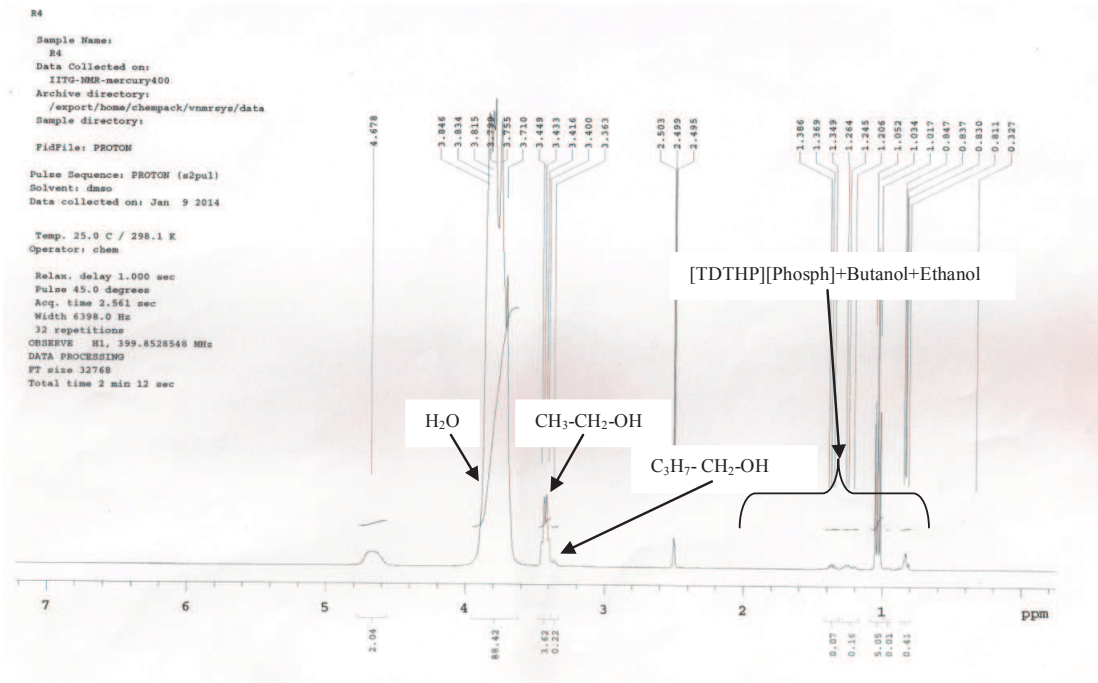

FIGURE 4.3: Raffinate phase ^{1}H NMR spectra for the system: [TDTHP][Phosph] (1) - Ethanol (2) - 1-Butanol (3) - Water (4) at T=298.15 K and p=1 atm.

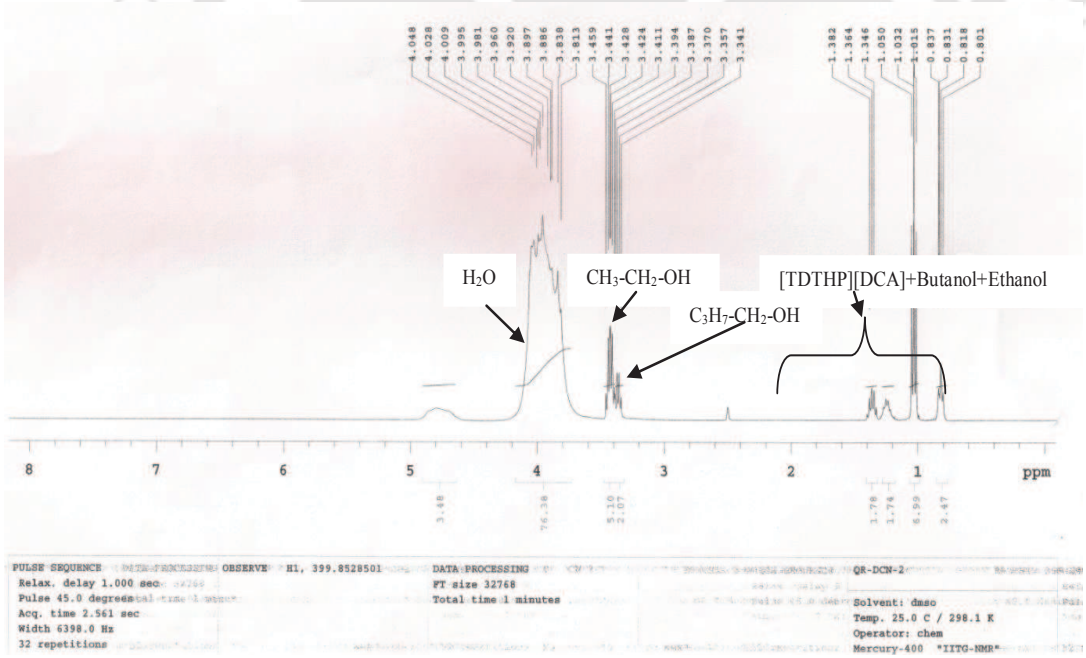

FIGURE 4.4: Raffinate phase ^{1}H NMR spectra for the system: [TDTHP][DCA] (1) - Ethanol (2) - 1-Butanol (3) - Water (4) at T=298.15 K and p=1 atm.

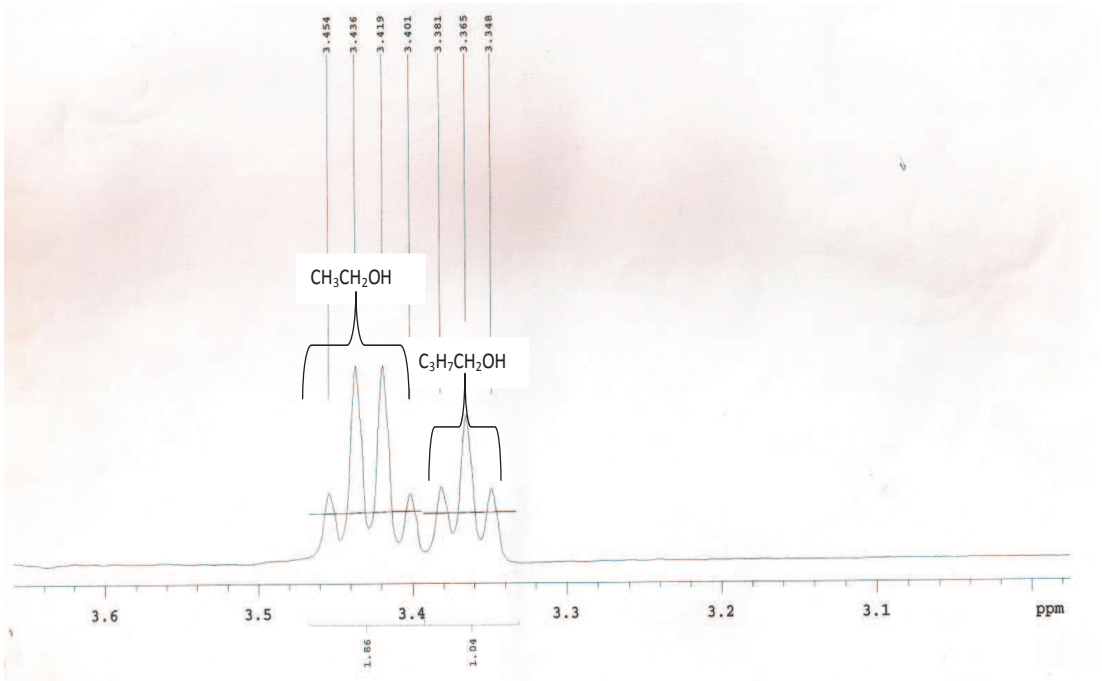

FIGURE 4.5: Alcohol peaks on ^{1}H NMR spectra expansion at T=298.15 K and p=1 atm.

for both alcohols were measured for different feed mole ratio of alcohols. The separation efficiency is represented by Distribution coefficient (β) and selectivity (S_i) for both alcohols (Eqs. 3.2-3.3 in Chapter 3).

For a specific degree of separation, the amount of solvent required is less in case of larger distribution coefficient. The butanol distribution coefficient (β_B) varied in the range of 3.55-122.5 and 5.37-43.84 for [TDTHP][Phosph] and [TDTHP][DCA] respectively. The ethanol distribution coefficient (β_E) varied within 3.31-20.36 and 3.09-12.86 for [TDTHP][Phosph] and [TDTHP][DCA] respectively (Table 4.1). Selectivity signifies the solvent ability for solute extraction. Higher selectivity indicates more solute diffusion from raffinate to extract phase resulting in better separation. For [TDTHP][Phosph] containing system, the butanol selectivity varied within 41.27-3708.99 which is higher than ethanol selectivity i.e 38.50-2583.93.

TABLE 4.1: Experimental tie lines and feed ratio of IL (1)- Ethanol (2)- 1-butanol (3)- Water (4) at T=298.15 K and p=1 atm.

Sr. No.	Extract Phase composition				Raffinate Phase composition				β_B	β_E	S_B	S_E	Feed Mole Ratio	
	x_{IL}	x_B	x_E	x_W	x_{IL}	x_B	x_E	x_W					E/B	W/IL
[TDTHP][Phosph] (1) - Ethanol (2) - 1-Butanol (3) - Water (4)														
1	0.109	0.469	0.359	0.063	0	0.012	0.065	0.923	39.08	5.52	572.60	80.92	1.569	36.324
2	0.042	0.497	0.423	0.038	0	0.022	0.056	0.922	22.59	7.55	548.13	183.27	0.785	36.324
3	0.221	0.245	0.398	0.137	0	0.002	0.039	0.958	122.50	10.21	856.61	71.36	2.615	19.373
4	0.051	0.649	0.273	0.027	0	0.016	0.042	0.943	40.56	6.50	1416.68	227.02	0.549	26.907
5	0.110	0.259	0.566	0.065	0	0.073	0.171	0.756	3.55	3.31	41.27	38.50	4.969	55.883
6	0.006	0.424	0.538	0.033	0	0.024	0.144	0.832	17.67	3.74	445.41	94.20	3.138	36.324
7	0.042	0.361	0.550	0.047	0	0.041	0.101	0.858	8.80	5.45	160.74	99.41	1.569	48.432
8	0.023	0.244	0.696	0.037	0	0.034	0.191	0.775	7.18	3.64	150.32	76.33	3.661	72.648
9	0.015	0.456	0.509	0.02	0	0.016	0.025	0.959	28.50	20.36	1366.58	976.26	0.268	36.324
10	0.004	0.516	0.473	0.007	0	0.019	0.025	0.956	27.16	18.92	3708.99	2583.93	0.268	72.648
11	0.009	0.672	0.296	0.023	0	0.014	0.021	0.965	48.00	14.10	2013.91	591.39	0.268	60.540
[TDTHP][DCA] (1) - Ethanol (2) - 1-Butanol (3) - Water (4)														
1	0.157	0.464	0.379	0	0	0.027	0.075	0.898	17.19	5.05	-	-	1.569	25.458
2	0.107	0.614	0.28	0	0	0.025	0.061	0.914	24.56	4.59	-	-	0.785	25.458

3	0.367	0.267	0.366	0	0	0.007	0.057	0.935	38.14	6.42	-	-	2.615	13.578
4	0.096	0.653	0.251	0	0	0.023	0.05	0.927	28.39	5.02	-	-	0.549	18.858
5	0.068	0.773	0.159	0	0.008	0.144	0.046	0.802	5.37	3.46	-	-	0.330	23.761
6	0.142	0.289	0.568	0	0.001	0.044	0.159	0.797	6.57	3.57	-	-	3.138	25.458
7	0.103	0.458	0.439	0	0	0.051	0.126	0.824	8.98	3.48	-	-	1.569	33.944
8	0.151	0.276	0.572	0	0	0.029	0.185	0.786	9.52	3.09	-	-	4.969	39.167
9	0.042	0.833	0.125	0	0	0.019	0.021	0.96	43.84	5.95	-	-	0.268	36.369
10	0.053	0.793	0.154	0	0	0.02	0.034	0.946	39.65	4.53	-	-	0.268	72.738
11	0.018	0.712	0.27	0	0	0.018	0.021	0.961	39.56	12.86	-	-	0.268	60.615

where x_W, x_B, x_E and x_{IL} represent mole fraction of water, 1-butanol, ethanol and IL respectively.

E/B and W/IL stand for feed molar ratio of ethanol to 1-butanol and water to IL respectively.

Uncertainty, u (mole fraction) $=\pm 10^{-3}$

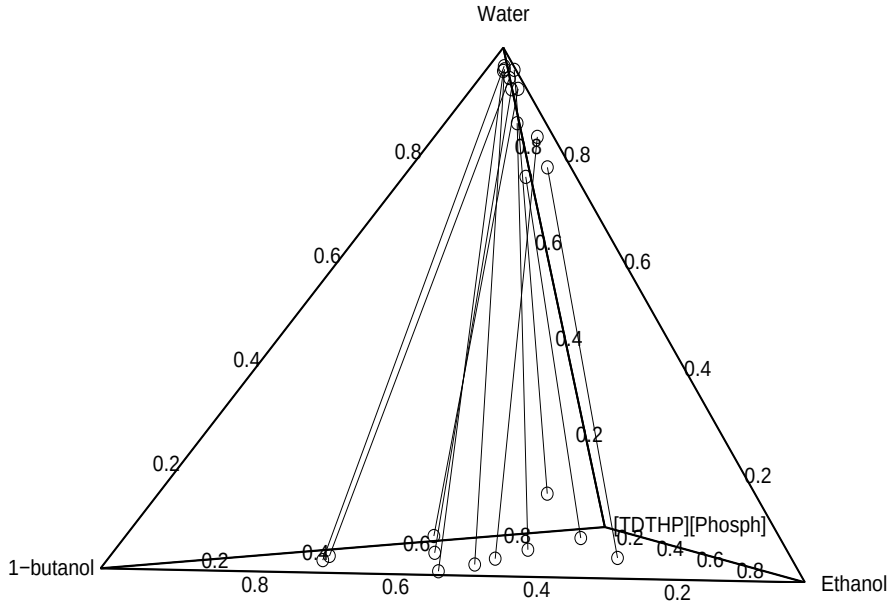

FIGURE 4.6: Experimental tie lines for the system: [TDTHP][Phosph] (1) - Ethanol (2) - 1-Butanol (3) - Water (4) at T=298.15 K and p=1 atm.

In the case of system containing [TDTHP][DCA], the water in extract phase was negligible i.e., within uncertainty values thereby resulting in infinite selectivity. Hence the results are not included in Table 4.1. For system containing [TDTHP][Phosph], the largest β_B (122.50) was found for 2.615 ethanol/butanol molar ratio and 19.373 water/[TDTHP][Phosph] molar ratio. The highest value of β_E was obtained at 0.268 ethanol/butanol molar ratio and 36.324 water/[TDTHP][Phosph] molar ratio. Water/[TDTHP][Phosph] molar ratio of 72.648 gave a higher S_B (3708.99) and S_E (2583.93) for ethanol to butanol molar ratio of 0.268. There was not much improvement in β_B (39.56-43.84) with varying water to [TDTHP][DCA] molar ratio when the ethanol/butanol molar ratio was kept constant at 0.268. On similar lines, β_E gave the largest value (12.86) for ethanol/butanol molar ratio of 0.268 and water/[TDTHP][DCA]

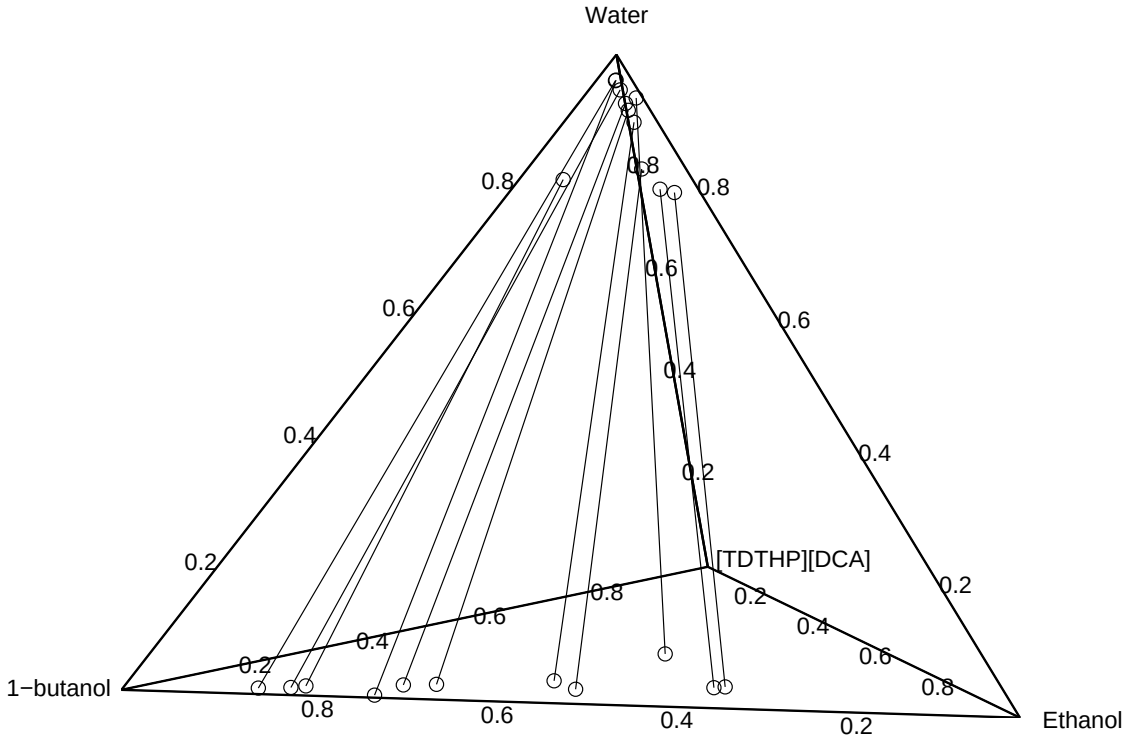

FIGURE 4.7: Experimental tie lines for the system: [TDTHP][DCA] (1) - Ethanol (2) - 1-butanol (3) - Water (4) at T=298.15 K and p=1 atm.

molar ratio of 60.615. It can be observed that β_B is always higher than β_E for both systems(Table. 4.1). It indicates both ILs are more selective for butanol separation than ethanol. This is primarily due to the lesser polarity index of butanol (4) than ethanol (5.2) hence dissolving easily in non polar ILs. β_B was found to be twelve times higher than β_E for lowest mole ratio (19.4) of water/[TDTHP][Phosph]. For lowest mole ratio (13.6) of water/[TDTHP][DCA], β_B was six times higher than β_E. In both cases, ethanol to butanol feed mole ratio was maintained at 2.6. For constant value of water/[TDTHP][Phosph] molar ratio of 36.32, β_E was found to increase with decreasing ethanol to butanol feed ratio. However β_B did not follow any specific trend. It was noted that β_B was seven times higher than β_E for ethanol to butanol feed molar ratio of 1.57. Similarly for water to [TDTHP][DCA] molar ratio of 25.46, β_B increased with

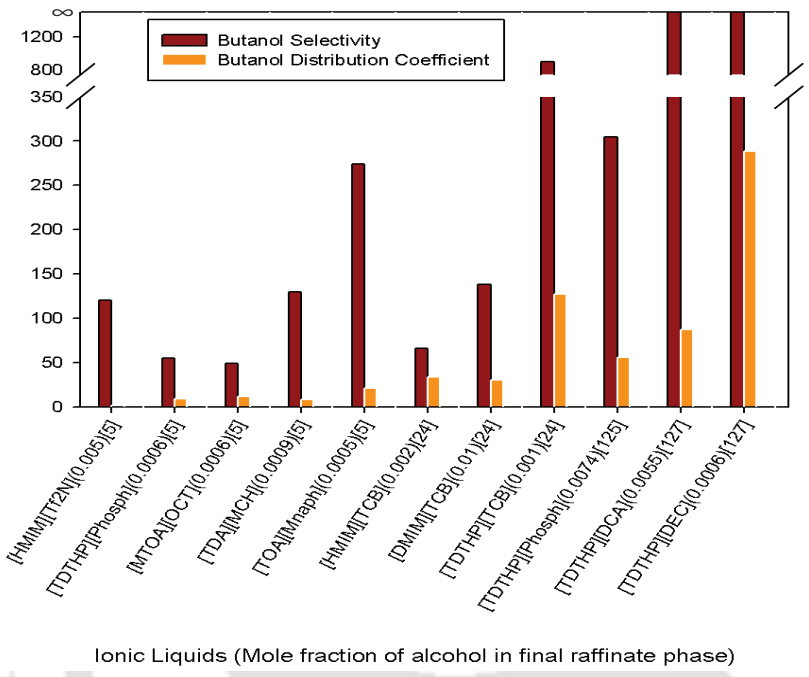

(A) Ternary systems

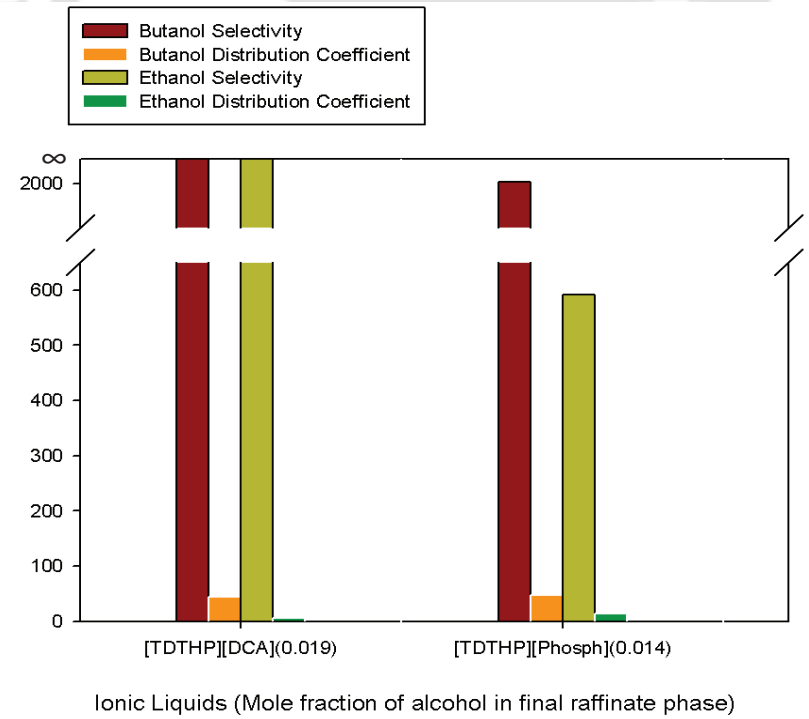

(B) Quaternary systems

FIGURE 4.8: Comparison of alcohol selectivity and distribution coefficients from (a)literature, (b)the present work

TABLE 4.2: NRTL and UNIQUAC interaction parameters for quaternary systems at T=298.15 K and p=1 atm.

i-j	NRTL Model Parameters				UNIQUAC Model Parameters			
	τ_{ij}	τ_{ji}	Obj^*	%RMSD**	A_{ij}/K	A_{ji}/K	Obj^*	%RMSD**
[TDTHP][Phosph] (1)- Ethanol (2)- 1-Butanol (3)- Water (4)								
1-2	19.85	17.20	-1.42 x10^{-3}	0.47	812.47	-621.74	-4.12 x10^{-3}	0.80
1-3	19.98	1.76			769.88	-603.32		
1-4	8.41	6.83			1493.6	-610.46		
2-3	6.97	2.07			-83.66	960.18		
2-4	14.15	5.07			894.60	-17.90		
3-4	11.11	3.47			754.54	77.52		
[TDTHP][DCA] (1)- Ethanol (2)- 1-Butanol (3)- Water (4)								
1-2	27.02	-27.60	-3.5 x10^{-4}	0.23	-276.38	252.26	-3.68 x10^{-3}	0.76
1-3	4.14	-12.17			-613.00	409.74		
1-4	9.97	-17.40			1495.30	-6.67		
2-3	1.21	3.22			-570.56	732.36		
2-4	11.33	3.49			1249.40	-86.93		
3-4	10.36	3.76			1114.40	-448.59		

* Calculated by Eq. 3.14

** Calculated by Eq. 3.15

decreasing ethanol to butanol feed molar ratio. β_B was 5.4 times higher than β_E at ethanol to butanol molar ratio of 0.78. These values are much higher than obtained by Kubiczek and Kamiński [51] for 1-hexyl-3-methylimidazolium hexafluorophosphate and 1-butyl-3-methylimidazolium bis(trifluoromethylsulfonyl)imide ILs.

For NRTL, UNIQUAC and COSMO-SAC models, modelling procedure is described in Chapter 3. For ethanol, UNIQUAC parameters, volume parameter (r) and surface

area parameter (q) were taken as 2.11 and 1.97 respectively. Here the maximization would occur with respect to 12 binary interaction parameters (τ_{ij} and A_{ij} for NRTL and UNIQUAC model respectively). The number of generation and the number of population (possible random solutions) in GA were specified at 200 and 100 [116]. Each solution represents the set of twelve parameters (A_{12}/τ_{12}, A_{13}/τ_{13}, A_{14}/τ_{14}, A_{21}/τ_{21}, A_{23}/τ_{23}, A_{24}/τ_{24}, A_{31}/τ_{31}, A_{32}/τ_{32}, A_{34}/τ_{34}, A_{41}/τ_{41}, A_{42}/τ_{42}, A_{43}/τ_{43}).

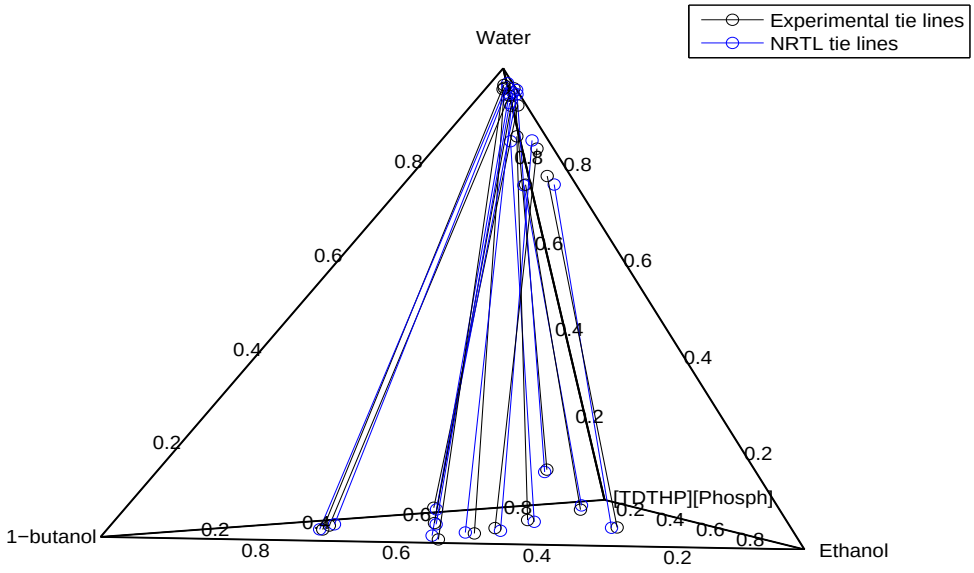

FIGURE 4.9: Experimental and NRTL predicted tie lines for the system: [TDTHP][Phosph] (1) - Ethanol (2) - 1-Butanol (3) - Water (4) at T=298.15 K and p=1 atm.

GA operators (crossover and mutation) alter the random solution after each iteration till the termination criteria is satisfied. The optimization results corresponding to the lowest *Obj* are reported in Table 4.2. For both quaternary systems, the tie lines predicted by NTRL and UNIQUAC are plotted with experimental tie lines in Figs. 4.9- 4.12. For system containing [TDTHP][Phosph], NRTL and UNIQUAC models gave RMSD values of 0.47% and 0.80% respectively. Similarly, NRTL and UNIQUAC models were

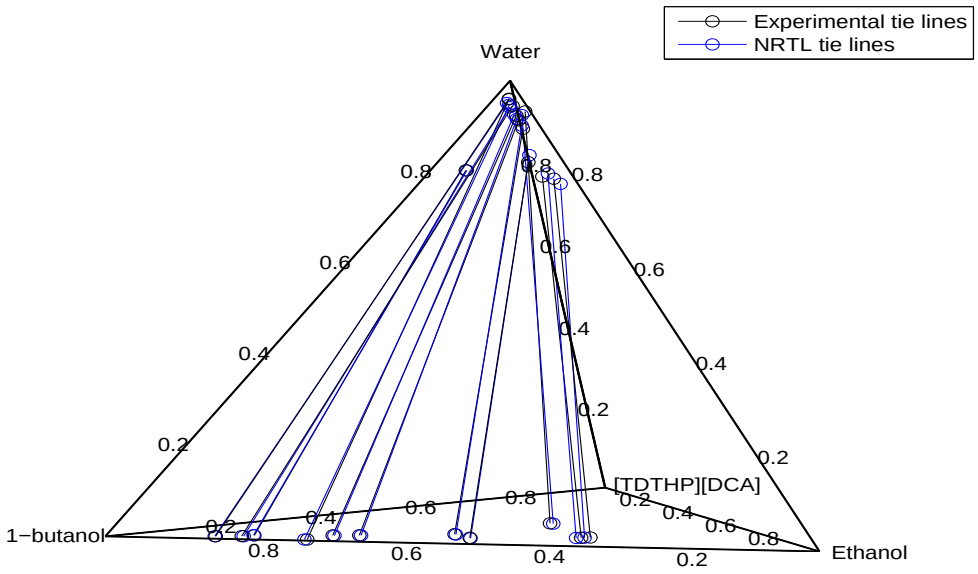

FIGURE 4.10: Experimental and NRTL predicted tie lines for the system: [TDTHP][DCA] (1) - Ethanol (2) - 1-Butanol (3) - Water (4) at T=298.15 K and p=1 atm.

correlated for [TDTHP][DCA] containing system with RMSD values at 0.23% and 0.76% respectively (Table 4.2). The COSMO-SAC deviation found for system containing [TDTHP][DCA] was 10.45% (Fig. 4.13). From the comparative study in Fig. 4.13, it can be seen that the deviation is mainly due to the extract phase composition. The raffinate phase compositions agrees reasonably well with COSMO-SAC model. It should be noted that we have not altered the COSMO-SAC parameters i.e effective area of a segment, misfit constant, cut off for hydrogen bonding and the hydrogen bonding constants for predicting the quaternary systems [94, 123, 129].

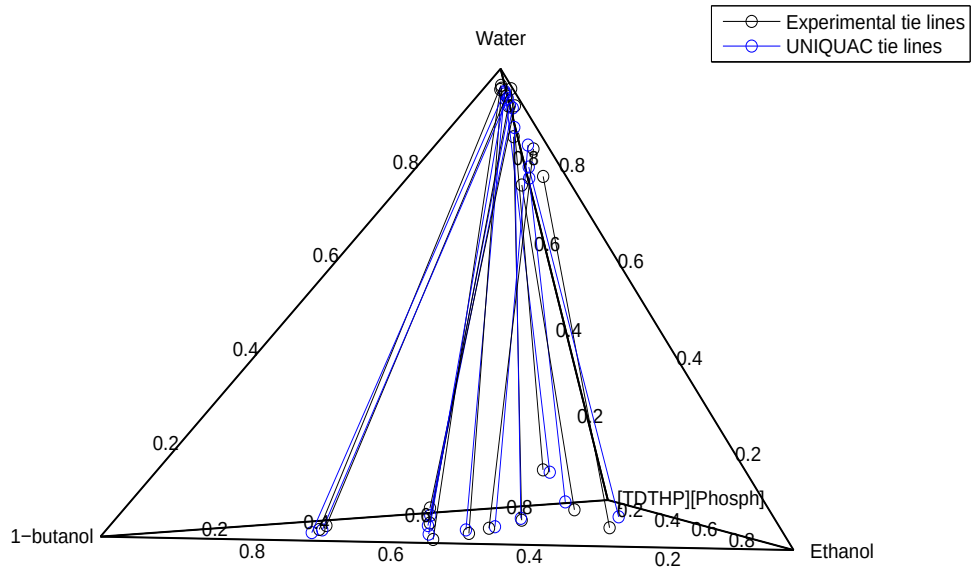

FIGURE 4.11: Experimental and UNIQUAC predicted tie lines for the system: [TDTHP][Phosph] (1) - Ethanol (2) - 1-Butanol (3) - Water (4) at T=298.15 K and p=1 atm.

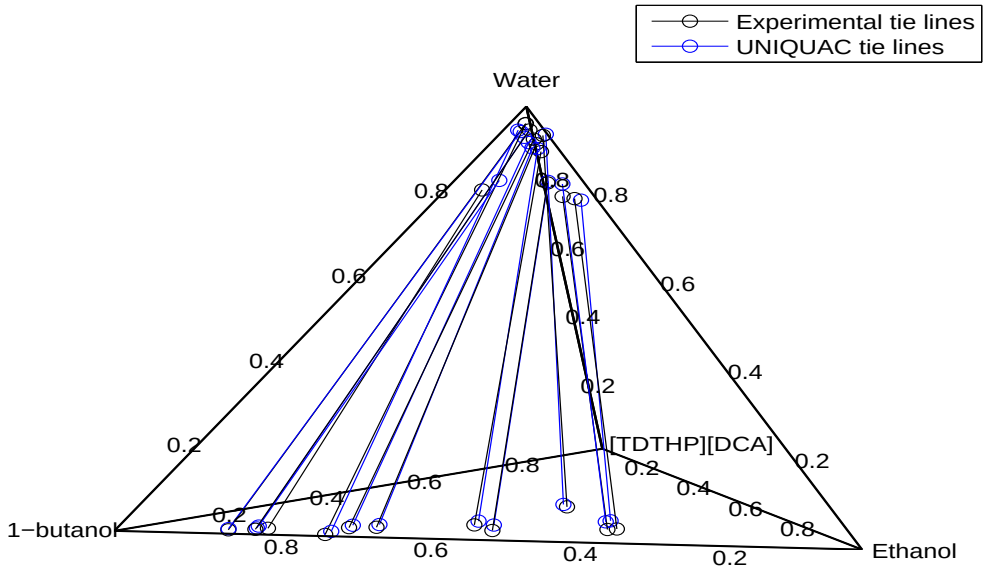

FIGURE 4.12: Experimental and UNIQUAC predicted tie lines for the system: [TDTHP][DCA] (1) - Ethanol (2) - 1-Butanol (3) - Water (4) at T=298.15 K and p=1 atm.

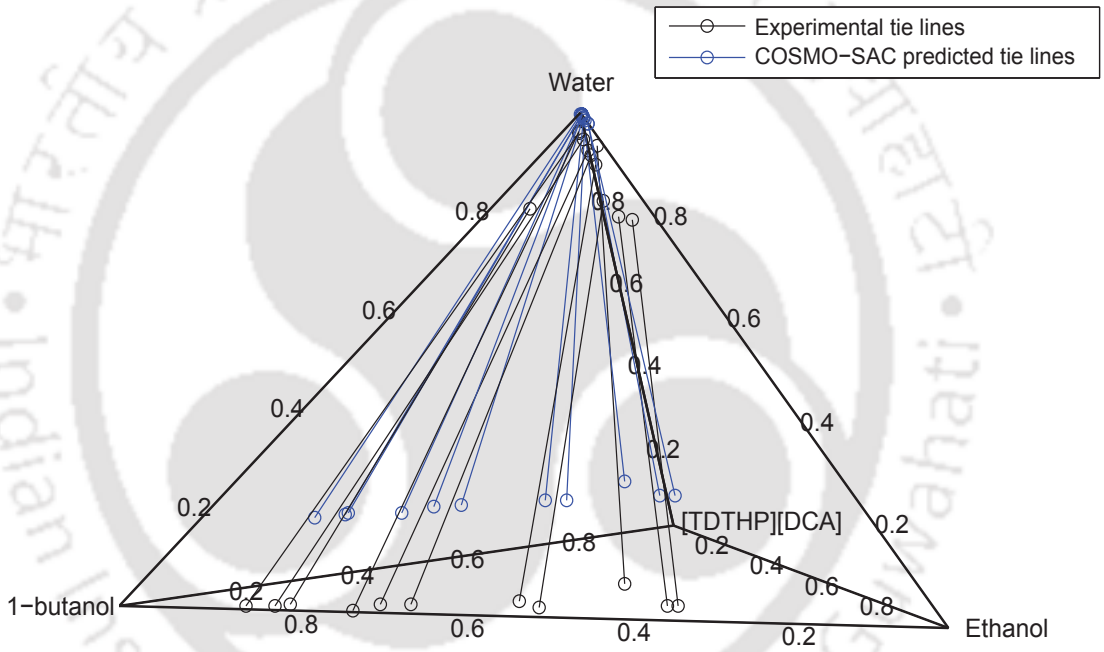

FIGURE 4.13: Experimental and COSMO-RS predicted tie lines for the system: [TDTHP][DCA] (1) - Ethanol (2) - 1-Butanol (3) - Water (4) at T=298.15 K and p=1 atm.

5

Optimization of Multistage Extractor

5.1 Introduction

Low volatile Phosphonium ILs have proved to be better solvents as compared to volatile organic solvents from our LLE experiments in Chapters 3 and 4. However the experiments were carried out in laboratory scale. The separation has not been implemented on an industrial scale till date. For transforming laboratory data into industrial application, process optimization study is necessary. In past, many popular stochastic algorithms such as Genetic Algorithm (GA) [130], Simulated Annealing (SA) [131], Particle Swarm Optimization (PSO) [132, 133], Ant Colony Optimization (ACO) [134, 135], Differential Evolution (DE) [136, 137] and Self-Organising Migrating Algorithm (SOMA) [138] have been investigated for optimization in science and engineering.

PSO is an evolutionary algorithm based on social behavior of birds in swarm. Initial position and velocity of each particle are initiated randomly. During simulation, each particle in swarm (population) updates its position and velocity based on its experience as well as neighbors' experience within the search space. PSO is robust as it evaluates fewer function values during simulation as compared to GA [139, 140]. Ethni et al. [141] have shown that PSO shows more success rate to reach the target optimum value as compared to SA. PSO is also more preferable than ACO due to high success rate and solution quality [142]. Keeping the shortcoming of other methodology in mind, we have chosen PSO technique for optimizing the flow rate and number of stages in a multistage extractor.

A multistage extractor containing more than two components requires detailed design like temperature, pressure, flow rate and composition on each stage. These are achieved

by solving material balance equations (M), phase equilibrium relation (E), mole fraction summation for each stage (S) and energy balance equations (H) better known as *MESH* Equations. In this work, the traditional Isothermal Sum Rate (ISR) method [143] has been considered for the stagewise calculation. We have tried to obtain the optimum number of stages and solvent flow rate by minimizing the multistage extractor cost for extraction of butanol and ethanol from aqueous solution using ILs; [TDTHP][DCA] and [TDTHP][Phosph].

5.2 Computational details

5.2.1 Isothermal Sum Rate (ISR) algorithm

A hypothetical column (Fig. 5.1) is considered in the model to formulate the optimization problem. The solvent enters at the bottom and feed enters at the top of the tray. The raffinate and extract compositions leaving each tray are assumed to be in equilibrium. Figure 5.2 shows the algorithm for Tsuboka-Katayama ISR method [143, 144]. The extractor model is considered isothermal as stream temperature is uniform and heat of mixing is negligible. The number of stages (N) and solvent (IL) flow rate (Sol) are input variables for ISR algorithm that are decided by PSO algorithm described in the next section. The feed (water and solutes) flow rate was taken as 100 kmol/hr. The feed compositions are 0.99767 mole fraction water, 0.002 mole fraction butanol and 0.00033 mole fraction ethanol which are identical with output composition of ABE fermentation process. Initially the feed, extract and raffinate flow rates; and compositions on each tray were derived based on linear interpolation with assumption of complete separation.

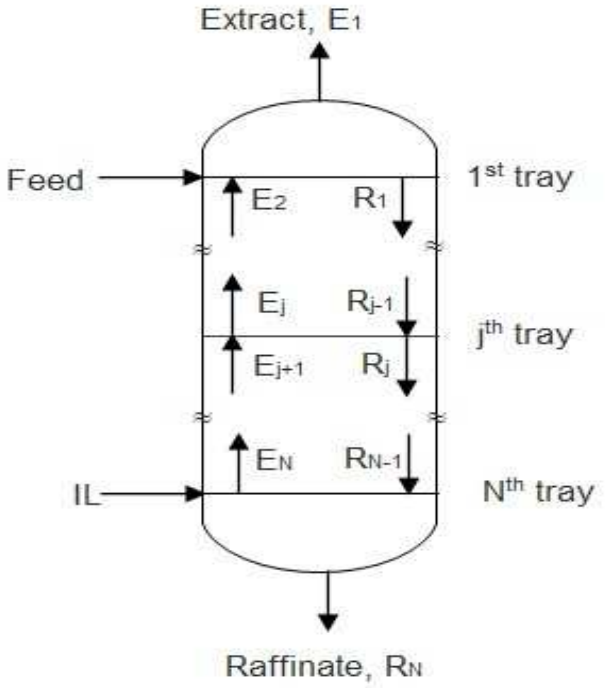

FIGURE 5.1: Hypothetical multistage Liquid-Liquid Extractor

The solvent was also assumed to be completely immiscible with water. The activity coefficients for each component (i) in both phases over every stage were then obtained from NRTL model. Binary Interaction Parameters (BIP) were derived from NRTL model and were directly regressed from our previous experimental work. BIP parameters for both quaternary systems are shown in Table 4.2 (Chapter 4). The distribution coefficients were then obtained by Eq. 5.1.

$$K_{i,j} = \frac{\gamma_{i,j}^{R}}{\gamma_{i,j}^{E}} \tag{5.1}$$

Here superscripts E and R indicate the extract (Solvent rich) and raffinate (Water rich) phases, respectively. $\gamma_{i,j}$ is the activity coefficient of component i in respective phase

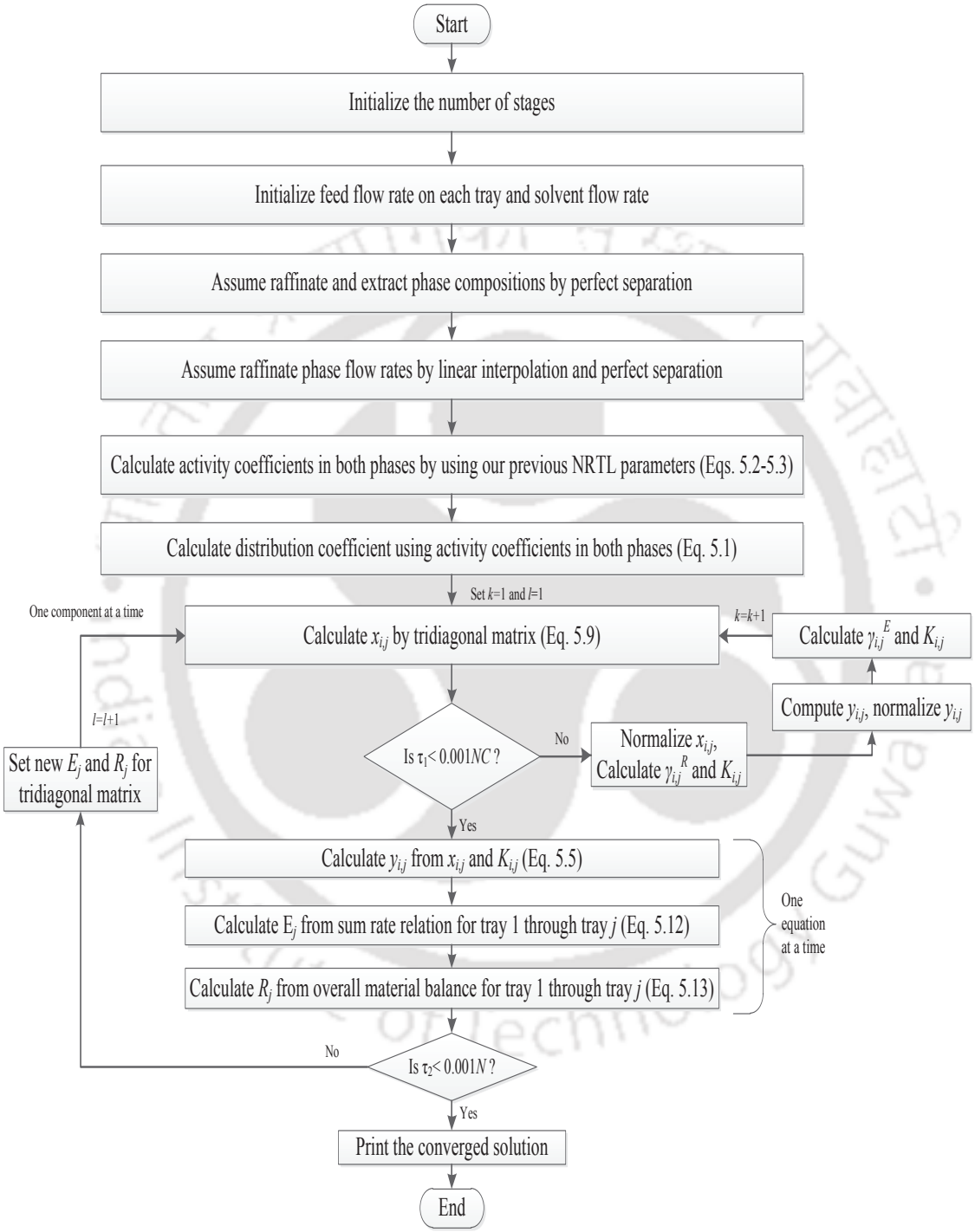

FIGURE 5.2: Tsuboka-Katayama ISR algorithm for liquid-liquid extraction

over j^{th} tray. Here $\gamma_{i,j}$'s are obtained from the BIP values i.e.

$$\gamma_{i,j}^{R} = f\left(\tau_{ia}, x_{i,j}, T\right) \tag{5.2}$$

and

$$\gamma_{i,j}^{E} = f\left(\tau_{ia}, y_{i,j}, T\right) \tag{5.3}$$

where T=298.15 K. $x_{i,j}$ and $y_{i,j}$ represent the compositions of component i in raffinate and extract phases, respectively from stage j. τ_{ia} is BIP for pair of components i and a. The overall material balance for component i over j^{th} tray is then given by

$$R_{j-1}x_{i,j-1} + E_{j+1}y_{i,j+1} + F_j z_{i,j} - R_j x_{i,j} - E_j y_{i,j} = 0 \tag{5.4}$$

where subscript i and j represent the component and the tray respectively. E and R represent the extract and raffinate flow rate in kmol/hr from a specific tray. F stands for feed flow rate in kmol/hr over a specific tray. The equilibrium relation for component i over j is given by

$$y_{i,j} = K_{i,j}x_{i,j} \tag{5.5}$$

From Eqs. 5.4 and 5.5, we have,

$$R_{j-1}x_{i,j-1} - (R_j + E_j K_{i,j})x_{i,j} + E_{j+1}K_{i,j+1}x_{i,j+1} = -F_j z_{i,j} \tag{5.6}$$

For the top (j=*1*) and bottom (j=N) stages, the raffinate (R_0) and extract(E_{N+1}) flow rates are zeros, respectively. So the simplified equations can be written as:

$$-(R_1 + E_1 K_{i,1}) x_{i,1} + E_2 K_{i,2} x_{i,2} = -F_1 z_{i,1} \tag{5.7}$$

$$R_{N-1} x_{i,N-1} - (R_N + E_N K_{i,N}) x_{i,N} = -F_N z_{i,N} \tag{5.8}$$

Eqs. 5.6- 5.8 can be arranged in the form of tridiagonal matrix,

$$\begin{pmatrix} B_1 & C_1 & 0 & 0 & 0 & 0 \\ A_2 & B_2 & C_2 & 0 & 0 & 0 \\ \cdots & \cdots & \cdots & \cdots & \cdots & \cdots \\ 0 & 0 & A_j & B_j & C_j & 0 \\ \cdots & \cdots & \cdots & \cdots & \cdots & \cdots \\ 0 & 0 & 0 & A_{N-1} & B_{N-1} & C_{N-1} \\ 0 & 0 & 0 & 0 & A_N & B_N \end{pmatrix} \begin{pmatrix} x_{i,1} \\ x_{i,2} \\ \cdots \\ x_{i,j} \\ \cdots \\ x_{i,N-1} \\ x_{i,N} \end{pmatrix} = \begin{pmatrix} D_1 \\ D_2 \\ \cdots \\ D_j \\ \cdots \\ D_{N-1} \\ D_N \end{pmatrix} \tag{5.9}$$

where A_j=R_{j-1}, B_j=-(R_j+$E_j K_{i,j}$), C_j=$E_{j+1} K_{i,j+1}$, D_j=$-F_j z_{i,j}$ for j=1 to N tray and component i. The tridiagonal matrix for each component was solved by direct method for sparse linear system in MATLAB. The new values of $x_{i,j}$ were compared with assumed values as per inner loop termination criteria (Eqs. 5.10- 5.11).

$$\tau_1 = \sum_{j=1}^{N} \sum_{i=1}^{C} \left| x_{i,j}^{(k-1)} - x_{i,j}^{k} \right| \tag{5.10}$$

where N and C represent total number of trays and total number of components, respectively. k is the inner loop index.

$$\tau_1 < 0.001NC \tag{5.11}$$

The new $x_{i,j}$ values were normalized and were then used to compute the activity coefficient in raffinate phase ($\gamma^R_{i,j}$) by Eq. 5.2 . Thereafter $K_{i,j}$ and $y_{i,j}$ were computed as per Eq. 5.1 and Eq. 5.5 respectively. The new $y_{i,j}$ values were again normalized and then used to compute $\gamma^E_{i,j}$ (Eq. 5.3) and $K_{i,j}$ (Eq. 5.1). The tridiagonal matrix was then solved with these new $K_{i,j}$ values till the termination criterion is satisfied (Eqs. 5.10- 5.11). After the convergence of inner loop, $x_{i,j}$ values were utilized to calculate $y_{i,j}$ (Eq. 5.5) using the new values of activity coefficients. New E_j values were then calculated from sum rate relation,

$$E_j^{(l+1)} = E_j^l \sum_{i=1}^{C} y_{i,j} \tag{5.12}$$

where l is the outer loop index. The outer loop termination criteria was considered as

$$\tau_2 = \sum_{j=1}^{N} \left(1 - \frac{E_j^l}{E_j^{(l+1)}}\right)^2 < 0.001N \tag{5.13}$$

For diverging solution, corresponding R_j values were obtained as:

$$R_j = E_{j+1} - E_1 + \sum_{1}^{j} F_j \tag{5.14}$$

The tridiagonal matrix with new extract and raffinate flow rates were now solved till the outer loop gets converged. The converged solution then consists of traywise composition

and flow rates of extract and raffinate leaving a particular tray. The solutes and solvent amount in final raffinate stream were then used as variables in cost (objective) function.

5.2.2 Particle Swarm Optimization (PSO) algorithm

The Particle swarm optimization is a stochastic optimization method based on swarm intelligence. It was first proposed by Kennedy [132, 133] recognizing the flocking behavior of birds as principle for optimization. Each particle in population (swarm) is represented by two vectors namely position and velocity. These vectors are updated by the past experience of particles and their neighbors. Inertial, cognitive and social components that play a major role in effectiveness and performance of PSO, update the vectors iteratively. In literature, there are many modified versions of PSO applied to various domains. The PSO algorithm is explained in Fig. 5.3

Each variable i is represented by *nop* (number of population) dimensional position and velocity vectors. Both vectors are initialized randomly within the search space. The corresponding objective function to each population is then calculated. The best position of variable i through the generation cycle is known as the individual best position ($p_{best,i}$) while the position of the best variable in its entire population is termed as global best position (g_{best}). The best positions are usually decided based on the minimum objective function values. The position (X_i) and velocity (V_i) of particle i at iteration k+1 are updated by,

$$V_i^{k+1} = w^k V_i^k + c_1 r_1 \left(p_{best,i}^k - X_i^k \right) + c_2 r_2 \left(g_{best}^k - X_i^k \right) \tag{5.15}$$

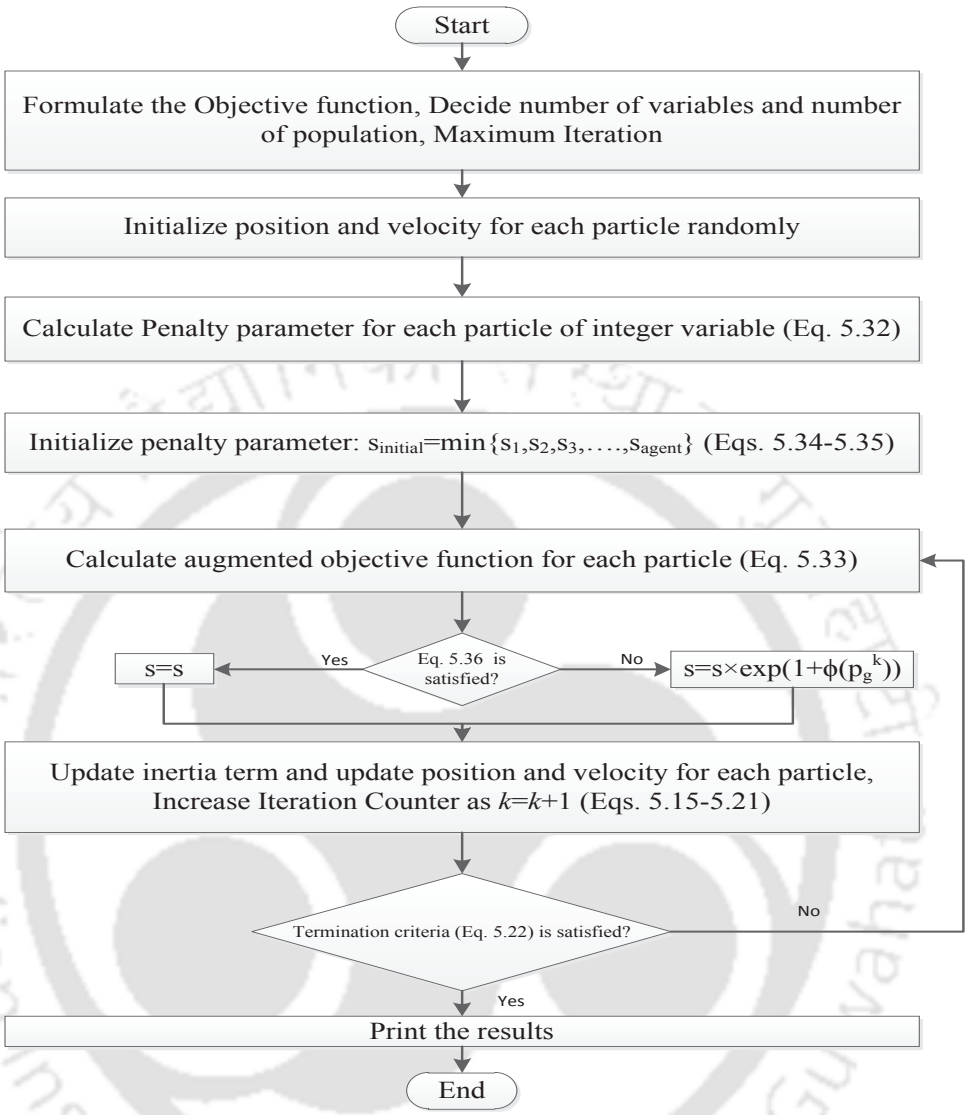

FIGURE 5.3: Particle Swarm Optimization Algorithm

$$X_i^{k+1} = X_i^k + V_i^{k+1} \tag{5.16}$$

where c_1 and c_2 are learning factors representing stochastic acceleration term weighting. Generally c_1=c_2=2 and r_1 and r_2 are random numbers generated separately from 0 to 1. $p_{best,i}^k$ represents the best position of variable i till the k^{th} iteration, while g_{best}^k is the best global position in swarm till the k^{th} iteration. w is the inertia weight term providing balance between global and local exploration ability. Among the various inertia term

mechanisms proposed by different authors, a simple mechanism with a Linear Decreasing Inertia Weight (LDIW) is proposed below:

$$w^k = w_{\max} - \frac{w_{\max} - w_{\min}}{iter_{\max}} \times k \tag{5.17}$$

where w_{max}=0.9, w_{min}=0.4. $iter_{max}$ is maximum number of iterations decided by the user. Arumugam and Rao [145] have proposed another strategy which is the inertia weight and acceleration coefficient based on global and local best values. The Global-average Local best Inertia Weight (GLbestIW) for variable i is,

$$w_i = \left(1.1 - \frac{g_{best}}{(p_{best,i})_{average}}\right) \tag{5.18}$$

and the Global-Local best Acceleration Coefficient (GLbestAC) is,

$$GLbestAC = \left(1 + \frac{g_{best}}{(p_{best,i})}\right) \tag{5.19}$$

Here $(p_{best,i})_{average}$ is the average of all the personal best values in specific generation. The velocity (V_i) of particle i is updated by,

$$V_i^{k+1} = w_i^k V_i^k + GLbestAC \times r\left(p_{best,i}^k + g_{best}^k - 2X_i^k\right) \tag{5.20}$$

where r is random number generated from 0 to 1. The updated velocity from Eq. 5.20 is then used to calculate the new position of particle.

$$X_i^{k+1} = X_i^k + V_i^{k+1} \tag{5.16}$$

The position and velocity bounds were applied to the updated vectors to keep the particles within search space. Position bounds were then decided from the problem variable bounds. The velocity is therefore clamped within $[-V_{max},V_{max}]$, where V_{max} is given by,

$$V_{\max} = (X_{UB} - X_{LB})/2 \tag{5.21}$$

where X_{UB} and X_{LB} represent the upper and lower limit for variable X respectively. Velocity bounds can be varied based on the necessity of the problem. Objective functions were then evaluated at updated positions and compared with past function values. The best values ($p^k_{best,i}$ and g^k_{best}) are improved upon continuously with each iteration. The optimization continues till the termination criteria is met. The termination criteria can be of maximum number of iterations. Generally the termination criteria is given by,

$$\sum_{n=1}^{nop} \frac{\left(X_n^{k+1} - X_n^k\right)^2}{nop} \leq 10^{-4} \tag{5.22}$$

where n is number of variables and nop is number of population.

5.2.3 Problem Formulation

The current work emphasizes on the cost optimization for multistage liquid liquid extractor with the implementation of PSO and ISR algorithms. The annualized cost (C_{Total}) was considered as an objective function that contains three parameters namely, (1) solvent lost in final raffinate ($C_{Solvent}$), (2) solute/solutes lost in final

raffinate(C_{Solute}) and (3) column capital cost($C_{Capital}$).

$$C_{Total} = C_{Solvent} + C_{Solute} + C_{Capital} \tag{5.23}$$

The cost for solvent and solute loss are defined as,

$$C_{Solvent} = R_N x_{BN}(kmol/hr) \times (24 \times 325)(hrs/year) \times MW_B \times P_B(INR/kg) \tag{5.24}$$

$$C_{Solute} = R_N x_{CN}(kmol/hr) \times (24 \times 325)(hrs/year) \times MW_C \times P_C(INR/kg) \tag{5.25}$$

where R_N, x_{BN} and x_{CN} are the raffinate flow rate, the solvent (B) and solute (C) composition in raffinate phase from Stage N, respectively. MW stands for Molecular weight. P stand for the price of component. Here ethanol and 1-butanol have been considered as solutes in the present work. The capital cost contains two components, packing cost (C_{pack}) and column cost (C_{col}). They are given as below:

$$C_{pack} = \left(\frac{\pi}{4}D^2\right) \times N \times HETS \times C^0_{pack} \tag{5.26}$$

where D,N, $HETS$ and C^0_{pack} are column diameter (m), total number of stages, Height Equivalent to Theoretical Stage (m) and packing cost per unit volume (INR/m^3) respectively. The column cost is given by

$$C_{col} = 1.4 \times \pi \times D \times N \times HETS \times T_S \times \rho_S \times C_S \tag{5.27}$$

Here, T_S,ρ_S and C_S are column thickness (m), steel (column material) density (kg/m^3) and steel cost per unit mass (INR/kg). Table 5.1 shows the values of different parameters

in cost equations.

TABLE 5.1: Cost function Parameters Values

Parameters	Value	Unit
Feed flow rate (F)	100	$kmol/hr$
Column diamater (D)	1 *	m
HETS	1 *	m
Packing cost (C^0_{pack})	11636.43 *	INR/m^3
Column thickness (T_S)	0.006 *	m
Steel density (ρ_S)	8000 *	kg/m^3
Steel cost (C_S)	296.39 *	INR/kg
[TDTHP][Phosph] cost	136172.40 **	INR/kg
[TDTHP][DCA] cost	237480 **	INR/kg
Butanol cost	744.76 **	INR/kg
Ethanol cost	2210.39 **	INR/kg

* Taken from Ubaidullah et al. [146]

** Taken from Sigma Aldrich Online price catalogue as on 7^{th} August 2014

With consideration of additional costs due to depreciation, interest and maintenance, 35% excess amount in terms of capital cost has been set to the final capital cost.

$$C_{Capital} = 1.35 \times (C_{pack} + C_{col}) \tag{5.28}$$

It was found that the objective function is highly non-linear in nature. The number of stages and solvent flow rate have been considered as decision variables. The Optimization

problem is then defined as,

$$Obj_C = C_{Total} \tag{5.29}$$

with bounds

$$2 < N < 10 \tag{5.30}$$

$$1 < Sol < 40 \tag{5.31}$$

where N and Sol are the number of stages and solvent flow rate in *kmol/hr*. The bounds limit has been decided based on our known experimental data of Chapter 4. Here, variable N is an integer variable while Sol is a continuous variable. So, the overall problem formulation is a Mixed Integer Non Linear Programming (MINLP).

Since one variable (N) is integer, penalty function for integer variable has been used in the optimization problem. For discrete variable, penalty functions in the form of *sine* and *elliptic* are widely used. Shin et al. [147] have shown that *elliptic* type functions are unstable as compared to *sine* type penalty functions. So, In this chapter, we have implemented *sine* type function [147] for single integer variable N.

$$\phi(x) = \frac{1}{2}\left[\sin\frac{2\pi\left\{x_m^c - \frac{1}{4}\left(d_{j+1} + 3d_j\right)\right\}}{d_{j+1} - d_j} + 1\right] \tag{5.32}$$

where x_m^c is the continuous design variable between discrete variables, d_j and d_{j+1}. Thus implementing penalty approach in optimization, the augmented objective function is defined as,

$$F(x) = Obj_C + s\phi(x) \tag{5.33}$$

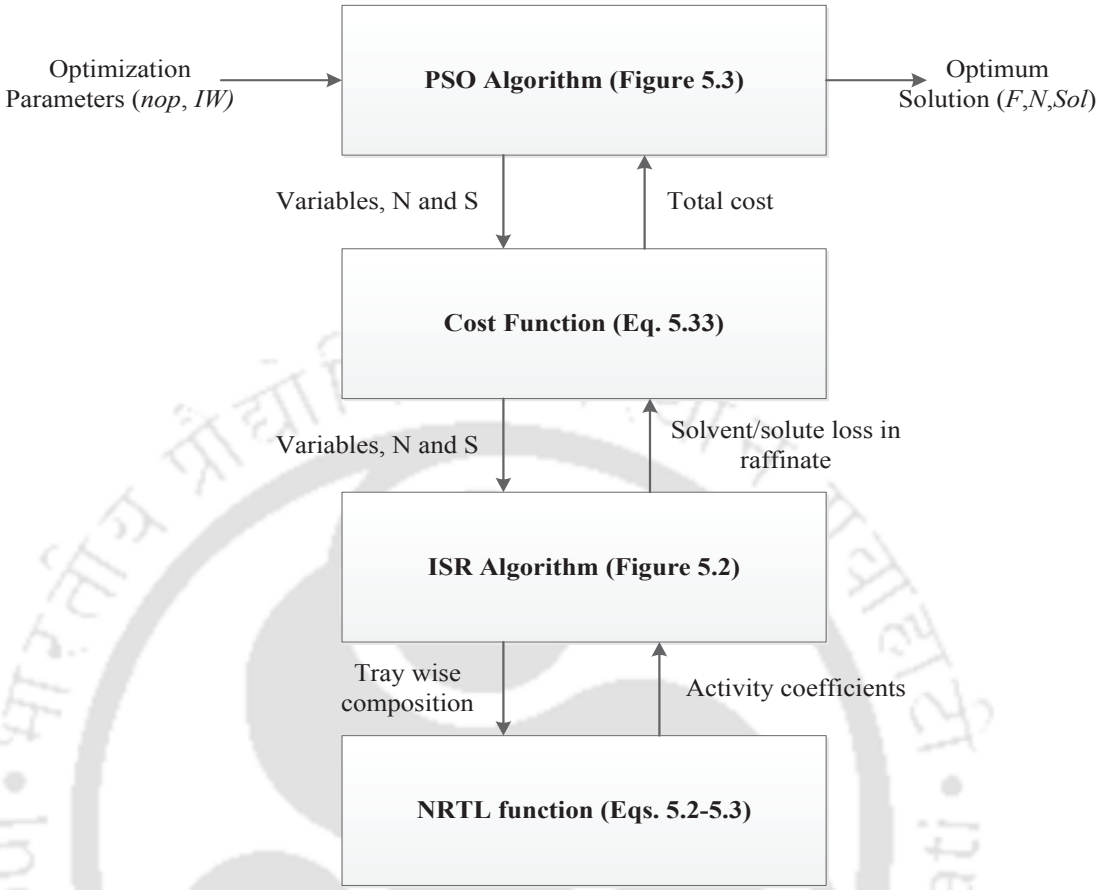

FIGURE 5.4: Optimization Strategy with Input/Output Variables

where s is penalty parameter. The initial values of s has been considered as,

$$s_{initial} = \min\{s_1, s_2, \cdots\cdots, s_{nop}\} \tag{5.34}$$

where nop is total number of populations and s is defined as,

$$s_i = 1 + \phi(x_i) \;\; where\, i = 1, 2, \cdots\cdots, nop \tag{5.35}$$

The penalty parameter through generation is updated based on tolerance (ε), where ε is a small positive number (=1). The termination criteria then is defined as,

$$\frac{\left|F\left(g_{best}^{k}\right) - Obj_{C}\left(g_{best}^{k}\right)\right|}{F\left(g_{best}^{k}\right)} \leq \varepsilon \tag{5.36}$$

If Eq. 5.36 is satisfied, s would be the same as old value. Otherwise it is updated as per Eq. 5.37 [148]

$$s = s \times \exp\left(1 + \phi\left(g_{best}^{k}\right)\right) \tag{5.37}$$

The optimization problem can then be rewritten in the following form,

$$\min \rightarrow F(N, Sol) \tag{5.38}$$

$$2 < N < 10 \tag{5.30}$$

$$1 < Sol < 40 \tag{5.31}$$

The PSO algorithm with penalty function is shown in Fig. 5.3. The whole optimization strategy was coded in MATLAB (Fig. 5.4 and APPENDIX B). The decision variables N and Sol were particles in swarm (Population). PSO algorithm then invokes the cost function (Eq. 5.33). Cost function thereafter calculates the capital cost using particle values. For solvent and solute loss cost, the ISR algorithm was used. The ISR algorithm then calculated the stagewise composition and flow rates with the help of activity coefficients generated by NRTL model (Eqs. 5.2- 5.3). For the NRTL model, we have used our own BIP (Table 4.2) measured in our previous experimental work. The PSO algorithm then execute and minimizes the augmented cost function (Eq. 5.33) till

the minimum sum of square error for all particles is achieved.

5.3 Results and Discussions

5.3.1 Tuning of PSO Parameters

Since PSO is a stochastic algorithm, its efficiency is tuned by different parameters like population size and inertia weight (Eqs. 5.17- 5.19, 5.32- 5.33). Initially the effect of these parameters on PSO efficiency was checked (Figure 5.3). The efficiency was analyzed by the evolution of different parameters like best solution, Success Rate (SR), Average number of ITerations (AIT), mean of the best solutions (*mean*) and Standard Deviation (SD). We have considered 50 individual runs of optimization for [TDTHP][DCA]-ethanol-1-butanol-water system in order to tune the parameters. The SR is defined as percentage of runs giving the best solution. AIT is defined as the mean of total iterations to achieve the best solution. *mean* and SD were calculated from the solutions across all 50 runs. The number of population (*nop*) considered for the study ranged from 10 to 100 with an increment of 10. Two inertia weight approaches (Eqs. 5.17-5.19) were studied for the optimization. Table 5.2 shows the SR and AIT for both inertia weight approaches with different population for [TDTHP][DCA]-ethanol-1-butanol-water system. LDIW shows high success rate as compared to GLbestIW. LDIW was found to decrease linearly independent of g_{best} and $p_{best,i}$ values (Eq. 5.17), thereby giving solution after higher number of generations. From Figs. 5.5-5.9, it can be seen that few local minima were evaluated far away from global minima at higher number of generations. It indicates higher number of generations

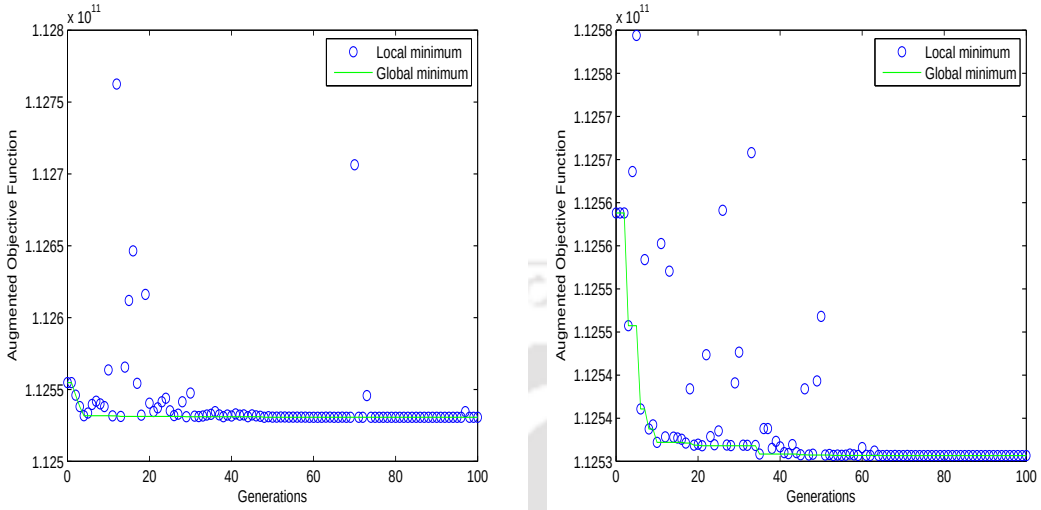

(A) (B)

FIGURE 5.5: Augmented Objective function (Eq. 5.33) Vs Generations for LD Inertia Weight for [TDTHP][DCA] (1) - Ethanol (2) - 1-Butanol (2) - Water (4) system at T=298.15 K and p=1 atm. (A) nop=10, (B)nop=20

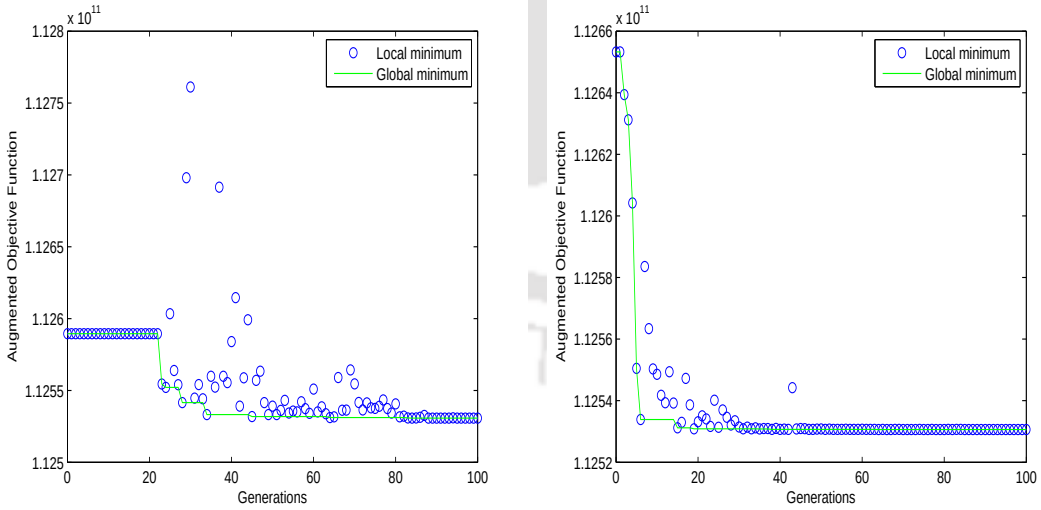

(A) (B)

FIGURE 5.6: Augmented Objective function (Eq. 5.33) Vs Generations for LD Inertia Weight for [TDTHP][DCA] (1) - Ethanol (2) -1-Butanol (3) - Water (4) system at T=298.15 K and p=1 atm. (A) nop=30, (B)nop=40

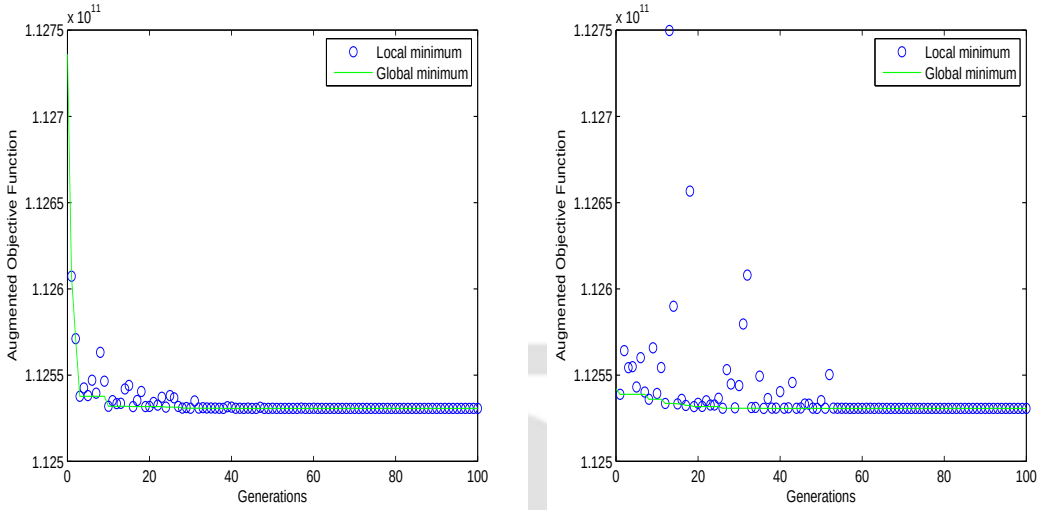

(A) (B)

FIGURE 5.7: Augmented Objective function (Eq. 5.33) Vs Generations for LD Inertia Weight for [TDTHP][DCA] (1) - Ethanol (2) - 1-Butanol (3) - Water (4) system at T=298.15 K and p=1 atm. (A) nop=50, (B)nop=60

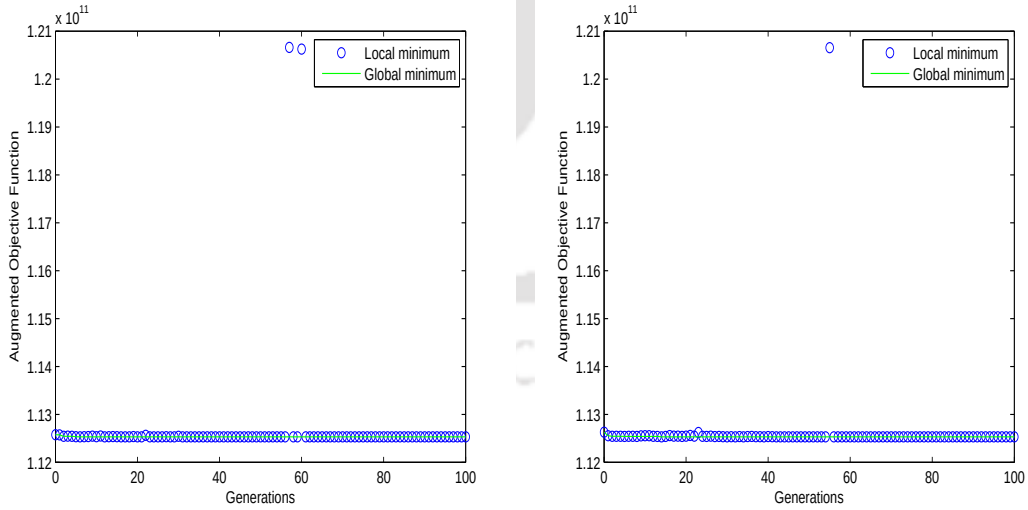

(A) (B)

FIGURE 5.8: Augmented Objective function (Eq. 5.33) Vs Generations for LD Inertia Weight for [TDTHP][DCA] (1) - Ethanol (2) - 1-Butanol (3) - Water (4) system at T=298.15 K and p=1 atm. (A) nop=70, (B)nop=80

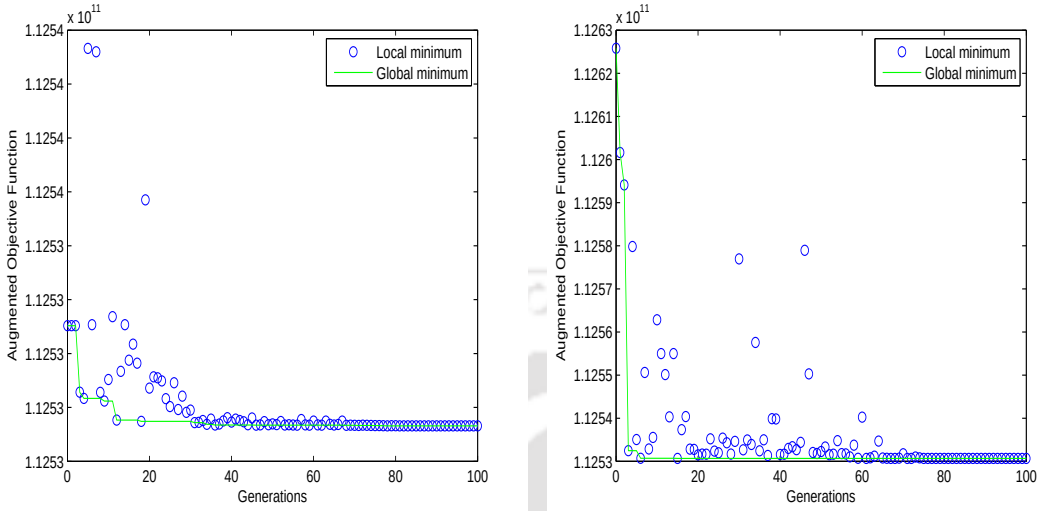

(A) (B)

FIGURE 5.9: Augmented Objective function (Eq. 5.33) Vs Generations for LD Inertia Weight for [TDTHP][DCA] (1) - Ethanol (2) -1-Butanol (3) - Water (4) system at T=298.15 K and p=1 atm. (A) nop=90, (B)nop=100

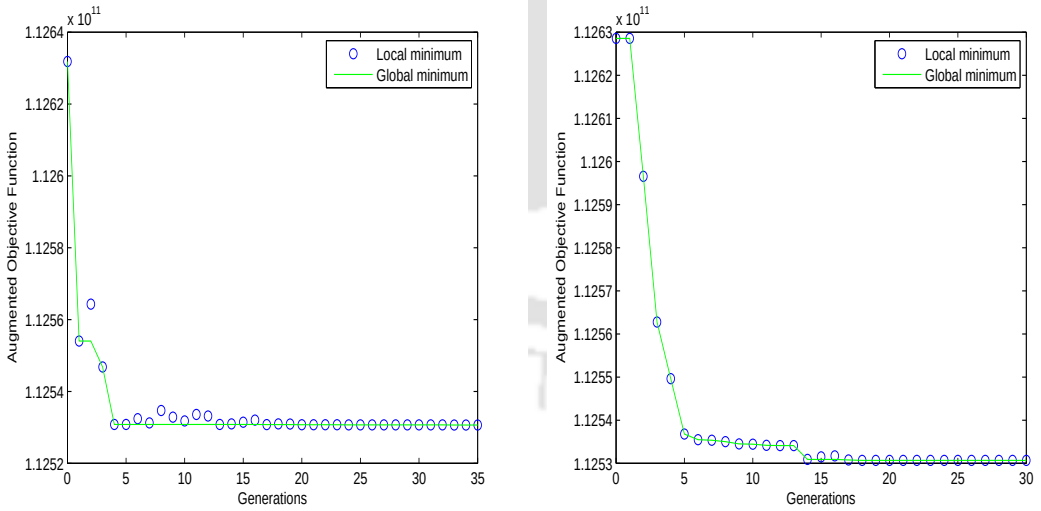

(A) (B)

FIGURE 5.10: Augmented Objective function (Eq. 5.33) Vs Generations for GLbest Inertia Weight for [TDTHP][DCA] (1) - Ethanol (2) - 1-Butanol (3) - Water (4) system at T=298.15 K and p=1 atm. (A) nop=10, (B)nop=20

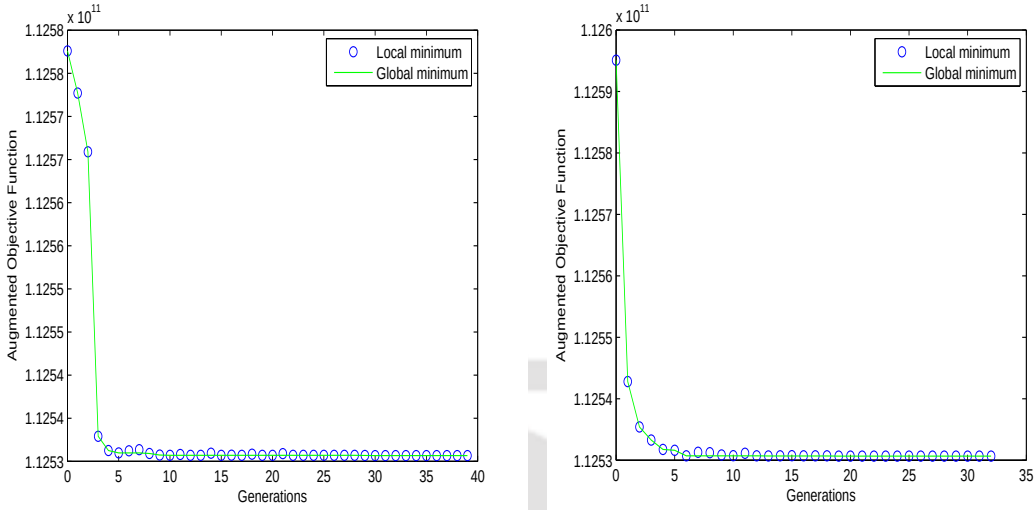

(A) (B)

FIGURE 5.11: Augmented Objective function (Eq. 5.33) Vs Generations for GLbest Inertia Weight for [TDTHP][DCA] (1) - Ethanol (2) - 1-Butanol (3) - Water (4) system at T=298.15 K and p=1 atm. (A) nop=30, (B)nop=40

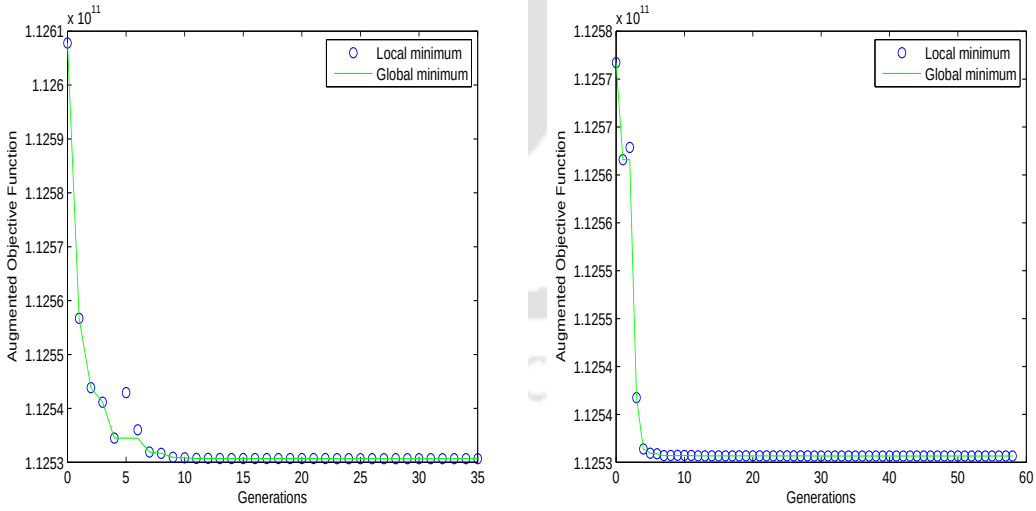

(A) (B)

FIGURE 5.12: Augmented Objective function (Eq. 5.33) Vs Generations for GLbest Inertia Weight for [TDTHP][DCA] (1) - Ethanol (2) - 1-Butanol (3) - Water (4) system at T=298.15 K and p=1 atm. (A) nop=50, (B)nop=60

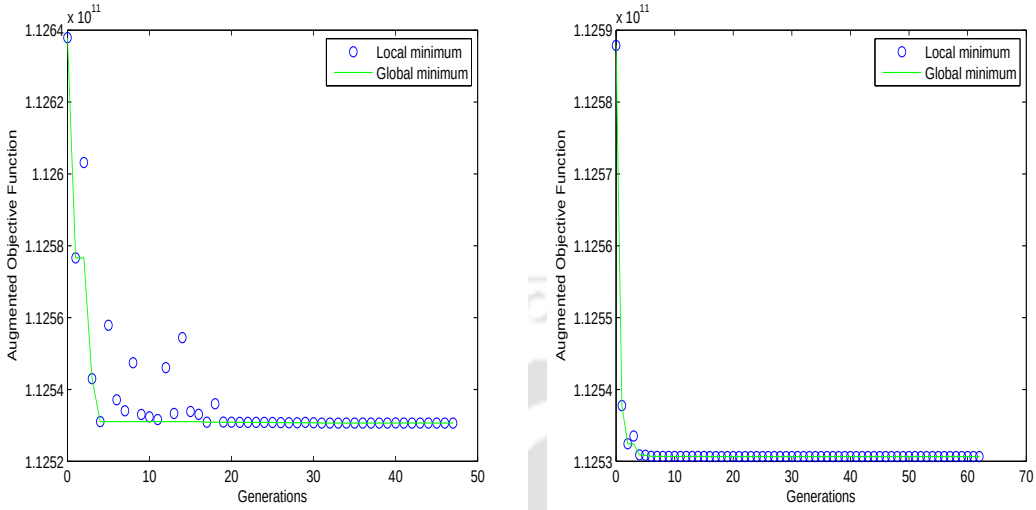

(A) (B)

FIGURE 5.13: Augmented Objective function (Eq. 5.33) Vs Generations for GLbest Inertia Weight for [TDTHP][DCA] (1) - Ethanol (2) - 1-Butanol (3) - Water (4) system at T=298.15 K and p=1 atm. (A) nop=70, (B)nop=80

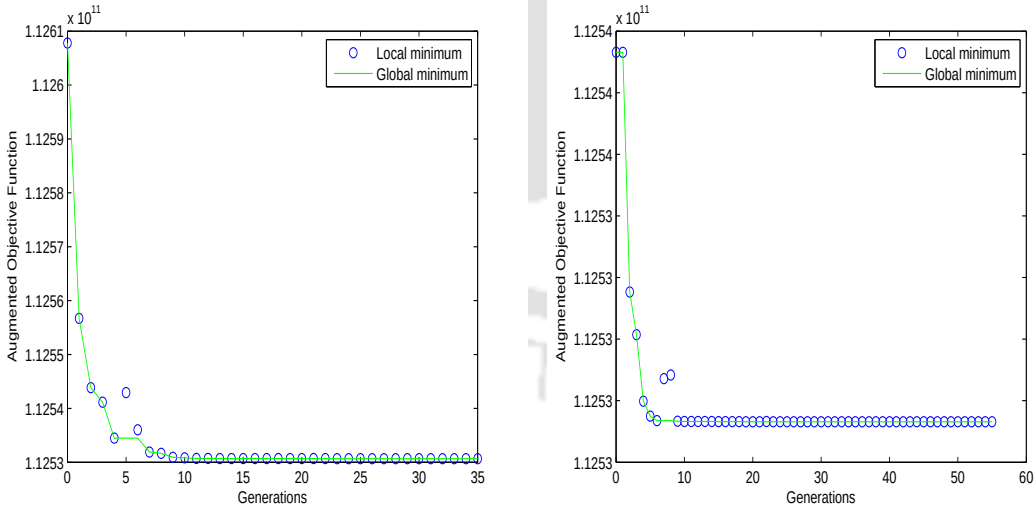

(A) (B)

FIGURE 5.14: Augmented Objective function (Eq. 5.33) Vs Generations for GLbest Inertia Weight for [TDTHP][DCA] (1) - Ethanol (2) - 1-Butanol (3) - Water (4) system at T=298.15 K and p=1 atm. (A) nop=90, (B)nop=100

TABLE 5.2: Parameter tuning and Efficiency analysis for [TDTHP][DCA] (1) - Ethanol (2) - 1-Butanol (3) - Water (4) system at T=298.15 K and p=1 atm.

Population Size	GLbestIW		LDIW	
	AIT	SR (%)	AIT	SR (%)
10	44	34	100	70
20	41	48	100	82
30	42	64	99	86
40	39	64	100	90
50	41	82	100	94
60	40	74	100	92
70	43	70	100	94
80	37	78	100	96
90	40	80	100	98
100	40	76	100	98

is required to achieve the termination criteria (Eq. 5.22). GLbestIW shows very few local minima at the initial generations (Figs. 5.10-5.14). Thus both GLbestIW and GLbestAC depend on g_{best} and $p_{best,i}$ values (Eqs. 5.18- 5.19) that converges faster. AIT for LDIW was approximately 2.5 times higher than GLbestIW. Thus GLbestIW was chosen for further study considering lesser function evaluations. Population containing 10 and 20 particles show SR less than 50% with GLbestIW. While population of 30 and 40 particles have similar SR and AIT. Higher *nop* (>50) did not improve upon the SR and AIT significantly. So we have chosen a population of 30 particles for optimization as less number of function evaluations are needed.

5.3.2 Cost Optimization results

The objective function (Eq. 5.33) was optimized for two systems, namely, [TDTHP][DCA]-ethanol-1-butanol-water and [TDTHP][Phosph]-ethanol-1-butanol-water. PSO converged at various best solutions with success rate as shown in Fig. 5.15. The minimum objective function was found to

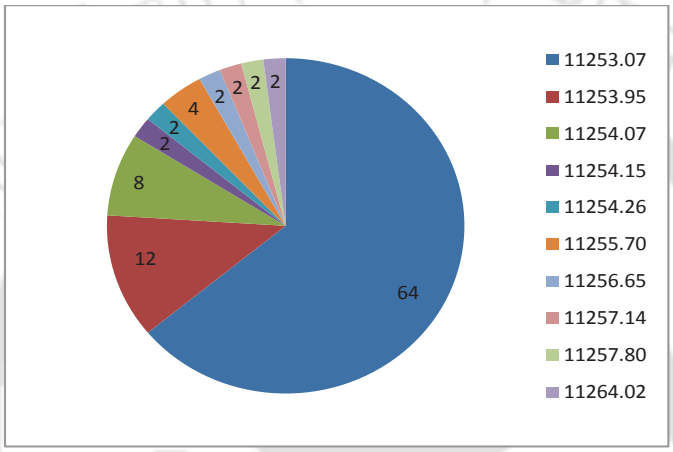

(A)

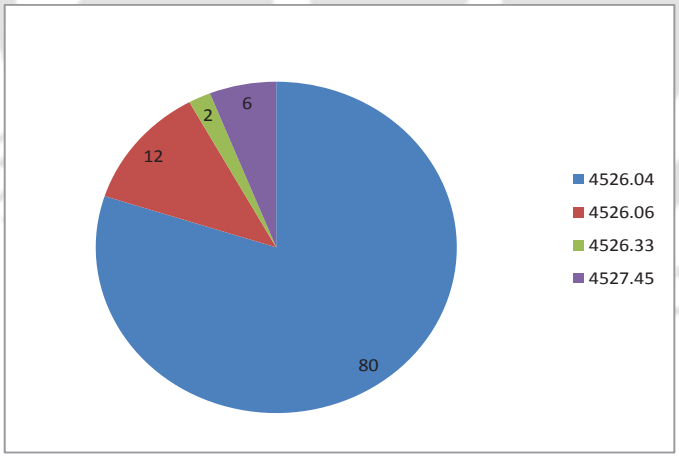

(B)

FIGURE 5.15: Optimized cost values (Eq. 5.33) in *crore INR/year* with success rate (%) for system: (a) [TDTHP][DCA] (1) - Ethanol (2) - 1-Butanol (3) - Water (4) and (b) [TDTHP][Phosph] (1) - Ethanol (2) - 1-Butanol (3) - Water (4) at T=298.15 K and p=1 atm.

be $1.1253 \cdot 10^{11}$ INR/year with SR of 64% for [TDTHP][DCA]-ethanol-1-butanol-water

system. Nine local minimum solutions were also found with SR 36%. For [TDTHP][Phosph]-ethanol-1-butanol-water system, the best solution was at $4.526 \cdot 10^{10}$ INR/year with SR 80%. There were other three local solutions with a low SR of 20%. The optimized parameters corresponding to best solution are shown in Table 5.3. For system containing [TDTHP][DCA], optimum number of stages and solvent flow rate were 3 and 3.9891 kmol/hr respectively. The optimum objective function value was found at 23^{th} generation and the convergence criteria was fully satisfied at 48^{th} generation. (Fig. 5.16). The AIT over the 50 runs to achieve this solution was 42. Similarly for [TDTHP][Phosph] containing system, optimum solution was found with 10 stages and 36.285 kmol/hr solvent flow rate. It was achieved in 15 generations with AIT equal to 13 (Table 5.3 and Fig. 5.17). The stagewise compositions and flow rates with respective to optimum solution for both systems are shown in Table 5.4. The [TDTHP][Phosph] containing system converged at an upper bound of N(=10).

From Table 5.4, it can be seen that the compositions are uniform for more than 6 stages. The butanol concentration decreases continuously with number of stages resulting in minimization of total cost. The revised upper bound (N=20-40) shows no improvement to get the solution within the bound regions. Therefore considering four decimal places as significant and physics of the problem, the present solution was considered as the optimum solution. The butanol concentration was reduced from 0.002 mole fraction in feed to 0.0012 mole fraction and 0.0004 mole fraction in raffinate phase for [TDTHP][DCA] and [TDTHP][Phosph] systems respectively (Table 5.4).

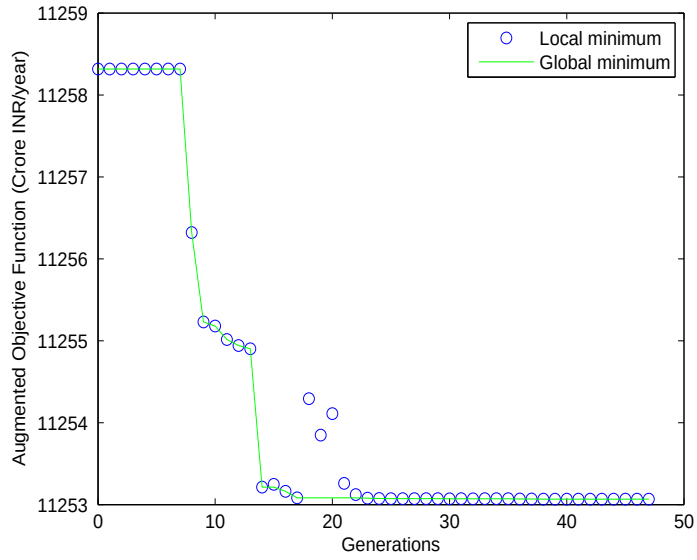

FIGURE 5.16: Optimized objective function (Eq. 5.33) with iterations for [TDTHP][DCA] (1) - Ethanol (2) - 1-Butanol (3) - Water (4) system at T=298.15 K and p=1 atm.

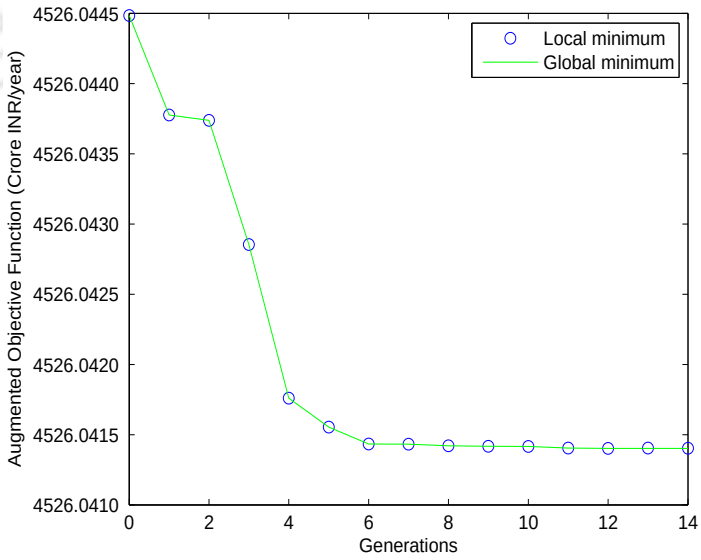

FIGURE 5.17: Optimized objective function (Eq. 5.33) with iterations for [TDTHP][Phosph] (1) - Ethanol (2) -1-Butanol (3) - Water (4) system at T=298.15 K and p=1 *atm.*

TABLE 5.3: Optimization results for multistage extractor at T=298.15 K and p=1 atm.

Total Cost (INR/year)	N	*Sol* (kmol/hr)	Losses in raffinate			Optimization Evaluation Parameters			
			IL loss (kmol/hr)	Butanol loss (kmol/hr)	Ethanol loss (kmol/hr)	AIT	SR (%)	Mean (INR/year)	SD (INR/year)
[TDTHP][DCA] (1) - Ethanol (2) - 1-Butanol (3) - Water (4)									
1.1253E+11	3	3.9891	0.1102	0.1183	0.0001	42	64	1.1254E+11	1.8330E+07
[TDTHP][Phosph] (1) - Ethanol (2) - 1-Butanol (3) - Water (4)									
4.5260E+10	10	36.2850	0.0551	0.0375	0.0321	13	82	4.5261E+10	3.3884E+06

TABLE 5.4: Stagewise optimized compositions and flow rates at T=298.15 K and p=1 atm.

Stage (j)	Compositions*				Flow rate (kmol/hr)
	x_W/y_W	x_B/y_B	x_E/y_E	x_{IL}/y_{IL}	
[TDTHP][DCA] (1) - Ethanol (2) - 1-Butanol (3) - Water (4)					
Extract Phase					
1	0.0020	0.0204	0.0082	0.9694	4.0014
2	0.0020	0.0179	0.0010	0.9791	4.0750
3	0.0020	0.0125	0.0001	0.9854	4.0489
Raffinate Phase					
1	0.9970	0.0019	0.0000	0.0011	100.0737
2	0.9972	0.0017	0.0000	0.0011	100.0476
3	0.9977	0.0012	0.0000	0.0011	99.9878
[TDTHP][Phosph] (1) - Ethanol (2) - 1-Butanol (3) - Water (4)					
Extract Phase					
1	0.0002	0.0045	0.0000	0.9953	36.4008
2	0.0002	0.0023	0.0000	0.9975	36.3792
3	0.0002	0.0012	0.0000	0.9986	36.3400
4	0.0003	0.0006	0.0000	0.9991	36.3195
5	0.0003	0.0003	0.0000	0.9994	36.3087
6	0.0003	0.0001	0.0000	0.9996	36.3031
7	0.0003	0.0000	0.0000	0.9996	36.3006
8	0.0003	0.0000	0.0000	0.9996	36.2992
9	0.0003	0.0000	0.0000	0.9997	36.2974
10	0.0002	0.0000	0.0000	0.9998	36.2936
Raffinate Phase					
1	0.9979	0.0012	0.0003	0.0006	99.9785
2	0.9983	0.0008	0.0003	0.0006	99.9392

3	0.9985	0.0006	0.0003	0.0006	99.9188
4	0.9986	0.0005	0.0003	0.0006	99.9079
5	0.9987	0.0004	0.0003	0.0006	99.9024
6	0.9987	0.0004	0.0003	0.0006	99.8998
7	0.9987	0.0004	0.0003	0.0006	99.8985
8	0.9987	0.0004	0.0003	0.0006	99.8966
9	0.9987	0.0004	0.0003	0.0006	99.8929
10	0.9987	0.0004	0.0003	0.0006	99.8842

* x and y refer to the raffinate (water rich) and extract (IL rich) phase composition respectively.

The extraction efficiency for solute is given by,

$$Efficiency(\%) = \frac{Solute\,in\,extract,\,kmol/hr}{Solute\,in\,feed,\,kmol/hr} \times 100 \tag{5.39}$$

[TDTHP][Phosph] gave butanol efficiency at 81.25% which was double than 40.85% as achieved by [TDTHP][DCA]. But [TDTHP][DCA] proved to be a better solvent for ethanol extraction (99.70% efficiency) as compared to [TDTHP][Phosph] (2.7% efficiency). It indicates that [TDTHP][Phosph] is more selective to butanol than ethanol. In summary [TDTHP][DCA] is a better solvent for simultaneous extraction of butanol and ethanol from aqueous solution. [TDTHP][Phosph] loss (0.0551 kmol/hr) in raffinate phase is half than that of [TDTHP][DCA] loss (0.1102 kmol/hr), as [TDTHP][Phosph] is more hydrophobic than [TDTHP][DCA] in water rich phase. It results in lesser total cost in extraction by [TDTHP][Phosph] even though possessing higher number of stages.

5.3.3 Effect of IL Cost on Optimization

An attempt has been made to study the impact of IL cost on cost function values as compared to other components. This is in keeping the mind that newer production technologies will reduce the IL cost in the future. Fifty optimization runs were performed with reduction in IL cost ranging through factors 1/1 to 1/10000 of the present cost. For

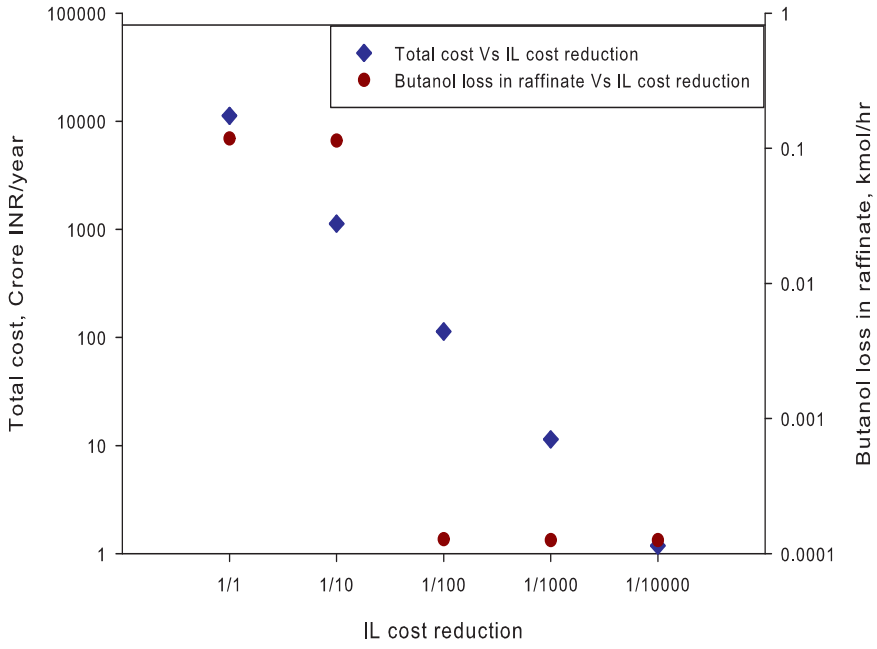

FIGURE 5.18: The effect of IL cost on total cost and butanol loss in raffinate for [TDTHP][DCA] (1) - Ethanol (2) - 1-Butanol (3) - Water (4) system at T=298.15 K and p=1 atm.

both systems, the optimized results are shown in Table 5.5 and Figs. 5.18- 5.19. It is observed that the total cost gradually decreases with IL cost reduction. [TDTHP][DCA] gave 100% butanol efficiency when IL cost was reduced by 100 times. The corresponding number of stages and solvent flow rate were 9 and 20.3997 kmol/hr respectively. Further reduction in IL cost (by 1000 and 10000 times) reduced the total cost with same butanol efficiency. The optimized number of stages was then 5 and solvent flow rate was 40

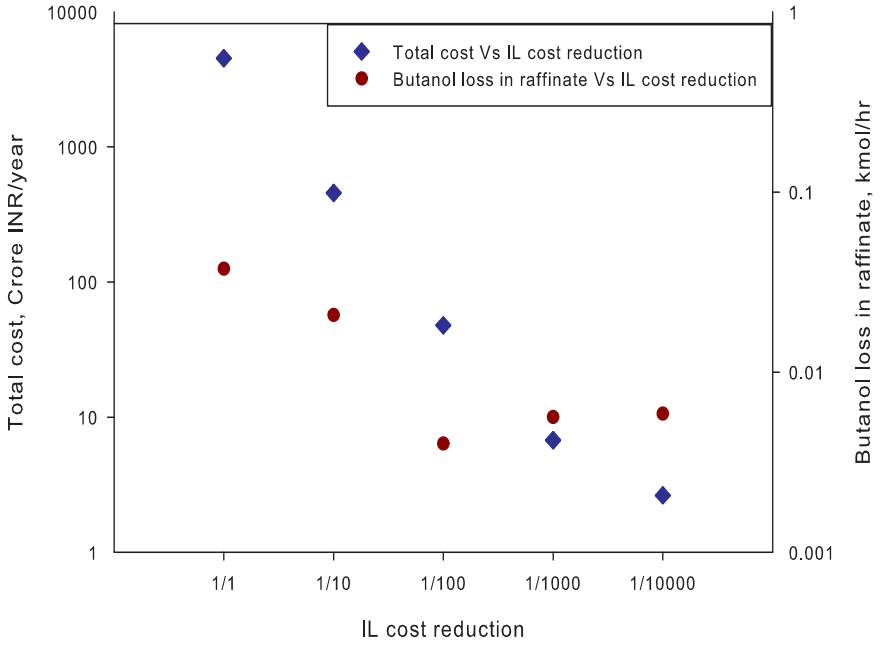

FIGURE 5.19: The effect of IL cost on total cost and butanol loss in raffinate for [TDTHP][Phosph] (1) - Ethanol (2) - 1-Butanol (3) - Water (4) system at T=298.15 K and p=1 atm.

kmol/hr. Similarly for [TDTHP][Phosph], 100 times reduction in IL cost show butanol efficiency of 98%. It also indicated a further improvement in ethanol efficiency from 2.7% to 24%. For [TDTHP][Phosph], the optimized flow rate was 11.9839 kmol/hr with ten stages.

TABLE 5.5: The effect of IL price on Optimization Results and Total cost (Eq. 5.33)

IL cost reduction	Total Cost (Crore INR/year)	N	*Sol* (kmol/hr)	IL loss in raffinate (kmol/hr)	Butanol loss in raffinate (kmol/hr)	Ethanol loss in raffinate (kmol/hr)
[TDTHP][DCA] (1) - Ethanol (2) - 1-Butanol (3) - Water (4)						
1/1	11253.1	3	3.9891	0.1102	0.1183	0.0001
1/10	1129.8	2	4.6987	0.1102	0.1138	0.0003
1/100	113.7	9	20.3997	0.1114	0.0001	0.0000
1/1000	11.4	5	40.0000	0.1114	0.0001	0.0000
1/10000	1.2	5	40.0000	0.1114	0.0001	0.0000
[TDTHP][Phosph] (1) - Ethanol (2) - 1-Butanol (3) - Water (4)						
1/1	4526.0	10	36.2850	0.0551	0.0375	0.0321
1/10	455.8	10	30.5992	0.0551	0.0207	0.0316
1/100	47.8	10	11.9839	0.0555	0.0040	0.0251
1/1000	6.8	10	9.5960	0.0556	0.0056	0.0233
1/10000	2.6	10	9.4108	0.0556	0.0059	0.0232

6

Conclusion and Future Scope

6.1 Research Conclusion

Due to the large number of ILs, it is impractical to measure the densities of all ILs experimentally. The NMPRNSM1 and NMSRK models, corresponding to predictive Soave-Redlich-Kwong (PSRK) equation of state with the PRNSM1 alpha function and the original SRK alpha function respectively can be used for the prediction of density of ILs. However it is evident that, irrespective of nature of IL, the improvement in prediction for the modified PSRK cohesion factor is around four times better than the original PSRK cohesion factor expression.

Improved mass transfer rates coupled with high separation efficiency was observed with [TDTHP][Phosph] for the separation of butanol-water mixtures. Larger values of butanol selectivity (81-323) indicate easier separation of butanol from water. The larger values of butanol distribution coefficient (19-59, 25-95 and 17-173 for [TDTHP][Phosph],[TDTHP][DCA] and [TDTHP][DEC] respectively) indicated a lesser solvent requirement for butanol-water separation. Higher butanol and ethanol selectivity indicated better separation of both alcohols from feed in quaternary systems too. Butanol was found to be more soluble in ILs as it contains longer carbon chain (non polar) than ethanol. As the concentration of butanol is almost six times higher than ethanol in ABE fermentation broth, the results can be used for selective extraction of butanol using optimized hybrid fermentation-extraction process. Acetone is highly volatile and can be evaporated easily from fermentation products, hence it has not been considered for extraction.

Furthermore, the raffinate phase was found to comprise mainly water with mole

composition as high as 99% for all systems. The slopes of the tie lines and the spread of two-phase region indicated greater separation. The NRTL and UNIQUAC models gave RMSD values less than unity for all systems indicating a better fit. Thus, phosphonium based ILs have performed as better solvents for extraction of butanol and ethanol from the aqueous solution. COSMO-SAC also predicted acceptable equilibrium data with deviation within 10%-20% for ternary and quaternary systems.

The combined strategy of PSO and ISR algorithm was adopted for the optimization of multistage extractor. GLbestIW gave less AIT (42) and satisfactory SR (64) as compared to conventional LDIW for nop=30. For system containing [TDTHP][DCA], the optimum solution was $1.1253 \cdot 10^{11}$ $INR/year$ with 3 stages and 3.9891 $kmol/hr$ solvent flow rate. [TDTHP][Phosph] gave lesser cost as it is economical than [TDTHP][DCA]. Furthermore IL loss in raffinate phase was less in case of [TDTHP][Phosph]. Ethanol efficiency was found to increase by nine times when [TDTHP][Phosph] cost reduces by 100 times. Thus [TDTHP][DCA] is proposed as a solvent for simultaneous extraction for both alcohols. Further a cost reduction of 100 times for [TDTHP][DCA] shows a complete extraction (almost 100%) for both alcohols.

6.2 Future Scope

MD Strategy was used to predict the density of pure ILs in the present work. Further, it can be implemented for the IL-water interface study for the prediction of solubility of IL and water in either phase. Thereafter, the butanol diffusivity in both phases can be predicted by mixing butanol as third component in IL-water binary mixtures.

The simulation can be repeated for different feed mixture of experiments carried out in the current research. Thus tie line data can be generated for ternary mixture by MD and can be compared with experimental tie line data. Further MD approach can be implemented for quaternary systems containing ethanol and butanol. On other side, the multistage extractor optimization can be studied with detailed design. The cost function can be optimized by the combination of the mutistage extractor with acetone distillation unit and solvent recovery unit. The results of PSO can also be compared with process simulator such as CHEMCAD.

Bibliography

[1] Dunford, N. T. *Food Ind. Bioprod. Bioprocess.* Wiley, 2012. ISBN 9781119946052. pp.195.

[2] Kaminski, W., Tomczak, E., and Gorak, A. Biobutanol - Production and purification methods. *Eco. Chem. Engg. Sci.*, **18**(1), 31–37, 2011.

[3] Durre, P. New insights and novel developments in clostridial acetone/butanol/isopropanol fermentation. *Appl. Microbiol. Biotechnol.*, **49** (6), 639–648, 1998.

[4] Durre, P. and Bahl, H. *Microbial Production of Acetone/Butanol/Isopropanol*, 229–268. Wiley-VCH Verlag GmbH, 2008.

[5] Garcia-Chavez, L. Y., Garsia, C. M., Schuur, B., and de Haan, A. B. Biobutanol recovery using nonfluorinated task-specific ionic liquids. *Ind. Eng. Chem. Res.*, **51** (24), 8293–8301, 2012.

[6] Li, J., Zhao, J., Zhao, M., Yang, Y., Jiang, W., and Yang, S. Screening and characterization of butanol-tolerant micro-organisms. *Lett. Appl. Microbiol.*, **50** (4), 373–379, 2010.

[7] Abdehagh, N., Tezel, F. H., and Thibault, J. Separation techniques in butanol production: Challenges and developments. *Biomass Bioenergy*, **60**, 222–246, 2014.

[8] Haung, H. J., Ramaswamy, S., and Liu, Y. Separation and Purification of Biobutanol during Bioconversion of Biomass. *Sep. Purif. Technol.*, **132**, 513–540, 2014.

[9] Qureshi, N., Hughes, S., Maddox, I. S., and Cotta, M. A. Energy-efficient recovery of butanol from model solutions and fermentation broth by adsorption. *Bioprocess Biosyst. Eng.*, **27**(4), 215–222, 2005.

[10] Davison, B. H. and Thompson, J. E. Continuous direct solvent extraction of butanol in a fermenting fluidized-bed bioreactor with immobilizedclostridium acetobutylicum. *Appl. Biochem. Biotechnol.*, **39-40**(1), 415–426, 1993.

[11] Anbarasan, P., Baer, Z. C., Sreekumar, S., Gross, E., Binder, J. B., Blanch, H. W., Clark, D. S., and Toste, F. D. Integration of chemical catalysis with extractive fermentation to produce fuels. *Nature*, **491**, 235–239, 2012.

[12] Kraemer, K., Harwardt, A., Bronneberg, R., and Marquardt, W. Separation of butanol from acetone-butanol-ethanol fermentation by a hybrid extraction-distillation process. *Comput. Chem. Eng.*, **35**(5), 949 – 963, 2011.

[13] Anderson, J. L. and Armstrong, D. W. Immobilized Ionic Liquids as High-Selectivity/High-Temperature/High-Stability Gas Chromatography Stationary Phases. *Anal. Chem.*, **77**(19), 6453–6462, 2005.

[14] Ribeiro, M. C. C. High Viscosity of Imidazolium Ionic Liquids with the Hydrogen Sulfate Anion: A Raman Spectroscopy Study. *J. Phys. Chem. B*, **116**(24), 7281–7290, 2012.

[15] Mukherjee, I., Manna, K., Dinda, G., Ghosh, S., and Moulik, S. P. Shear-and temperature-dependent viscosity behavior of two phosphonium-based ionic liquids and surfactant triton X-100 and their biocidal activities. *J. Chem. Eng. Data*, **57** (5), 1376–1386, 2012.

[16] Neves, C. M. S. S., Carvalho, P. J., Freire, M. G., and Coutinho, J. A. Thermophysical properties of pure and water-saturated tetradecyltrihexylphosphonium-based ionic liquids. *J. Chem. Thermodyn.*, **43**(6), 948–957, 2011.

[17] Freire, M. G., Carvalho, P. J., Gardas, R. L., Santos, L. M., Marrucho, I. M., and Coutinho, J. A. Solubility of water in tetradecyltrihexylphosphonium-based ionic liquids. *J. Chem. Eng. Data*, **53**(10), 2378–2382, 2008.

[18] Wasserscheid, P. and Keim, W. Ionic Liquids-New Solutions for Transition Metal Catalysis. *Angew. Chem. Int. Ed.*, **39**(21), 3772–3789, 2000.

[19] Fredlake, C. P., Crosthwaite, J. M., Hert, D. G., Aki, S. N., and Brennecke, J. F. Thermophysical Properties of Imidazolium-Based Ionic Liquids. *J. Chem. Eng. Data*, **49**(4), 954–964, 2004.

[20] Welton, T. Room-Temperature Ionic Liquids. Solvents for Synthesis and Catalysis. *Chem. Rev.*, **99**(8), 2071–2084, 1999.

[21] Ha, S. H., Mai, N. L., and Koo, Y. M. Butanol recovery from aqueous solution into ionic liquids by liquid–liquid extraction. *Proc. Biochem*, **45**(12), 1899–1903, 2010.

[22] Simoni, L. D., Chapeaux, A., Brennecke, J. F., and Stadtherr, M. A. Extraction of biofuels and biofeedstocks from aqueous solutions using ionic liquids. *Comp. Chem. Eng.*, **34**(9), 1406–1412, 2010.

[23] Chapeaux, A., Simoni, L. D., Ronan, T. S., Stadtherr, M. A., and Brennecke, J. F. Extraction of alcohols from water with 1-hexyl-3-methylimidazolium bis (trifluoromethylsulfonyl) imide. *Green Chem.*, **10**(12), 1301–1306, 2008.

[24] Domanska, U. and Krolikowski, M. Extraction of butan-1-ol from water with ionic liquids at T= 308.15 K. *J. Chem. Thermodyn.*, **53**, 108–113, 2012.

[25] Hu, X., Yu, J., and Liu, H. Liquid-liquid equilibria of the system 1-(2-hydroxyethyl)-3-methylimidozolium tetrafluoroborate or 1-(2-hydroxyethyl)-2, 3-dimethylimidozolium tetrafluoroborate+ water+ 1-butanol at 293.15 K. *J. Chem. Eng. Data*, **51**(2), 691–695, 2006.

[26] Xiao, L., Su, D., Yue, C., and Wu, W. Protic ionic liquids: A highly efficient catalyst for synthesis of cyclic carbonate from carbon dioxide and epoxides. *J. CO2 Util.*, **6**, 1 – 6, 2014.

[27] Ying, A., Li, Z., Ni, Y., Xu, S., Hou, H., and Hu, H. Novel multiple-acidic ionic liquids: Green and efficient catalysts for the synthesis of bis-indolylmethanes under solvent-free conditions. *J. Ind. Eng. Chem.*, 2014. doi: http://dx.doi.org/10.1016/j.jiec.2014.09.019.

[28] Zhuo, K., Du, Q., Bai, G., Wang, C., Chen, Y., and Wang, J. Hydrolysis of cellulose catalyzed by novel acidic ionic liquids. *Carbohydr. Polym.*, **115**, 49 – 53, 2015.

[29] Tao, F. R., Zhuang, C., Cui, Y. Z., and Xu, J. Dehydration of glucose into 5-hydroxymethylfurfural in SO3H-functionalized ionic liquids. *Chin. Chem. Lett.*, **25**(5), 757 – 761, 2014.

[30] Cota, I., Medina, F., Gonzalez-Olmos, R., and Iglesias, M. Alanine-supported protic ionic liquids as efficient catalysts for aldol condensation reactions. *C. R. Chimie*, **17**(1), 18 – 22, 2014.

[31] Matuszek, K., Chrobok, A., Coleman, F., Seddon, K. R., and Swadzba-Kwasny, M. Tailoring ionic liquid catalysts: structure, acidity and catalytic activity of protonic ionic liquids based on anionic clusters, [(HSO4)(H2SO4)x]- (x = 0, 1, or 2). *Green Chem.*, **16**(7), 3463–3471, 2014.

[32] Li, H., Bhadury, P. S., Song, B., and Yang, S. Immobilized functional ionic liquids: efficient, green, and reusable catalysts. *RSC Adv.*, **2**(33), 12525–12551, 2012.

[33] Salminen, E., Maki-Arvela, P., Virtanen, P., Salmi, T., Warna, J., and Mikkola, J. P. Kinetics upon Isomerization of α,β-Pinene Oxides over Supported Ionic Liquid Catalysts Containing Lewis Acids. *Ind. Eng. Chem. Res.*, **53**(52), 20107–20115, 2014.

[34] Nehra, P., Khungar, B., Pericherla, K., Sivasubramanian, S. C., and Kumar, A. Imidazolium ionic liquid-tagged palladium complex: an efficient catalyst for the heck and suzuki reactions in aqueous media. *Green Chem.*, **16**(9), 4266–4271, 2014.

[35] Beier, M. J., Andanson, J.-M., Mallat, T., Krumeich, F., and Baiker, A. Ionic Liquid-Supported Pt Nanoparticles as Catalysts for Enantioselective Hydrogenation. *ACS Catal.*, **2**(3), 337–340, 2012.

[36] Cai, F., Zhao, M., Wang, Y., Wang, F., and Xiao, G. Phosphoric-based ionic liquids as solvents to separate the azeotropic mixture of ethanol and hexane. *J. Chem. Thermodyn.*, **81**, 177 – 183, 2015.

[37] Ram, N. M., Naidoo, P., Letcher, T. M., and Ramjugernath, D. (Liquid+liquid) equilibria for mixtures of dodecane and ethanol with alkylsulfate-based ionic liquids. *J. Chem. Thermodyn.*, **81**, 95 – 100, 2015.

[38] Garcia, S., Garcia, J., Larriba, M., Torrecilla, J. S., and Rodriguez, F. Sulfonate-Based Ionic Liquids in the Liquid liquid Extraction of Aromatic Hydrocarbons. *J. Chem. Eng. Data*, **56**(7), 3188–3193, 2011.

[39] Garcia, S., Larriba, M., Garcia, J., Torrecilla, J. S., and Rodriguez, F. Liquid-Liquid Extraction of Toluene from Heptane Using 1-Alkyl-3-methylimidazolium Bis(trifluoromethylsulfonyl)imide Ionic Liquids. *J. Chem. Eng. Data*, **56**(1), 113–118, 2011.

[40] Papaiconomou, N., Vite, G., Goujon, N., Leveque, J. M., and Billard, I. Efficient removal of gold complexes from water by precipitation or liquid-liquid extraction using ionic liquids. *Green Chem.*, **14**, 2050–2056, 2012.

[41] Manohar, C. V., Banerjee, T., and Mohanty, K. Co-solvent effects for aromatic extraction with ionic liquids. *J. Mol. Liq.*, **180**, 145 – 153, 2013.

[42] Shah, M. R., Anantharaj, R., Banerjee, T., and Yadav, G. D. Quaternary (liquid+liquid) equilibria for systems of imidazolium based ionic liquid+thiophene+pyridine+cyclohexane at 298.15 K: Experiments and quantum chemical predictions. *J. Chem. Thermodyn.*, **62**, 142 – 150, 2013.

[43] Santos, E., Albo, J., and Irabien, A. Acetate based Supported Ionic Liquid Membranes (SILMs) for CO2 separation: Influence of the temperature. *J. Membr. Sci.*, **452**, 277 – 283, 2014.

[44] Li, P., Paul, D. R., and Chung, T. S. High performance membranes based on ionic liquid polymers for CO2 separation from the flue gas. *Green Chem.*, **14**(4), 1052–1063, 2012.

[45] Shiflett, M. B., Niehaus, A. M. S., and Yokozeki, A. Separation of N2O and CO2 Using Room-Temperature Ionic Liquid [bmim][BF4]. *J. Phys. Chem. B*, **115**(13), 3478–3487, 2011.

[46] Shiflett, M. B., Niehaus, A. M. S., and Yokozeki, A. Separation of CO2 and H2S Using Room-Temperature Ionic Liquid [bmim][MeSO4]. *J. Chem. Eng. Data*, **55** (11), 4785–4793, 2010.

[47] Tome, L. C., Patinha, D. J. S., Freire, C. S. R., Rebelo, L. P. N., and Marrucho, I. M. Co2 separation applying ionic liquid mixtures: the effect of mixing different anions on gas permeation through supported ionic liquid membranes. *RSC Adv.*, **3**(30), 12220–12229, 2013.

[48] Pereiro, A. B. and Rodriguez, A. Ternary Liquid-Liquid Equilibria Ethanol + 2-Butanone + 1-Butyl-3-methylimidazolium Hexafluorophosphate, 2-Propanol + 2-Butanone + 1-Butyl-3-methylimidazolium Hexafluorophosphate, and 2-Butanone + 2-Propanol + 1,3-Dimethylimidazolium Methyl Sulfate at 298.15 K. *J. Chem. Eng. Data*, **52**(6), 2138–2142, 2007.

[49] Nann, A., Held, C., and Sadowski, G. Liquid-liquid equilibria of 1-butanol/water/IL systems. *Ind. Eng. Chem. Res.*, **52**(51), 18472–18482, 2013.

[50] Davis, S. and Morton III, S. Investigation of ionic liquids for the separation of butanol and water. *Sep. Sci. Technol.*, **43**(9-10), 2460–2472, 2008.

[51] Kubiczek, A. and Kamiński, W. Ionic liquids for the extraction of n-butanol from aqueous solutions. *Proc. ECOpole*, **7**(1), 125–131, 2013.

[52] Heitmann, S., Stoffers, M., and Lutze, P. Integrated processing for the separation of biobutanol. Part B: model-based process analysis. *Green Process. Synth.*, **2**(2), 121–141, 2013.

[53] Chowdhury, S. A., Scott, J. L., and MacFarlane, D. R. Ternary mixtures of phosphonium ionic liquids + organic solvents + water. *Pure Appl. Chem.*, **80** (6), 1325–1335, 2008.

[54] Matsumoto, M., Panigrahi, A., Murakami, Y., and Kondo, K. Effect of Ammonium- and Phosphonium-Based Ionic Liquids on the Separation of Lactic Acid by Supported Ionic Liquid Membranes (SILMs). *Membranes*, **1**(2), 98–108, 2011.

[55] Martak, J. and Schlosser, S. Liquid-liquid equilibria of butyric acid for solvents containing a phosphonium ionic liquid. *Chem. Pap.*, **62**(1), 42–50, 2008.

[56] Reid, R. C., Prausnitz, J. M., and Sherwood, T. K. *The properties of gases and liquids*. McGraw-Hill, New York, 1977. ISBN 9780070517905.

[57] Mchaweh, A., Alsaygh, A., Nasrifar, K., and Moshfeghian, M. A simplified method for calculating saturated liquid densities. *Fluid Phase Equilib.*, **224**(2), 157 – 167, 2004.

[58] Valderrama, J. O. and Zarricueta, K. A simple and generalized model for predicting the density of ionic liquids. *Fluid Phase Equilib.*, **275**(2), 145 – 151, 2009.

[59] Nasrifar, K. and Moshfeghian, M. A saturated liquid density equation in conjunction with the Predictive-Soave-Redlich-Kwong equation of state for pure refrigerants and LNG multicomponent systems. *Fluid Phase Equilib.*, **153**(2), 231 – 242, 1998.

[60] Ji, W. R. and Lempe, D. A. Density improvement of the SRK equation of state. *Fluid Phase Equilib.*, **130**(2), 49 – 63, 1997.

[61] Joshipura, M. H., Dabke, S. P., and Subrahmanyam, N. Modeling vapour pressure using compound specific cohesion factor relationship. *J. Taiwan Inst. Chem. Eng.*, **41**(5), 570 – 578, 2010.

[62] *Instruction Manual DMA 4100M, DMA 4500M, DMA 5000M*. Anton Paar GmbH, 2009.

[63] Valderrama, J. O., Forero, L. A., and Rojas, R. E. Critical Properties and Normal Boiling Temperature of Ionic Liquids. Update and a New Consistency Test. *Ind. Eng. Chem. Res.*, **51**(22), 7838–7844, 2012.

[64] Valderrama, J. O. and Robles, P. A. Critical Properties, Normal Boiling Temperatures, and Acentric Factors of Fifty Ionic Liquids. *Ind. Eng. Chem. Res.*, **46**(4), 1338–1344, 2007.

[65] Valderrama, J. O., Sanga, W. W., and Lazzus, J. A. Critical Properties, Normal Boiling Temperature, and Acentric Factor of Another 200 Ionic Liquids. *Ind. Eng. Chem. Res.*, **47**(4), 1318–1330, 2008.

[66] Valderrama, J. O. and Rojas, R. E. Critical Properties of Ionic Liquids. Revisited. *Ind. Eng. Chem. Res.*, **48**(14), 6890–6900, 2009.

[67] Rudkin, J. Equation predicts vapor pressures. *Chem. Eng.*, **22**, 202, 1961.

[68] Hanwell, M. D., Curtis, D. E., Lonie, D. C., Vandermeersch, T., Zurek, E., and Hutchison, G. R. Avogadro: an advanced semantic chemical editor, visualization, and analysis platform. *J. Cheminf.*, **4**(1), 1 – 17, 2012.

[69] Breneman, C. M. and Wiberg, K. B. Determining atom-centered monopoles from molecular electrostatic potentials. The need for high sampling density in formamide conformational analysis. *J. Comput. Chem.*, **11**(3), 361–373, 1990.

[70] Martinez, L., Andrade, R., Birgin, E. G., and Martinez, J. M. PACKMOL: A package for building initial configurations for molecular dynamics simulations. *J. Comput. Chem.*, **30**(13), 2157–2164, 2009.

[71] Kale, L., Skeel, R., Bhandarkar, M., Brunner, R., Gursoy, A., Krawetz, N., Phillips, J., Shinozaki, A., Varadarajan, K., and Schulten, K. NAMD2: Greater Scalability for Parallel Molecular Dynamics. *J. Comput. Phys.*, **151**(1), 283 – 312, 1999.

[72] Sieffert, N. and Wipff, G. The [BMI][Tf_2N] Ionic Liquid/Water Binary System: A Molecular Dynamics Study of Phase Separation and of the Liquid-Liquid Interface. *J. Phys. Chem. B*, **110**(26), 13076–13085, 2006.

[73] Krolikowska, M. and Hofman, T. Densities, isobaric expansivities and isothermal compressibilities of the thiocyanate-based ionic liquids at temperatures(298.15-338.15 K) and pressures up to 10 MPa. *Thermochim. Acta*, **530**, 1 – 6, 2012.

[74] Freire, M. G., Teles, A. R. R., Rocha, M. A. A., Schroder, B., Neves, C. M. S. S., Carvalho, P. J., Evtuguin, D. V., Santos, L. M. N. B. F., and Coutinho, J. A. P. Thermophysical Characterization of Ionic Liquids Able To Dissolve Biomass. *J. Chem. Eng. Data*, **56**(12), 4813–4822, 2011.

[75] Seki, S., Kobayashi, T., Kobayashi, Y., Takei, K., Miyashiro, H., Hayamizu, K., Tsuzuki, S., Mitsugi, T., and Umebayashi, Y. Effects of cation and anion on physical properties of room-temperature ionic liquids. *J. Mol. Liq.*, **152**, 9 – 13, 2010.

[76] Domanska, U. and Krolikowski, M. Measurements of activity coefficients at infinite dilution for organic solutes and water in the ionic liquid 1-ethyl-3-methylimidazolium methanesulfonate. *J. Chem. Thermodyn.*, **54**, 20 – 27, 2012.

[77] Ficke, L. E., Novak, R. R., and Brennecke, J. F. Thermodynamic and Thermophysical Properties of Ionic Liquid + Water Systems. *J. Chem. Eng. Data*, **55**(11), 4946–4950, 2010.

[78] Froba, A., Rausch, M., Krzeminski, K., Assenbaum, D., Wasserscheid, P., and Leipertz, A. Thermal Conductivity of Ionic Liquids: Measurement and Prediction. *Int. J. Thermophys.*, **31**(11), 2059–2077, 2010.

[79] Shiflett, M. B. and Yokozeki, A. Phase Behavior of Carbon Dioxide in Ionic Liquids: [emim][Acetate], [emim][Trifluoroacetate], and [emim][Acetate] + [emim][Trifluoroacetate] Mixtures. *J. Chem. Eng. Data*, **54**(1), 108–114, 2009.

[80] Rosenboom, J. G., Afzal, W., and Prausnitz, J. M. Solubilities of some organic solutes in 1-ethyl-3-methylimidazolium acetate. chromatographic measurements and predictions from COSMO-RS. *J. Chem. Thermodyn.*, **47**, 320–327, 2012.

[81] Quijada-Maldonado, E., Boogaart, S. d., Lijbers, J. H., W., M. G., and Haan, A. B. d. Experimental densities, dynamic viscosities and surface tensions of the ionic liquids series 1-ethyl-3-methylimidazolium acetate and dicyanamide and their binary and ternary mixtures with water and ethanol at T=(298.15 to 343.15K). *J. Chem. Thermodyn.*, **51**, 51 – 58, 2012.

[82] Schmidt, H., Stephan, M., Safarov, J., Kul, I., Nocke, J., M., A. I., and Hassel, E. Experimental study of the density and viscosity of 1-ethyl-3-methylimidazolium ethyl sulfate. *J. Chem. Thermodyn.*, **47**, 68 – 75, 2012.

[83] Regueira, T., Lugo, L., and Fernandez, J. High pressure volumetric properties of 1-ethyl-3-methylimidazolium ethylsulfate and 1-(2-methoxyethyl)-1-methyl-pyrrolidinium bis(trifluoromethylsulfonyl)imide. *J. Chem. Thermodyn.*, **48**, 213 – 220, 2012.

[84] Nieto de Castro, C. A., Langa, E., Morais, A. L., Matos Lopes, M. L., Lourenco, M. J., Santos, F. J., Santos, M. S. C., Canongia Lopes, J. N., Veiga, H. I., Macatrao, M., Esperanca, J. M., Marques, C. S., Rebelo, L. P., and Afonso, C. A. Studies on the density, heat capacity, surface tension and infinite dilution diffusion with the ionic liquids [C4mim][NTf2], [C4mim][dca], [C2mim][EtOSO3] and [Aliquat][dca]. *Fluid Phase Equilib.*, **294**, 157 – 179, 2010. Ionic Liquids Special Issue.

[85] Matkowska, D., Goldon, A., and Hofman, T. Densities, Excess Volumes, Isobaric Expansivities, and Isothermal Compressibilities of the 1-Ethyl-3-methylimidazolium Ethylsulfate + Ethanol System at Temperatures (283.15 to 343.15) K and Pressures from (0.1 to 35) MPa. *J. Chem. Eng. Data*, **55**(2), 685–693, 2010.

[86] Hofman, T., Goldon, A., Nevines, A., and Letcher, T. M. Densities, excess volumes, isobaric expansivity, and isothermal compressibility of the (1-ethyl-3-methylimidazolium ethylsulfate+methanol) system at temperatures (283.15 to 333.15)K and pressures from (0.1 to 35)MPa. *J. Chem. Thermodyn.*, **40**(4), 580 – 591, 2008.

[87] McHale, G., Hardacre, C., Ge, R., Doy, N., Allen, R. W. K., MacInnes, J. M., Bown, M. R., and Newton, M. I. Density-Viscosity Product of Small-Volume Ionic Liquid Samples Using Quartz Crystal Impedance Analysis. *Anal. Chem.*, **80**(15), 5806–5811, 2008.

[88] Arce, A., Soto, A., Ortega, J., and Sabater, G. Viscosities and Volumetric Properties of Binary and Ternary Mixtures of Tris(2-hydroxyethyl) Methylammonium Methylsulfate + Water + Ethanol at 298.15 K. *J. Chem. Eng. Data*, **53**(3), 770–775, 2008.

[89] Hwang, I. C., Park, S. J., and Han, K. J. Vapor-liquid equilibria at 333.15K and excess molar volumes and deviations in molar refractivity at 298.15K for mixtures of diisopropyl ether, ethanol and ionic liquids. *Fluid Phase Equilib.*, **309**(2), 145 – 150, 2011.

[90] Hwang, I. C., Kwon, R. H., and Park, S. J. Azeotrope breaking for the system ethyl tert-butyl ether (ETBE)+ethanol at 313.15K and excess properties at 298.15K for mixtures of ETBE and ethanol with phosphonium-based ionic liquids. *Fluid Phase Equilib.*, **344**, 32 – 37, 2013.

[91] Diogo, J. C. F., Caetano, F. J. P., Fareleira, J. M. N. A., Wakeham, W. A., Afonso, C. A. M., and Marques, C. S. Viscosity Measurements of the Ionic Liquid Trihexyl(tetradecyl)phosphonium Dicyanamide [P6,6,6,14][dca] Using the Vibrating Wire Technique. *J. Chem. Eng. Data*, **57**(4), 1015–1025, 2012.

[92] Fraser, K. J. and MacFarlane, D. R. Phosphonium-Based Ionic Liquids: An Overview. *Aust. J. Chem.*, **62**, 309 – 321, 2009.

[93] Brennecke, J. F. and Maginn, E. J. Ionic liquids: innovative fluids for chemical processing. *AIChE J.*, **47**(11), 2384–2389, 2001.

[94] Varma, N. R., Ramalingam, A., and Banerjee, T. Experiments, correlations and COSMO-RS predictions for the extraction of benzothiophene from n-hexane using imidazolium-based ionic liquids. *Chem. Eng. J.*, **166**(1), 30–39, 2011.

[95] Anantharaj, R. and Banerjee, T. Liquid-liquid equilibria for quaternary systems of imidazolium based ionic liquid + thiophene + pyridine + iso-octane at 298.15 K: Experiments and quantum chemical predictions. *Fluid Phase Equilib.*, **312**, 20 – 30, 2011.

[96] Potdar, S., Anantharaj, R., and Banerjee, T. Aromatic Extraction Using Mixed Ionic Liquids: Experiments and COSMO-RS Predictions. *J. Chem. Eng. Data*, **57** (4), 1026–1035, 2012.

[97] Heintz, A. Recent developments in thermodynamics and thermophysics of non-aqueous mixtures containing ionic liquids. A review. *J. Chem. Thermodyn.*, **37**(6), 525 – 535, 2005.

[98] Kumar, A. A. P. and Banerjee, T. Thiophene separation with ionic liquids for desulphurization: A quantum chemical approach. *Fluid Phase Equilib.*, **278**, 1 – 8, 2009.

[99] Arce, A., Earle, M. J., Rodriguez, H., Seddon, K. R., and Soto, A. Bis(trifluoromethyl)sulfonylamide ionic liquids as solvents for the extraction of aromatic hydrocarbons from their mixtures with alkanes: effect of the nature of the cation. *Green Chem.*, **11**(3), 365–372, 2009.

[100] Cheruku, S. and Banerjee, T. Liquid-Liquid Equilibrium Data for 1-Ethyl-3-methylimidazolium Acetate-Thiophene-Diesel Compound: Experiments and Correlations. *J. Solution Chem.*, **41**(5), 898–913, 2012.

[101] Garcia, J., Fernandez, A., Torrecilla, J. S., Oliet, M., and Rodriguez, F. Ternary Liquid-Liquid Equilibria Measurement for Hexane and Benzene with the Ionic Liquid 1-Butyl-3-methylimidazolium Methylsulfate at T = (298.2, 313.2, and 328.2) K. *J. Chem. Eng. Data*, **55**(1), 258–261, 2010.

[102] Gonzalez, E. J., Calvar, N., Gomez, E., and Dominguez, A. Separation of Benzene from Linear Alkanes (C6-C9) Using 1-Ethyl-3-Methylimidazolium Ethylsulfate at T = 298.15 K. *J. Chem. Eng. Data*, **55**(9), 3422–3427, 2010.

[103] Meindersma, G. W., Podt, A., Klaren, M. B., and de Haan, A. B. Separation of Aromatic and Aliphatic Hydrocarbons with Ionic Liquids. *Chem. Eng. Commun.*, **193**(11), 1384–1396, 2006.

[104] Melo, C. I., Bogel-Lukasik, R., da Ponte, M. N., and Bogel-Lukasik, E. Ammonium ionic liquids as green solvents for drugs. *Fluid Phase Equilib.*, **338**, 209 – 216, 2013.

[105] Deenadayalu, N., Ngcongo, K. C., Letcher, T. M., and Ramjugernath, D. Liquid-Liquid Equilibria for Ternary Mixtures (an Ionic Liquid + Benzene + Heptane or Hexadecane) at T = 298.2 K and Atmospheric Pressure. *J. Chem. Eng. Data*, **51**(3), 988–991, 2006.

[106] Letcher, T. M. and Deenadayalu, N. Ternary liquid-liquid equilibria for mixtures of 1-methyl-3-octyl-imidazolium chloride + benzene + an alkane at T=298.2 K and 1 atm. *J. Chem. Thermodyn.*, **35**(1), 67 – 76, 2003.

[107] Gonzalez, E. J., Calvar, N., Gonzalez, B., and Dominguez, A. Separation of toluene from alkanes using 1-ethyl-3-methylpyridinium ethylsulfate ionic liquid at T = 298.15 K and atmospheric pressure. *J. Chem. Thermodyn.*, **42**(6), 752 – 757, 2010.

[108] Gottlieb, H. E., Kotlyar, V., and Nudelman, A. NMR Chemical Shifts of Common Laboratory Solvents as Trace Impurities. *J. Org. Chem.*, **62**(21), 7512–7515, 1997.

[109] Spectral database for organic compounds (SDBS). "http://sdbs.riodb.aist.go.jp/", 2012. accessed on 10 February.

[110] Richter, K., Birkner, A., and Mudring, A. V. Stability and growth behavior of transition metal nanoparticles in ionic liquids prepared by thermal evaporation: how stable are they really? *Phys. Chem. Chem. Phys.*, **13**(15), 7136–7141, 2011.

[111] Cascon, H. and Choudhary, S. Separation performance and stability of PVDF-co-HFP/alkylphosphonium dicyanamide ionic liquid gel-based membrane in pervaporative separation of 1-butanol. *Sep. Sci. Technol.*, **48**(11), 1616–1626, 2013.

[112] Garbuz, S., Skopenko, V., Khavryuchenko, V., and Gerasimchuk, N. Quantum-chemical simulation of dicyanamide and tricyanomethanide ion solvation. *Theor. Exp. Chem.*, **25**(1), 83–86, 1989.

[113] Renon, H. and Prausnitz, J. M. Local compositions in thermodynamic excess functions for liquid mixtures. *AIChE J.*, **14**(1), 135–144, 1968.

[114] Abrams, D. S. and Prausnitz, J. M. Statistical thermodynamics of liquid mixtures: a new expression for the excess gibbs energy of partly or completely miscible systems. *AIChE J.*, **21**(1), 116–128, 1975.

[115] Banerjee, T., Singh, M. K., Sahoo, R. K., and Khanna, A. Volume, surface and UNIQUAC interaction parameters for imidazolium based ionic liquids via polarizable continuum model. *Fluid phase equilib.*, **234**(1), 64–76, 2005.

[116] Singh, M. K., Banerjee, T., and Khanna, A. Genetic algorithm to estimate interaction parameters of multicomponent systems for liquid–liquid equilibria. *Comp. Chem. Engg.*, **29**(8), 1712–1719, 2005.

[117] Wang, S. and Sandler, S. I. Refinement of COSMO-SAC and the Applications. *Ind. Eng. Chem. Res.*, **46**(22), 7275–7288, 2007.

[118] Frisch, M. J., Trucks, G. W., Schlegel, H. B., Scuseria, G. E., Robb, M. A., Cheeseman, J. R., Montgomery Jr., J. A., Vreven, T., Kudin, K. N., Burant, J. C., Millam, J. M., Iyengar, S. S., Tomasi, J., Barone, V., Mennucci, B., Cossi, M., Scalmani, G., Rega, N., Petersson, G. A., Nakatsuji, H., Hada, M., Ehara, M., Toyota, K., Fukuda, R., Hasegawa, J., Ishida, M., Nakajima, T., Honda, Y., Kitao, O., Nakai, H., Klene, M., Li, X., Knox, J. E., Hratchian, H. P., Cross, J. B., Bakken, V., Adamo, C., Jaramillo, J., Gomperts, R., Stratmann, R. E., Yazyev, O., Austin, A. J., Cammi, R., Pomelli, C., Ochterski, J. W., Ayala, P. Y., Morokuma, K., Voth, G. A., Salvador, P., Dannenberg, J. J., Zakrzewski, V. G., Dapprich, S., Daniels, A. D., Strain, M. C., Farkas, O., Malick, D. K., Rabuck, A. D., Raghavachari, K., Foresman, J. B., Ortiz, J. V., Cui, Q., Baboul, A. G., Clifford, S., Cioslowski, J., Stefanov, B. B., Liu, G., Liashenko, A., Piskorz, P., Komaromi, I., Martin, R. L., Fox, D. J., Keith, T., Al-Laham, M. A., Peng, C. Y., Nanayakkara, A., Challacombe, M., Gill, P. M. W., Johnson, B., Chen, W., Wong, M. W., Gonzalez, C., and Pople, J. A. Gaussian 03, Revision C.02. Gaussian, Inc., Wallingford, CT, 2004.

[119] Kim, K. and Jordan, K. D. Comparison of Density Functional and MP2 Calculations on the Water Monomer and Dimer. *J. Phys. Chem.*, **98**(40), 10089–10094, 1994.

[120] Perdew, J. P. Density-functional approximation for the correlation energy of the inhomogeneous electron gas. *Phys. Rev. B*, **33**(12), 8822–8824, 1986.

[121] Schaefer, A., Huber, C., and Ahlrichs, R. Fully optimized contracted gaussian basis sets of triple zeta valence quality for atoms Li to Kr. *J. Chem. Phys.*, **100** (8), 5829–5835, 1994.

[122] Sosa, C., Andzelm, J., Elkin, B. C., Wimmer, E., Dobbs, K. D., and Dixon, D. A. A local density functional study of the structure and vibrational frequencies of molecular transition-metal compounds. *J. Phys. Chem.*, **96**(16), 6630–6636, 1992.

[123] Mohanty, S., Banerjee, T., and Mohanty, K. Quantum chemical based screening of ionic liquids for the extraction of phenol from aqueous solution. *Ind. Eng. Chem. Res.*, **49**(6), 2916–2925, 2010.

[124] Banerjee, T., Verma, K. K., and Khanna, A. Liquid-liquid equilibrium for ionic liquid systems using COSMO-RS: Effect of cation and anion dissociation. *AIChE J.*, **54**(7), 1874–1885, 2008.

[125] Rabari, D. and Banerjee, T. Biobutanol and n-propanol recovery using a low density phosphonium based ionic liquid at T= 298.15 K and p= 1 atm. *Fluid Phase Equilib.*, **355**, 26–33, 2013.

[126] Neves, C. M., Granjo, J. F., Freire, M. G., Robertson, A., Oliveira, N. M., and Coutinho, J. A. Separation of ethanol-water mixtures by liquid-liquid extraction using phosphonium-based ionic liquids. *Green Chem.*, **13**, 1517–1526, 2011.

[127] Rabari, D. and Banerjee, T. Experimental and Theoretical Studies on the Effectiveness of Phosphonium-Based Ionic Liquids for Butanol Removal at T= 298.15 K and p = 1 atm. *Ind. Eng. Chem. Res.*, **53**(49), 18935–18942, 2014.

[128] Reusch, W. Nuclear magnetic resonance spectroscopy. `http://www2.chemistry.msu.edu/faculty/reusch/VirtTxtJml/Spectrpy/nmr/nmr1.htm`, 2014. accessed on 24 May.

[129] Verma, V. K. and Banerjee, T. Ionic liquids as entrainers for water+ ethanol, water+ 2-propanol, and water+ THF systems: A quantum chemical approach. *J. Chem. Thermodyn.*, **42**(7), 909–919, 2010.

[130] Goldberg, D. E. *Genetic Algorithms in Search, Optimization and Machine Learning*. Addison-Wesley Longman Publishing Co., Inc., Boston, MA, USA, 1st edition, 1989. ISBN 0201157675.

[131] Kirkpatrick, S., Gelatt, C. D., and Vecchi, M. P. Optimization by Simulated Annealing. *Science*, **220**(4598), 671–680, 1983.

[132] Eberhart, R. and Kennedy, J. A new optimizer using particle swarm theory. In *Proceedings of the Sixth International Symposium on Micro Machine and Human Science*, 39–43, Oct 1995.

[133] Kennedy, J. and Eberhart, R. Particle swarm optimization. In *Proceedings of IEEE International Conference on Neural Networks*, 4, 1942–1948, Nov 1995.

[134] Colorni, A., Dorigo, M., and Maniezzo, V. Distributed Optimization by Ant Colonies. In *Proceedings of the First European conference on Artificial Life*, 134–142, 1991.

[135] Dorigo, M. *Optimization, Learning and Natural Algorithms (in Italian)*. PhD thesis, Dipartimento di Elettronica, Politecnico di Milano, Milan, Italy, 1992.

[136] Storn, R. and Price, K. Differential evolution - A Simple and Efficient Heuristic for global Optimization over Continuous Spaces. *J. Global Optim.*, **11**(4), 341–359, 1997.

[137] Storn, R. On the usage of differential evolution for function optimization. In *Proceedings of Biennial Conference of the North American on Fuzzy Information Processing Society*, 519–523, Jun 1996.

[138] Zelinka, I. Soma - Self-Organizing Migrating Algorithm. In *New Optimization Techniques in Engineering*, 141 of *Studies in Fuzziness and Soft Computing*, 167–217. Springer Berlin Heidelberg, 2004. ISBN 978-3-642-05767-0.

[139] Hassan, R., Cohanim, B. E., and de Weck, O. L. A Comparison of Particle Swarm Optimization and the Genetic Algorithm. In *46th AIAA/ASME/ASCE/AHS/ASC Structures, Structural Dynamics, and Materials Conference*, number AIAA-2005-1897, Austin, Texas, April 2005. American Institute of Aeronautics and Astronautics.

[140] Sivanandam, S. N. and Deepa, S. N. A comparative Study Using Genetic Algorithm and Particle Swarm Optimization for Lower Order System Modelling. *International Journal of the Computer, the Internet and Management*, **17**(3), 1–10, 2009.

[141] Ethni, S. A., Zahawi, B., Giaouris, D., and Acarnley, P. P. Comparison of particle swarm and simulated annealing algorithms for induction motor fault identification. In *Proceedings of 7th IEEE International Conference on Industrial Informatics*, 470–474, June 2009.

[142] Elbeltagi, E., Hegazy, T., and Grierson, D. Comparison among five evolutionary-based optimization algorithms. *Adv. Eng. Inform.*, **19**(1), 43 – 53, 2005.

[143] Tsuboka, T. and Katayama, T. General design algorithm based on pseudo-equilibrium concept for multistage multi-component liquid-liquid separation processes. *J. Chem. Eng. Jpn.*, **9**(1), 40–45, 1976.

[144] Seader, J. D. and Henley, E. J. *Separation Process Principles*. Wiley India Pvt. Ltd., New Delhi, India, 2nd edition, 2010. ISBN 9788126509270.

[145] Arumugam, M. S. and Rao, M. On the improved performances of the particle swarm optimization algorithms with adaptive parameters, cross-over operators and root mean square (RMS) variants for computing optimal control of a class of hybrid systems. *Appl. Soft. Comput.*, **8**(1), 324 – 336, 2008.

[146] Ubaidullah, S., Upadhyay, R., Raut, S., and Rahman, I. Optimization of Continuous Extraction Column and Solvent Selection Using Differential Evolution Technique. *J. Inst. Eng.: Series E*, **93**(1), 49–54, 2012.

[147] Shin, D. K., Gurdal, Z., and Griffin, O. H. A penalty approach for nonlinear optimization with discrete design variables. *Eng. Optimiz.*, **16**(1), 29–42, 1990.

[148] Kitayama, S., Arakawa, M., and Yamazaki, K. Penalty function approach for the mixed discrete nonlinear problems by particle swarm optimization. *Struct. Multidiscip. O.*, **32**(3), 191–202, 2006.

Appendix A

NAMD Configuration File

```
#############################################################
## JOB DESCRIPTION                                         ##
#############################################################

# 150 molecules of [TDTHP][DEC] or [TDTHP][DCA] IL


#############################################################
## ADJUSTABLE PARAMETERS                                   ##
#############################################################

structure          ../common/TDDEC150.psf #or /TDDCA150.psf
coordinates        ../02_Heating/TDDEC150_heat.coor #or /TDDCA150_heat.coor
extendedSystem     ../02_Heating/TDDEC150_heat.xsc #or /TDDCA150_heat.xsc

set temperature    300
set outputname     TDDEC150_eq #or TDDCA150_eq
set restart    0

# Continuing a job from the restart files
if {$restart} {
set inputname      myinput
Coordinates        $inputname.restart.coor
Velocities         $inputname.restart.vel  ;
extendedSystem     $inputname.xsc
}

firsttimestep      0


#############################################################
## SIMULATION PARAMETERS                                   ##
#############################################################

# Input
paraTypeCharmm     on
parameters         ../common/TDTHP-DEC.params #or /TDTHP-DCA.params
if {$restart-1} {
temperature        $temperature
}

# Force-Field Parameters
exclude            scaled1-4
1-4scaling         0.5
cutoff             15.0
switching          on
switchdist         13.5
pairlistdist       16.5


# Integrator Parameters
```

```
timestep            1.0  ;# 1fs/step
nonbondedFreq       1
vdwGeometricSigma   yes
fullElectFrequency  2
stepspercycle       20
pairlistsperCycle   2

# Periodic Boundary Conditions
if {0} {
cellBasisVector1    74.2    0.   0.0
cellBasisVector2     0.0  73.2   0.0
cellBasisVector3     0.0    0   126.1
cellOrigin           0.0   0.0  25.9

# PME (for full-system periodic electrostatics)
PME                 yes
PMEGridSpacing      1.0

#manual grid definition
#PMEGridSizeX        74.2
#PMEGridSizeY        73.2
#PMEGridSizeZ        126.1
}
wrapAll             on

# Constant Temperature Control
if {1} {
langevin            on    ;# do langevin dynamics
langevinDamping     1     ;# damping coefficient (gamma) of 1/ps
langevinTemp        $temperature
langevinHydrogen    off    ;# don't couple langevin bath to hydrogens
}

# Constant Pressure Control (variable volume)
if {1} {
useGroupPressure      yes ;# needed for rigidBonds
useFlexibleCell       no
useConstantArea       no

langevinPiston        on
langevinPistonTarget  1.01325 ;#  in bar -> 1 atm
langevinPistonPeriod  100.0
langevinPistonDecay   50.0
langevinPistonTemp    $temperature
}

# Fixed Atoms Constraint (set PDB beta-column to 1)
if {0} {
fixedAtoms          on
#fixedAtomsForces    on #Is it necessary?
fixedAtomsFile      ../../02_Heating/IL20-Mixed_heat.coor
fixedAtomsCol       B
}

# IMD Settings (can view sim in VMD)
if {0} {
IMDon           on
IMDport         3000    ;# port number (enter it in VMD)
```

```
IMDfreq         1       ;# send every 1 frame
IMDwait         no      ;# wait for VMD to connect before running?
}

# Output
outputName          $outputname

restartfreq         500     ;# 500steps = every 1ps
dcdfreq             250
outputEnergies      100
outputPressure      100

binaryoutput        no
binaryrestart       no

#############################################################
## EXTRA PARAMETERS                                        ##
#############################################################


#############################################################
## EXECUTION SCRIPT                                        ##
#############################################################

# Equilibration
seed                1010
numsteps            2000000             # Number of integration steps
```

[TDTHP][DCA] Parameter File

```
BONDS
!
!V(bond)=Kb(b-b0)**2
!Kb:kcal/mole
!bo:A
!
!atom type              Kb              b0
!
!TDTHP
P3  CT  424.2352    1.810  !
CT  HC  339.9857    1.090  !
CT  CT  267.9254    1.529  !

!DCA
N3  CZ  502.6291    1.310  !
CZ  NZ  925.6692    1.157  !

!TIP3P WATER
OW  HT   450.0000      0.9572 !

ANGLES
!
!V(angle)=Ktheta(Theta-Theta0)**2
!
!Ktheta:Kcal/mole
!Theta0:degrees
!
!atom types     Ktheta      Theta0
!TDTHP
CT  P3  CT  72.634      109.500  !
HC  CT  P3  46.594      110.100  !
CT  CT  P3  60.839      115.200  !
CT  CT  CT  58.353      112.700  !
CT  CT  HC  37.500      110.700  !
HC  CT  HC  32.995      107.800  !

!DCA
CZ  N3  CZ  43.260      118.500  !
N3  CZ  NZ  50.789      175.200  !

!TIP3P Water
HT   OW   HT     55.0000  104.52 !

DIHEDRALS
!
!V(dihedral)=Kchi(1+cos(n(chi)-delta))
!
!Kchi:Kcal/mol
!n:multiplicity
!delta:degrees
!
!atom types         Kchi        n   delta
!TDTHP
CT  P3  CT  HC    0.0000    1     0 !
CT  P3  CT  HC    0.0000    2   180 !
```

```
CT  P3  CT  HC    0.1108    3     0 !
CT  P3  CT  CT    0.0000    1     0 !
CT  P3  CT  CT    0.0000    2   180 !
CT  P3  CT  CT    0.1354    3     0 !
P3  CT  CT  HC    0.0000    1     0 !
P3  CT  CT  HC    0.0000    2   180 !
P3  CT  CT  HC    0.0556    3     0 !
P3  CT  CT  CT   -0.3881    1     0 !
P3  CT  CT  CT    0.1181    2   180 !
P3  CT  CT  CT   -0.0854    3     0 !
HC  CT  CT  HC    0.0000    1     0 !
HC  CT  CT  HC    0.0000    2   180 !
HC  CT  CT  HC    0.1590    3     0 !
CT  CT  CT  HC    0.0000    1     0 !
CT  CT  CT  HC    0.0000    2   180 !
CT  CT  CT  HC    0.1830    3     0 !
CT  CT  CT  CT    0.8700    1     0 !
CT  CT  CT  CT   -0.0785    2   180 !
CT  CT  CT  CT    0.1395    3     0 !

!DCA
NZ  CZ  N3  CZ    0.4876    1     0 !
NZ  CZ  N3  CZ    0.0000    2   180 !
NZ  CZ  N3  CZ    0.0000    3     0 !

NONBONDED
!
!V(Lennard-Jones)=Eps,i,j[(Rmin,i,j/ri,j)**12-2(Rmin,i,j/ri,j)**6]
!
!epsilon:Kcal/mol,Eps,i,j=sqrt(eps,i*eps,j)
!Rmin/2:A,Rmin,i,j=Rmin/2,i + Rmin/2,j
!
!atom   ignored     epsilon     Rmin/2
!TDTHP
P3    0.000000    -0.2000    2.0990  !
CT    0.000000    -0.0660    1.9643  !
HC    0.000000    -0.0300    1.4031  !

!DCA
N3    0.000000    -0.1700    1.8240  !
CZ    0.000000    -0.0660    1.8521  !
NZ    0.000000    -0.1700    1.7959  !

!TIP3P Water
HT      0.000000  -0.046000     0.224500 !
OW      0.000000  -0.152100     1.768200 !

END
```

[TDTHP][DCA] PDB File

```
HEADER
TITLE     Built with Packmol
REMARK   Packmol generated pdb file
REMARK   Home-Page: http://www.ime.unicamp.br/~martinez/packmol
REMARK
ATOM      1  C1  TDT A   1    2.160   10.815  19.567  1   0    TD1 C
ATOM      2  P1  TDT A   1    3.257   10.666  18.096  1   0    TD1 P
ATOM      3  C2  TDT A   1    4.304   12.167  18.054  1   0    TD1 C
ATOM      4  C3  TDT A   1    3.650   13.526  18.349  1   0    TD1 C
ATOM      5  C4  TDT A   1    4.707   14.643  18.382  1   0    TD1 C
ATOM      6  C5  TDT A   1    4.203   15.972  18.966  1   0    TD1 C
ATOM      7  C6  TDT A   1    3.104   16.703  18.179  1   0    TD1 C
ATOM      8  C7  TDT A   1    3.539   17.200  16.796  1   0    TD1 C
ATOM      9  C8  TDT A   1    2.461   17.987  16.032  1   0    TD1 C
ATOM     10  C9  TDT A   1    2.016   19.339  16.621  1   0    TD1 C
ATOM     11  C10 TDT A   1    3.107   20.429  16.692  1   0    TD1 C
ATOM     12  C11 TDT A   1    3.845   20.534  18.033  1   0    TD1 C
ATOM     13  C12 TDT A   1    4.918   21.629  18.051  1   0    TD1 C
ATOM     14  C13 TDT A   1    5.638   21.764  19.397  1   0    TD1 C
ATOM     15  C14 TDT A   1    6.715   22.854  19.413  1   0    TD1 C
ATOM     16  C15 TDT A   1    7.428   22.983  20.761  1   0    TD1 C
ATOM     17  C16 TDT A   1    1.336   9.581   19.995  1   0    TD1 C
ATOM     18  C17 TDT A   1    2.014   8.718   21.066  1   0    TD1 C
ATOM     19  C18 TDT A   1    1.179   7.497   21.466  1   0    TD1 C
ATOM     20  C19 TDT A   1    1.825   6.646   22.564  1   0    TD1 C
ATOM     21  C20 TDT A   1    0.984   5.428   22.953  1   0    TD1 C
ATOM     22  C21 TDT A   1    4.433   9.266   18.212  1   0    TD1 C
ATOM     23  C22 TDT A   1    3.898   7.860   17.886  1   0    TD1 C
ATOM     24  C23 TDT A   1    5.014   6.810   17.966  1   0    TD1 C
ATOM     25  C24 TDT A   1    4.526   5.404   17.604  1   0    TD1 C
ATOM     26  C25 TDT A   1    5.635   4.347   17.643  1   0    TD1 C
ATOM     27  C26 TDT A   1    5.142   2.946   17.278  1   0    TD1 C
ATOM     28  C27 TDT A   1    2.193   10.404  16.633  1   0    TD1 C
ATOM     29  C28 TDT A   1    1.311   11.576  16.146  1   0    TD1 C
ATOM     30  C29 TDT A   1    1.920   12.334  14.959  1   0    TD1 C
ATOM     31  C30 TDT A   1    1.025   13.473  14.459  1   0    TD1 C
ATOM     32  C31 TDT A   1    1.470   14.085  13.122  1   0    TD1 C
ATOM     33  C32 TDT A   1    2.852   14.746  13.150  1   0    TD1 C
ATOM     34  N1  DCA A   1    5.720   10.994  15.421  1   0    TD1 N
ATOM     35  C33 DCA A   1    5.417   10.135  14.679  1   0    TD1 C
ATOM     36  N2  DCA A   1    5.120   9.197   13.829  1   0    TD1 N
ATOM     37  C34 DCA A   1    4.111   8.405   14.100  1   0    TD1 C
ATOM     38  N3  DCA A   1    3.217   7.680   14.311  1   0    TD1 N
ATOM     39  H1  TDT A   1    1.495   11.650  19.325  1   0    TD1 H
ATOM     40  H2  TDT A   1    2.785   11.165  20.395  1   0    TD1 H
ATOM     41  H3  TDT A   1    1.076   8.965   19.128  1   0    TD1 H
ATOM     42  H4  TDT A   1    0.380   9.938   20.390  1   0    TD1 H
ATOM     43  H5  TDT A   1    2.202   9.337   21.954  1   0    TD1 H
ATOM     44  H6  TDT A   1    2.999   8.386   20.719  1   0    TD1 H
ATOM     45  H7  TDT A   1    0.188   7.830   21.801  1   0    TD1 H
ATOM     46  H8  TDT A   1    1.001   6.873   20.581  1   0    TD1 H
ATOM     47  H9  TDT A   1    1.998   7.268   23.451  1   0    TD1 H
ATOM     48  H10 TDT A   1    2.816   6.314   22.231  1   0    TD1 H
ATOM     49  H11 TDT A   1    0.000   5.726   23.328  1   0    TD1 H
ATOM     50  H12 TDT A   1    1.470   4.840   23.735  1   0    TD1 H
```

```
ATOM     51  H13 TDT A   1    0.822   4.765   22.097  1   0   TD1 H
ATOM     52  H14 TDT A   1    4.869   9.305   19.218  1   0   TD1 H
ATOM     53  H15 TDT A   1    5.228   9.539   17.511  1   0   TD1 H
ATOM     54  H16 TDT A   1    3.481   7.843   16.876  1   0   TD1 H
ATOM     55  H17 TDT A   1    3.090   7.583   18.571  1   0   TD1 H
ATOM     56  H18 TDT A   1    5.449   6.804   18.976  1   0   TD1 H
ATOM     57  H19 TDT A   1    5.823   7.099   17.286  1   0   TD1 H
ATOM     58  H20 TDT A   1    4.080   5.430   16.603  1   0   TD1 H
ATOM     59  H21 TDT A   1    3.720   5.107   18.290  1   0   TD1 H
ATOM     60  H22 TDT A   1    6.089   4.329   18.642  1   0   TD1 H
ATOM     61  H23 TDT A   1    6.436   4.642   16.953  1   0   TD1 H
ATOM     62  H24 TDT A   1    4.366   2.602   17.970  1   0   TD1 H
ATOM     63  H25 TDT A   1    5.956   2.215   17.307  1   0   TD1 H
ATOM     64  H26 TDT A   1    4.716   2.925   16.270  1   0   TD1 H
ATOM     65  H27 TDT A   1    1.579   9.536   16.893  1   0   TD1 H
ATOM     66  H28 TDT A   1    2.846   10.055  15.830  1   0   TD1 H
ATOM     67  H29 TDT A   1    1.071   12.271  16.959  1   0   TD1 H
ATOM     68  H30 TDT A   1    0.350   11.157  15.836  1   0   TD1 H
ATOM     69  H31 TDT A   1    2.913   12.712  15.224  1   0   TD1 H
ATOM     70  H32 TDT A   1    2.087   11.619  14.145  1   0   TD1 H
ATOM     71  H33 TDT A   1    0.970   14.262  15.222  1   0   TD1 H
ATOM     72  H34 TDT A   1    0.000   13.096  14.344  1   0   TD1 H
ATOM     73  H35 TDT A   1    0.722   14.826  12.814  1   0   TD1 H
ATOM     74  H36 TDT A   1    1.455   13.305  12.351  1   0   TD1 H
ATOM     75  H37 TDT A   1    2.901   15.530  13.913  1   0   TD1 H
ATOM     76  H38 TDT A   1    3.080   15.213  12.187  1   0   TD1 H
ATOM     77  H39 TDT A   1    3.648   14.027  13.357  1   0   TD1 H
ATOM     78  H40 TDT A   1    4.815   12.140  17.084  1   0   TD1 H
ATOM     79  H41 TDT A   1    5.084   11.966  18.799  1   0   TD1 H
ATOM     80  H42 TDT A   1    3.136   13.501  19.316  1   0   TD1 H
ATOM     81  H43 TDT A   1    2.889   13.753  17.598  1   0   TD1 H
ATOM     82  H44 TDT A   1    5.113   14.788  17.376  1   0   TD1 H
ATOM     83  H45 TDT A   1    5.552   14.305  18.993  1   0   TD1 H
ATOM     84  H46 TDT A   1    5.062   16.646  19.072  1   0   TD1 H
ATOM     85  H47 TDT A   1    3.846   15.789  19.988  1   0   TD1 H
ATOM     86  H48 TDT A   1    2.771   17.553  18.785  1   0   TD1 H
ATOM     87  H49 TDT A   1    2.220   16.060  18.073  1   0   TD1 H
ATOM     88  H50 TDT A   1    3.831   16.345  16.175  1   0   TD1 H
ATOM     89  H51 TDT A   1    4.447   17.808  16.895  1   0   TD1 H
ATOM     90  H52 TDT A   1    1.574   17.349  15.924  1   0   TD1 H
ATOM     91  H53 TDT A   1    2.821   18.164  15.011  1   0   TD1 H
ATOM     92  H54 TDT A   1    1.576   19.195  17.615  1   0   TD1 H
ATOM     93  H55 TDT A   1    1.195   19.702  15.994  1   0   TD1 H
ATOM     94  H56 TDT A   1    2.648   21.404  16.484  1   0   TD1 H
ATOM     95  H57 TDT A   1    3.833   20.272  15.883  1   0   TD1 H
ATOM     96  H58 TDT A   1    4.309   19.575  18.289  1   0   TD1 H
ATOM     97  H59 TDT A   1    3.113   20.733  18.827  1   0   TD1 H
ATOM     98  H60 TDT A   1    4.459   22.591  17.788  1   0   TD1 H
ATOM     99  H61 TDT A   1    5.656   21.427  17.264  1   0   TD1 H
ATOM    100  H62 TDT A   1    4.901   21.972  20.185  1   0   TD1 H
ATOM    101  H63 TDT A   1    6.095   20.801  19.663  1   0   TD1 H
ATOM    102  H64 TDT A   1    6.260   23.816  19.147  1   0   TD1 H
ATOM    103  H65 TDT A   1    7.453   22.645  18.628  1   0   TD1 H
ATOM    104  H66 TDT A   1    6.725   23.233  21.562  1   0   TD1 H
ATOM    105  H67 TDT A   1    8.191   23.766  20.738  1   0   TD1 H
ATOM    106  H68 TDT A   1    7.924   22.048  21.042  1   0   TD1 H
END
```

[TDTHP][DCA] PSF File

```
PSF

       1 !NTITLE
 REMARKS VMD-generated NAMD/X-Plor PSF structure file

     106 !NATOM
       1 TD1  1    TDT  N1   NZ    -0.813247       14.0067           0
       2 TD1  1    TDT  C1   CZ     0.698705       12.0107           0
       3 TD1  1    TDT  N2   N3    -0.770851       14.0067           0
       4 TD1  1    TDT  C2   CZ     0.698722       12.0107           0
       5 TD1  1    TDT  N3   NZ    -0.813330       14.0067           0
       6 TD1  1    TDT  P1   P3     0.331869       30.9738           0
       7 TD1  1    TDT  C3   CT    -0.130331       12.0107           0
       8 TD1  1    TDT  C4   CT    -0.150988       12.0107           0
       9 TD1  1    TDT  C5   CT     0.091967       12.0107           0
      10 TD1  1    TDT  H1   HC     0.066084        1.0079           0
      11 TD1  1    TDT  H2   HC     0.083769        1.0079           0
      12 TD1  1    TDT  C6   CT    -0.071679       12.0107           0
      13 TD1  1    TDT  H3   HC    -0.005087        1.0079           0
      14 TD1  1    TDT  H4   HC     0.017687        1.0079           0
      15 TD1  1    TDT  C7   CT    -0.014130       12.0107           0
      16 TD1  1    TDT  H5   HC     0.023218        1.0079           0
      17 TD1  1    TDT  H6   HC     0.023417        1.0079           0
      18 TD1  1    TDT  C8   CT     0.202206       12.0107           0
      19 TD1  1    TDT  H7   HC     0.006699        1.0079           0
      20 TD1  1    TDT  H8   HC     0.001089        1.0079           0
      21 TD1  1    TDT  C9   CT    -0.215989       12.0107           0
      22 TD1  1    TDT  H9   HC    -0.034771        1.0079           0
      23 TD1  1    TDT  H10  HC    -0.035219        1.0079           0
      24 TD1  1    TDT  H11  HC     0.049570        1.0079           0
      25 TD1  1    TDT  H12  HC     0.062070        1.0079           0
      26 TD1  1    TDT  H13  HC     0.047274        1.0079           0
      27 TD1  1    TDT  C10  CT     0.101576       12.0107           0
      28 TD1  1    TDT  H14  HC     0.090929        1.0079           0
      29 TD1  1    TDT  H15  HC     0.070089        1.0079           0
      30 TD1  1    TDT  C11  CT    -0.081811       12.0107           0
      31 TD1  1    TDT  H16  HC     0.015496        1.0079           0
      32 TD1  1    TDT  H17  HC    -0.005966        1.0079           0
      33 TD1  1    TDT  C12  CT     0.001161       12.0107           0
      34 TD1  1    DCA  H18  HC     0.023665        1.0079           0
      35 TD1  1    DCA  H19  HC     0.025861        1.0079           0
      36 TD1  1    DCA  C13  CT     0.196030       12.0107           0
      37 TD1  1    DCA  H20  HC    -0.002341        1.0079           0
      38 TD1  1    DCA  H21  HC     0.003619        1.0079           0
      39 TD1  1    TDT  C14  CT    -0.229728       12.0107           0
      40 TD1  1    TDT  H22  HC    -0.031933        1.0079           0
      41 TD1  1    TDT  H23  HC    -0.033511        1.0079           0
      42 TD1  1    TDT  H24  HC     0.051142        1.0079           0
      43 TD1  1    TDT  H25  HC     0.066091        1.0079           0
      44 TD1  1    TDT  H26  HC     0.052938        1.0079           0
      45 TD1  1    TDT  C15  CT    -0.109953       12.0107           0
      46 TD1  1    TDT  C16  CT     0.075905       12.0107           0
      47 TD1  1    TDT  H27  HC     0.081818        1.0079           0
      48 TD1  1    TDT  H28  HC     0.060757        1.0079           0
      49 TD1  1    TDT  C17  CT    -0.070587       12.0107           0
```

```
  50 TD1  1    TDT  H29  HC     0.020059        1.0079          0
  51 TD1  1    TDT  H30  HC    -0.002961        1.0079          0
  52 TD1  1    TDT  C18  CT     0.000894       12.0107          0
  53 TD1  1    TDT  H31  HC     0.020536        1.0079          0
  54 TD1  1    TDT  H32  HC     0.023393        1.0079          0
  55 TD1  1    TDT  C19  CT     0.206693       12.0107          0
  56 TD1  1    TDT  H33  HC    -0.003791        1.0079          0
  57 TD1  1    TDT  H34  HC     0.003212        1.0079          0
  58 TD1  1    TDT  C20  CT    -0.210557       12.0107          0
  59 TD1  1    TDT  H35  HC    -0.037667        1.0079          0
  60 TD1  1    TDT  H36  HC    -0.038131        1.0079          0
  61 TD1  1    TDT  H37  HC     0.045039        1.0079          0
  62 TD1  1    TDT  H38  HC     0.060586        1.0079          0
  63 TD1  1    TDT  H39  HC     0.046587        1.0079          0
  64 TD1  1    TDT  C21  CT    -0.119791       12.0107          0
  65 TD1  1    TDT  C22  CT     0.033587       12.0107          0
  66 TD1  1    TDT  H40  HC     0.064650        1.0079          0
  67 TD1  1    TDT  H41  HC     0.082792        1.0079          0
  68 TD1  1    TDT  C23  CT    -0.002938       12.0107          0
  69 TD1  1    TDT  H42  HC     0.005400        1.0079          0
  70 TD1  1    TDT  H43  HC     0.026053        1.0079          0
  71 TD1  1    TDT  C24  CT     0.030553       12.0107          0
  72 TD1  1    TDT  H44  HC     0.009754        1.0079          0
  73 TD1  1    TDT  H45  HC     0.008310        1.0079          0
  74 TD1  1    TDT  C25  CT     0.054550       12.0107          0
  75 TD1  1    TDT  H46  HC    -0.006781        1.0079          0
  76 TD1  1    TDT  H47  HC    -0.015793        1.0079          0
  77 TD1  1    TDT  C26  CT     0.036790       12.0107          0
  78 TD1  1    TDT  H48  HC    -0.017428        1.0079          0
  79 TD1  1    TDT  H49  HC    -0.016810        1.0079          0
  80 TD1  1    TDT  C27  CT     0.041215       12.0107          0
  81 TD1  1    TDT  H50  HC    -0.016473        1.0079          0
  82 TD1  1    TDT  H51  HC    -0.013731        1.0079          0
  83 TD1  1    TDT  C28  CT     0.029418       12.0107          0
  84 TD1  1    TDT  H52  HC    -0.018035        1.0079          0
  85 TD1  1    TDT  H53  HC    -0.016811        1.0079          0
  86 TD1  1    TDT  C29  CT     0.040228       12.0107          0
  87 TD1  1    TDT  H54  HC    -0.016835        1.0079          0
  88 TD1  1    TDT  H55  HC    -0.018100        1.0079          0
  89 TD1  1    TDT  C30  CT     0.103152       12.0107          0
  90 TD1  1    TDT  H56  HC    -0.019364        1.0079          0
  91 TD1  1    TDT  H57  HC    -0.018513        1.0079          0
  92 TD1  1    TDT  C31  CT    -0.023374       12.0107          0
  93 TD1  1    TDT  H58  HC    -0.033092        1.0079          0
  94 TD1  1    TDT  H59  HC    -0.033266        1.0079          0
  95 TD1  1    TDT  C32  CT     0.028799       12.0107          0
  96 TD1  1    TDT  H60  HC    -0.011218        1.0079          0
  97 TD1  1    TDT  H61  HC    -0.010813        1.0079          0
  98 TD1  1    TDT  C33  CT     0.204438       12.0107          0
  99 TD1  1    TDT  H62  HC    -0.015355        1.0079          0
 100 TD1  1    TDT  H63  HC    -0.015325        1.0079          0
 101 TD1  1    TDT  C34  CT    -0.210951       12.0107          0
 102 TD1  1    TDT  H64  HC    -0.045893        1.0079          0
 103 TD1  1    TDT  H65  HC    -0.045687        1.0079          0
 104 TD1  1    TDT  H66  HC     0.039558        1.0079          0
 105 TD1  1    TDT  H67  HC     0.049349        1.0079          0
 106 TD1  1    TDT  H68  HC     0.039914        1.0079          0
```

```
104 !NBOND: bonds
  1       2       2       3       3       4       4       5
  6       7       6      45       6      64       6       8
  7      10       7      11       7       9       8      27
  8      29       8      28       9      12       9      13
  9      14      12      15      12      16      12      17
 15      20      15      18      15      19      18      21
 18      22      18      23      21      24      21      25
 21      26      27      32      27      30      27      31
 30      35      30      34      30      33      33      36
 33      37      33      38      36      39      36      40
 36      41      39      42      39      44      39      43
 45      47      45      46      45      48      46      49
 46      50      46      51      49      53      49      52
 49      54      52      55      52      56      52      57
 55      58      55      59      55      60      58      61
 58      62      58      63      64      65      64      67
 64      66      65      70      65      68      65      69
 68      71      68      72      68      73      71      76
 71      74      71      75      74      77      74      78
 74      79      77      82      77      80      77      81
 80      83      80      84      80      85      83      88
 83      86      83      87      86      89      86      90
 86      91      89      94      89      92      89      93
 92      95      92      96      92      97      95     100
 95      98      95      99      98     101      98     102
 98     103     101     104     101     105     101     106

201 !NTHETA: angles
  1       2       3       2       3       4       3       4       5
  7       6      45       7       6      64       7       6       8
 45       6      64       8       6      45       8       6      64
 10       7      11       9       7      10       6       7      10
  9       7      11       6       7      11       6       7       9
  6       8      27       6       8      29       6       8      28
 27       8      29      27       8      28      28       8      29
  7       9      12       7       9      13       7       9      14
 12       9      13      12       9      14      13       9      14
  9      12      15       9      12      16       9      12      17
 15      12      16      15      12      17      16      12      17
 12      15      20      12      15      18      12      15      19
 18      15      20      19      15      20      18      15      19
 15      18      21      15      18      22      15      18      23
 21      18      22      21      18      23      22      18      23
 18      21      24      18      21      25      18      21      26
 24      21      25      24      21      26      25      21      26
  8      27      32      30      27      32      31      27      32
  8      27      30       8      27      31      30      27      31
 27      30      35      27      30      34      27      30      33
 34      30      35      33      30      35      33      30      34
 30      33      36      30      33      37      30      33      38
 36      33      37      36      33      38      37      33      38
 33      36      39      33      36      40      33      36      41
 39      36      40      39      36      41      40      36      41
 36      39      42      36      39      44      36      39      43
 42      39      44      42      39      43      43      39      44
 46      45      47       6      45      47      47      45      48
  6      45      46      46      45      48       6      45      48
```

```
 45      46      49      49      46      50      49      46      51
 45      46      50      45      46      51      50      46      51
 52      49      53      53      49      54      46      49      53
 52      49      54      46      49      52      46      49      54
 49      52      55      49      52      56      49      52      57
 55      52      56      55      52      57      56      52      57
 52      55      58      52      55      59      52      55      60
 58      55      59      58      55      60      59      55      60
 55      58      61      55      58      62      55      58      63
 61      58      62      61      58      63      62      58      63
  6      64      65       6      64      67       6      64      66
 65      64      67      65      64      66      66      64      67
 68      65      70      64      65      70      69      65      70
 64      65      68      68      65      69      64      65      69
 71      68      72      71      68      73      65      68      71
 72      68      73      65      68      72      65      68      73
 68      71      76      74      71      76      75      71      76
 68      71      74      68      71      75      74      71      75
 71      74      77      77      74      78      77      74      79
 71      74      78      71      74      79      78      74      79
 80      77      82      81      77      82      74      77      82
 80      77      81      74      77      80      74      77      81
 77      80      83      77      80      84      77      80      85
 83      80      84      83      80      85      84      80      85
 86      83      88      80      83      88      87      83      88
 80      83      86      86      83      87      80      83      87
 89      86      90      89      86      91      83      86      89
 90      86      91      83      86      90      83      86      91
 86      89      94      92      89      94      93      89      94
 86      89      92      86      89      93      92      89      93
 89      92      95      95      92      96      95      92      97
 89      92      96      89      92      97      96      92      97
 98      95     100      99      95     100      92      95     100
 98      95      99      92      95      98      92      95      99
 95      98     101      95      98     102      95      98     103
101      98     102     101      98     103     102      98     103
 98     101     104     104     101     105     104     101     106
 98     101     105      98     101     106     105     101     106

290 !NPHI: dihedrals
  1       2       3       4       2       3       4       5
 45       6       7      10      45       6       7      11
 45       6       7       9      64       6       7      10
 64       6       7      11      64       6       7       9
  8       6       7      10       8       6       7      11
  8       6       7       9       7       6      45      47
  7       6      45      46       7       6      45      48
 64       6      45      47      64       6      45      46
 64       6      45      48       8       6      45      47
  8       6      45      46       8       6      45      48
  7       6      64      65       7       6      64      67
  7       6      64      66      45       6      64      65
 45       6      64      67      45       6      64      66
  8       6      64      65       8       6      64      67
  8       6      64      66       7       6       8      27
  7       6       8      29       7       6       8      28
 45       6       8      27      45       6       8      29
 45       6       8      28      64       6       8      27
```

```
64   6   8  29  64   6   8  28
10   7   9  12  10   7   9  13
10   7   9  14  11   7   9  12
11   7   9  13  11   7   9  14
 6   7   9  12   6   7   9  13
 6   7   9  14   6   8  27  32
 6   8  27  30   6   8  27  31
29   8  27  32  29   8  27  30
29   8  27  31  28   8  27  32
28   8  27  30  28   8  27  31
 7   9  12  15   7   9  12  16
 7   9  12  17  13   9  12  15
13   9  12  16  13   9  12  17
14   9  12  15  14   9  12  16
14   9  12  17   9  12  15  20
 9  12  15  18   9  12  15  19
16  12  15  20  16  12  15  18
16  12  15  19  17  12  15  20
17  12  15  18  17  12  15  19
12  15  18  21  12  15  18  22
12  15  18  23  20  15  18  21
20  15  18  22  20  15  18  23
19  15  18  21  19  15  18  22
19  15  18  23  15  18  21  24
15  18  21  25  15  18  21  26
22  18  21  24  22  18  21  25
22  18  21  26  23  18  21  24
23  18  21  25  23  18  21  26
32  27  30  35  32  27  30  34
32  27  30  33   8  27  30  35
 8  27  30  34   8  27  30  33
31  27  30  35  31  27  30  34
31  27  30  33  27  30  33  36
27  30  33  37  27  30  33  38
35  30  33  36  35  30  33  37
35  30  33  38  34  30  33  36
34  30  33  37  34  30  33  38
30  33  36  39  30  33  36  40
30  33  36  41  37  33  36  39
37  33  36  40  37  33  36  41
38  33  36  39  38  33  36  40
38  33  36  41  33  36  39  42
33  36  39  44  33  36  39  43
40  36  39  42  40  36  39  44
40  36  39  43  41  36  39  42
41  36  39  44  41  36  39  43
47  45  46  49  47  45  46  50
47  45  46  51   6  45  46  49
 6  45  46  50   6  45  46  51
48  45  46  49  48  45  46  50
48  45  46  51  45  46  49  53
45  46  49  52  45  46  49  54
50  46  49  53  50  46  49  52
50  46  49  54  51  46  49  53
51  46  49  52  51  46  49  54
53  49  52  55  53  49  52  56
53  49  52  57  54  49  52  55
54  49  52  56  54  49  52  57
```

46	49	52	55	46	49	52	56
46	49	52	57	49	52	55	58
49	52	55	59	49	52	55	60
56	52	55	58	56	52	55	59
56	52	55	60	57	52	55	58
57	52	55	59	57	52	55	60
52	55	58	61	52	55	58	62
52	55	58	63	59	55	58	61
59	55	58	62	59	55	58	63
60	55	58	61	60	55	58	62
60	55	58	63	6	64	65	70
6	64	65	68	6	64	65	69
67	64	65	70	67	64	65	68
67	64	65	69	66	64	65	70
66	64	65	68	66	64	65	69
70	65	68	71	70	65	68	72
70	65	68	73	64	65	68	71
64	65	68	72	64	65	68	73
69	65	68	71	69	65	68	72
69	65	68	73	72	68	71	76
72	68	71	74	72	68	71	75
73	68	71	76	73	68	71	74
73	68	71	75	65	68	71	76
65	68	71	74	65	68	71	75
76	71	74	77	76	71	74	78
76	71	74	79	68	71	74	77
68	71	74	78	68	71	74	79
75	71	74	77	75	71	74	78
75	71	74	79	71	74	77	82
71	74	77	80	71	74	77	81
78	74	77	82	78	74	77	80
78	74	77	81	79	74	77	82
79	74	77	80	79	74	77	81
82	77	80	83	82	77	80	84
82	77	80	85	81	77	80	83
81	77	80	84	81	77	80	85
74	77	80	83	74	77	80	84
74	77	80	85	77	80	83	88
77	80	83	86	77	80	83	87
84	80	83	88	84	80	83	86
84	80	83	87	85	80	83	88
85	80	83	86	85	80	83	87
88	83	86	89	88	83	86	90
88	83	86	91	80	83	86	89
80	83	86	90	80	83	86	91
87	83	86	89	87	83	86	90
87	83	86	91	90	86	89	94
90	86	89	92	90	86	89	93
91	86	89	94	91	86	89	92
91	86	89	93	83	86	89	94
83	86	89	92	83	86	89	93
94	89	92	95	94	89	92	96
94	89	92	97	86	89	92	95
86	89	92	96	86	89	92	97
93	89	92	95	93	89	92	96
93	89	92	97	89	92	95	100
89	92	95	98	89	92	95	99
96	92	95	100	96	92	95	98

```
 96      92      95      99      97      92      95     100
 97      92      95      98      97      92      95      99
100      95      98     101     100      95      98     102
100      95      98     103      99      95      98     101
 99      95      98     102      99      95      98     103
 92      95      98     101      92      95      98     102
 92      95      98     103      95      98     101     104
 95      98     101     105      95      98     101     106
102      98     101     104     102      98     101     105
102      98     101     106     103      98     101     104
103      98     101     105     103      98     101     106

  0 !NIMPHI: impropers


  0 !NDON: donors


  0 !NACC: acceptors


  0 !NNB

  0       0       0       0       0       0       0       0
  0       0       0       0       0       0       0       0
  0       0       0       0       0       0       0       0
  0       0       0       0       0       0       0       0
  0       0       0       0       0       0       0       0
  0       0       0       0       0       0       0       0
  0       0       0       0       0       0       0       0
  0       0       0       0       0       0       0       0
  0       0       0       0       0       0       0       0
  0       0       0       0       0       0       0       0
  0       0       0       0       0       0       0       0
  0       0       0       0       0       0       0       0
  0       0       0       0       0       0       0       0
  0       0

  1       0 !NGRP
  0       0       0
```

[TDTHP][DEC] Parameter File

```
BONDS
!
!V(bond)=Kb(b-b0)**2
!Kb:kcal/mole
!bo:A
!
!atom type              Kb              b0
!
!TDTHP
P3  CT  424.2352    1.810  !
CT  HC  339.9857    1.090  !
CT  CT  267.9254    1.529  !

!DEC
C   CT  167.5000    1.522  !
C   O2  328.0000    1.250  !


!TIP3P WATER
OW  HT   450.0000      0.9572 !

ANGLES
!
!V(angle)=Ktheta(Theta-Theta0)**2
!
!Ktheta:Kcal/mole
!Theta0:degrees
!
!atom types     Ktheta      Theta0
!TDTHP
CT  P3  CT  72.634      109.500  !
HC  CT  P3  46.594      110.100  !
CT  CT  P3  60.839      115.200  !
CT  CT  CT  58.353      112.700  !
CT  CT  HC  37.500      110.700  !
HC  CT  HC  32.995      107.800  !

!DEC
C   CT  CT  31.500      111.100  !
C   CT  HC  17.500      109.500  !
CT  C   O2  35.000      117.000  !
O2  C   O2  40.000      126.000  !

!TIP3P Water
HT   OW   HT     55.0000  104.52 !

DIHEDRALS
!
!V(dihedral)=Kchi(1+cos(n(chi)-delta))
!
!Kchi:Kcal/mol
!n:multiplicity
!delta:degrees
!
!atom types         Kchi        n   delta
```

```
!TDTHP
CT  P3  CT  HC    0.0000    1     0 !
CT  P3  CT  HC    0.0000    2   180 !
CT  P3  CT  HC    0.1108    3     0 !
CT  P3  CT  CT    0.0000    1     0 !
CT  P3  CT  CT    0.0000    2   180 !
CT  P3  CT  CT    0.1354    3     0 !
P3  CT  CT  HC    0.0000    1     0 !
P3  CT  CT  HC    0.0000    2   180 !
P3  CT  CT  HC    0.0556    3     0 !
P3  CT  CT  CT   -0.3881    1     0 !
P3  CT  CT  CT    0.1181    2   180 !
P3  CT  CT  CT   -0.0854    3     0 !
HC  CT  CT  HC    0.0000    1     0 !
HC  CT  CT  HC    0.0000    2   180 !
HC  CT  CT  HC    0.1590    3     0 !
CT  CT  CT  HC    0.0000    1     0 !
CT  CT  CT  HC    0.0000    2   180 !
CT  CT  CT  HC    0.1830    3     0 !
CT  CT  CT  CT    0.8700    1     0 !
CT  CT  CT  CT   -0.0785    2   180 !
CT  CT  CT  CT    0.1395    3     0 !

!DEC
HC  CT  CT  C     0.6500    3     0 !
CT  CT  CT  C     0.6500    3     0 !
CT  CT  C   O2    0.0000    2     0 !
HC  CT  C   O2    0.0000    2     0 !

IMPROPER
!
!V(improper) = Kpsi(psi - psi0)**2
!
!Kpsi: kcal/mole/rad**2
!psi0: degrees
!note that the second column of numbers (0) is ignored
!
!atom types           Kpsi                   psi0
O2  O2  CT  C     0.0000    2     0 !
C   O2  O2  CT    0.0000    2     0 !
O2  CT  O2  C     0.0000    2     0 !

NONBONDED
!
!V(Lennard-Jones)=Eps,i,j[(Rmin,i,j/ri,j)**12-2(Rmin,i,j/ri,j)**6]
!
!epsilon:Kcal/mol,Eps,i,j=sqrt(eps,i*eps,j)
!Rmin/2:A,Rmin,i,j=Rmin/2,i + Rmin/2,j
!
!atom   ignored     epsilon     Rmin/2
!TDTHP
P3    0.000000    -0.2000    2.0990  !
CT    0.000000    -0.0660    1.9643  !
HC    0.000000    -0.0300    1.4031  !

!DEC
C     0.000000    -0.1200    0.9250  !
O2    0.000000    -0.2000    0.8000  !
```

```
!TIP3P Water
HT       0.000000  -0.046000     0.224500 !
OW       0.000000  -0.152100     1.768200 !

END
```

[TDTHP][DEC] PDB File

```
HEADER
TITLE     Built with Packmol
REMARK   Packmol generated pdb file
REMARK   Home-Page: http://www.ime.unicamp.br/~martinez/packmol
REMARK
ATOM      1  C1  TDT A   1    5.139   12.500  50.071  1   0    TDE C
ATOM      2  C2  TDT A   1    5.041   11.454  48.940  1   0    TDE C
ATOM      3  C3  TDT A   1    6.090   10.339  49.016  1   0    TDE C
ATOM      4  C4  TDT A   1    5.846   9.244   47.973  1   0    TDE C
ATOM      5  C5  TDT A   1    6.893   8.127   48.014  1   0    TDE C
ATOM      6  C6  TDT A   1    6.644   7.033   46.972  1   0    TDE C
ATOM      7  P1  TDT A   1    6.274   13.926  49.864  1   0    TDE P
ATOM      8  C7  TDT A   1    6.362   14.768  51.503  1   0    TDE C
ATOM      9  C8  TDT A   1    5.058   14.950  52.297  1   0    TDE C
ATOM     10  C9  TDT A   1    5.307   15.687  53.620  1   0    TDE C
ATOM     11  C10 TDT A   1    4.073   15.791  54.531  1   0    TDE C
ATOM     12  C11 TDT A   1    2.874   16.574  53.972  1   0    TDE C
ATOM     13  C12 TDT A   1    3.163   18.046  53.658  1   0    TDE C
ATOM     14  C13 TDT A   1    1.940   18.848  53.181  1   0    TDE C
ATOM     15  C14 TDT A   1    0.795   19.061  54.189  1   0    TDE C
ATOM     16  C15 TDT A   1    1.153   19.878  55.449  1   0    TDE C
ATOM     17  C16 TDT A   1    1.561   19.049  56.675  1   0    TDE C
ATOM     18  C17 TDT A   1    1.903   19.904  57.900  1   0    TDE C
ATOM     19  C18 TDT A   1    2.284   19.081  59.135  1   0    TDE C
ATOM     20  C19 TDT A   1    2.631   19.934  60.361  1   0    TDE C
ATOM     21  C20 TDT A   1    3.011   19.104  61.589  1   0    TDE C
ATOM     22  C21 TDT A   1    8.012   13.425  49.533  1   0    TDE C
ATOM     23  C22 TDT A   1    8.426   13.320  48.056  1   0    TDE C
ATOM     24  C23 TDT A   1    9.822   12.706  47.907  1   0    TDE C
ATOM     25  C24 TDT A   1    10.281  12.645  46.446  1   0    TDE C
ATOM     26  C25 TDT A   1    11.644  11.970  46.264  1   0    TDE C
ATOM     27  C26 TDT A   1    12.103  11.926  44.804  1   0    TDE C
ATOM     28  C27 TDT A   1    5.706   15.044  48.553  1   0    TDE C
ATOM     29  C28 TDT A   1    4.320   15.685  48.730  1   0    TDE C
ATOM     30  C29 TDT A   1    3.944   16.513  47.492  1   0    TDE C
ATOM     31  C30 TDT A   1    2.549   17.137  47.604  1   0    TDE C
ATOM     32  C31 TDT A   1    2.093   17.904  46.353  1   0    TDE C
ATOM     33  C32 TDT A   1    2.921   19.152  46.033  1   0    TDE C
ATOM     34  H1  TDT A   1    4.163   12.961  50.244  1   0    TDE H
ATOM     35  H2  TDT A   1    5.420   12.024  51.019  1   0    TDE H
ATOM     36  H3  TDT A   1    5.094   11.926  47.956  1   0    TDE H
ATOM     37  H4  TDT A   1    4.044   11.006  49.019  1   0    TDE H
ATOM     38  H5  TDT A   1    6.093   9.899   50.025  1   0    TDE H
ATOM     39  H6  TDT A   1    7.089   10.754  48.850  1   0    TDE H
ATOM     40  H7  TDT A   1    4.848   8.810   48.128  1   0    TDE H
ATOM     41  H8  TDT A   1    5.843   9.712   46.984  1   0    TDE H
ATOM     42  H9  TDT A   1    6.918   7.677   49.017  1   0    TDE H
ATOM     43  H10 TDT A   1    7.887   8.561   47.852  1   0    TDE H
ATOM     44  H11 TDT A   1    5.674   6.550   47.127  1   0    TDE H
ATOM     45  H12 TDT A   1    7.411   6.253   47.015  1   0    TDE H
ATOM     46  H13 TDT A   1    6.647   7.446   45.959  1   0    TDE H
ATOM     47  H14 TDT A   1    8.161   12.474  50.054  1   0    TDE H
ATOM     48  H15 TDT A   1    8.637   14.159  50.057  1   0    TDE H
ATOM     49  H16 TDT A   1    8.422   14.323  47.614  1   0    TDE H
ATOM     50  H17 TDT A   1    7.703   12.736  47.476  1   0    TDE H
```

```
ATOM     51  H18 TDT A   1    9.816   11.692  48.325  1   0   TDE H
ATOM     52  H19 TDT A   1    10.554  13.274  48.500  1   0   TDE H
ATOM     53  H20 TDT A   1    10.323  13.664  46.038  1   0   TDE H
ATOM     54  H21 TDT A   1    9.521   12.117  45.858  1   0   TDE H
ATOM     55  H22 TDT A   1    11.598  10.949  46.661  1   0   TDE H
ATOM     56  H23 TDT A   1    12.397  12.494  46.868  1   0   TDE H
ATOM     57  H24 TDT A   1    11.388  11.381  44.180  1   0   TDE H
ATOM     58  H25 TDT A   1    13.073  11.431  44.703  1   0   TDE H
ATOM     59  H26 TDT A   1    12.201  12.933  44.387  1   0   TDE H
ATOM     60  H27 TDT A   1    5.700   14.454  47.614  1   0   TDE H
ATOM     61  H28 TDT A   1    6.482   15.813  48.453  1   0   TDE H
ATOM     62  H29 TDT A   1    4.287   16.324  49.621  1   0   TDE H
ATOM     63  H30 TDT A   1    3.565   14.904  48.869  1   0   TDE H
ATOM     64  H31 TDT A   1    4.697   17.298  47.350  1   0   TDE H
ATOM     65  H32 TDT A   1    4.001   15.862  46.613  1   0   TDE H
ATOM     66  H33 TDT A   1    2.512   17.812  48.472  1   0   TDE H
ATOM     67  H34 TDT A   1    1.822   16.342  47.807  1   0   TDE H
ATOM     68  H35 TDT A   1    1.045   18.197  46.486  1   0   TDE H
ATOM     69  H36 TDT A   1    2.109   17.224  45.492  1   0   TDE H
ATOM     70  H37 TDT A   1    2.939   19.845  46.880  1   0   TDE H
ATOM     71  H38 TDT A   1    2.505   19.691  45.178  1   0   TDE H
ATOM     72  H39 TDT A   1    3.958   18.906  45.786  1   0   TDE H
ATOM     73  H40 TDT A   1    6.835   15.739  51.317  1   0   TDE H
ATOM     74  H41 TDT A   1    7.078   14.192  52.098  1   0   TDE H
ATOM     75  H42 TDT A   1    4.614   13.971  52.510  1   0   TDE H
ATOM     76  H43 TDT A   1    4.325   15.495  51.699  1   0   TDE H
ATOM     77  H44 TDT A   1    5.705   16.687  53.408  1   0   TDE H
ATOM     78  H45 TDT A   1    6.099   15.165  54.172  1   0   TDE H
ATOM     79  H46 TDT A   1    4.386   16.252  55.477  1   0   TDE H
ATOM     80  H47 TDT A   1    3.743   14.777  54.792  1   0   TDE H
ATOM     81  H48 TDT A   1    2.066   16.508  54.707  1   0   TDE H
ATOM     82  H49 TDT A   1    2.486   16.081  53.072  1   0   TDE H
ATOM     83  H50 TDT A   1    3.927   18.109  52.873  1   0   TDE H
ATOM     84  H51 TDT A   1    3.609   18.530  54.536  1   0   TDE H
ATOM     85  H52 TDT A   1    1.529   18.361  52.288  1   0   TDE H
ATOM     86  H53 TDT A   1    2.286   19.835  52.845  1   0   TDE H
ATOM     87  H54 TDT A   1    0.366   18.097  54.486  1   0   TDE H
ATOM     88  H55 TDT A   1    -0.007  19.577  53.649  1   0   TDE H
ATOM     89  H56 TDT A   1    0.289   20.492  55.731  1   0   TDE H
ATOM     90  H57 TDT A   1    1.951   20.592  55.206  1   0   TDE H
ATOM     91  H58 TDT A   1    2.418   18.409  56.435  1   0   TDE H
ATOM     92  H59 TDT A   1    0.740   18.366  56.930  1   0   TDE H
ATOM     93  H60 TDT A   1    1.047   20.548  58.143  1   0   TDE H
ATOM     94  H61 TDT A   1    2.726   20.586  57.649  1   0   TDE H
ATOM     95  H62 TDT A   1    1.459   18.403  59.389  1   0   TDE H
ATOM     96  H63 TDT A   1    3.139   18.435  58.893  1   0   TDE H
ATOM     97  H64 TDT A   1    1.777   20.578  60.607  1   0   TDE H
ATOM     98  H65 TDT A   1    3.455   20.612  60.109  1   0   TDE H
ATOM     99  H66 TDT A   1    2.195   18.439  61.891  1   0   TDE H
ATOM    100  H67 TDT A   1    3.251   19.741  62.446  1   0   TDE H
ATOM    101  H68 TDT A   1    3.887   18.477  61.391  1   0   TDE H
ATOM    102  O1  DEC A   1    5.111   13.739  45.929  1   0   TDE O
ATOM    103  C33 DEC A   1    0.956   14.864  35.016  1   0   TDE C
ATOM    104  C34 DEC A   1    0.953   15.049  36.536  1   0   TDE C
ATOM    105  C35 DEC A   1    2.082   14.290  37.241  1   0   TDE C
ATOM    106  C36 DEC A   1    2.094   14.473  38.762  1   0   TDE C
ATOM    107  C37 DEC A   1    3.223   13.710  39.465  1   0   TDE C
ATOM    108  C38 DEC A   1    3.247   13.899  40.986  1   0   TDE C
```

```
ATOM    109  C39 DEC A    1    4.371   13.128  41.683  1    0    TDE C
ATOM    110  C40 DEC A    1    4.415   13.333  43.201  1    0    TDE C
ATOM    111  C41 DEC A    1    5.532   12.540  43.880  1    0    TDE C
ATOM    112  C42 DEC A    1    5.686   12.745  45.402  1    0    TDE C
ATOM    113  O2  DEC A    1    6.403   11.906  46.008  1    0    TDE O
ATOM    114  H69 DEC A    1    6.501   12.799  43.431  1    0    TDE H
ATOM    115  H70 DEC A    1    5.413   11.466  43.701  1    0    TDE H
ATOM    116  H71 DEC A    1    4.539   14.395  43.434  1    0    TDE H
ATOM    117  H72 DEC A    1    3.450   13.047  43.640  1    0    TDE H
ATOM    118  H73 DEC A    1    5.337   13.427  41.250  1    0    TDE H
ATOM    119  H74 DEC A    1    4.266   12.057  41.460  1    0    TDE H
ATOM    120  H75 DEC A    1    3.343   14.969  41.216  1    0    TDE H
ATOM    121  H76 DEC A    1    2.280   13.591  41.405  1    0    TDE H
ATOM    122  H77 DEC A    1    4.188   14.025  39.046  1    0    TDE H
ATOM    123  H78 DEC A    1    3.132   12.640  39.234  1    0    TDE H
ATOM    124  H79 DEC A    1    2.178   15.543  38.998  1    0    TDE H
ATOM    125  H80 DEC A    1    1.128   14.152  39.174  1    0    TDE H
ATOM    126  H81 DEC A    1    2.001   13.221  37.005  1    0    TDE H
ATOM    127  H82 DEC A    1    3.047   14.614  36.829  1    0    TDE H
ATOM    128  H83 DEC A    1   -0.012   14.722  36.941  1    0    TDE H
ATOM    129  H84 DEC A    1    1.032   16.118  36.773  1    0    TDE H
ATOM    130  H85 DEC A    1    0.139   15.417  34.542  1    0    TDE H
ATOM    131  H86 DEC A    1    1.892   15.216  34.573  1    0    TDE H
ATOM    132  H87 DEC A    1    0.841   13.809  34.743  1    0    TDE H
END
```

[TDTHP][DEC] PSF File

```
PSF

       1 !NTITLE
 REMARKS VMD-generated NAMD/X-Plor PSF structure file

     132 !NATOM
       1 TDE  1    TDT  C1   CT     0.412622       12.0107           0
       2 TDE  1    TDT  C2   CT    -0.160857       12.0107           0
       3 TDE  1    TDT  C3   CT     0.067578       12.0107           0
       4 TDE  1    TDT  C4   CT     0.077664       12.0107           0
       5 TDE  1    TDT  C5   CT     0.092139       12.0107           0
       6 TDE  1    TDT  C6   CT    -0.112108       12.0107           0
       7 TDE  1    TDT  P1   P3     0.004618       30.9738           0
       8 TDE  1    TDT  C7   CT     0.032418       12.0107           0
       9 TDE  1    TDT  C8   CT    -0.066094       12.0107           0
      10 TDE  1    TDT  C9   CT     0.044427       12.0107           0
      11 TDE  1    TDT  C10  CT     0.043813       12.0107           0
      12 TDE  1    TDT  C11  CT     0.161565       12.0107           0
      13 TDE  1    TDT  C12  CT     0.034358       12.0107           0
      14 TDE  1    TDT  C13  CT     0.027226       12.0107           0
      15 TDE  1    TDT  C14  CT    -0.325644       12.0107           0
      16 TDE  1    TDT  C15  CT    -0.010805       12.0107           0
      17 TDE  1    TDT  C16  CT    -0.010259       12.0107           0
      18 TDE  1    TDT  C17  CT     0.082769       12.0107           0
      19 TDE  1    TDT  C18  CT     0.091444       12.0107           0
      20 TDE  1    TDT  C19  CT     0.079587       12.0107           0
      21 TDE  1    TDT  C20  CT    -0.215389       12.0107           0
      22 TDE  1    TDT  C21  CT     0.072670       12.0107           0
      23 TDE  1    TDT  C22  CT     0.113522       12.0107           0
      24 TDE  1    TDT  C23  CT     0.089968       12.0107           0
      25 TDE  1    TDT  C24  CT    -0.135600       12.0107           0
      26 TDE  1    TDT  C25  CT     0.033428       12.0107           0
      27 TDE  1    TDT  C26  CT     0.012310       12.0107           0
      28 TDE  1    TDT  C27  CT    -0.047418       12.0107           0
      29 TDE  1    TDT  C28  CT     0.048002       12.0107           0
      30 TDE  1    TDT  C29  CT     0.051805       12.0107           0
      31 TDE  1    TDT  C30  CT     0.166524       12.0107           0
      32 TDE  1    TDT  C31  CT     0.023986       12.0107           0
      33 TDE  1    TDT  C32  CT     0.028339       12.0107           0
      34 TDE  1    TDT  H1   HC    -0.336547        1.0079           0
      35 TDE  1    TDT  H2   HC    -0.010879        1.0079           0
      36 TDE  1    TDT  H3   HC    -0.013125        1.0079           0
      37 TDE  1    TDT  H4   HC     0.082469        1.0079           0
      38 TDE  1    TDT  H5   HC     0.094164        1.0079           0
      39 TDE  1    TDT  H6   HC     0.084197        1.0079           0
      40 TDE  1    TDT  H7   HC    -0.162446        1.0079           0
      41 TDE  1    TDT  H8   HC     0.049240        1.0079           0
      42 TDE  1    TDT  H9   HC     0.097037        1.0079           0
      43 TDE  1    TDT  H10  HC     0.076549        1.0079           0
      44 TDE  1    TDT  H11  HC    -0.123036        1.0079           0
      45 TDE  1    TDT  H12  HC     0.037839        1.0079           0
      46 TDE  1    TDT  H13  HC     0.013022        1.0079           0
      47 TDE  1    TDT  H14  HC    -0.060732        1.0079           0
      48 TDE  1    TDT  H15  HC     0.046534        1.0079           0
      49 TDE  1    TDT  H16  HC     0.049782        1.0079           0
```

```
 50 TDE  1    TDT  H17  HC     0.172761        1.0079          0
 51 TDE  1    TDT  H18  HC     0.026141        1.0079          0
 52 TDE  1    TDT  H19  HC     0.032349        1.0079          0
 53 TDE  1    TDT  H20  HC    -0.325652        1.0079          0
 54 TDE  1    TDT  H21  HC    -0.013945        1.0079          0
 55 TDE  1    TDT  H22  HC    -0.014912        1.0079          0
 56 TDE  1    TDT  H23  HC     0.078899        1.0079          0
 57 TDE  1    TDT  H24  HC     0.091104        1.0079          0
 58 TDE  1    TDT  H25  HC     0.081429        1.0079          0
 59 TDE  1    TDT  H26  HC    -0.199927        1.0079          0
 60 TDE  1    TDT  H27  HC     0.026446        1.0079          0
 61 TDE  1    TDT  H28  HC     0.084356        1.0079          0
 62 TDE  1    TDT  H29  HC     0.107514        1.0079          0
 63 TDE  1    TDT  H30  HC    -0.038627        1.0079          0
 64 TDE  1    TDT  H31  HC     0.016645        1.0079          0
 65 TDE  1    TDT  H32  HC     0.036614        1.0079          0
 66 TDE  1    TDT  H33  HC    -0.050405        1.0079          0
 67 TDE  1    TDT  H34  HC     0.032293        1.0079          0
 68 TDE  1    TDT  H35  HC     0.031386        1.0079          0
 69 TDE  1    TDT  H36  HC    -0.008774        1.0079          0
 70 TDE  1    TDT  H37  HC     0.025136        1.0079          0
 71 TDE  1    TDT  H38  HC     0.019259        1.0079          0
 72 TDE  1    TDT  H39  HC     0.005586        1.0079          0
 73 TDE  1    TDT  H40  HC     0.011485        1.0079          0
 74 TDE  1    TDT  H41  HC     0.012717        1.0079          0
 75 TDE  1    TDT  H42  HC    -0.005820        1.0079          0
 76 TDE  1    TDT  H43  HC     0.004375        1.0079          0
 77 TDE  1    TDT  H44  HC     0.006167        1.0079          0
 78 TDE  1    TDT  H45  HC    -0.024010        1.0079          0
 79 TDE  1    TDT  H46  HC     0.004788        1.0079          0
 80 TDE  1    TDT  H47  HC     0.005026        1.0079          0
 81 TDE  1    TDT  H48  HC    -0.011750        1.0079          0
 82 TDE  1    TDT  H49  HC     0.008423        1.0079          0
 83 TDE  1    TDT  H50  HC     0.006772        1.0079          0
 84 TDE  1    TDT  H51  HC     0.051624        1.0079          0
 85 TDE  1    TDT  H52  HC     0.007567        1.0079          0
 86 TDE  1    TDT  H53  HC     0.008228        1.0079          0
 87 TDE  1    TDT  H54  HC    -0.091129        1.0079          0
 88 TDE  1    TDT  H55  HC    -0.006734        1.0079          0
 89 TDE  1    TDT  H56  HC    -0.006197        1.0079          0
 90 TDE  1    TDT  H57  HC    -0.016476        1.0079          0
 91 TDE  1    TDT  H58  HC     0.018635        1.0079          0
 92 TDE  1    TDT  H59  HC     0.018647        1.0079          0
 93 TDE  1    TDT  H60  HC     0.157744        1.0079          0
 94 TDE  1    TDT  H61  HC     0.012367        1.0079          0
 95 TDE  1    TDT  H62  HC     0.010222        1.0079          0
 96 TDE  1    TDT  H63  HC    -0.315532        1.0079          0
 97 TDE  1    TDT  H64  HC    -0.018418        1.0079          0
 98 TDE  1    TDT  H65  HC    -0.020456        1.0079          0
 99 TDE  1    TDT  H66  HC     0.072135        1.0079          0
100 TDE  1    TDT  H67  HC     0.078837        1.0079          0
101 TDE  1    TDT  H68  HC     0.072413        1.0079          0
102 TDE  1    DEC  O1   O2     0.899565       15.9994          0
103 TDE  1    DEC  C33  CT    -0.294283       12.0107          0
104 TDE  1    DEC  C34  CT     0.196195       12.0107          0
105 TDE  1    DEC  C35  CT     0.033905       12.0107          0
106 TDE  1    DEC  C36  CT     0.033910       12.0107          0
107 TDE  1    DEC  C37  CT    -0.126221       12.0107          0
```

```
108 TDE  1    DEC  C38  CT    -0.024843       12.0107          0
109 TDE  1    DEC  C39  CT    -0.024846       12.0107          0
110 TDE  1    DEC  C40  CT    -0.014504       12.0107          0
111 TDE  1    DEC  C41  CT     0.013826       12.0107          0
112 TDE  1    DEC  C42  C      0.013825       12.0107          0
113 TDE  1    DEC  O2   O2     0.110847       15.9994          0
114 TDE  1    DEC  H69  HC    -0.001316        1.0079          0
115 TDE  1    DEC  H70  HC    -0.001315        1.0079          0
116 TDE  1    DEC  H71  HC    -0.110639        1.0079          0
117 TDE  1    DEC  H72  HC    -0.025811        1.0079          0
118 TDE  1    DEC  H73  HC    -0.025811        1.0079          0
119 TDE  1    DEC  H74  HC    -0.020249        1.0079          0
120 TDE  1    DEC  H75  HC     0.017304        1.0079          0
121 TDE  1    DEC  H76  HC     0.017304        1.0079          0
122 TDE  1    DEC  H77  HC     0.189114        1.0079          0
123 TDE  1    DEC  H78  HC     0.006293        1.0079          0
124 TDE  1    DEC  H79  HC     0.006293        1.0079          0
125 TDE  1    DEC  H80  HC    -0.334184        1.0079          0
126 TDE  1    DEC  H81  HC    -0.029194        1.0079          0
127 TDE  1    DEC  H82  HC    -0.029193        1.0079          0
128 TDE  1    DEC  H83  HC     0.071925        1.0079          0
129 TDE  1    DEC  H84  HC     0.071000        1.0079          0
130 TDE  1    DEC  H85  HC     0.071925        1.0079          0
131 TDE  1    DEC  H86  HC    -0.849340        1.0079          0
132 TDE  1    DEC  H87  HC    -0.841479        1.0079          0

130 !NBOND: bonds
  1       2       1       7       1      34       1      35
  2       3       2      37       2      36       3       4
  3      38       3      39       4      41       4       5
  4      40       5      43       5       6       5      42
  6      46       6      44       6      45       7       8
  7      22       7      28       8      74       8      73
  8       9       9      76       9      10       9      75
 10      77      10      11      10      78      11      12
 11      79      11      80      12      13      12      81
 12      82      13      84      13      83      13      14
 14      86      14      15      14      85      15      16
 15      88      15      87      16      90      16      89
 16      17      17      18      17      91      17      92
 18      94      18      19      18      93      19      20
 19      95      19      96      20      98      20      21
 20      97      21      99      21     100      21     101
 22      48      22      23      22      47      23      49
 23      50      23      24      24      52      24      25
 24      51      25      53      25      26      25      54
 26      27      26      55      26      56      27      57
 27      58      27      59      28      60      28      61
 28      29      29      30      29      62      29      63
 30      64      30      65      30      31      31      32
 31      66      31      67      32      33      32      68
 32      69      33      70      33      71      33      72
102     112     103     131     103     104     103     130
103     132     104     105     104     128     104     129
105     127     105     106     105     126     106     124
106     125     106     107     107     122     107     108
107     123     108     109     108     120     108     121
109     118     109     110     109     119     110     116
```

```
110     117     110     111     111     114     111     112
111     115     112     113

255 !NTHETA: angles
  2       1       7       2       1      34       2       1      35
  7       1      34       7       1      35      34       1      35
  1       2       3       1       2      37       1       2      36
  3       2      37       3       2      36      36       2      37
  2       3       4       2       3      38       2       3      39
  4       3      38       4       3      39      38       3      39
  3       4      41       3       4       5       3       4      40
  5       4      41      40       4      41       5       4      40
  4       5      43       4       5       6       4       5      42
  6       5      43      42       5      43       6       5      42
  5       6      46       5       6      44       5       6      45
 44       6      46      45       6      46      44       6      45
  8       7      22       8       7      28       1       7       8
 22       7      28       1       7      22       1       7      28
 73       8      74       7       8      74       9       8      74
  7       8      73       9       8      73       7       8       9
  8       9      76       8       9      10       8       9      75
 10       9      76      75       9      76      10       9      75
  9      10      77      11      10      77      77      10      78
  9      10      11       9      10      78      11      10      78
 12      11      79      10      11      12      12      11      80
 10      11      79      79      11      80      10      11      80
 13      12      81      13      12      82      11      12      13
 81      12      82      11      12      81      11      12      82
 83      13      84      12      13      84      14      13      84
 12      13      83      14      13      83      12      13      14
 15      14      86      13      14      86      85      14      86
 13      14      15      15      14      85      13      14      85
 16      15      88      16      15      87      14      15      16
 87      15      88      14      15      88      14      15      87
 15      16      90      89      16      90      17      16      90
 15      16      89      15      16      17      17      16      89
 16      17      18      16      17      91      16      17      92
 18      17      91      18      17      92      91      17      92
 19      18      94      93      18      94      17      18      94
 19      18      93      17      18      19      17      18      93
 20      19      95      20      19      96      18      19      20
 95      19      96      18      19      95      18      19      96
 19      20      98      21      20      98      97      20      98
 19      20      21      19      20      97      21      20      97
 20      21      99      20      21     100      20      21     101
 99      21     100      99      21     101     100      21     101
 23      22      48       7      22      48      47      22      48
  7      22      23      23      22      47       7      22      47
 22      23      49      22      23      50      22      23      24
 49      23      50      24      23      49      24      23      50
 23      24      52      23      24      25      23      24      51
 25      24      52      51      24      52      25      24      51
 24      25      53      26      25      53      53      25      54
 24      25      26      24      25      54      26      25      54
 25      26      27      25      26      55      25      26      56
 27      26      55      27      26      56      55      26      56
 26      27      57      26      27      58      26      27      59
 57      27      58      57      27      59      58      27      59
```

```
 60      28      61       7      28      60      29      28      60
  7      28      61      29      28      61       7      28      29
 30      29      62      28      29      30      30      29      63
 28      29      62      62      29      63      28      29      63
 64      30      65      29      30      64      31      30      64
 29      30      65      31      30      65      29      30      31
 30      31      32      32      31      66      32      31      67
 30      31      66      30      31      67      66      31      67
 33      32      68      33      32      69      31      32      33
 68      32      69      31      32      68      31      32      69
 32      33      70      32      33      71      32      33      72
 70      33      71      70      33      72      71      33      72
104     103     131     130     103     131     131     103     132
104     103     130     104     103     132     130     103     132
103     104     105     103     104     128     103     104     129
105     104     128     105     104     129     128     104     129
106     105     127     104     105     127     126     105     127
104     105     106     106     105     126     104     105     126
124     106     125     105     106     124     107     106     124
105     106     125     107     106     125     105     106     107
106     107     122     108     107     122     122     107     123
106     107     108     106     107     123     108     107     123
107     108     109     107     108     120     107     108     121
109     108     120     109     108     121     120     108     121
108     109     118     110     109     118     118     109     119
108     109     110     108     109     119     110     109     119
116     110     117     109     110     116     111     110     116
109     110     117     111     110     117     109     110     111
110     111     114     112     111     114     114     111     115
110     111     112     110     111     115     112     111     115
102     112     113     102     112     111     111     112     113

366 !NPHI: dihedrals
  7       1       2       3       7       1       2      37
  7       1       2      36      34       1       2       3
 34       1       2      37      34       1       2      36
 35       1       2       3      35       1       2      37
 35       1       2      36       2       1       7       8
  2       1       7      22       2       1       7      28
 34       1       7       8      34       1       7      22
 34       1       7      28      35       1       7       8
 35       1       7      22      35       1       7      28
  1       2       3       4       1       2       3      38
  1       2       3      39      37       2       3       4
 37       2       3      38      37       2       3      39
 36       2       3       4      36       2       3      38
 36       2       3      39       2       3       4      41
  2       3       4       5       2       3       4      40
 38       3       4      41      38       3       4       5
 38       3       4      40      39       3       4      41
 39       3       4       5      39       3       4      40
  3       4       5      43       3       4       5       6
  3       4       5      42      41       4       5      43
 41       4       5       6      41       4       5      42
 40       4       5      43      40       4       5       6
 40       4       5      42       4       5       6      46
  4       5       6      44       4       5       6      45
 43       5       6      46      43       5       6      44
```

```
43   5   6  45  42   5   6  46
42   5   6  44  42   5   6  45
22   7   8  74  22   7   8  73
22   7   8   9  28   7   8  74
28   7   8  73  28   7   8   9
 1   7   8  74   1   7   8  73
 1   7   8   9   8   7  22  48
 8   7  22  23   8   7  22  47
28   7  22  48  28   7  22  23
28   7  22  47   1   7  22  48
 1   7  22  23   1   7  22  47
 8   7  28  60   8   7  28  61
 8   7  28  29  22   7  28  60
22   7  28  61  22   7  28  29
 1   7  28  60   1   7  28  61
 1   7  28  29  74   8   9  76
74   8   9  10  74   8   9  75
73   8   9  76  73   8   9  10
73   8   9  75   7   8   9  76
 7   8   9  10   7   8   9  75
 8   9  10  77   8   9  10  11
 8   9  10  78  76   9  10  77
76   9  10  11  76   9  10  78
75   9  10  77  75   9  10  11
75   9  10  78  77  10  11  12
77  10  11  79  77  10  11  80
 9  10  11  12   9  10  11  79
 9  10  11  80  78  10  11  12
78  10  11  79  78  10  11  80
79  11  12  13  79  11  12  81
79  11  12  82  10  11  12  13
10  11  12  81  10  11  12  82
80  11  12  13  80  11  12  81
80  11  12  82  81  12  13  84
81  12  13  83  81  12  13  14
82  12  13  84  82  12  13  83
82  12  13  14  11  12  13  84
11  12  13  83  11  12  13  14
84  13  14  86  84  13  14  15
84  13  14  85  83  13  14  86
83  13  14  15  83  13  14  85
12  13  14  86  12  13  14  15
12  13  14  85  86  14  15  16
86  14  15  88  86  14  15  87
13  14  15  16  13  14  15  88
13  14  15  87  85  14  15  16
85  14  15  88  85  14  15  87
88  15  16  90  88  15  16  89
88  15  16  17  87  15  16  90
87  15  16  89  87  15  16  17
14  15  16  90  14  15  16  89
14  15  16  17  90  16  17  18
90  16  17  91  90  16  17  92
15  16  17  18  15  16  17  91
15  16  17  92  89  16  17  18
89  16  17  91  89  16  17  92
16  17  18  94  16  17  18  19
16  17  18  93  91  17  18  94
```

91	17	18	19	91	17	18	93
92	17	18	94	92	17	18	19
92	17	18	93	94	18	19	20
94	18	19	95	94	18	19	96
93	18	19	20	93	18	19	95
93	18	19	96	17	18	19	20
17	18	19	95	17	18	19	96
95	19	20	98	95	19	20	21
95	19	20	97	96	19	20	98
96	19	20	21	96	19	20	97
18	19	20	98	18	19	20	21
18	19	20	97	98	20	21	99
98	20	21	100	98	20	21	101
19	20	21	99	19	20	21	100
19	20	21	101	97	20	21	99
97	20	21	100	97	20	21	101
48	22	23	49	48	22	23	50
48	22	23	24	7	22	23	49
7	22	23	50	7	22	23	24
47	22	23	49	47	22	23	50
47	22	23	24	22	23	24	52
22	23	24	25	22	23	24	51
49	23	24	52	49	23	24	25
49	23	24	51	50	23	24	52
50	23	24	25	50	23	24	51
23	24	25	53	23	24	25	26
23	24	25	54	52	24	25	53
52	24	25	26	52	24	25	54
51	24	25	53	51	24	25	26
51	24	25	54	53	25	26	27
53	25	26	55	53	25	26	56
24	25	26	27	24	25	26	55
24	25	26	56	54	25	26	27
54	25	26	55	54	25	26	56
25	26	27	57	25	26	27	58
25	26	27	59	55	26	27	57
55	26	27	58	55	26	27	59
56	26	27	57	56	26	27	58
56	26	27	59	60	28	29	30
60	28	29	62	60	28	29	63
61	28	29	30	61	28	29	62
61	28	29	63	7	28	29	30
7	28	29	62	7	28	29	63
62	29	30	64	62	29	30	65
62	29	30	31	28	29	30	64
28	29	30	65	28	29	30	31
63	29	30	64	63	29	30	65
63	29	30	31	64	30	31	32
64	30	31	66	64	30	31	67
65	30	31	32	65	30	31	66
65	30	31	67	29	30	31	32
29	30	31	66	29	30	31	67
30	31	32	33	30	31	32	68
30	31	32	69	66	31	32	33
66	31	32	68	66	31	32	69
67	31	32	33	67	31	32	68
67	31	32	69	68	32	33	70
68	32	33	71	68	32	33	72

```
 69      32      33      70      69      32      33      71
 69      32      33      72      31      32      33      70
 31      32      33      71      31      32      33      72
131     103     104     105     131     103     104     128
131     103     104     129     130     103     104     105
130     103     104     128     130     103     104     129
132     103     104     105     132     103     104     128
132     103     104     129     103     104     105     127
103     104     105     106     103     104     105     126
128     104     105     127     128     104     105     106
128     104     105     126     129     104     105     127
129     104     105     106     129     104     105     126
127     105     106     124     127     105     106     125
127     105     106     107     104     105     106     124
104     105     106     125     104     105     106     107
126     105     106     124     126     105     106     125
126     105     106     107     124     106     107     122
124     106     107     108     124     106     107     123
125     106     107     122     125     106     107     108
125     106     107     123     105     106     107     122
105     106     107     108     105     106     107     123
122     107     108     109     122     107     108     120
122     107     108     121     106     107     108     109
106     107     108     120     106     107     108     121
123     107     108     109     123     107     108     120
123     107     108     121     107     108     109     118
107     108     109     110     107     108     109     119
120     108     109     118     120     108     109     110
120     108     109     119     121     108     109     118
121     108     109     110     121     108     109     119
118     109     110     116     118     109     110     117
118     109     110     111     108     109     110     116
108     109     110     117     108     109     110     111
119     109     110     116     119     109     110     117
119     109     110     111     116     110     111     114
116     110     111     112     116     110     111     115
117     110     111     114     117     110     111     112
117     110     111     115     109     110     111     114
109     110     111     112     109     110     111     115
114     111     112     102     114     111     112     113
110     111     112     102     110     111     112     113
115     111     112     102     115     111     112     113

  3 !NIMPHI: impropers
112     102     113     111     102     111     113     112
113     102     111     112

  0 !NDON: donors


  0 !NACC: acceptors


  0 !NNB

  0       0       0       0       0       0       0       0
  0       0       0       0       0       0       0       0
  0       0       0       0       0       0       0       0
```

```
         0          0          0          0          0          0          0          0
         0          0          0          0          0          0          0          0
         0          0          0          0          0          0          0          0
         0          0          0          0          0          0          0          0
         0          0          0          0          0          0          0          0
         0          0          0          0          0          0          0          0
         0          0          0          0          0          0          0          0
         0          0          0          0          0          0          0          0
         0          0          0          0          0          0          0          0
         0          0          0          0          0          0          0          0
         0          0          0          0          0          0          0          0
         0          0          0          0          0          0          0          0
         0          0          0          0          0          0          0          0
         0          0          0          0

         1          0 !NGRP
         0          0          0
```

Appendix B

Master File

```
function main
% Copyright with Dr. Tamal Banerjee at IIT Guwahati (India).
fileID = fopen('exp1.txt','w');
global xbc  % Raffinate loss
% Fifty run for optimization strategy
for i=1:50
    sol=pso(i);
outp=[sol xbc];
fprintf(fileID,'%f\t',outp);
fprintf(fileID,'\n');
end
fclose(fileID);
end
```

PSO function

```
function[solution]=pso(cnt)
format short

% Optimization Parameters Initialization
popsize = 30;   % Size of the swarm
npar = 2;       % Dimension of the problem
maxit = 100;    % Maximum number of iterations

% Variable Bounds
stage_low=2;    % Lower bound for number of stages (N)
stage_high=10;  % Upper bound for number of stages (N)
flow_low=1;     % Lower bound for solvent flow rate (S)
flow_high=10;   % Upper bound for solvent flow rate (S)
% Linear Decreasing Interia weight limit
wmin=0.4;
wmax=0.9;

% Velocity limits
vmax(1)=((stage_high-stage_low)*0.5);
vmax(2)=((flow_high-flow_low)*0.5);

% Particles Position and Velocity Initialization
par(:,1)=(stage_high-stage_low).*rand(popsize,1) + stage_low;
par(:,2)=(flow_high-flow_low).*rand(popsize,1) + flow_low; % Solvent flow rate
vel = zeros(popsize,npar) ;

% Penalty Parameter
dj=floor(par(:,1));
dj1=ceil(par(:,1));
ph=zeros(popsize,1);
count=1;
for i=1:popsize
if dj(i)~=dj1(i)
ph(i)=(sin((2*pi*(par(i,1)-(0.25*(dj1(i)+(3*dj(i))))))./(dj1(i)-dj(i))))+1)/2;
```

```
sd=1+ph(i);
sd_array(count)=sd;
count=count+1;
end
end
smin=min(sd_array);

% Initial cost value evaluation
cost1=test1(par);

% Initial Augmented Cost evaluation
cost=cost1+smin*ph;
minc(1)=min(cost); % min cost
meanc(1)=mean(cost); % mean cost
globalmin=minc(1); % initialize global minimum
% Initialize local minimum for each particle
localpar = par; % location of local minima
localcost = cost; % cost of local minima
% Finding best particle in initial population
[globalcost,indx] = min(cost);
indx;
globalpar=par(indx,:);
epsi=1; % Termination criteria for Penalty parameter update

iter = 0; % counter
s=smin;
while iter < maxit
iter = iter + 1;
xxold=par(:,1);
yyold=par(:,2);

%Penalty parameter update
penalty_cost=abs(globalcost-cost1(indx));
if abs(globalcost)<=epsi
    terminal=penalty_cost;
else
    terminal=penalty_cost/abs(globalcost);
end
 if terminal<=epsi
     s=s;
 else
     s=s*exp(1+ph(indx));
 end

% Global Local Best Inertia Weight (GLBestIW) calculation
pbest_avg(1)=mean(globalpar(:,1));
pbest_avg(2)=mean(globalpar(:,2));
pbest(:,1)=localpar(:,1);
pbest(:,2)=localpar(:,2);
w(1)=(1.1-(globalpar(1)/pbest_avg(1)));
w(2)=(1.1-(globalpar(2)/pbest_avg(2)));
c1=(1+(globalpar(1)./pbest(:,1)));
c2=(1+(globalpar(1)./pbest(:,2)));

% Linear Decreasing Inertia Weight (LDIW) calculation
w(iter)=(wmax-(((wmax-wmin)/maxit)*iter));

% Velocity Update for variable N
```

```
% GLBestIW
vel(:,1)=w(1)*vel(:,1)+rand(1,1)*c1.*(pbest(:,1)+globalpar(1)-(2.*par(:,1)));
% LDIW
%vel(:,1) = w(iter)*vel(:,1) + 2*rand(1,1).*(localpar(:,1)-par(:,1)) +
                    % 2*rand(1,1).*(ones(popsize,1)*globalpar(:,1)-par(:,1));

% Velocity Bounds for variable N
vel_over(:,1)=vel(:,1)<=vmax(1);
vel_under(:,1)=vel(:,1)>=(-vmax(1));
vel(:,1)=vel(:,1).*vel_over(:,1)+(not(vel_over(:,1))*vmax(1));
vel(:,1)=vel(:,1).*vel_under(:,1)+(not(vel_under(:,1))*(-vmax(1)));

% Velocity Update for variable S
%GLBestIW
vel(:,2)=w(2)*vel(:,2)+rand(1,1)*c2.*(pbest(:,2)+globalpar(2)-(2.*par(:,2)));
% LDIW
% vel(:,2) = w(iter)*vel(:,2) +  2*rand(1,1).*(localpar(:,2)-par(:,2)) +
                    % 2*rand(1,1).*(ones(popsize,1)*globalpar(:,2)-par(:,2));

% Velocity Bounds for variable S
vel_over(:,2)=vel(:,2)<=vmax(2);
vel_under(:,2)=vel(:,2)>=(-vmax(2));
vel(:,2)=vel(:,2).*vel_over(:,2)+(not(vel_over(:,2))*vmax(2));
vel(:,2)=vel(:,2).*vel_under(:,2)+(not(vel_under(:,2))*(-vmax(2)));

par = par + vel; % updates particle position

% Particel Position Bounds
overlimit(:,1)=par(:,1)<=stage_high;
underlimit(:,1)=par(:,1)>=stage_low;
overlimit(:,2)=par(:,2)<=flow_high;
underlimit(:,2)=par(:,2)>=flow_low;
par(:,1)=par(:,1).*overlimit(:,1)+(not(overlimit(:,1))*stage_high);
par(:,1)=par(:,1).*underlimit(:,1)+(not(underlimit(:,1))*stage_low);
par(:,2)=par(:,2).*overlimit(:,2)+(not(overlimit(:,2))*flow_high);
par(:,2)=par(:,2).*underlimit(:,2)+(not(underlimit(:,2))*flow_low);

% Penalty function for variable N
dj=floor(par(:,1));
dj1=ceil(par(:,1));
ph=zeros(popsize,1);
for i=1:popsize
if dj(i)~=dj1(i)
ph(i)=(sin((2*pi*(par(i,1)-(0.25*(dj1(i)+(3*dj(i)))))./(dj1(i)-dj(i))))+1)/2;
end
end
% Cost update
cost1=test1(par);
cost=cost1+s.*ph;
% Updating the best local position for each particle
bettercost = cost < localcost;
localcost = localcost.*not(bettercost) + cost.*bettercost;
localpar(find(bettercost),:) = par(find(bettercost),:);
% Updating index g
[temp, t] = min(localcost);

% Best global value update
if temp<globalcost
```

```
globalpar=par(t,:); indx=t; globalcost=temp;
end
cost1=test1(localpar)
solution=[iter globalpar globalcost] % print output each;
xx=par(:,1);
yy=par(:,2);
zz=cost;
% PSO termination criteria
termxx=(xx-xxold).^2;
termyy=(yy-yyold).^2;
if (((sum(termxx)/popsize)<=0.0001)&((sum(termyy)/popsize)<=0.0001))
    break;
end
minc(iter+1)=min(cost); % min for this
globalmin(iter+1)=globalcost; % best min so far
meanc(iter+1)=mean(cost); % avg. cost for
end

% Augmented objective function plot for each run
figure(cnt)
iters=0:length(minc)-1;
plot(iters,minc,'bo',iters,globalmin,'g-');
legend('Local minimum','Global minimum')
xlabel('Generations');ylabel('Augmented Objective Function');
end
```

Cost function

```
function f=test1(x)
[m,n]=size(x);
f=zeros(m,1);
Dc=1;    % Diameter of the column (m)
HETS=1;  % Height Equivalent to Theoritical Stages (m)
Costpack=11636.43; % Cost of the packing (INR/m3)
Ct=0.006;  % Thickness of the Column (m)
raws=8000; % Density of column material steel (kg/m3)
Csteel=296.39; % Cost of column material steel (INR/kg)
for i=1:m
    y=lle(x(i,:));  % ISR Function calling
% Cost of [TDTHP][Phosph] loss in raffinate
% C1=(y(1)*24*325*773.27*136172.4);
C1=(y(1)*24*325*550.91*237480); % Cost of [TDTHP][DCA] loss in raffinate
% Cost of butanol and ethanol loss in raffinate
C2=(y(2)*24*325*74.12*744.76)+(y(3)*24*325*46.07*2210.3929);
Cpack=(((pi/4)*Dc^2)*x(i,1)*HETS*Costpack); % Cost of the packing
Ccol=(3.14*1.4*Dc*x(i,1)*Ct*raws*Csteel);  % Column Cost
% Column cost with 35% excess amount(depreciation, interest & Maintanance)
C3=(1.35*(Cpack+Ccol));
f(i)=(C1)+C2+(C3); % Total Cost
end
end
```

ISR function

```
 function [xbc]=lle(var1)% clear all;
global xbc
format long;
z=0; % Inner Loop index for termination
w=0; % Outer Loop index for termination
N=round(var1(1));  % Rounding of Variable N
NOC=4;             % Number of components
C=0.2;             % Ethanol flow rate in feed (kmol/hr)
D=0.033;           % Butanol flow rate in feed (kmol/hr)
A=100-C-D;         % Water flow rate in feed (kmol/hr)
B=var1(2);         % Solvent flow rate

%Variables Initialization
F=zeros(N,1);          % Feed Flow rate stagewise (kmol/hr)
E=zeros(N,1);          % Extract Flow rate stagewise (kmol/hr)
R=zeros(N,1);          % Raffinate Flow rate stagewise (kmol/hr)
K=zeros(N,NOC);        % Stagewise Distribution Constant
xij=zeros(N,NOC);      % Stagewise Raffinate Phase Composition
yij=zeros(N,NOC);      % Stagewise Extract Phase Composition
xf=zeros(N,NOC);       % Feed Composition stagewise for all components
E_new=zeros(N,1);

G1=C/N;                 % Butanol removal in each stage (kmol/hr)
G2=D/N;                 % Ethanol removal in each stage (kmol/hr)


F(1)=A+C+D; % Feed flow rate to stage 1 (kmol/hr)
F(N)=B;     % Feed flow rate to stage N (kmol/hr)
xf(1,:)=[A/(A+C+D) C/(A+C+D) D/(A+C+D) 0]; % Feed composition on stage 1
xf(N,:)=[0 0 0 1]; % Feed composition on stage N

k=N;
% Stagewise composition and flow rate (kmol/hr) assuming perfect separation
for i=1:N
    xij(i,1)=A/((A+C+D)-(i*G1)-(i*G2));
    xij(i,2)=(C-(i*G1))/((A+C+D)-(i*G1)-(i*G2));
    xij(i,3)=(D-(i*G2))/((A+C+D)-(i*G1)-(i*G2));
    yij(i,2)=(k*G1)/(B+(k*G1)+(k*G2));
    yij(i,3)=(k*G2)/(B+(k*G1)+(k*G2));
    yij(i,4)=B/(B+(k*G1)+(k*G2));
    E(i)=B+(k*G1)+(k*G2);
    k=k-1;
end
for i=1:N-1
    R(i)=E(i+1)-E(1)+sum(F(1:i));
end
R(N)=A;
K1=nrtl(xij,N,NOC)./nrtl(yij,N,NOC); % NRTL function calling
oldx=xij;
Tau_2=N;

while(Tau_2>(0.00001*N))
K=K1;
Tau_1=N*NOC;
tempx=oldx;

while(Tau_1>(0.001*N*NOC))
xij_old=tempx;
```

```
[xij]=tridiagonal(E,R,K,NOC,N,xf,F); % Tridiagonal function calling
tempx= xij;
Kold=K;
 row_sumx=sum(xij,2);
    for i=1:N
        xij(i,:)=xij(i,:)/row_sumx(i);
    end
K=nrtl(xij,N,NOC)./nrtl(yij,N,NOC);
yij=K.*xij;
    row_sumy=sum(yij,2);
    for i=1:N
        yij(i,:)=yij(i,:)/row_sumy(i);
    end
K=nrtl(xij,N,NOC)./nrtl(yij,N,NOC);
Tau_1=0;
for i=1:N
 for j=1:NOC
 Tau_1=Tau_1+(abs(xij_old(i,j)-tempx(i,j)));
end
end
z=z+1
if z>10000
    break
end
end
yij=Kold.*tempx;
for i=1:N
    E_new(i)=E(i)*sum(yij(i,:));
end

for i=1:N-1
    R(i)=E_new(i+1)-E_new(1)+sum(F(1:i));
end

R(N)=-E_new(1)+sum(F(1:N));

Tau_2=0;
for i=1:N
  Tau_2=Tau_2+(((E_new(i)-E(i))/E_new(i))^2);
end
E=E_new;
w=w+1
if w>10000
    break
end
end
xbc(1)=R(N)*tempx(N,4); % Solvent loss in last stage raffinate
xbc(2)=R(N)*tempx(N,2); % Butanol loss in last stage raffinate
xbc(3)=R(N)*tempx(N,3); % Ethanol loss in last stage raffinate
 end
```

NRTL function

```
function gamma=nrtl(x,N,NOC)
gamma=zeros(N,NOC);
temp_x=x;
```

```
for j=1:N
    x=temp_x(j,:);
    alpha=0.3;
% Binary Interaction parameters from Experiments
% Water Butanol Ethanol [TDTHP][Phosph]
%a=[0 3.47 5.07 6.83;11.11 0 2.07 1.76;14.15 6.97 0 17.20;8.41 19.98 19.85 0];
% Water Butanol Ethanol [TDTHP][DCA]
a=[0 3.33 -29.54 5.59;13.5 0 -29.56 3.61;4.24 37.85 0 -2.16;3.97 39.99 33.7 0];
tau=a;
G=exp(-alpha*tau);
sum_Gx=x*G;
sum_Gtaux=x*(G.*tau);
for i=1:length(x)
    s(i,:)=(x.*G(i,:)./sum_Gx).*(tau(i,:)-sum_Gtaux./sum_Gx);
end
gamma(j,:)=exp(sum_Gtaux./sum_Gx+(sum(s,2))');
end
```

Tridiagonal Matrix function

```
function [x]=tridiagonal(E,R,K,NOC,N,xf,F)
tridg=zeros(N);
x=zeros(N,NOC);

for i=1:NOC
   D=zeros(N,1);
    %Tridiagonal matrix starts
    for j=1:N
       tridg(j,j)=(-R(j)-(E(j)*K(j,i)));
       D(j)=-F(j)*xf(j,i);
   end

   for j=2:N
       tridg(j,j-1)=R(j-1);
       tridg(j-1,j)=E(j)*K(j,i);
   end
   %Tridiagonal matrix ends
   x(:,i)=tridg\D;
end
```

List of Publications

International Journals

- **Dharamashi Rabari**, Tamal Banerjee, "**Biobutanol and n-propanol recovery using a low densityphosphonium based ionic liquid at T = 298.15 K and p = 1 atm**," *Fluid Phase Equilbria*, 355: 26-33, 2013.
- C V Manohar, **Dharamashi Rabari**, A Ananth Praveen Kumar, Tamal Banerjee, Kaustubha Mohanty, "**Liquid-liquid equilibria studies on ammonium and phosphonium based ionic liquid-aromatic-aliphatic component at T = 298.15 K and p = 1 bar: Correlations and a-priori predictions**," *Fluid Phase Equilbria*, 360: 392-400, 2013.
- **Dharamashi Rabari**, Nikunj Patel, Milind Joshipura, Tamal Banerjee, "**Densities of Six Commercial Ionic Liquids: Experiments and Prediction Using a Cohesion Based Cubic Equation of State**," *Journal of Chemical & Engineering Data*, 59: 571-578, 2014.
- **Dharamashi Rabari**, Tamal Banerjee, "**Experimental and Theoretical Studies on the Effectiveness of Phosphonium-Based Ionic Liquids for Butanol Removal at T = 298.15 K and p = 1 atm**," , 53: 18935-18942, 2014.

Manuscript Revised and Submitted

- **Dharamashi Rabari**, Tamal Banerjee, "**Preferential Extraction of Butanol from Acetone-Butanol-Ethanol (ABE) Process by Phosphonium based Ionic Liquids**," *The Journal of Chemical Thermodynamics.*

Manuscript Submitted

- **Dharamashi Rabari**, Tamal Banerjee, "**Particle Swarm Optimization of a Multistage Extractor for Lower Alcohols Enhancement using Phosphonium Ionic Liquids**," *Computers and Chemical Engineering.*